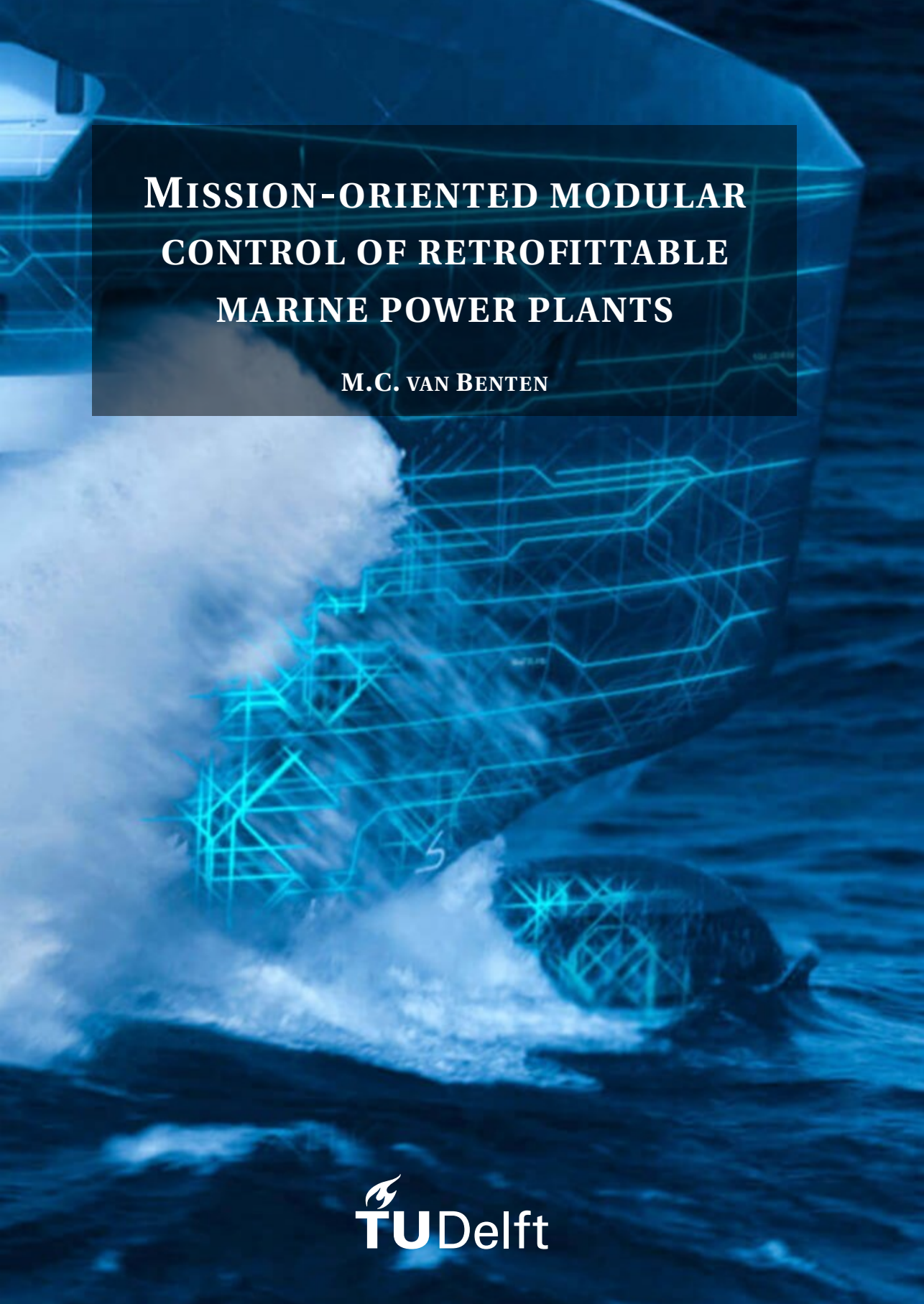

Mission-oriented modular control of retrofittable marine power plants

M.C. van Benten

TU Delft

MISSION-ORIENTED MODULAR CONTROL OF RETROFITTABLE MARINE POWER PLANTS

by

M.C. VAN BENTEN

Master Thesis

in partial fulfilment of the requirements for the degree of

Master of Science
in Mechanical Engineering

at the Department Maritime and Transport Technology of Faculty Mechanical, Maritime and Materials Engineering of Delft University of Technology
to be defended publicly on Tuesday July 12 ,2022 at 1415 PM.

Student number:	4555767		
MSc track:	Multi-Machine Engineering		
Report number:	2022.MME.8673		
Supervisors:	Dr. V. Reppa,		
	N. Kougiatsos (MSc)		
Thesis committee:	Prof. dr. R.R. Negenborn,	TU Delft,	Chair
	Dr. V. Reppa,	TU Delft,	Supervisor
	N. Kougiatsos (MSc)	TU Delft,	Supervisor
Date:	June, 2022		

Cover photo [1]

An electronic version of this thesis is available at http://repository.tudelft.nl/

TU Delft Delft University of Technology

PREFACE

Dear reader,

This thesis is the last step towards completing my Master of Science in Mechanical Engineering at the University of Technology in Delft. It has been quite the journey, which started with the track Multi-Machine Engineering. During the second year of my masters, I did a literature study under the supervision of Vasso Reppa and Nikos Kougiatsos, where I reviewed the state-of-the-art of the propulsion control in marine vessels. I found that, although there is a great variety in propulsion control systems, no literature considered modular use of the equipment in the power plant. To this end, in collaboration with Vasso, Nikos, and Royal IHC, the main idea for this thesis was proposed.

Soon after the initial proposal the main course of the thesis was set, and after the approval of Rudy Negenborn, the journey began. In this work, you may find information about different missions of ships, how these missions dictate the required power, and also how this affects the power plants and the control systems found in various marine vessels. It is shown how this leads to a mission-oriented design of the control system, where equipment can be added, replaced, or removed. Although I did not specialize in control engineering, my skills with MATLAB, developed during the master, greatly helped to resolve most problems, and I am proud to present you my work.

I want to start by thanking Vasso and Nikos for their daily supervision and assistance. Nikos is a PhD researcher, and his field of work is very closely related to the topic of this thesis, so he was always able to provide insightful comments and detailed explanations when I found some obstacles. Vasso's input was aimed more towards the presentation and design of the control systems, and was also very helpful with maintaining the right course, and keeping track of the main goal of the thesis. Also, I want to thank Rudy, who was able to provide good feedback during meetings, as he knows a great deal about this topic, and a lot of his work is used in this thesis.

Finally, I want to thank my parents, friends and my girlfriend for their support, motivation, and guidance, not only during this thesis, but also during my entire studies at the TU Delft. This journey would not have been the same without you.

I wish you a pleasant reading,

M.C. van Benten
Delft, June 2022

SUMMARY

Marine vessels execute many missions during their life cycle, each associated with a different required power profile. The required power is to be provided by the power plant, which has a fixed set of equipment such as diesel engines, generator sets, electric machines, and batteries. Consequently, as the control system is designed for the vessel's power plant, this is also fixed. However, in practice the fixed power plant layout may not suffice for generating the power demand dictated by a new mission. This may lead to inefficient use of components, risk of overloading components, or the inability to deliver the required power. To handle this issue, equipment modifications such as additions, removals or replacements would probably be necessary, along with modifications in the power plant control system. To enable the seamless operation of the power plant control system after the modifications is essential for guaranteeing safety and reducing the downtime, which could be achieved by a control architecture that allows for modular use of the power plant components.

RESEARCH QUESTION

This thesis aims to design a modular control system for varying missions and retrofittable power plants. In this regard, the following research question is addressed:

"How can mission-oriented modular control of marine vessels be designed?"

In order to answer this question, first the correlation between the mission and the power profile, and the required automation modifications of the power plant and the control system to meet the demand of the different power profiles should be investigated. Next, a control architecture can be designed for the proposed power plant to ensure safety, where after the controller can be verified and the performance can be assessed. In order to achieve this, the following subquestions are considered:

1. What is the state-of-the art in marine power plant control?
2. How to model the correlation between the mission and the power profile of the vessel?
3. How to model the correlation between the power profile for a mission and the needed modifications in automation of the control systems and the power plant?
4. How can a modular control architecture be designed to meet the proposed automation and power plant modifications?
5. How to verify the performance (stability and robustness) of the developed modular control scheme?

APPROACH

First the state-of-the-art in marine power plant control is discussed. It is found that typically, the control of vessel's power plants consist of two levels; a primary level with local controllers for the power plant components, and a secondary level that determines the distribution of the required power to the various components in the power plant, also refered to as the power split. The control strategies to determine the power split depends on the type of vessels and their operations, and there are numerous seen in literature. To this end, a taxonomy is provided, including the type of power plant equipment, control strategy, and type of control system seen in the most common type of vessels: service ships, cargo ships, and passenger ships. Service ships, such as tugboats and offshore support vessels, often have hybrid power plants, including diesel engines, electric machines, generator sets and batteries. To this end, Energy Consumption Minimization Strategy (ECMS), power control, or power management is often used to provide the optimal power split between the components. Cargo ships, such as container ships, bulk carriers, and tankers, use a more wide range of control strategies. As container ships often still have a single mechanical engine for propulsion, and generator sets to provide the power for the auxiliary loads, the control system often consists of a single level, using simple shaft speed controllers. Bulk carriers sometimes have battery packs installed to help provide the optimal power split when deck cranes are used, but propulsion is still realized with a single mechanical engine. Also, tankers shipping liquefied natural gas (LNG) often use the boil-off gas to provide fuel for the gas engines, which are also used to power the auxiliary systems. Therefore, ECMS or power management is also seen for bulk carriers and tankers. At last, passenger ships, such as cruise ships and ferries are discussed. Ferries travel short distances, with mechanical engines for propulsion, and mostly they have a controllable-pitch propeller, hence combinator curve control is often seen, and no secondary level control is required. Furthermore, as the power plants of large cruise ships provide both propulsion power, but also a large amount of electric power for many (small) users, power plants are equipped with multiple generator sets and batteries, and often electric motors are used for propulsion. Also, batteries are often charged using shore power when the vessels are at quay. This results in the need for ECMS or power control.

Second, the correlation between the mission and the power profile of the vessel is presented. A general definition for a mission is proposed, which gives details about the type of cargo, time for the mission, and where the mission will be executed. Using this definition, the type of vessel and its parameters, and the operational modes, such as *transit*, *standby*, *loading/unloading*, or *dynamic positioning* required for the mission can be derived. Using the operational modes and the time for the mission, an estimate of the vessel speed for each operational mode is proposed, and this helps determine the operational environment, such as waves, currents, and winds during the route of the vessel. Finally, the found aspects are used to find the required propulsion and auxiliary power during the mission, resulting in the power profile.

Third, the correlation between the power profile and the automation modifications for the control system and power plant are discussed. Examples of different tugboat

and cargo ship missions, power profiles, and power plants are used to show that for a certain vessel with a certain power plant, a higher power demand results in additional equipment such as generator sets or batteries, and vice versa. Also, instead of adding equipment, components can be replaced. As most control systems consist of two levels; a secondary level to determine the power split, and a primary level including the controllers for each power plant component, for equipment modifications such as the described additions, removals, or replacements, the control system has to be able to automatically adapt. More specifically, in order to determine the power split, often ECMs is used, requiring a cost function and constraints, based on the layout of the power plant. As the layout of the power plant changes for each equipment modification, the control system needs to be able to facilitate multiple power plant layouts. Using this, a modular control architecture is proposed.

The modular control architecture of this thesis is designed for a hybrid power plant, which uses a diesel engine and induction motor connected to the propeller, two diesel generator sets, and a variable amount of batteries. Standard PI controllers in the primary level are used for all the components but the batteries, and an ECMS structure in the secondary level is used to determine the power split. As mentioned above, ECMS uses the layout of the power plant to determine the power split. To limit the possible layouts of the power plant, this thesis only considers battery modifications. Now, based on the idea of supervisory switching control [2], a bank of secondary controllers is proposed, using an ECMS structure based on each possible layout of the power plant. As the only change in the power plant layout is the amount of batteries, and there is a physical limit of K_{max} batteries in the power plant, due to limited space, the bank of controllers contains $K_{max}+1$ secondary level controllers (also a controller for no batteries is required). In order to select the required controller, a supervisor is designed. The latter uses the power profile for the mission, and based on this power profile, the required batteries for the mission are determined, and the corresponding secondary level controller is selected from the bank. Assuming the batteries chosen by the supervisor are installed in the power plant, the primary level can be initialized, as for each battery there is a constraint module in the primary level, which provides a limit to the power that can be assigned/requested and communicates this to the selected secondary level controller. At last, if it is assumed that a fault diagnosis is properly designed and installed, the supervisor is designed to cope with battery faults. It has to be noted that no design for this fault diagnosis is presented in this thesis, only a certain output signal is assumed and used by the supervisor.

At last, the performance, with respect to stability and robustness, of the modular control architecture is verified using simulations based on a typical mission of a tugboat. Using a given power profile as a baseline, variations in the mission are correlated to variations of the power profile, and in total four different power profiles are compiled, corresponding to four different missions. Each of these missions is used to simulate the behavior of the modular control architecture, in a Simulink/MATLAB environment. The supervisor, secondary level, primary level, and the power plant components are monitored, and the tracking errors with respect to the required propulsion and auxiliary

power, but also of the reference-signals that have to be followed by the power plant components, are determined. Using these errors, but also with figures showing the power split and the SOC of the batteries, the performance of the modular control architecture with respect to stability and robustness is verified.

CONCLUSIONS

In this thesis, the correlation between the mission and the power profile, and also the correlation between the power profile and the automation modifications, are clearly described. It is shown that different missions lead to different power profiles, which on their turn lead to equipment modifications of the power plant. In order to facilitate these equipment modifications, a modular power plant architecture is designed, consisting of a supervisor, a bank of secondary level controllers, and a primary level. Then, using variations in the mission of a tugboat, different power profiles are compiled, used to show the performance of the modular control architecture. The results show good performance with respect to stability and robustness, with a relative tracking error of 3% for the propulsion power, and 11% for the auxiliary power. Further research is required in order to allow modular use of other power plant components than the batteries, and the correlation between the mission and the power profile can also be further investigated.

CONTENTS

List of Figures

List of Tables

NOMENCLATURE

Abbreviations

AC	Alternating Current
AHTS	Anchor Handling Tug Supply vessel
B	Battery
CSDE	Constant Speed Diesel Engine
DC	Direct Current
DE	Diesel Engine
DG	Diesel Generator Set
DWT	Dead Weight Tonnage
ECMS	Equivalent Consumption Minimization Strategy
EM	Electric Machine
EMS	Energy Management Strategy
ESS	Energy Storage System
FC	Frequency Converter
G	Generator
GS	Generator Set
IM	Induction Motor
KPI	Key Performance Indicator
LNG	Liquefied Natural Gas
M	Motor
ME	Main Engine
MOP	Measure of Performance
OSCV	Offshore Construction Vessel
OSV	Offshore Support Vessel

PF	Power Profile
PSV	Platform Supply Vessel
PTI	Power Take In
PTO	Power Take Off
RMSE	Root-Mean-Square Error
RORO	Roll-On Roll-Off
SFOC	Specific Fuel Oil Consumption
SI	Scatter Index
SOC	State-of-Charge
SSC	Supervisory Switching Control
TEU	Twenty-foot Equivalent Unit
WHR	Waste Heat Recovery
ZES	Zero Emission Services

Greek

Δt	Discrete time step
η_D	Propulsive efficiency
η_H	Hull efficiency
η_O	Open-water efficiency
η_R	Relative rotative efficiency
η_T	Transmission efficiency
η_B	Battery efficiency
η_{DG}	Diesel generator set efficiency
η_{EM}	Electric machine efficiency
η_{FC}	Frequency converter efficiency
η_{gb}	Gearbox efficiency
η_{IM}	Induction motor efficiency
η_S	Shaft efficiency

γ_0	General multiplying factor
γ_1	Multiplying factor for sea state
γ_2	Multiplying factor for wind at sea
γ_3	Multiplying factor for currents of sea
γ_4	Multiplying factor for water depth
γ_5	Multiplying factor for waterway width
γ_6	Multiplying factor for fouling of hull
γ_7	Multiplying factor for displacement of vessel
λ	Fraction expressing reserve power in terms of maximum power
∇	Displacement of vessel
ω_{DE}	Diesel engine shaft speed
$\omega_{DE,ref}$	Diesel engine reference shaft speed
ω_{DG}	Diesel generator set shaft speed
$\omega_{DG,ref}$	Diesel generator set reference shaft speed
ω_{IM}	Induction motor rotor speed
$\omega_{IM,ref}$	Induction motor reference rotor speed
$\omega_{IM,slip}$	Induction motor slip speed
$\omega_{IM,s}$	Induction motor stator speed
ω_p	Propeller speed
$\omega_{p,ref}$	Propeller reference speed
ρ	Density of seawater
τ_{DE}	Torque buildup constant of diesel engine
τ_{DG}	Torque buildup constant of diesel generator set engine

Lowercase

a	Coefficient of proportionality between propulsion power and vessel speed
a_1^{DE}	Constant for SFOC relation diesel engine
a_1^{DG}	Constant for SFOC relation diesel generator set

a_2^{DE}	Constant for SFOC relation diesel engine
a_2^{DG}	Constant for SFOC relation diesel generator set
a_3^{DE}	Constant for SFOC relation diesel engine
a_3^{DG}	Constant for SFOC relation diesel generator set
a_4^{DE}	Constant for SFOC relation diesel engine
a_5^{DE}	Constant for SFOC relation diesel engine
a_6^{DE}	Constant for SFOC relation diesel engine
$a_{B,0}$	Constant for voltage-SOC relation constant of battery
$a_{B,1}$	Constant for voltage-SOC relation constant of battery
$a_{G,0}$	Constant for voltage-current relation of diesel generator set
$a_{G,1}$	Constant for voltage-current relation of diesel generator set
c_0	Nominal resistance factor
$\mathbf{c_0}$	List containing the nominal resistance factor for each operational mode during the mission
c_1	Scaling factor
c_{eqv}	Equivalent consumption of battery
c_s	Currents of sea
d	Draught of vessel
$e_{\omega,DE}$	Shaft speed error of diesel engine
$e_{\omega,DG}$	Shaft speed error of diesel generator set
$e_{\omega,IM}$	Rotor speed error of induction motor
$e_{Q,DE}$	Torque error of diesel engine
$e_{V,DG}$	Voltage error of diesel generator set
f_{grid}	Grid frequency
f_h	Fouling of the hull
h	Water depth
i	Number of shaft lines
i_{DE}	Gear ratio of diesel engine

i_{IM}	Gear ratio of induction motor
k_{DE}	Torque constant of diesel engine
k_{DG}	Torque constant of diesel generator set engine
k_{IM}	Dimensionless constant of induction motor
m_B	Equivalent fuel consumption of battery
m_{DE}	Fuel consumption of diesel engine
m_{DG}	Fuel consumption of diesel generator set engine
$m_{f,DE}$	Fuel index of diesel engine
$m_{f,DG}$	Fuel index of diesel generator set engine
m_s	Sea margin
m_T	Total fuel consumption of power plant
$\dot{m}_T$	Fuel consumption rate of power plant
n_p	Propeller speed in rotations per second
p_{DG}	Poles of diesel generator set
p_{IM}	Poles of induction motor
$r_{2/1}$	Ratio of battery capacity between battery type 2 and battery type 1
s	Slip of induction motor
s_{eqv}	Equivalence factor for battery fuel consumption
s_s	Sea state
t_0	Starting time of the mission
t_{end}	Ending time of the mission
t_{fault}	Time at which a battery fails
t_m	Total mission time
w_s	Wind at sea
w_w	Waterway width
y_{fault}	Fault signal output of the fault diagnosis

Uppercase

C_0	Battery capacity in Ampere-second
$\boldsymbol{C}_0$	Vector containing the capacity in Ampere-second of the batteries in the power plant
C_B	Cost associated with power from or to the battery
C_{GS}	Cost associated with power from the generator set
C_{ME}	Cost associated with power from the main engine
C_p	Propeller constant
C_{tot}	Total cost for a certain power split
$C_{V/f}$	Constant ratio between stator frequency and input voltage of induction motor
D	Propeller diameter
D_{DE}	Damping of diesel engine
D_{IM}	Damping of induction motor
E_0	Battery capacity in Joule
$\boldsymbol{E}_0$	Vector containing the capacity in Joule of the batteries in the power plant
$E_{B,max}$	Maximum energy capacity of batteries in power plant
$E_{B,plant}$	Required energy capacity of batteries in power plant
$\mathbf{E}_K$	Matrix containing the total capacity of each battery configuration of the power plant
F_{bp}	Bollard pull
F_{tow}	Towing force
$\mathbf{F_{tow}}$	List containing the towing force for each operational mode during the mission
H	Amount of harbours to visit
I_B	Output current battery
I_{DG}	Output current diesel generator set
I_X	Excitation current diesel generator set
J_{DE}	Inertia of diesel engine

J_{DG}	Inertia of diesel generator set shaft
J_{IM}	Inertia of induction motor
J_{tot}	Total inertia of diesel engine, induction motor, gearbox, and shaft
K	Number of batteries in the power plant
K_{config}	Maximum number of configurations with batteries in the power plant
$K_{I,DE}$	Integral gain diesel engine controller
K_{I,DG_ω}	Integral gain diesel generator set shaft speed controller
K_{I,DG_V}	Integral gain diesel generator set voltage controller
$K_{I,IM}$	Integral gain induction motor controller
K_{max}	Maximum number of batteries in the power plant
$K_{P,DE}$	Proportional gain diesel engine controller
K_{P,DG_ω}	Proportional gain diesel generator set shaft speed controller
K_{P,DG_V}	Proportional gain diesel generator set voltage controller
$K_{P,IM}$	Proportional gain induction motor controller
K_Q	Propeller thrust coefficient
K_T	Propeller torque coefficient
$\mathcal{L}$	Set of type of vessel and its characteristics, defined by the inputs
L_{DG}	Inductance of diesel generator set
$L_{r,IM}$	Rotor inductance induction motor
$L_{s,IM}$	Stator inductance induction motor
$\mathcal{M}$	Set of measurement units associated with the physical properties
O_e	Operational environment
$\mathbf{O_e}$	List containing the operational environment along the route
$\mathbf{O_H}$	List containing the required operational modes between two harbours
O_m	Operational mode
$\mathbf{O_m}$	List containing the operational modes required during the mission
$\mathcal{P}$	Set of capabilities (operational modes) defined by the inputs and the features-of-interest

P_{aux}	Auxiliary power
$\mathbf{P_{aux}}$	List containing the auxiliary power for each point P along the route
$P_{aux,plant}$	Auxiliary power provided by power plant
P_B	Power of battery
$\boldsymbol{P}_B$	Vector containing the battery power for the batteries as determined by the secondary level
$\boldsymbol{P}_{B,assign}$	Vector containing the battery power assigned to each of the batteries in the power plant
$\mathbf{P}_{B,con}$	List containing the battery constraints provided by the battery constraints modules
$\mathbf{P}_{B,con,assign}$	List containing the battery constraints of each battery in the power plant as input to the secondary level
$P_{B,max}$	Maximum power of battery
$P_{B,min}$	Minimum power of battery
P_B^{max}	Maximum power of battery determined by battery constraint module
P_B^{min}	Minimum power of battery determined by battery constraint module
$P_{B,SOC}^{max}$	Maximum power of battery considering SOC
$P_{B,SOC}^{min}$	Minimum power of battery considering SOC
$P_{B,V}^{max}$	Maximum power of battery considering output voltage
$P_{B,V}^{min}$	Minimum power of battery considering output voltage
P_D	Propulsion power
$\mathbf{P_D}$	List containing the propulsion power for each point P along the route
$P_{D,elec}$	Propulsion power expressed in electric load of induction motor
$P_{D,error}$	Propulsion power error
P_{DE}	Power of diesel engine
P_{DE}^{max}	Maximum power of diesel engine
P_{DG}	Power of diesel generator set
P_{DG}^{max}	Maximum power of diesel generator set
P_{DG}^{opt}	Power of diesel generator set at the most efficient working point

P_E	Effective power
P_{EM}	Power of electric machine
$P_{EM,max}$	Maximum power of electric machine
$P_{EM,min}$	Minimum power of electric machine
P_{GS}	Power of generator set
$P_{GS,max}$	Maximum power of generator set
$P_{GS,min}$	Minimum power of generator set
P_{hotel}	Power required for the hotel load
$P_{IM,elec}$	Electric power of induction motor
$P_{IM,grid}$	Power from the grid required for the induction motor
$P^{max}_{IM,grid}$	Maximum power from the grid required for the induction motor
$P_{IM,mec}$	Mechanical power of induction motor
$P^{max}_{IM,mec}$	Maximum mechanical power of induction motor
P_{ME}	Power of main engine
$P_{ME,max}$	Maximum power of main engine
$P_{ME,min}$	Minimum power of main engine
P_p	Propeller power
P_{plant}	Required power plant power
$P_{plant,max}$	Maximum power of power plant
$P_{service}$	Power required for the service load
$\mathbf{P_{tot}}$	List containing the total power for each point P along the route
$\mathcal{Q}$	Set of physical properties associated with inputs, outputs, and parameters
Q_{DE}	Diesel engine torque
$Q_{DE,ref}$	Diesel engine torque reference
$Q_{DG,DE}$	Diesel generator set engine torque
$Q_{DG,G}$	Diesel generator set generator torque
Q_{IM}	Induction motor torque
Q_p	Propeller torque

$Q_{p,DE}$	Diesel engine torque delivered to propeller
$Q_{p,IM}$	Induction motor torque delivered to propeller
R	Hull resistance
R_A	Air resistance
R_B	Battery resistance
R_{DG}	Load resistance of diesel generator set
$R_{DG,int}$	Internal resistance of diesel generator set
R_E	Eddy resistance
R_F	Frictional resistance
$R_{r,IM}$	Rotor resistance induction motor
$R_{s,IM}$	Stator resistance induction motor
R_T	Total hull resistance
R_W	Wave resistance
$\overline{\mathbf{S}}_{\mathbf{O_m}}$	List containing the travelled distance for each operational mode during the mission
$\mathbf{S_m}$	List containing P points (x,y) defining the route of the vessel
SOC_{avg}	Average SOC of battery
SOC_{max}	Maximum SOC of battery
SOC_{min}	Minimum SOC of battery
T_a	Ambient temperature
$\mathbf{T}_{\mathbf{O_m}}$	List containing the duration of each required operational mode for the mission
T_p	Propeller thrust
$\mathcal{U}$	Set of inputs defined by the mission
V	Vessel speed
V_0	Diesel generator set induced voltage
V_{avg}	Average battery voltage
V_B	Battery output voltage
$V_{B,max}$	Minimum battery output voltage

$V_{B,min}$	Maximum battery output voltage
V_{DG}	Diesel generator set output voltage
$V_{DG,ref}$	Diesel generator set reference output voltage
V_{IM}	Induction motor input voltage
V_{OC}	Battery open-circuit voltage
$\mathbf{V_{O_m}}$	List containing the vessel speed for each operational mode during the mission
X	Type of cargo
X_{DG}	Internal reactance of diesel generator set
$\mathbf{X_p}$	List containing vessel characteristics
X_v	Type of vessel
$\mathbf{X}_\nabla$	List containing the vessel displacement for each operational mode during the mission
$\mathcal{Y}$	Set of outputs defined by the parameters and features-of-interest
$\mathcal{Z}$	Set of parameters affected by the input, features-of-interest and capabilities

1

INTRODUCTION

1.1. MOTIVATION

Marine vessels are used for many purposes, such as shipping cargo, (supporting) offshore operations, transporting passengers, or even to tow other marine vessels. During their lifetime they execute many missions, and each mission requires power, either for propulsion or for other tasks. The required power is generated by the power plant, which consists of the power supply and the propulsion plant. The power supply often consists of generator sets and batteries, and the propulsion plant often consists of diesel engines and/or electric motors, coupled to a propeller to provide the propulsion power. How the power plant is designed is partly based on the mission statement which includes the expected missions the vessel will execute [3], and during a mission, vessels can operate using several operational modes. Each operational mode implies a certain amount of power from the power plant, so for each mission a power profile can be constructed, which shows the required power versus the time or frequency of occurrence [4]. From such a profile, the minimum amount of equipment in the power plant to deliver the required amount of power can be derived. However, each mission results in a different amount of required power for each operational mode, since for each mission there are different environmental conditions (such as wind, waves and currents) and operational conditions (e.g. the frequency of the required actions of the vessel, such as loading or unloading cargo, sail across open sea or towing another vessel). Therefore, the power profile depends on the mission, hence each mission implies a certain required amount of equipment in the power plant.

For example, consider a bulk carrier with two missions: transport iron ore from A to B, and from A to C. The total travelled distance may be the same, but the sea state may be very different, resulting in high waves and strong currents for one mission and a calm sea for the other. Furthermore, the operational conditions in the port may be different. At port B the cargo is unloaded by port cranes, while at port C the vessel has to unload the cargo itself. These differences in the environmental and operational conditions, result in

varying power profiles (e.g. extra power is required for the deck cranes to perform the unloading operation). This motivates for a reconfigurable power plant, where equipment can be replaced, added or removed, and a modular control system which can adapt to changes in the power plant. Using this approach, each mission can be executed with the required amount of equipment for the power plant, which could improve the efficiency of the vessel, reduce the operating cost, and improve the ability to stay competitive in the future.

Furthermore, not only at the start and end of each mission, but also during the mission it can be beneficial to change equipment. If for example a vessel visits a harbour for a short amount of time, the batteries of the power supply could be charged, but since vessel's time at the harbour is limited, it is more useful to replace the battery with a fully charged one. However, if the battery is not exactly the same, the vessel cannot use it since the control system is designed for a specific set of equipment. Therefore, a control system that is designed for modular use of the equipment in the power plant, where the replaced battery does not have to be identical, has to be investigated.

In addition, with respect to automated sailing, imagine a vessel which sails across the ocean, and a generator breaks down. There is no crew to fix the generator, so either the vessel has to wait for backup, which can lead to substantial delays and high costs, or the vessel finds a way to accommodate this fault and operate with the remaining equipment to continue with the mission. When the vessel docks at the destination harbour, the problem can be fixed, minimizing the delays and costs. This can be realized if the control system allows modular use of the equipment in the power plant, since this scenario is equivalent to the removal of equipment as described in the previous example.

1.2. BACKGROUND

The previous section highlighted the need for a scalable and modular power plant control system to increase the reconfigurability of the vessel's systems. From the operation side of view, this novelty could enable a more efficient use of the same vessel for many different missions. To this end, this section will discuss power plants and their control systems in current marine vessels. Furthermore, this section illustrates the relation between the mission and the power profile of the vessel, and also how the power profile implies design choices for the power plant.

MISSION AND POWER PROFILE

The power plant of a vessel provides the required power for propulsion, but also for the auxiliary loads. The equipment and layout of a power plant, but also the type of mission that can be executed, strongly depends on the type of vessel. To highlight a few different types: cargo ships are specialized to transport a certain type of cargo from one port to another, cruise ships and ferries transport people over short and long distance routes, offshore vessels operate in near the coast or at deep sea with a variety of functions, such as supplying oil-platforms and pipe-laying, and tugboats (service vessels) in most cases assist incoming and outgoing cargo ships in the port. Each type of vessel has different

missions. For example, a typical mission of a cargo ship consists of:

- Loading the cargo
- Maneuvering to open sea (guided by a tugboat)
- Transit (sail to destination)
- Maneuvering to the assigned location at the port (guided by a tugboat)
- Unloading the cargo

Most of the time is spent in transit mode with constant slow speed [5], resulting in a constant propulsion load. Since the required power for the auxiliary systems is also mostly constant [6], the total power demand is constant during most of the mission. This constant power profile is in broad contrast with the power profile of a tugboat, whose typical mission can be described as follows:

- Standby at port
- Transit (sail to vessel that has to be assisted)
- Waiting (if vessel is not ready yet, wait till assist is needed)
- Assist vessel
- Transit (sail back to standby area)

This mission induces a much more time-varying power demand. For standby and waiting, the propulsion power is low, of the same order of magnitude as the auxiliary power, and together they comprise more than half of the mission time [6, 7]. For transit, the propulsion power demand is already higher, and for assisting the vessel, nearly all available propulsion power may be used, but only for a short amount of time.

Concluding, the mission for the cargo ship induces a constant power demand, while the power demand of mission for the tugboat is time-varying. How the power demand varies throughout the mission, can be illustrated with the power profile. A typical power profile shows the required power (y-axis), against the time or frequency of occurrence (x-axis), and is shown in Figure 1.1 for the cargo ship and the tugboat.

POWER PLANT

The power profile affects the design of the power plant [9], since the power plant produces the required power for propulsion and the auxiliary loads [10–12]. How propulsive power is generated, is determined by the type of propulsion, and there are three types of propulsion: mechanical, electric, and hybrid [13], depicted in Figure 1.2. With mechanical propulsion, the main engine (often a diesel engine) drives a shaft, which is either directly coupled to the propeller (direct propulsion), or through a gearbox (geared propulsion). This type of propulsion is mostly used for ships with constant power profiles. With electric propulsion, the shaft is driven by an electric motor instead of a diesel

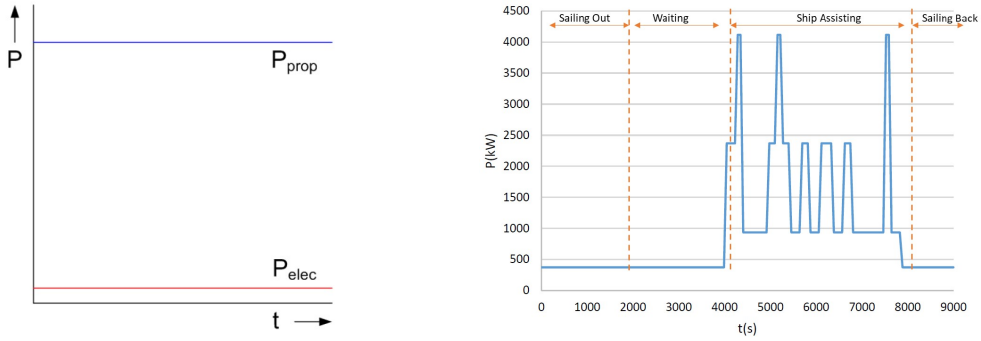

(a) Typical power profile of a cargo ship[6]

(b) Typical power profile of a tugboat [8]

Figure 1.1: Power profiles of a cargo ship and tugboat

engine. This removes the need of a gearbox, so the propeller is directly connected to the shaft. The latest step is hybrid propulsion, which is a combination between mechanical and electric propulsion. It typically has a diesel engine and an electric machine coupled to the same shaft. This is especially beneficial for ships with varying speeds, since for high ship speeds, the diesel engine provides propulsion power, and for low ship speeds the electric machine can be used as a motor (M), to take over the propulsion to avoid inefficient use of the diesel engine in part load [13]. Furthermore, the electric machine can be used as motor to boost the engine, also known as Power Take In (PTI), or as a generator (G) to generate power, also known as Power Take Off (PTO).

How the power for the auxiliary loads (hotel load and onboard systems) is generated, strongly depends on the type of power supply. Just as for the propulsion, there are three types of power supply: mechanical, electric, and hybrid, shown in Figure 1.2, Figure 1.3a, and Figure 1.3b, respectively. Mechanical power supply consists of diesel generator sets, electric power supply only consists of a type of energy storage system (ESS), and hybrid power supply consists of both generator sets and an ESS. The main task of the power supply is to deliver the required power for the auxiliary loads. However, when the vessel uses electric or hybrid propulsion, the power supply can also provide the required power for electric motors. Furthermore, the ESS can be charged, either by the PTO (in case of hybrid propulsion) or the generator sets (in case of hybrid power supply), but it can also be charged with power from the shore [14]. Next to the power supply, the propulsion system can also be used to generate auxiliary power, using the aforementioned PTO.

Which type of propulsion and power supply is used, depends on the type of vessel. Cargo ships often use mechanical propulsion and a mechanical power supply, and in some cases a shaft generator is installed (PTO) to generate power for the auxiliary loads [15]. Although electric propulsion is not interesting for cargo ships, since direct propulsion has proven to be more efficient [16], mechanical or hybrid propulsion with a hybrid power supply could improve the performance due to more efficient use of the equipment in the power plant [17, 18]. Passenger ships use electric propulsion, since it is the

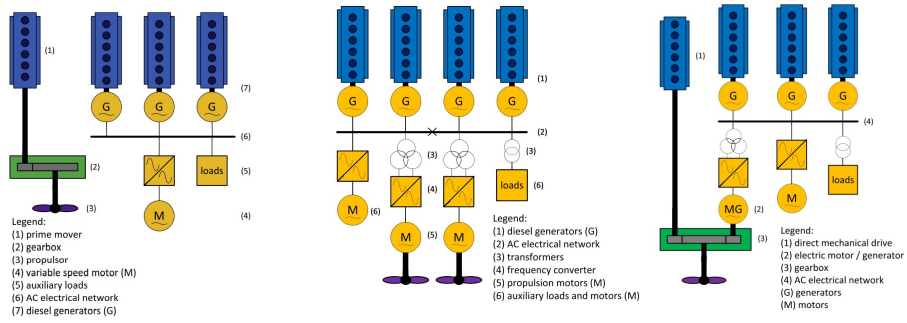

(a) Example of mechanical propulsion and power supply

(b) Example of electric propulsion and mechanical power supply

(c) Example of hybrid propulsion and mechanical power supply

Figure 1.2: Different types of propulsion with mechanical power supply [13]

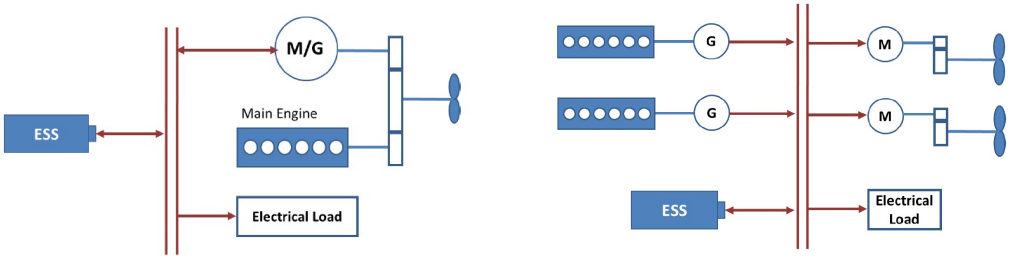

(a) Example of hybrid propulsion with electric power supply

(b) Example of electric propulsion with hybrid power supply

Figure 1.3: Different types of propulsion and power supply [8]

most efficient approach to combine the propulsion load and the high hotel load [19, 20], and mostly a hybrid power supply, using power from the shore to charge the ESS [21]. Service ships do not have a standard layout for their power plants, due to the variety of ships and functions within this category, but mostly electric or hybrid propulsion is used since these ships have varying power profiles. The most seen power supply is either mechanical or hybrid. For more detailed information about the used power plant layout and equipment on different type of ships, the reader is refered to [22].

As mentioned in section 1.1, there is need for a reconfigurable marine power plant. Although extensive literature study has shown that such a power plant is not yet applied in existing marine vessels [22], future vessels may be equipped with such a power plant. Wärtsillä and partners [23], forming ZES (Zero Emission Services), propose the modular use of batteries on inland barges. The concept is based on the use of replaceable battery containers (ZESPacks), which will be charged with energy from renewable sources. If a ZESPack is depleted, it can be replaced by a charged one at access points, which will be placed along the route of the vessel.

1

OPERATIONAL AND ENVIRONMENTAL CONDITIONS

During each mission, the power plant is subject to certain operational conditions, for example the different operational modes describing the required 'actions' for the vessel, and environmental conditions, for example the waves, wind, and currents at sea. As mentioned in section 1.1, these conditions, which act as constraints for the power plant, are changing during and between missions. The changes in operational and environmental conditions affect the required power of the vessel, hence from an operational point of view, it could be beneficial to have a vessel which could operate in a wide, flexible range of environmental and operational conditions, due to modular use of equipment. However, before this can be realized, an understanding of the current marine control system is required.

MARINE CONTROL SYSTEM

The control system of the power plant is part of the marine control system, and the latter can be divided in two main parts [24]: real-time control and monitoring, and operational and business enterprise management, see Figure 1.4. For vessel design, the area of real-time control is most important, and the real-time control systems of marine vessels are more and more developed in a hierarchical, distributed architecture. Most of these systems can be divided into three levels [25–28]:

- Local optimizer
- High-level plant control
- Low-level control

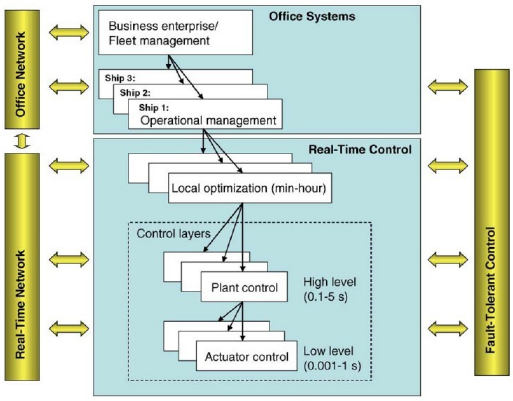

Figure 1.4: Control structure of marine vessels [24]

The local optimizer is also known as the guidance and navigation system. While it is part of the control system, it is not a controller. This system consists of motion and position sensors, a vessel observer, and set-point/path generator [26, 29] to measure the position and motion of the ship, determine the operational mode, generate the desired path

for the ship, and to provide the reference signals for the high-level control. The authors describe the high-level plant control (part of the power plant control) to be directly under the supervision of the guidance and navigation system, but using the work of [29] it can be argued that instead, a general high-level control level fulfills this position. This general high-level includes the path-following controller, which uses the reference signal and the generated path from the guidance and navigation system to determine the reference signals for the high-level plant control and other controllers, for example the rudder control. The high-level plant control determines the distribution of power, energy, and thrust, and generates the set-points for the low-level control. This layer consists of the controllers of the main engine, electric machines, battery system, generator sets, and propellers. The authors of [13] also discuss different levels of control, and focus more on the propulsion of the ship. They state that the propulsion control consists of three levels: a primary level (corresponding to the low-level control), secondary level (corresponding to the high-level plant control), and a tertiary level (corresponding to the input from the general high-level control). Using this information and the general control architectures presented in [30], a schematic of the ship control architecture is made and can be seen in Figure 1.5. For this example, hybrid propulsion with mechanical power supply is used. It can be seen that this division in control can be classified as hierarchical control with the guidance and navigation system on top (the tertiary level), multiple agents in the secondary level (a general secondary level controller and a secondary level power plant controller), and multiple agents in the primary level. Furthermore, the used sensors and actuators are shown for the primary level controllers.

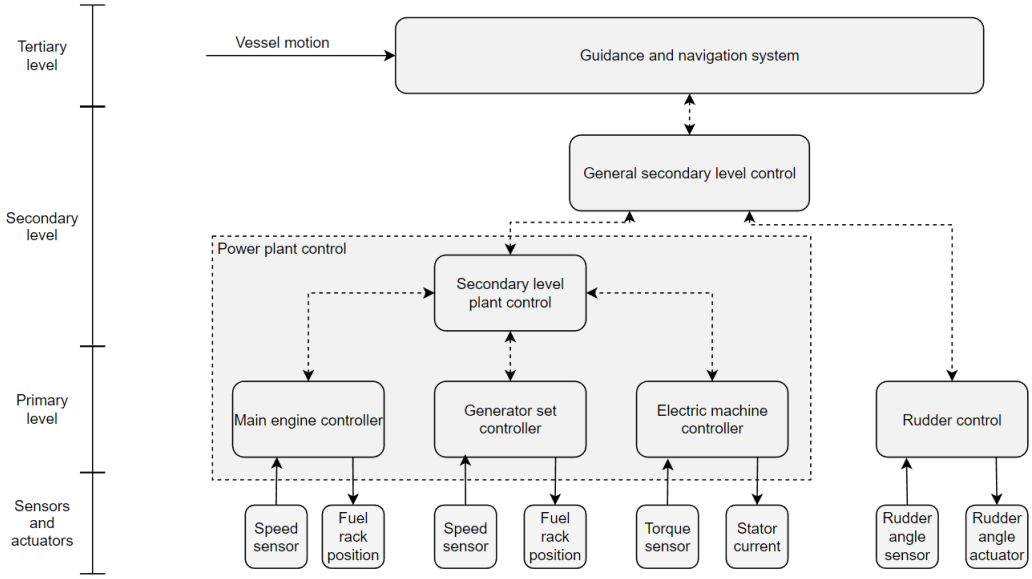

Figure 1.5: General control architecture of a marine vessel

1

1.3. PROBLEM STATEMENT AND RESEARCH QUESTIONS

This thesis aims to design a modular control system for varying missions and retrofittable power plants. In this regard, the following research question is addressed:

"How can mission-oriented modular control of marine vessels be designed?"

In order to answer this question, first the correlation between the mission and the power profile, and the required automation modifications of the power plant and the control system to meet the demand of the different power profiles should be investigated. Next, a control architecture can be designed for the proposed power plant to ensure safety, where after the controller can be verified and the performance can be assessed. In order to achieve this, the following subquestions are considered:

1. What is the state-of-the art in marine power plant control?
2. How to model the correlation between the mission and the power profile of the vessel?
3. How to model the correlation between the power profile for a mission and the needed modifications in automation of the control systems and the power plant?
4. How can a modular control architecture be designed to meet the proposed automation and power plant modifications?
5. How to verify the performance (stability and robustness) of the developed modular control scheme?

1.4. APPROACH

First, information of different vessel missions, power profiles, and power plants needs to be gathered. This information should be analyzed to find a correlation between the power profile and the mission of the ship. It is also important to understand why the power profiles can be different, and why or how certain missions differ from each other. Second, examples of power plants can be analyzed and a correlation between the power profiles and the power plant can be determined. Furthermore, a general understanding of the way the power plant is designed in correlation to the mission can also be important. Due to the fluctuations in missions and power profiles, modifications for the power plant can be determined. Each modification in the power plant implies different operational conditions for the control system. Therefore, if all the possible modifications are identified, the controller can be automated to adapt to each change. This could be realized with supervisory switching control, where at each time step the control system compares the measurements of the system to a set of models, where each model is connected to a controller. The model that best describes the current situation is selected, and therefore the system applies the best controller for that situation. The stability and robustness of the proposed modular control scheme needs to be verified to ensure safe operation of the vessel, so simulations will be used to illustrate this.

These steps lead to a model of the correlation between the mission of the vessel and the power profile, and also to the correlation between the power profile and needed modifications to the power plant and the control system. Furthermore, it leads to a design for a modular control system for a retrofittable power plant. Simulations will demonstrate the stability and robustness of the designed control system.

1.5. SCOPE

Since a lot of data needs to be gathered, and there are a lot of different vessels, it is not realistic to include all of them. Naval ships will be excluded, since there is little available information, especially about the missions and power profiles. Only the most common types of vessels from the main categories of merchant vessels are used for analysis [31], which can be seen in Table 1.1. With respect to the power plant, the stability of the grid will not be investigated. Instead, the focus is to determine the needed automation and modifications to the plant to be able to handle each mission, and design stable controllers for the proposed power plant. Modifications for the power plant consist of adding, removing, or replacing equipment. To verify the stability and robustness of the designed controllers, simulations are used, rather than theoretical verification.

Category	Type of Ship
Service Ships	Tugboats
	Offshore Support Vessels
	Research Vessels
Cargo Ships	Container Ships
	Bulk Carriers
	Tankers
Passenger Ships	Ferries
	Cruise Ships

Table 1.1: Type of ships in different categories

1.6. OUTLINE

In this chapter, power plants of different type of vessels are discussed, and it is argued that there is need for a retrofittable power plant with and a modular control system. Therefore, Chapter 2 describes the state-of-the-art of marine power plant control systems, and proposes an approach that could enable modular use of the equipment in the power plant, based on supervisory switching control. Furthermore, since it is illustrated that the mission affects the power profile, and the latter affects the required equipment in the power plant, Chapter 3 discusses both the correlation between the mission and the power profile, and the correlation between the power profile and the required modifications of the power plant. Even more, it is shown how the control system has to be automated to facilitate these modifications. Then, based on these findings, Chapter 4 presents a modular control architecture to meet the required automation and power plant modifications. The designed control architecture is verified in Chapter 5 using

1

simulations to check stability and robustness. Finally, this thesis is concluded in Chapter 6, and future recommendations, e.g. further steps with the designed controller, are discussed. The outline of this thesis is visualized in Figure 1.6.

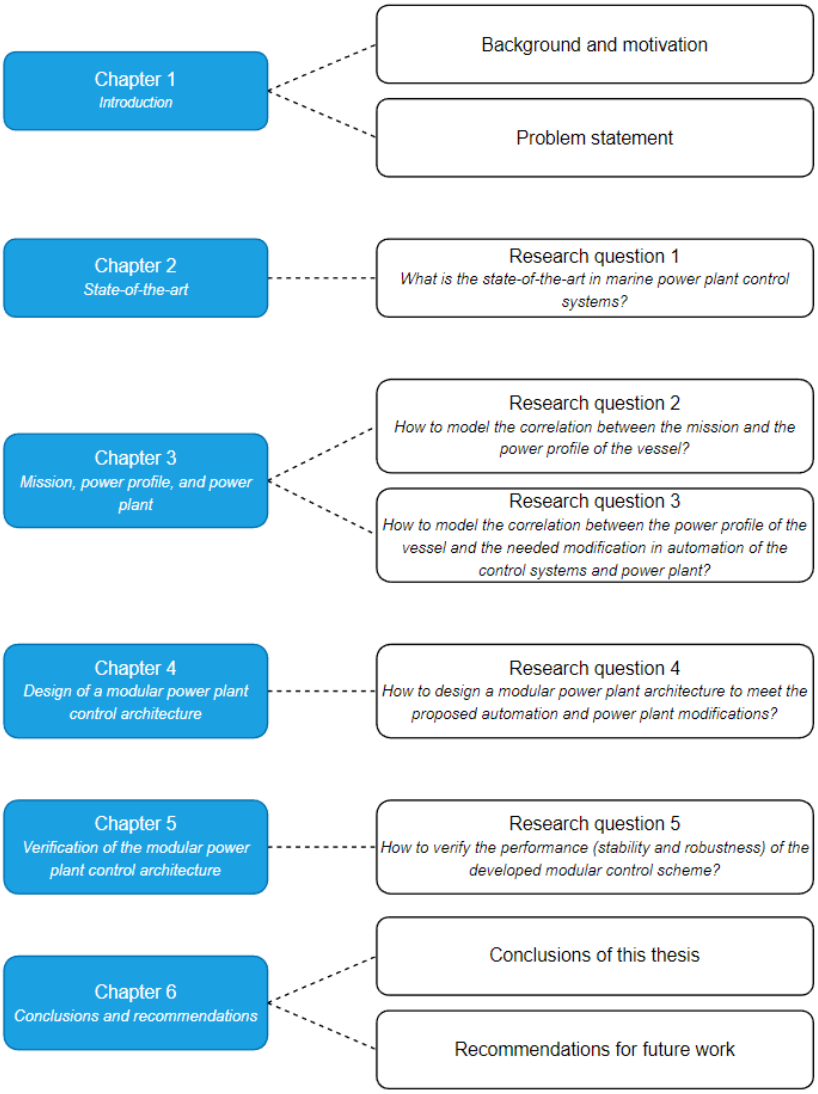

Figure 1.6: Outline of thesis

2

STATE-OF-THE-ART

This chapter addresses the first research question: "What is the state-of-the-art in marine power plant control systems?", by discussing current power plant control strategies, as used in service ships, cargo ships, and passenger ships. Furthermore, it will discuss promising developments the concept of supervisory switching control, which could be useful regarding the design of an modular control system for a retrofittable power plant.

2.1. STATE-OF-THE-ART IN MARINE POWER PLANT CONTROL

The three vessel categories are divided in different types, as shown in Table 1.1. They will be discussed separately, since each type fulfills a different purpose.

2.1.1. SERVICE SHIPS

The ships is this category are characterized by the variety of their operations, and the service ships within this category that will be discussed in this thesis are tugboats, offshore support vessels, and research vessels.

TUGBOATS

A typical tugboat can be seen in Figure 2.1, and these vessels are used mostly to assist cargo vessels to maneuver in the harbour. Their typical mission consists of: standby/waiting for instructions, transit to a vessel that needs assistance, assist the vessel trough the harbour, and then transit back to the quay [7, 8]. This results in a varying power profile, and consequently, a hybrid power supply generates the required power for auxiliary loads and the propulsion system, where the latter is either electric or hybrid [32, 33]. Their control systems therefore mainly focus on the optimal power split for the generator sets and the ESS in the power supply, and between the main engine and electric machine for hybrid propulsion, often by using an Equivalent Consumption Minimization Strategy (ECMS) [4, 6, 12], power management [7, 34], or coordinated control [32]. Another control strategy is proposed by the author of [8], which uses dynamic programming to solve a minimization problem to provide the optimal power split with minimum emissions.

(a) Typical harbour tug: Damen ASD-tug 2810 'Smit Elbe' [6]

(b) Two tugboats maneuvering a cargo vessel [35]

Figure 2.1: Examples of tugboats

OFFSHORE SUPPORT VESSELS

Since oil and gas exploitation moved to deep sea areas by the end of the 20th century, drill rigs and platforms were developed and a new type of ship was needed: the offshore support vessel (OSV) [36], and there are many types of OSV's [37, 38]. They are not only used to serve oil and gas exploration and production, but also to provide necessary supplies, materials, fuels and other reserves for all sorts of project which take place in deep sea. Regardless of their differences, OSV's can be placed in three main categories [39, 40]:

- Platform supply vessel (PSV): used to supply drilling ships, offshore construction vessels and production platforms with the necessary items.
- Anchor handling tug supply vessels (AHTS): used to place platform anchors in the right position, recovering anchors and relocating them if needed.
- Offshore construction vessel (OSCV): used for building and maintainting platforms, well heads, under-water pumping units, pipelines and power cables. Often designed with a large open deck with cranes, moon pools, pipe storage and cable carousels.

In Figure 2.2 these three type of OSVs can be seen, and since they all execute precise operations, dynamic positioning is an important feature of these vessels. Although they have such varying tasks, they all follow a certain mission profile. Either they are docked/ standby at the harbour, standby at sea waiting for instructions, in transit, or they use dynamic positioning. An important note is that AHTS vessels have an additional mode, where high bollard pull is needed to place, recover, or relocate anchors. To facilitate these missions, different type of power plants are used. While hybrid propulsion and a hybrid power supply is emerging , most vessels of this kind use electric propulsion with a mechanical power supply [36, 41, 42], and their power plant control systems focus on the optimal power split between the different generator sets, for which the authors of [9, 43] propose two algorithms, a genetic algorithm and a particle swarm algorithm.

(a) Platform supply vessel from DNV GL [44]

(b) Anchor handling tug supply vessel 'MMA Centurion' [45]

(c) Offshore construction vessel 'Polar Queen' [46]

Figure 2.2: Examples of offshore support vessels

RESEARCH VESSELS

Another important task of service ships, is performing research at sea. Two examples of research vessels are shown in Figure 2.3, and each research vessels is designed for specific missions, for example seismic surveys, polar research, fishing research, naval/defence research, or oil exploitation [47]. For a fishing research vessel, such as shown in Figure 2.3a, a typical mission includes the following operational modes: maneuvering with low to intermediate speed, navigating with high speed, and fishing. For the last mode the vessel operates at low speed, but has a high load due to drag force of the fishing gear [48]. This results in a power profile where the required propulsion power is high for both low and high vessel speeds. Therefore, the authors propose to use hybrid propulsion with a hybrid power supply, to replace the mechanical propulsion with a PTO to generate auxiliary power. For a small coastal research vessel [49], the mission consists of maneuvering with low speed in waters with a small water depth, or navigating at open sea, which results in a power profile with high loads for high vessel speeds, and low loads for low vessel speeds. The vessel is required to have zero-emission modes, so the power plant of this vessel supports hybrid propulsion and a hybrid power supply. The control system is rule-based, which results in pre-programmed scenario's to operate the power plant.

(a) Fishing research vessel 'G. Dellaporta' [48]

(b) Polar research vessel [47]

Figure 2.3: Two examples of research vessels

2.1.2. CARGO SHIPS

The most widely known cargo ships are general cargo ships, container ships, bulk carriers, and tankers. General cargo ships are very important for the shipping industry, and have a very broad range of operations. However, because there is limited available information about their specifics, they will not be discussed.

CONTAINER SHIPS

A large share (≈ 55%) of the world trade is transported with container ships [50], of which an example can be seen in Figure 2.4. A typical characteristic of this type of vessels is the use of a single, long two-stroke, slow-speed, turbocharged, two-stroke diesel engine as main engine, directly coupled to a fixed pitch propeller [51]. In recent years,

Figure 2.4: Maersk Mc-Kinney Møller Triple-E Ship [52]

they adapted (super) slow steaming as main operating mode to avoid high emissions [5, 53]. Therefore, the propulsion in these vessels is mechanical, mostly with a mechanical power supply, but recently hybrid power supply has been proposed for use in container ships to reduce emissions even further [18]. A typical mission for a container ship consists of: loading containers, maneuvering out of the harbour, transit at open sea, maneuver into the destination harbour, and unloading the cargo. Loading and unloading of containers is done with quay cranes, and maneuvering in the harbour is mostly done

by tugboats. As a result, their power plant control systems are focused on maintaining the required shaft speed, by regulating the fuel intake of the engines [54–56].

BULK CARRIERS

Instead of containers, bulk carriers transport bulk cargo such as sand, iron ore, wood pellets, or steel coils. In Figure 2.5 and example of a typical bulk carrier can be seen. Because a typical mission of a bulk carrier is almost the same as that of a container ship,

Figure 2.5: Bulk Carrier 'Berge Snaefell' of Berge Bulk [57]

bulk carriers also use mechanical propulsion and mechanical power supply. However, they have more auxiliary loads than container ships, since they often use deck cranes to load or unload cargo. For this reason, the authors of [17, 58] investigated the use of hybrid propulsion and a hybrid power supply on these ships, and concluded that it could be beneficial. The power plant control system would use an Equivalent Energy Minimiztion Strategy (ECMS), to provide the optimal power split between the generator sets and the ESS, but also to switch the electric machine between PTO and PTI mode. Furthermore, by extracting heat from exhaust gases, also known as Waste Heat Recovery (WHR), the required auxiliary power can be reduced [59].

TANKERS

The missions of this type of vessel have much in common with the missions for container ships and bulk carriers, only tankers transport liquids and gases, such as oil, chemicals, and Liquefied Natural Gas (LNG). The latter is highly pressurized during transport, and the gas is allowed to boil off to prevent too high pressures. An example of an LNG tanker can be seen in 2.6, and it can be noted that the cargo holds are spherical, to accommodate the high pressure. The boil-off gas can be used as fuel for the propulsion of the vessel [19]. As a result, early LNG tankers used steam engines as main power sources, until combustion engines were able to use this gas as a fuel. Today these combustion engines are coupled to generators to deliver the power for the auxiliary loads, and for the electric propulsion motors [61]. Their power plant control systems are not much described. Tankers used to transport oil and chemicals mainly use mechanical propulsion and a mechanical power supply, resulting in a power plant control system that regulates the fuel intake of the engines [62]. Recent studies propose the use of hybrid propulsion

Figure 2.6: LNG Tanker 'Arctic Princess' [60]

[63, 64], but also the use of a hybrid power supply, where power management is used to provide the power split between the generator sets and the ESS [15]. Another interesting control system for the power plant is described by the authors of [65], where a shuttle tanker uses supervisory switching control, which switches between controllers for the power plant, depending on the desired operational mode.

2.1.3. PASSENGER SHIPS

Not only cargo, but also passengers are transported, and this is the main task of ferries and cruise ships. Next to passengers, ferries are often also able to transport cargo, mostly in the form of vehicles which can be loaded on the deck or in the belly of the ship. Cruise ships transport solely passengers, and in contrast to ferries, they travel long distances, even across continents.

FERRIES

Ferries are used to transport a small amount passengers across a small river [66], but also to transport many passengers together with either cars, trucks, or even trains [67], and in literature the latter is refered to as RORO (roll-on roll-of), of which an example is shown in Figure 2.7. Their typical mission is therefore quite similar to the missions of

Figure 2.7: Example of a RORO ferry [68]

cargo ships: loading passengers (and cargo), maneuvering away from the quay, transit at open water (if the ferry is used for larger distances), maneuvering to the destination quay, unloading the passengers (and cargo). To execute these missions, different types of propulsion, power supply, and control systems are used. Older ferries often still use mechanical propulsion [33, 66, 69–73], and also mechanical power supply [66], with control systems that focuses on maintaining the desired shaft speed by regulating the fuel intake of the engines. Newer ferries or improved designs use electric propulsion [21, 33, 66, 74], which is combined with a hybrid power supply [21, 33, 66]. The control of the used power plant is not much described, but the authors of [21] mention speed control for the electric machines and diesel generators, and the authors of [75] use shaft speed control for the electric podded propulsion, to maintain the desired ship speed. Furthermore, the author of [74] proposes multiple Energy Management Strategies (EMS) for optimal control of the hybrid power supply.

CRUISE SHIPS

Cruise ships are one of the most challenging and advanced type of vessels, due to the high hotel and service loads because of their accommodations and facilities [76]. Therefore, large cruise ships present an integrated power system [77], which can be considered as a microgrid, with a large power source and many small users. An example of a cruise ship can be seen in Figure 2.8. Using the work of the authors of [77, 79–81], their typi-

Figure 2.8: Cruise ship 'Coral Princess' [78]

cal mission is deduced. A cruise ship is either at port, maneuvering (in and out of the port), or navigating (sailing at open waters). The latter corresponds to the transit mode of cargo ships, only with higher ship speeds. To execute the missions and facilitate the hotel loads, a power plant with electric propulsion with mechanical power supply is often used [77, 81–84]. A hybrid power supply is introduced by [80, 85] to further improve fuel efficiency. There is also mention of cruise ships with mechanical propulsion instead of electric [79], and even where gas turbines are used to propel the ship and a steam turbine produces power for the electric loads [82]. Unfortunately, there is limited information about the control systems of cruise ship power plants. Shaft speed control is

mentioned by the authors of [83], and also the authors of [84] discuss this, coupling it to a strategy to control the delivered power of the propeller. The authors of [85] discuss load following and cycle charging control of the hybrid power supply, which implies a certain order of draining and charging the of hybrid systems.

2.1.4. TAXONOMY OF POWER PLANT CONTROL STRATEGIES

As shown, there are many different vessels, power plant, and control systems. In order to give a useful overview of the gathered information of the discussed vessels, a taxonomy containing the type of vessel, propulsion, power supply, type of controller, and the control strategy can be made, and can be found below.

Category	Paper	Year	Type of Ship	Power Plant					
				Level	Propulsion	Power Supply	Control Strategy	Input	Output
Service Ships	[4]	2016	Tugboat	High	Electric	Hybrid	ECMS	Total power	Power split
	[32]	2020	Tugboat	High	Electric	Hybrid	Coordinated control	Total power	Power split
	[6]	2011	Tugboat	High	Hybrid	Hybrid	ECMS	Total power	Power split
	[7]	2015	Tugboat	High	Electric	Hybrid	Power management	Total power	Power split
	[8]	2019	Tugboat	High	Electric	Hybrid	Dynamic programming	Total power	Power split
	[12]	2018	Tugboat	High	Electric	Hybrid	Rule based ECMS A-ECMS Dynamic programming	Total power	Power split
	[34]	2016	Tugboat	High	Electric	Hybrid	Power management	Total power	Power split
	[9]	2015	OSV	High	Electric	Mechanical	Power control	Total power	Power split
	[43]	2015	OSV	High	Electric	Mechanical	Power control	Total power	Power split
	[49]	2018	Research Vessel	High	Hybrid Electric	Hybrid	Rule based	Operational mode	Power split

Cargo Ships	[54]	2009	Container Ship	Low	Mechanical	-	Shaft speed control Torque prediction	Shaft speed Shaft torque	Fuel intake
	[5]	2016	Container Ship	Low	Mechanical	Mechanical	Shaft speed control	Shaft speed	Fuel intake
	[55]	2019	Container Ship	Low	Mechanical	-	Shaft speed control	Shaft speed	Fuel intake
	[56]	2000	Container Ship	Low	Mechanical	-	Shaft speed control Torque prediction	Shaft speed Shaft torque	Fuel intake
	[17]	2016	Bulk Carrier	High	Mechanical Hybrid	Hybrid	ECMS	Total power	Power split
	[63]	2020	Tanker	High	Mechanical Hybrid	Mechanical	Rule based	Control mode	Power split
	[64]	2019	Tanker	High	Mechanical Hybrid	Mechanical Hybrid	Rule based	Control mode	Power split
	[62]	2019	Tanker	High	Mechanical	Mechanical	Rule based	Control mode	Power split
	[15]	2016	Tanker	High	Mechanical	Hybrid	Power management	Total power	Power split
	[65]	2011	Tanker	High	Electric	-	Supervisory switching control	Operational mode	Best fitting controller
Passenger Ships	[69]	1999	Ferry	Low	Mechanical	-	Combinator curve control	Shaft speed	Fuel intake
	[71]	1997	Ferry	Low	Mechanical	-	Shaft speed control	Shaft speed	Fuel intake
	[70]	2004	Ferry	Low	Mechanical	-	Combinator curve control	Shaft speed	Fuel intake
	[72]	1999	Ferry	Low	Mechanical	-	Combinator curve control	Shaft speed	Fuel intake
	[73]	2002	Ferry	Low	Mechanical	-	Combinator curve control	Shaft speed	Fuel intake
	[74]	2017	Ferry	High	Electric	Hybrid	EMS	Total power	Power split
	[75]	2020	Ferry	Low	Podded Electric	-	Shaft speed control	Shaft speed	Propeller torque
	[83]	2016	Cruise Ship	Low	Electric	Mechanical	Shaft speed control	Shaft speed	Motor voltage frequency
	[84]	2017	Cruise Ship	Low	Electric	Mechanical	Shaft speed control Power control	Shaft speed Motor power	Motor torque
	[85]	2019	Cruise Ship	High	Electric	Hybrid	Load following and cycle charging	Total power	Power split

Table 2.1: Taxonomy of power plant control strategies

$*$: It has to be noted that, for vessels with a hybrid power supply containing more than one batteries, the batteries are modeled as one, meaning that from the perspective of the control system, there is only a single battery in the power plant (while there are in fact more than one installed)

2.2. SUPERVISORY SWITCHING CONTROL

The previous section discussed power plants which are fixed in layout and equipment, and based on that, the control system is designed. In order to operate a retrofittable power plant, its control system needs to facilitate modifications, such as adding, removing or replacing equipment. In other words, the controller must be able to operate under varying operational conditions. Such a control architecture is proposed by authors [86] for a shuttle tanker, where multiple controllers are integrated in one system, and a supervisor applies the best controller for each situation. This is called supervisory switching control (SSC), but is also known as hybrid control, since it combines both discrete (switching between controllers) and continuous (power plant) systems [87].

The basis for this type of control was first introduced by Hespanha [88]. In his time as PhD student he developed a strategy to switch between multiple controllers for the marine power plant, creating a stable closed-loop system. At each time step, a supervisor compares the output of the actual system with a set of models, and determines which model best describes the current situation. Each model is connected to a controller, so when a model is selected, the system switches to the appropriate controller. Furthermore, the system can also include observers for each controller, if the required states can not be directly measured. A year later, Hespanha improved the design, by including a method to cope with modeling uncertainty [89]. For more detailed work on supervisory switching control, the reader is refered to [90–92]. The different models included in the supervisory switching controller depend on different control objectives, constraints and dynamic response of the controlled system [93]. This can be visually described within a three-dimensional space, as shown in Figure 2.9, with the following three parameters:

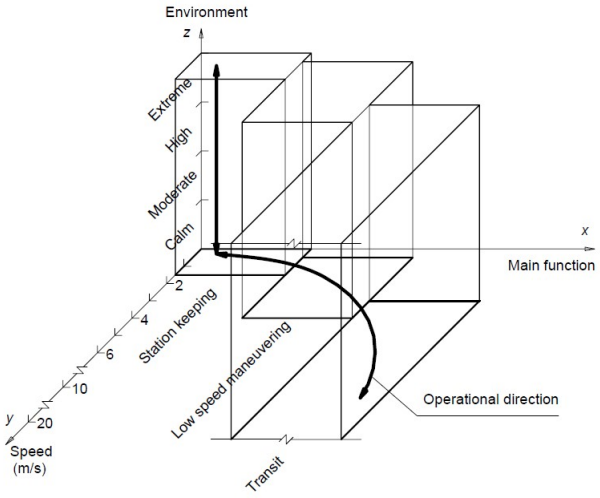

Figure 2.9: Three-dimensional space for control objectives [93]

- Main function / Operational modes (x-axis)
- Speed (y-axis)
- Environment (z-axis)

Changes in these three parameters results in changes of the objectives, constraints, and dynamic response of the system, so for different regions in the three-dimensional space, different controllers can be designed.

Using the work above, the authors of [94] design a supervisory switching controller for dynamic positioning, as shown in Figure 2.10a. The system contains a set of models to describe the environment, in this case the sea state, from calm to extreme. It compares the expected output of each model with the actual output of the system, and selects the model which gives the smallest error. The system then automatically switches to the corresponding controller. The same authors also design a supervisory switching controller where the bank of controllers is based on the operational modes [86]. Next to a controller for each operational mode, a controller for the transition between two sequential operational modes is included, which improves smooth switching between operational modes. More work on this specific application of supervisory switching control can also be found in [65, 95, 96], and a schematic can be seen in Figure 2.10b.

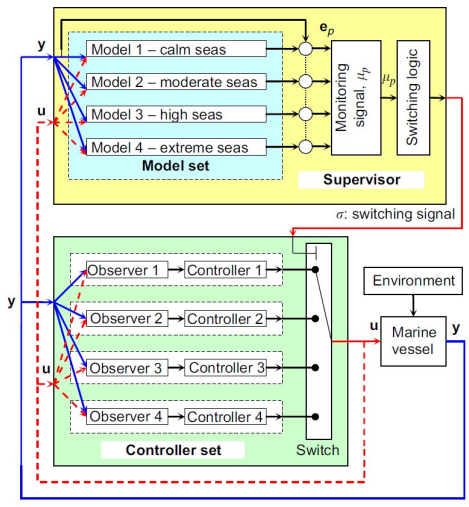

(a) Example of supervisory switching control with switching based on environmental conditions [94]

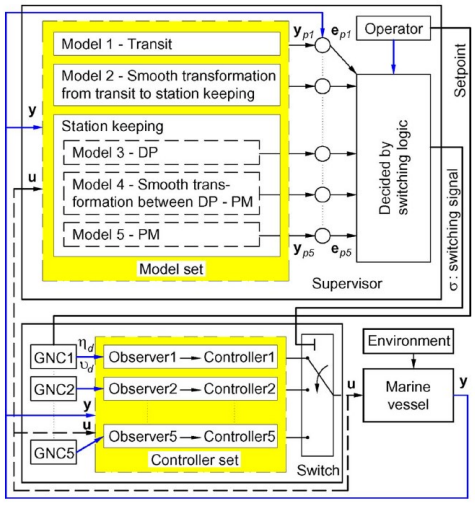

(b) Example of supervisory switching control with with switching based on operational conditions[86]

Figure 2.10: Supervisory switching control: switching based on environmental and operational conditions

Next to the control focused on a vessel operating alone, also for the coordination of vessels sailing in formation, supervisory switching control can be used [97]. The authors describe operational modes for the vessels such as coordinated path following,

coordinated formation, and coordinated dynamic positioning. They use a supervisory switching control architecture with a controller for each mode, and also a controller for the transition between modes, to ensure smooth switching. At last, another application of supervisory switching control is described by the authors of [98], where a supervisory switching control architecture is used to switch between different thrust allocation methods. Concluding, SSC serves a variety of purposes, and therefore, in Chapter 4 it will be discussed if this could be used for the design of a modular power plant control architecture.

2.3. CONCLUDING REMARKS

In this chapter the first subquestion: "What is the state-of-the art in marine power plant control?", is answered, by means of a literature review.

It is seen that there are many control strategies used for marine vessels, each with their own characteristics, and therefore a large taxonomy is shown. It is found that today, many marine vessels use a multi-level control system, where a control strategy such as ECMS, power control, power management, or a rule-based control strategy determines the power split for the power plant component. Furthermore, it is found that there is, to the best knowledge of the authors, no literature where multiple batteries are treated as individual batteries, as they are approximated to be a single, larger battery, from the perspective of the control system. Also, no vessels are found which have a control system that allows for modular use of components, without the need for tuning afterwards, hence supervisory switching control is proposed as a possible solution. In the next chapter, the correlation between the mission and the power profile will be discussed, together with the correlation between the power profile and the needed automation modifications of the control system and power plant, such that in Chapter 4 a design for a modular control architecture can be proposed, in order to allow modular use of the power plant components.

3

Mission, Power Profile, and Power Plant

In this chapter, two research questions will be adressed. Section 3.1 will discuss the research the question: "How to model the correlation between the mission and the power profile?", and section 3.2 discusses the question: "How to model the correlation between the power profile for a mission and the needed modifications in automation of the control systems and the power plant?", where after this can be used, together with the state-of-the-art in marine power plant control, to design a modular power plant control architecture. It will be shown that the correlation between the mission and the power profile depends on many factors, and that different power profiles can lead to a change in the desired layout (hence the desired equipment) of the power plant, resulting in the required automation modifications for the control system.

3.1. Correlation between the Mission and the Power Profile

"A tugboat is waiting (standby) at quay at the port of Rotterdam, when it gets the assignment to assist an incoming container ship. It then sails to the specified location (transit), waits (standby) for the ship to arrive and assist it into the harbour, as quickly and safe as possible, to the right unloading location (e.g. a container terminal), where after the tugboat returns (transit) to a position along the quay. This container ship, which has containers from New York, is first unloaded and loaded again with quay cranes. When this is finished, tugboats assist it out of the harbour, back to open sea, where the vessel sets sail (transit) to Shanghai, where it will arrive within two months."

The above can be an example of two different mission statements, each for a specific type of marine vessel. They describe the type of vessel, the activities of the vessel, such as

standby, transit, assist, loading/unloading (also refered to as operational modes), areas and locations where it will sail, and how much time there is available. However, in literature, there is no consensus about a general definition of a mission, only descriptions, just as the example shown above. To this end, this thesis proposes a general definition for a mission, so it can be used to investigate the correlation between a mission and the power profile of a vessel. Using the example from above, this definition has to include the type of operation that has to be executed, thus specifying the type of cargo that has to be transported, the locations/areas for this operation, and if there is a certain time limit in which the mission has to be finished. Before giving a general definition, the example of the tugboat and container ship is re-written into:

- Transport a container vessel from open sea to a container terminal of the port of Rotterdam, as fast and safe as possible.
- Transport containers from New York, via Rotterdam, to Shanghai, within two months.

Next to these descriptions, it is assumed that the starting time and date of the mission are clearly specified, hence this results in the following general definition of mission:

"Transport X from A to B (optionally via C, D, etc.), leaving at t_0 (time and date), arriving at destination at t_{end} (time and date)."

From this definition, but also from the given examples, it can directly be seen that the type of cargo (X) determines the type of vessel. The above definition also gives information about the harbours that are to be visited, resulting in the required operational modes and the route of the vessel (where the vessel has to operate), which gives information about the operational environment. Furthermore, it specifies the total mission time t_m (where $t_m = t_{end} - t_0$), which affects the speed of the vessel, and therefore dictates the environmental conditions and operational modes at each point in time during the mission. How this information eventually helps to find the power profile, can be seen in Figure 3.1, where a simplified model of the correlation between the mission and the power profile can be seen. The most important is the hull resistance, which combines multiple aspects such as the type of vessel, the operational modes and the speed to the propulsion power. The operational environment, the type of vessel, and the operational modes are the main contributors to the auxiliary power. If the latter and the propulsion power are known, the power profile can be found, either by stating them as separate power demands, or as their sum. For that matter, first the contribution of the propulsion and auxiliaries to the power profile will be discussed before they are further investigated, where the rest of this section will elaborate on each aspect of Figure 3.1, and shows how they affect the power profile.

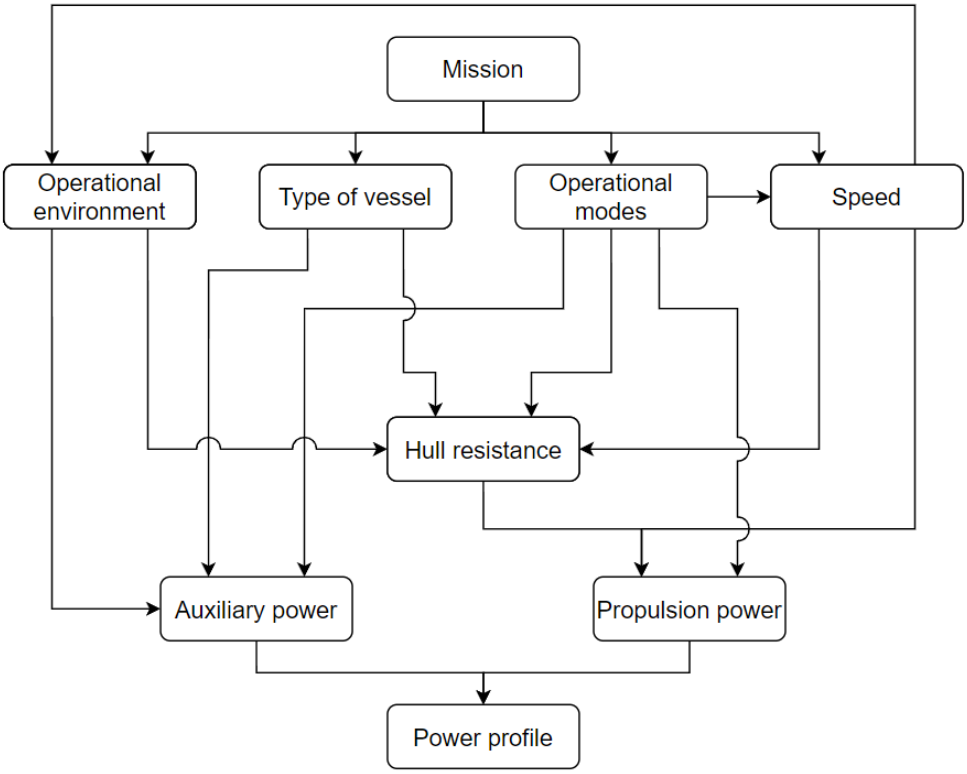

Figure 3.1: Simplified model of the correlation between the mission and power profile

3.1.1. POWER PROFILE

A thorough analysis has been done on power profiles for different type of vessels, which can be found in Appendix B. To ensure usefulness and validity, only vessels for which multiple papers with useful information are found, are further used in this thesis. The power profile consists of the required propulsion and the auxiliary power for the mission, as can be seen in Figure 1.1. It is observed that there are mainly 5 types of power profiles, based on the behavior and the importance of the propulsion and auxiliary power throughout the mission, and this is shown in Table 3.1.

An important note is that with respect to the propulsion power, the auxiliary power is approximately constant during the whole mission for all type of vessels, just as the authors of [85, 99] indicate. However, there still are some fluctuations of the auxiliary power, which for example depend on the operational environment. Furthermore, it is observed that the propulsion power is an important aspect for all type of vessels, which is as expected, since the whole purpose of a vessel can not be fulfilled without adequate propulsion power. Therefore, first the propulsion will be discussed, followed by the auxiliary power.

Type of vessel		Power profile			
		Propulsion power		Auxiliary power	
		Behaviour	Importance	Behaviour	Importance
Cargo ships	Container ship	Constant	High	Constant	Negligible
	Bulk carrier, Tanker	Constant	High	Constant	Low
Service ships	Tugboat	Varying	High	Constant	Low
	OSV	Varying	High	Constant	Moderate
Passenger ships	Cruise ship	Varying	High	Varying	High

Table 3.1: Different type of power profiles

3.1.2. PROPULSION POWER

Moving a vessel through the water requires power. The minimum amount of required power is refered to as the effective power (P_E), and consists of the product of the vessels speed (V) and hull resistance (R) [100]:

$$P_E = R * V \tag{3.1}$$

where the hull resistance is the force exerted on the hull by the water during the vessels motion. This resistance force is extensively discussed by the authors of [100–104]. They all describe the total resistance, consisting of different components. Combining their work, the main components of the hull resistance at calm sea are:

- Frictional resistance (R_F): the force that is a resultant of the tangential forces on the hull as a result of the boundary layer along the hull
- Wave resistance (R_W): the drag that is the result of waves generated by the ship. The kinetic and potential energy in the waves has to be generated by the propulsion system
- Eddy resistance (R_E): due to the flow separation, particularly at the aft of the vessel, eddy currents are generated which also cause a loss of energy of the vessel
- Air resistance (R_A): the air resistance is caused by the flow of air over the ship (with no wind present). It is affected by the shape of the vessel above the waterline, the area of that shape, and the vessel speed. Since a part of the hull contributes to this component is often seen as a contribution to the total hull resistance

The total hull resistance is the sum of these components:

$$R_T = R_F + R_W + R_E + R_A \tag{3.2}$$

The different components, and also their contribution relative to the total resistance are shown in Figure 3.2. This relative contribution is not constant, but depends on the vessel speed. For higher ship speeds, the wave resistance increases more than the other resistance components, so the contribution of each component to the total resistance

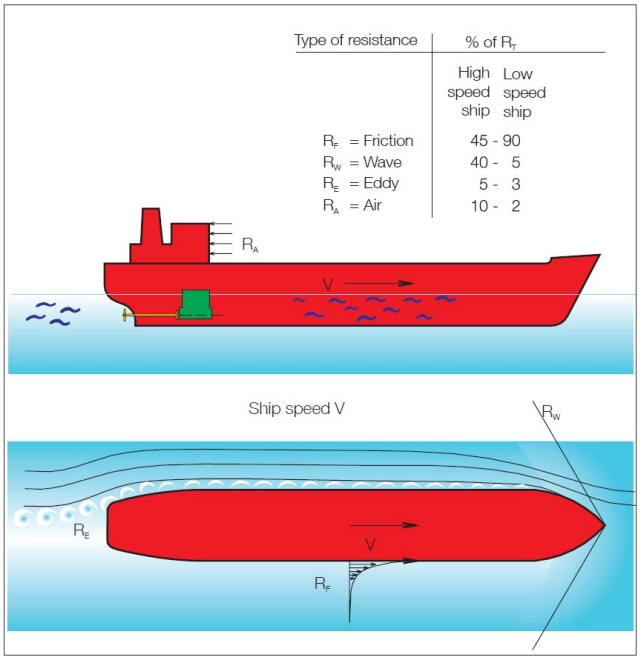

Figure 3.2: Total ship resistance and components (calm sea) [103]

changes. Typical high speed vessels are passenger ships, while typical low speed vessels are for example cargo ships.

The aforementioned contributions are determined for calm sea conditions. In reality, the sea can be very rough, and this affects the total hull resistance. This is often described as the *sea margin*, which takes into account the waves, often refered to as the sea state (s_s), the wind (w_s), but also the currents of the sea (c_s). This sea margin is a factor which can be multiplied with the total hull resistance for calm sea (this statement is verified in Appendix A). Depending on the route of the vessel, the average increase of resistance is 20-35%, but it can range up to 50-100%. Deviations from this average are not unusual, and it is even found that for a typical 14000 DWT bulk carrier, the sea margin (m_s) reaches values up to 220%, with an average of 100% [103].

$$m_s = f(s_s, w_s, c_s) \tag{3.3}$$

Next to the added resistance due to the conditions of the sea, the condition of the hull also changes throughout the vessels lifetime. The paint film of the hull will break down, erosion starts, marine plants will grow on the surface of the hull, and the hull can even get damaged due to bad weather. This is called *fouling* (f_h), which can cause the resistance of the vessel to increase 15-35% throughout its lifetime [101, 103].

Instead of an increase in resistance at open sea, inland vessels also experience more resistance due to waterway conditions. The depth of the waterway, but also the width of

the waterway can result in extra frictional resistance (ΔR_F). The depth of the waterway (h) with respect to the draught of the vessel (d) determines the impact on the resistance. The water depth is classified with respect to this ratio (h/d), which is shown in Table 3.2. For deep water there is no effect of the added resistance, but it is already noticeable in medium deep water, significant in shallow water and dominant in very shallow water, where the resistance can increase up to 200% (depending on speed of the vessel) [99]. Furthermore, waterways with restricted width (w_w), such as canals, increase the resistance of the vessel due to the proximity of the canal walls [104].

Classification	Range	Effect
Deep water	$h/d > 3.0$	No effect
Medium deep water	$1.5 < h/d < 3.0$	Noticeable
Shallow water	$1.2 < h/d < 1.5$	Significant
Very shallow water	$h/d < 1.2$	Dominant

Table 3.2: Classification of water depth [105]

In general, since most of the components of the hull resistance increase proportional to the square of the speed, the total hull resistance also shows this correlation. Only for high vessel speeds the wave friction R_W increases much faster, which is the reason for the difference between low speed and high speed contributions to the total hull resistance in Figure 3.2. Furthermore, it implies a speed barrier, meaning that for a certain speed an increase in power will not result in an increase in speed, as it is all converted to wave energy [103]. Still it is common to approximate the total hull resistance using a scaling factor (c_1) and the vessel speed (V):

$$R_T = c_1 * V^2 \tag{3.4}$$

In Figure 3.3 two customized speed-resistance curves can be seen which are based on speed-resistance curves found in [99–101]. For low speeds, the power increases proportional to the speed squared, but for higher speeds, it increases faster. This means V has a higher power (e.g. V^3 or V^4) for high speeds. The exact value of this higher power depends on the specific vessel and on the speed.

The factor c_1 is often not constant, but contains a nominal resistance factor c_0, which is speed dependent, and a multiplying factor γ_0:

$$c_1 = \gamma_0 * c_0(V) \tag{3.5}$$

The aforementioned sea state (s_s), wind (w_s), currents (c_s), water depth (h), water width (w_w) , fouling (f_h), but also variations in displacement (∇) of the vessel are captured by the multiplying factor γ [100]:

$$\begin{aligned}\gamma_0 &= f(s_s, w_s, c_s, h, w_w, f_h, \nabla) \\ &= \gamma_1(s_s) * \gamma_2(w_s) * \gamma_3(c_s) * \gamma_4(h) * \gamma_5(w_w) * \gamma_6(f_h) * \gamma_7(\nabla)\end{aligned} \tag{3.6}$$

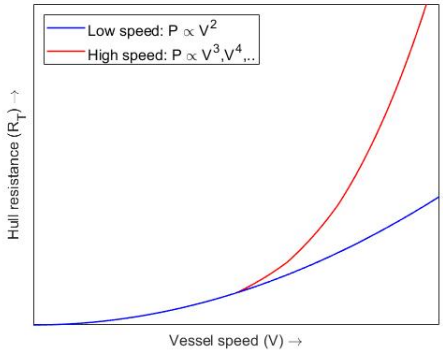

Figure 3.3: Relation between vessel speed and total hull resistance [104]

where in general the following bound for γ_0 is found [100]:

$$1 \leq \gamma_0 \leq 3 \tag{3.7}$$

This bound can be exceeded, but this only occurs for very rough sea conditions. The speed dependent factor c_0 is often smaller for low vessel speed, so that means that for low speeds, the required power decreases faster than the speed squared. However, since it is often assumed that for low vessel speeds, the quadratic relation between the required power and the vessel speed holds [100], this results in the assumption that the nominal resistance factor c_0 is constant for low vessel speeds.

Using the found relations for the resistance of the vessel, an expression for the effective power can be given, and it can be seen that there is a cubic relation between the vessel speed and the effective power, which means that for a doubling of the speed, the required power is multiplied by a factor eight. It is therefore quite costly to operate at high speeds.

$$P_E = c_1 * V^3 \tag{3.8}$$

In practice, the specific relation between the effective power and the speed also depends on the type of vessel. This results in a relation where the power is not exactly proportional to the cube of the speed: often more power is required. Therefore, a more general form of Equation 3.8 is used:

$$P_E = c_1 * V^a \tag{3.9}$$

where next to c_1, also a depends on the type of vessel. The authors of [103] describe parameter a for multiple cargo ships, and this is shown in Table 3.3. The exact value of c_1 depends on the used notation for the effective power (kW or W) and speed of the vessel (kn or ms^{-1}), but for each vessel it is a bounded parameter. The authors of [64] discuss the relation between the speed of a vessel and the effective power for a tanker,

Type of vessel	a
Large container ships	4.0
Medium container ships, RoRo ships	3.5
Tankers and bulk carriers	3.2

Table 3.3: Rate of proportionality of effective power and vessel speed for different type of vessels [103]

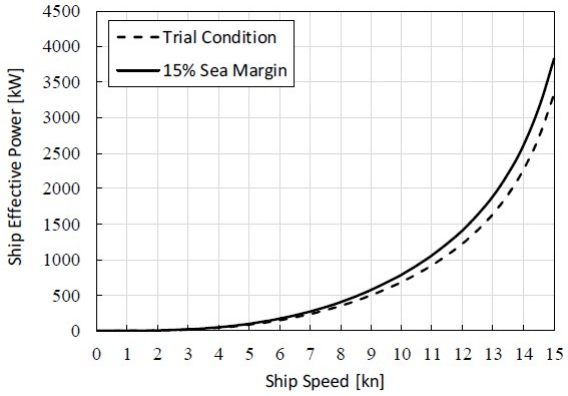

Figure 3.4: Effective power versus ship speed [64]

which is shown in Figure 3.4. Using ®MATLAB, this relation is approximated for low vessel speeds and shown in Equation 3.10:

$$\begin{aligned} P &= 0.55 * V^{3.10} && (0 < V < 12) && \text{(Trial Condition)} \\ P &= 0.64 * V^{3.09} && (0 < V < 12) && \text{(15\% Sea Margin)} \end{aligned} \tag{3.10}$$

As can be seen in Equation 3.10, in a is approximately 3.1, which is a deviation of 3% from the given value in Table 3.3, and it is found that the effective power required for the 15% sea margin can indeed be found by just increasing the factor c_1 for the trial condition with the stated sea margin ($0.55 * 1.15 \approx 0.64$). A detailed analysis of this can be found in Appendix A. Still, this effective power is only a theoretical minimum of the power required to propel the vessel. In fact, the propulsion power (the power delivered to all the propellers) is greater than the effective power P_E, since there are losses due to conversion from propeller power to actual thrust, which can easily reach up to more than 30%. Therefore, the following relation between the effective power and the propulsion power is used:

$$\begin{aligned} P_D &= \frac{P_E}{\eta_D} \\ \eta_D &= \eta_H * \eta_O * \eta_R \end{aligned} \tag{3.11}$$

where P_D is the propulsion power (the power delivered to the propellers) and η_D is the propulsive efficiency, η_H is the hull efficiency, η_R the relative rotative efficiency, and η_O

the propeller open-water efficiency. Furthermore, the propulsion power is not equal to the power that has to be delivered by the power plant, due to losses in the transmission:

$$P_{plant} = \frac{P_D}{\eta_T}$$
$$\eta_T = \eta_S * \eta_{gb} \tag{3.12}$$

where P_{plant} is the power delivered by the power plant, and η_T is the transmission efficiency, consisting of the the shaft efficiency η_S and the gearbox efficiency η_{gb}

For the propulsive and transmission efficiency the following average values are found [99, 106, 107]:

$$0.4 \leq \eta_D \leq 0.6 \qquad \text{for tugboats} \tag{3.13}$$
$$0.6 \leq \eta_D \leq 0.7 \qquad \text{for cargo vessels} \tag{3.14}$$
$$0.95 \leq \eta_T \leq 0.98 \qquad \text{in general} \tag{3.15}$$

Finally, an expressions for the propulsion power based on all the parameters discussed in this section is given in Equation 3.16:

$$P_D = \frac{f(s_s, w_s, c_s, h, w_w, f_h, \nabla) * c_0 * V^a}{\eta_D} \tag{3.16}$$

Still, there might be need for more propulsion power due to the vessel performing a specific task during its mission. For a tugboat assisting a vessel, there is a lot of towing force required, while this is not included in Equation 3.16. Not only is this important for tugboats, but also for OSVs (re)locating an anchor, or towing a drilling platform/rig the towing force plays an important role. In all examples, the required towing force F_{tow} has to be delivered by the propeller, hence this contributes to the propulsion power. For $V = 0$, the towing force is equal to the thrust T_p delivered by the propeller [108], but if $V > 0$, a part of the thrust is required to overcome the resistance R_T:

$$T_p = F_{tow} \qquad V = 0$$
$$T_p = F_{tow} + R_T \qquad V > 0 \tag{3.17}$$

The thrust T_p is produced by the propeller, which requires power. In Equation 3.16, R_T is already covered for, so the additional power to generate F_{tow} can be found by:

$$\Delta P = F_{tow} * V \qquad V > 0 \tag{3.18}$$

However, in literature it can be seen that the maximum required towing force, the bollard pull F_{bp}, is produced when $V = 0$, and in the analysis in Appendix B it can be found that for instance tugboats regularly operate near this operation point. Therefore, a different approach is considered. Instead of relating the extra power for the towing force to the

vessel speed, the shaft speed can be used. The authors of [26] discuss the relation between the propeller thrust T_p, the propeller torque Q_p, the propeller power P_p and the propeller speed n_p as:

$$T_p = K_T \rho D^4 |n_p| n_p \tag{3.19}$$

$$Q_p = K_Q \rho D^5 |n_p| n_p \tag{3.20}$$

$$P_p = 2\pi n_p Q_p = 2\pi K_Q \rho D^5 |n_p| n_p^2 \tag{3.21}$$

where ρ is the density of the seawater (ρ = 1025 kg/m^3), D is the diameter of the propeller, and K_T and K_Q are the thrust and torque coefficients, typically around 0.4 and 0.06, accounting for the thrust and torque losses, respectively [26, 109]. Using these relations, the relation between the propeller thrust T_p and propulsion power P_D can be given as:

$$P_D = P_p = |T_p|^{\frac{3}{2}} \frac{2\pi K_Q}{\sqrt{\rho} D K_T^{\frac{3}{2}}} \tag{3.22}$$

As mentioned, not all propeller thrust is required to deliver the towing force. Therefore, F_{tow} is substituted for T_p in Equation 3.22 to find the required power for the towing force. Furthermore, since this directly gives the power delivered by the propeller(s), it can also be refered to as the additional propulsion power ΔP_D, such that:

$$\Delta P_D = |F_{tow}|^{\frac{3}{2}} \frac{2\pi K_Q}{\sqrt{\rho} D K_T^{\frac{3}{2}}} \tag{3.23}$$

where K_Q, K_T, and D depend on the type of vessel X_v, and the towing force depends both on the type of vessel X_v, but also on the operational mode O_m. Using this result, the required power is given by Equation 3.24.

$$P_D(X_v, O_e, O_m, V) = \frac{f(s_s, w_s, c_s, h, w_w, f_h, \nabla) * c_0 * V^a}{\eta_D} + |F_{tow}|^{\frac{3}{2}} \frac{2\pi K_Q}{\sqrt{\rho} D K_T^{\frac{3}{2}}} \tag{3.24}$$

where $a, f_h, \eta_D, D, K_Q, K_T$ depend on the type of vessel X_v, ∇ and F_{tow} depend on both the type of vessel X_v, but also on the operational mode O_m, since for the same vessel, the displacement (∇) increases when the vessel is *loaded*, and the towing force has different values for different vessels and is only used for certain operational modes. The environmental factors (s_s, w_s, c_s, h, w_w) depend on the operational environment O_e, and c_0 depends both on the type of vessel X_v and the vessel speed V.

3.1.3. AUXILIARY POWER

The auxiliary power (P_{aux}) includes all the power required to operate the vessel, next to the power required for propulsion. As already mentioned in the previous section, for most vessels this load is often constant throughout a mission. Furthermore, it is often a lot less than the required propulsion power. In Table 3.4 the typical proportion of auxiliary and propulsion power of the total power can be seen for several type of vessels. How this data is derived can be seen in Appendix B.

Type of vessel		Auxiliary Power	Propulsion Power
Service ships	Tugboat	2% - 20%	80% - 98%
	OSV	6% - 20%	13% - 85%
Cargo ships	Container Ship	1% - 7%	93% - 99%
	Bulk Carrier	2% - 10%	90% - 98%
	Tanker	6% - 18%	82% - 94%
Passenger ships	Cruise Ship	34% - 42%	58% - 66%

Table 3.4: Proportion of propulsion power and auxiliary power from minimum installed power of different type of vessels

As can be seen from Table 3.4, for service and cargo ships the proportion of the auxiliary power is very small, and in some cases even negligible, while for cruise ships, the auxiliary power is an important factor. The reason for this difference is due to the many passenger and facilities on board, which leads to a significant amount of electricity use, heating and/or cooling.

To get a better understanding of the auxiliary loads (especially for cruise ships), it is often split in two type of loads: electric and thermal. The electric load is also refered to as the hotel load (P_{hotel}), and consists of electric power required for the on-board systems, guidance, computers and communication devices, electric power required for air conditioning, but also lighting, etc. [110, 111]. The thermal load mainly consists of power required for boilers, which produce heat for passenger and crew accommodation, engine room, tank heating, and fresh water production, and is also refered to as service load ($P_{service}$) [76, 77, 79]. An example of these loads are shown in Figure 3.5, where these loads are described during a mission in a cold and warm environment. It can be seen that the hotel and service loads are subject to variation, caused by both ambient temperature T_a (average load) and time t (minimum and maximum load). An important note is that this influence of time has a cycle of approximately a day, which only makes sense, since passengers facilities are reduced in the night, leading to lower power requirements. Based on Figure 3.5, the thermal load increases when comparing a cold environment with a warm environment (34% increase in the range between the minimum and maximum, and 23% increase in the average load), while on the other hand, the electric load decreases (7% decrease in both range and average load). The operational environment determines the ambient temperature T_a during the mission, resulting in the following relations:

$$P_{hotel}(X_v, T_a, t) = P_{hotel,c}(X_v) + \Delta P_{hotel}(X_v, T_a, t)$$
$$P_{service}(X_v, T_a, t) = P_{service,c}(X_v) + \Delta P_{service}(X_v, T_a, t) \quad (3.25)$$

where $P_{hotel,c}$ and $P_{service,c}$ are the constant hotel and service loads, based on the type of vessel X_v, and ΔP_{hotel} and $\Delta P_{service}$ are the change in both power demands, also depending on the X_v and T_a, but the high fluctuation from minimum to maximum (as seen in Figure 3.5) depends on the time t.

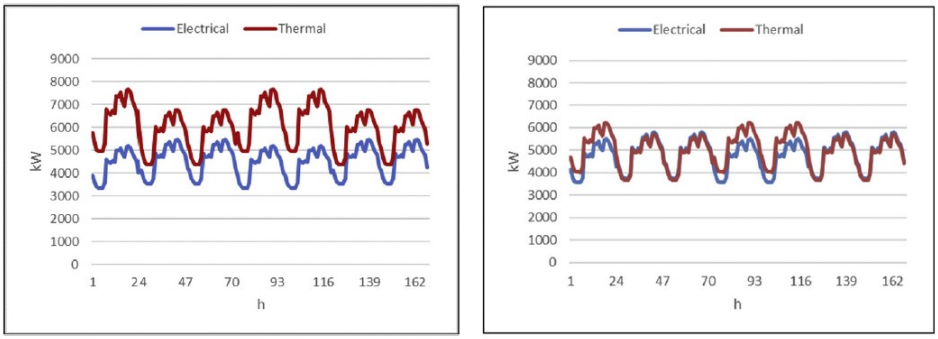

Figure 3.5: Electrical and thermal demand for a cruise ship in a cold environment (left) and in a warm environment (right) [76]

Next to the operational environment, the operational modes (O_m) also affect the auxiliary power. Consider a bulk carrier, loaded with the help of quay cranes of harbor A, but it needs to unload the cargo using its own deck cranes at another harbor B. As can be deduced, more auxiliary power would be required from the vessel's power plant in the case of the second harbor. Based on the work of [58, 112], using deck cranes for *loading/unloading* can lead to 26% increase of the required auxiliary power (for this particular mode). Since the power required for the deck cranes is an electric, non-propulsive load, it is categorized as hotel load. Also, this example specifies that there is only an extra load when the cranes are used, hence it can be captured in the additional hotel load ΔP_{hotel}. Furthermore, the authors of [113] show that a crude oil tanker has an extra load (with respect to other tankers) during the unloading of the cargo. The auxiliary boilers are used to supply exhaust gas to the inert gas systems, which are used to maintain sufficiently low oxygen levels in cargo tanks to prevent explosions. With data provided by the authors, it is estimated that this leads to 400% increase of the required boiler power. This increase of power can be captured in $\Delta P_{service}$.

At last, from the work of [18], a direct relation between the type of vessel and the required auxiliary power is seen. The authors indicate that for transportation of reefer containers (a container that is temperature-controlled), a reefer container ship is required, which can lead to an increase of 66% of the total auxiliary power. This can be seen as an

increase of the constant hotel load $P_{hotel,c}$.

Concluding, the given examples lead to a more complete definition of the auxiliary power:

$$P_{hotel}(O_m, T_a, X_v, t) = P_{hotel,c}(X_v) + \Delta P_{hotel}(O_m, T_a, X_v, t)$$

$$P_{service}(O_m, T_a, X_v, t) = P_{service,c}(X_v) + \Delta P_{service}(O_m, T_a X_v, t)$$

$$\begin{aligned} P_{aux}(O_m, T_a, X_v, t) &= P_{hotel}(O_m, T_a, X_v, t) + P_{service}(O_m, T_a, X_v, t) \\ &= P_{hotel,c}(X_v) + P_{service,c}(X_v) \\ &\quad + \Delta P_{hotel}(O_m, T_a, X_v, t) + \Delta P_{service}(O_m, T_a, X_v, t) \\ &= P_{aux,c}(X_v) + \Delta P_{aux}(O_m, T_a, X_v, t) \end{aligned} \tag{3.26}$$

where P_{hotel} and $P_{service}$ contain the required hotel and service power, and P_{aux} contains the total required auxiliary power. In literature however, for tugboats it is found that mostly, ΔP_{aux} is negligible compared to the amount of propulsion power, since they are designed for towing of large cargo vessels. For other vessels the contribution varies, which will be discussed in Section 3.2.1. Furthermore, as the time dependency of ΔP_{aux} is only (clearly) seen for cruise ships, it will be disregarded in later sections. Therefore, the final approximation of the required auxiliary power is given by 3.27:

$$P_{aux}(X_v, O_m, T_a) = P_{aux,c}(X_v) + \Delta P_{aux}(O_m, T_a, X_v) \tag{3.27}$$

Since the propulsion power and the auxiliary power both are affected by multiple aspects, they should be discussed. Therefore, the most important aspect which is required to model the propulsion and auxiliary power throughout the mission, the operational modes, will be discussed in the next section.

3.1.4. OPERATIONAL MODES

Each operational mode describes a distinct part of the mission, and is mainly characterized by the specific power demand and the speed of the vessel. For example, the standby mode of a tugboat requires very little power since the propulsion power demand is very low, but the assisting mode requires a tremendous amount of propulsion power to tow and maneuver the cargo ship in or out of the harbour. In Table 3.5 an overview of the main operational modes of the investigated vessels can be seen, and it can be noticed that there are a lot of identical modes. An important note is that the same operational mode can result in different power requirements, such as the operational mode *maneuvering*. For cargo ships this mode requires very little power, since mostly the maneuvering is realized with tugboats, but since passenger ships and research vessels use their own propulsion system for maneuvering, they require relatively more power for this mode. Also the *loading/unloading* mode can result in very different power requirements. Where a bulk carrier might use it's own deck cranes to load the cargo, the passengers of a cruise ship bring themselves on board, and since for the latter solely passengers are the 'cargo', it is more appropriate to use *boarding/unboarding*. For more detail about the operational modes, the reader is refered to Appendix B, where each operational mode can be found with an indication for the required power, vessel speed, and a short description.

Service ships		Cargo ships		Passenger ships	
Tugboat	Standby Transit Assist-low Assist-high	Container ship	Standby Loading/unloading Maneuvering Transit	Cruise ship	Standby Boarding/unboarding Maneuvering Transit low/high
OSV	Standby Transit Assist Dynamic positioning	Bulk carrier	Standby Loading/unloading Maneuvering Transit	Ferry*	Standby Loading/unloading Maneuvering Transit
Research Vessel*	Standby Transit Maneuvering Mission related mode	Tanker	Standby Loading/unloading Maneuvering Transit		

Table 3.5: Overview of the main operational modes of service ships, cargo ships, and passenger ships

* : Unfortunately, for research vessels and ferries not enough information can be found for further analysis, hence these will not be used in this thesis from here on

While Table 3.5 describes the main operational modes of each vessel, the required operational modes (and order of executing them) for a mission depend on the route of the vessel, which on its turn depends on the harbours that have to be visited (e.g. A and B in the definition of the mission given above). Take for example a container vessel, which has to transport containers from Rotterdam (A) to Shanghai (B). In the harbour of Rotterdam, the vessel could start in *standby*, then *load* containers, *maneuver* out of the harbour, *transit* across open sea to Shanghai, *maneuver* into the harbour, *unload* containers, to end in *standby* again. However, the vessel can also start directly with the *loading* of containers, then *maneuver* to another terminal, *load* more containers, *ma-*

neuver out of the harbour, *transit* to Shanghai, *standby* in front of the harbour (there could be some congestion causing the vessel to wait a certain amount of time before it can enter the harbour), *maneuver* into the harbour, *unload* a part of the containers at terminal 1, *maneuver* to terminal 2, *unload* the rest of the containers, and then mission has ended.

However, it is not in the scope of this thesis to investigate the different combinations of operational modes. Instead, to be able to provide a correlation between the mission and the power profile, it is assumed that for each mission the required sequence of operational modes is as short as possible (e.g. vessels do not have to wait in front of a harbour). This results in an expression that contains the required sequence of operational modes to complete a mission between only two harbours , $\mathbf{O_H}(X_v)$, where the specific entries depend on the type of vessel X_v. An example for a tugboat and an OSV be seen in 3.28:

$$\begin{aligned}\mathbf{O_H}(\textit{Tugboat}) &= \{\textit{Standby} \quad \textit{Transit} \quad \textit{Assist-low} \quad \textit{Assist-high} \quad \textit{Assist-low} \quad \textit{Transit} \quad \textit{Standby}\}\\ \mathbf{O_H}(\textit{OSV}) &= \{\textit{Standby} \quad \textit{Transit} \quad \textit{Assist} \quad \textit{Dynamic positioning} \quad \textit{Assist} \quad \textit{Transit} \quad \textit{Standby}\}\end{aligned} \tag{3.28}$$

Now for a mission with more than two harbours, the sequences of operational modes $\mathbf{O_H}$ can just be added together, such that for any mission, the required operational modes are described by:

$$\mathbf{O_m}(X_v, H) = \{\mathbf{O_H}(X_v),\ ...,\ \mathbf{O_H}(X_v)\} \tag{3.29}$$

where the amount of entries (each entry is equal to $\mathbf{O_H}$) to $\mathbf{O_m}$ is equal to $H-1$, with H the amount of harbours, derived from the mission description.

3.1.5. OPERATIONAL ENVIRONMENT AND SPEED

The operational environment is an important aspect for both the propulsion and the auxiliary power, but also for the speed of the vessel. To determine the operational environment, the locations of the harbours that are visited during the mission are required, which are specified by the mission $(A, B, C, D, ...)$. If each harbour can be described by a longitude $x \in \mathbb{R}$ and a latitude $y \in \mathbb{R}$, then a route $\mathbf{S_m}$ containing the required route, or path of the vessel can be constructed. Using Assumption 3.1, the route of the vessel can be described as:

$$\mathbf{S_m} = \{S_i\}_{i=1,...,P} = \{(x_i, y_i)\}_{i=1,...,P} \tag{3.30}$$

ASSUMPTION **3.1** *The route of the vessel between the harbours can be discretized in a certain amount of way-points P, such that between two consecutive points, only one operational mode is used, and that the route is described with good accuracy*

ASSUMPTION **3.2** *The route of a vessel between two harbours is always the same*

Now, since $\mathbf{S_m}$ describes the route of the vessel, it determines the operational environment during the mission. Using weather forecasts, data of previous voyages, etc. the environmental conditions such as wave height, currents, wind speed and direction with respect to the course of the vessel, and the ambient temperature can be determined for each specified way-point in $\mathbf{S_m}$. However, at which point in time these way-points are visited depends on the speed of the vessel. To make an estimate of this, Assumption 3.2 is used. Based on this assumption, historical data can be used to find the relative duration (β) of each operational mode in $\mathbf{O_m}$ which are used to execute a mission along route $\mathbf{S_m}$, and by combining this with the total mission time (t_m), the time spend in each operational mode (T_{O_m}) can be defined as:

$$t_m = t_{end} - t_0 \tag{3.31}$$

$$\mathbf{T_{O_m}} = t_m \begin{Bmatrix} \beta_1 \\ \dots \\ \beta_F \end{Bmatrix} = \begin{Bmatrix} t_{O_m,1} \\ \dots \\ t_{O_m,F} \end{Bmatrix} \tag{3.32}$$

where F is the length of $\mathbf{O_m}$ ($F \leq P$) and $\beta_i \in [0,1]$ is the relative duration of each operational mode such that $\sum_{i=1}^{F} \beta_i = 1$. Furthermore, using the discretized path of the vessel $\mathbf{S_m}$, the distance between two consecutive way-points can be approximated as:

$$\bar{s}_i = \sqrt{(x_{i+1} - x_i)^2 + (y_{i+1} - y_i)^2} \quad , 1 \leq i \leq P-1 \tag{3.33}$$

Using this approximation, the traveled distance for each operational mode can be expressed as:

$$\mathbf{\bar{S}_{O_m}} = \left\{ \sum_{i \in \mathbf{I_j}} \bar{s}_i \right\}_{j=1,\dots,F} \tag{3.34}$$

where $\mathbf{I_j}$ is the set of consecutive way-points for which the operational mode j does not change. Now, given the duration and travelled distance of each operational mode, the average speed (V_{O_m}) of each operational mode can be expressed as:

$$\mathbf{V_{O_m}} = \left\{ \frac{S_{O_m(i)}}{T_{O_m(i)}} \right\}_{i=1,\dots,F} \tag{3.35}$$

Finally, now using Assumption 3.1 and Assumption 3.2, the route of the vessel $\mathbf{S_m}$, the operational modes along this route $\mathbf{O_m}$, the duration of these modes $\mathbf{T_{O_m}}$ and the average speed of the modes $\mathbf{V_{O_m}}$ (hence along the route) are known, a forecast of the operational environment along the route can be made, such that the operational environment $\mathbf{O_e}_{,i}$ of way-point i is described by the sea state (s_s), currents of the sea (c_s), wind (w_s), ambient temperature (T_a), water depth (h), and waterway with (w_w), resulting in:

$$\mathbf{O_e}(\mathbf{S_m}, \mathbf{V_{O_m}}) = \{ s_{s,i} \quad c_{s,i} \quad w_{s,i} \quad T_{a,i} \quad h_i \quad w_{w,i} \}_{i=1,\dots,P} \tag{3.36}$$

3.1.6. TYPE OF VESSEL

The remainder of the required information to compute the power profile is given by or derived from the type of vessel X_v, which is based on the cargo X (where X specifies the type of cargo: *containers*, *iron ore*, *crude oil*, *passengers*, but also the specified amount, volume, or weight of the cargo). For example, if $X = 27000$ *Containers*, then a container ship with at least a capacity of 27000 containers is required. Using Assumption 3.3, the required parameters of the vessel are given by 3.37:

ASSUMPTION **3.3** *For a given mission and type of cargo X, the type of vessel X_v is known, together with the required parameters (size, efficiencies, etc.) of that vessel*

$$\mathbf{X_p}(X_v) = \{a,\ D,\ f_h,\ K_Q,\ K_T,\ \eta_D\} \tag{3.37}$$

Next to these parameters, the type of vessel X_v in combination with the used operational mode O_m gives information about the displacement ∇, hence the displacement of the vessel for each of its operational modes during the mission is captured in $\mathbf{X}_\nabla$:

$$\mathbf{X}_\nabla(\mathbf{O_m}, X_v) = \begin{Bmatrix} \nabla_1 \\ \dots \\ \nabla_F \end{Bmatrix} \tag{3.38}$$

where ∇ matches the displacement of vessel X_v for each operational mode in $\mathbf{O_m}$. Furthermore, the speed dependent parameter c_0 is also known for each operational mode during the mission:

$$\mathbf{c_0}(\mathbf{V_{O_m}}, X_v) = \begin{Bmatrix} c_{0,1} \\ \dots \\ c_{0,F} \end{Bmatrix} \tag{3.39}$$

where $\mathbf{c_0}$ depends on both the speed $\mathbf{V_{O_m}}$ and the vessel X_v. Furthermore, for vessels such as tugboats and OSVs, the towing force of the operational mode assist can now be expressed as:

$$\mathbf{F_{tow}}(\mathbf{O_m}, X_v) = \begin{Bmatrix} F_{tow,1} \\ \dots \\ F_{tow,F} \end{Bmatrix} \tag{3.40}$$

Finally, the described parameters and variables of the above sections can be combined to construct the power profile, which will be discussed in the next section.

3.1.7. MODEL OF CORRELATION MISSION AND POWER PROFILE

To construct the power profile, the propulsion and auxiliary power demand should be computed for each way-point of the route of the vessel, where after they can be plotted, either separately, or added together to find the total power demand during the mission. In the above sections, first the propulsion and auxiliary power are approximated, and then the inputs to construct them were discussed. This information is combined in 3.41, 3.42 and 3.43, and using these expressions, the power profile can be found. In addition, Algorithm 1 shows an algorithm which summarizes the required steps taken in this chapter to arrive at the power profile, based on the required inputs, such as the mission of the vessel.

$$\mathbf{P_D} = \left\{P_{D,i}\right\}_{i=1,\dots,P} = \left\{\frac{f(s_{s,i}, w_{s,i}, c_{s,i}, h_i, w_{w,i}, f_{h,i}, \nabla_{g(i)}) * c_{0,g(i)} * V^a_{O_m,g(i)}}{\eta_D} + |F_{tow,g(i)}|^{\frac{3}{2}} \frac{2\pi K_Q}{\sqrt{\rho} D K_T^{\frac{3}{2}}}\right\}_{i=1,\dots,P} \tag{3.41}$$

$$\mathbf{P_{aux}} = \left\{P_{aux,i}\right\}_{i=1,\dots,P} = \left\{P_{aux,c}(X_v) + \Delta P_{aux,i}(O_{m,g(i)}, T_{a,i}, X_v)\right\}_{i=1,\dots,P} \tag{3.42}$$

$$\mathbf{P_{tot}} = \mathbf{P_D} + \mathbf{P_{aux}} \tag{3.43}$$

where $g(i)$ is a mapping of way-point i, as these inputs are found using $\mathbf{O_m}$, hence they have $F \leq P$ elements. Furthermore, to adequately visualise the correlation between the mission and the power profile, a concept called "relation-graph" is used, found in the work of [114], which is a graphical way of describing the relation between multiple sets of "things". To this end, the first step is to sort the information given in this chapter into different classes, which are the inputs ($\mathcal{U}$), features-of-interest ($\mathcal{L}$), capabilities ($\mathcal{P}$), parameters ($\mathcal{Z}$), measurement units ($\mathcal{M}$), physical properties ($\mathcal{Q}$), and outputs ($\mathcal{Y}$). Each of the mentioned classes is a set of "things" of different types:

- $\mathcal{U}$: Inputs derived from the definition of the mission
  - $\mathcal{U} = \{u\}$
  - $u = \{A,\ B,\ t_0,\ t_m,\ X\}$
- $\mathcal{L}$: Type of vessel and characteristics based on X
  - $\mathcal{L} = \{l\}$
  - $l = \{X_v,\ a,\ D\ ,f_h,\ K_Q,\ K_T,\ \eta_D\}$
- $\mathcal{P}$: Required operating modes for vessel X_v throughout the mission
  - $\mathcal{P} = \{\ O_{M,1},\ ...,\ O_{M,end}\}$
- $\mathcal{Z}$: Parameters affected by the inputs, features-of-interest and capabilities
  - $\mathcal{Z} = \{z_1,\ ...,\ z_{end}\}$
  - $z_t = \{\ S_m,\ F_{tow}(t),\ O_e(t),\ \nabla(t),\ V_{O_m}(t),\ c_0(t)\}$
  - $O_e(t) = \{s_s(t),\ c_s(t),\ w_s(t),\ T_a(t),\ h(t),\ w_w(t)\}$

- $\mathcal{Q}$: Physical properties for parameters, inputs, and outputs
  - $\mathcal{Q} = \{Q_{\mathcal{U}}, Q_{\mathcal{Z}}, Q_{\mathcal{Y}}\}$
  - $Q_{\mathcal{U}} = \{Time\}$
  - $Q_{\mathcal{Z}} = \{Speed, Temperature, Height, Width, Direction, Draught, Flow\}$
  - $Q_{\mathcal{Y}} = \{Power\}$
- $\mathcal{M}$: Measuring units corresponding to the physical properties
  - $\mathcal{M} = \{kW, °C, m, deg, kn, s\}$
- $\mathcal{Y}$: Outputs of the model, resulting from the inputs $\mathcal{U}$
  - $\mathcal{Y} = \{y_1, ..., y_{end}\}$
  - $y_t = \{P_{tot}(t), P_D(t), P_{aux}(t)\}$

Since these sets are related to each other, the second step is to describe the specific relation between two sets. Take for example the inputs $\mathcal{U}$ and the capabilities $\mathcal{P}$. The relation between these sets can be descibed using vertices, or arrows, denoted as $E^{(\mathcal{U},\mathcal{P})}$. Using this definition, the relation graph is denoted as $\mathcal{G}(\mathcal{U},\mathcal{P},E^{(\mathcal{U},\mathcal{P})})$, and this can be seen in Figure 3.6.

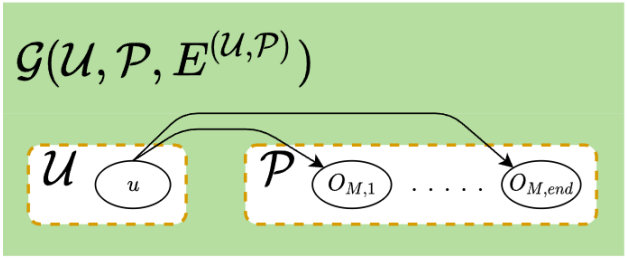

Figure 3.6: Relation-graph between inputs $\mathcal{U}$ and capabilities $\mathcal{P}$

Finally, the relation between each of the described sets can be found in this chapter, and it is found that ten distinct relation graphs can be constructed:

- $\mathcal{G}(\mathcal{U},\mathcal{P},E^{(\mathcal{U},\mathcal{P})})$
- $\mathcal{G}(\mathcal{U},\mathcal{L},E^{(\mathcal{U},\mathcal{L})})$
- $\mathcal{G}(\mathcal{U},\mathcal{Z},E^{(\mathcal{U},\mathcal{Z})})$
- $\mathcal{G}(\mathcal{U},\mathcal{Q},E^{(\mathcal{U},\mathcal{Q})})$
- $\mathcal{G}(\mathcal{P},\mathcal{Z},E^{(\mathcal{P},\mathcal{Z})})$
- $\mathcal{G}(\mathcal{L},\mathcal{P},E^{(\mathcal{L},\mathcal{P})})$
- $\mathcal{G}(\mathcal{L},\mathcal{Y},E^{(\mathcal{L},\mathcal{Y})})$
- $\mathcal{G}(\mathcal{Z},\mathcal{Y},E^{(\mathcal{Z},\mathcal{Y})})$
- $\mathcal{G}(\mathcal{Y},\mathcal{Q},E^{(\mathcal{Y},\mathcal{Q})})$
- $\mathcal{G}(\mathcal{Q},\mathcal{M},E^{(\mathcal{Q},\mathcal{M})})$

Combining these ten relation graphs results in Figure 3.7 , where all the relations between the sets are indicated with arrow, but to improve readability, only six relation graphs are shown with colors.

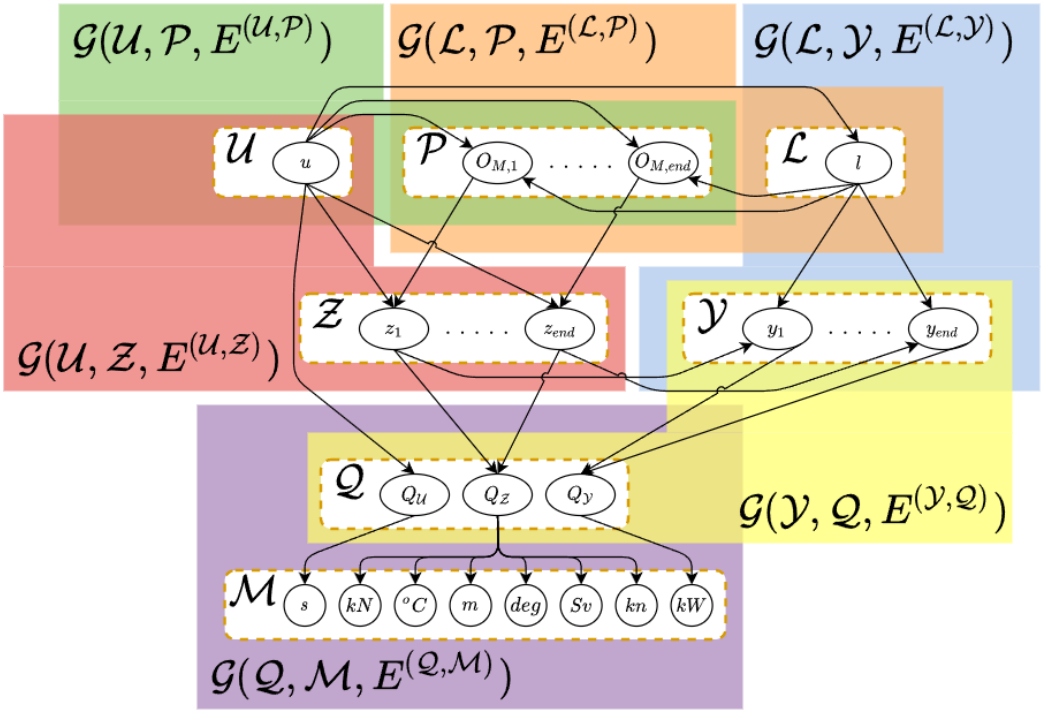

Figure 3.7: Relation-graph for the correlation between the mission and the power profile

To conclude, up till now this chapter has provided an answer to the research question: "How to model the correlation between the mission and the power profile of the vessel?", by constructing a graphical model, but also by providing an algorithm that can be used to approximate the expected power profile for a given mission. The next part of this chapter will discuss how variations in power profiles for a vessel can lead to modifications of its power plant, and which automation of the power plant control system is required to facilitate such modifications.

Algorithm 1: Correlation between mission and power profile

Input: Derived from mission definition or historic data

$X \leftarrow$ type of cargo

$X_v \leftarrow$ type of vessel based on (1)

$\mathbf{X_p} \leftarrow$ characteristics of vessel based on (2) (*eq. 3.37*)

$\mathbf{O_H} \leftarrow$ required operational modes between two harbours based on (2) (*eq. 3.28*)

$\mathbf{H} \leftarrow$ harbours to be visited (locations)

$\mathbf{S_m} \leftarrow$ list of coordinates (x, y) of the discretized route of the vessel based on (5) (*eq. 3.30*)

$t_0 \leftarrow$ starting time of mission

$t_{end} \leftarrow$ ending time of mission

$t_m \leftarrow t_{end} - t_0$, total mission time

$\mathbf{O_m} \leftarrow$ required operational modes for the mission, where

for $i = 1 : (length(\mathbf{H}) - 1)$ **do**

  $\mathbf{O_m}(i) = \mathbf{O_H}(X_v)$

end

$\mathbf{T_{O_m}} \leftarrow$ duration of each operational mode, where

for $i = 1 : length(\mathbf{O_m})$ **do**

  $\beta(i) =$ relative duration of operational mode $\mathbf{O_m}(i)$

  $\mathbf{T_{O_m}}(i) = t_m \cdot \beta(i)$

end

$\mathbf{S_{O_m}} \leftarrow$ traveled distance for each operational mode of (10), where

$\mathbf{I_j} \leftarrow$ set of consecutive points of $\mathbf{S_m}$ for which operational mode j does not change, and

for $i = 1 : length(\mathbf{S_m})$ **do**

  $\bar{s}(i) = \sqrt{(x_{i+1} - x_i)^2 (y_{i+1} - y_i)^2}$

end

for $j = 1 : length(\mathbf{O_m})$ **do**

  $\mathbf{S_{O_m}}(j) = \sum_{i \in \mathbf{I_j}} \bar{s}(i)$

end

$\mathbf{V_{O_m}} \leftarrow$ average speed for each operational mode of (10), where

for $i = 1 : length(\mathbf{O_m})$ **do**

  $\mathbf{V_{O_m}}(i) = \frac{S_{Om}(i)}{T_{Om}(i)}$

end

$\mathbf{F_{tow}} \leftarrow$ towing force for operational mode *assist*, where ;
for $i = 1 : length(\mathbf{O_m})$ **do**
    if $\mathbf{O_m}(i) == Assist$ **then**
        $\mathbf{F_{tow}}(i) = F_{tow}$
    else
        $\mathbf{F_{tow}}(i) = 0$
    end
end
$\mathbf{X_\nabla} \leftarrow$ displacement of the vessel during the mission (*eq. 3.38*) ;
$\mathbf{c_0} \leftarrow$ coefficient depending on the vessel speed of (27) (*eq. 3.39*) ;
$\mathbf{O_e} \leftarrow$ operational environment along the route defined in (6) (*eq. 3.36*) ;

Output: Power demands to construct the power profile ;

$\mathbf{P_D} \leftarrow$ propulsion power demand during mission, using (3,27,31,41,40,39) (*eq. 3.24*) ;
$\mathbf{P_{aux}} \leftarrow$ auxiliary power demand during mission, using (2,10,41) (*eq. 3.26*) ;
$\mathbf{P_{tot}} \leftarrow \mathbf{P_D} + \mathbf{P_{aux}}$, total power demand during the mission;

3.2. CORRELATION BETWEEN THE POWER PROFILE, POWER PLANT, AND CONTROL SYSTEMS

In the previous section, the correlation between the mission and the power profile is discussed. In this section, an answer to the research question: "How to model the correlation between the power profile for a mission and the needed modifications in automation of the control systems and the power plant?" will be formulated. Therefore, first the power profile is more discussed, and it is shown that the behavior and importance of the two components that build up the power profile (the propulsion power and the auxiliary power) depend on the type of vessel. Furthermore, it is shown how different power profiles can lead to modifications of the power plant, and at last the required automation of the power plant control system is discussed.

3.2.1. VARIATIONS OF THE POWER DEMAND AND POWER PROFILE

During a mission, several operational modes are used. Therefore it is only to be expected that the power demand varies during the mission, since each operational modes has different power requirements. Still, for a vessel that executes twice the same mission, the two corresponding power profiles could differ, caused by e.g. different conditions at sea. Therefore, this section discusses the effect of these different conditions at sea, but also of other causes for varying power demands and power profiles. Depending on the type of vessel, there are different reasons for a change in required power, hence they will be discussed separately. Furthermore, since the total power demand consist of the propulsion power and the auxiliary power, it is useful to know their relative importance (which shows how much to they contribute to the total). In Table 3.6 this can be seen, and the required information is extracted from the works used for Appendix B.

Type of vessel		Total power							
		Propulsion power				Auxiliary power			
Passenger ships	Cruise ship	Maneuvering		Transit low	Transit high	Standby	Boarding/ unboarding	Maneuvering	Transit low	Transit high
		8-10%		17-56%	41-75%	20-27%	20-27%	25-33%	25-48%	29-48%
Cargo ships		Maneuvering		Transit		Standby	Loading/ unloading	Maneuvering	Transit	
	Container ship	1-7%		93-99%		1-11%	1-11%	1-11%	1-7%	
	Bulk carrier	1-6%		90-98%		3-12%	4-17%	3-12%	3-11%	
	Tanker	3-7%		82-94%		8-21%	8-25%	8-21%	6-18%	
Service ships	OSV	Assist	Dynamic positioning	Transit		Standby	Assist	Dynamic positioning	Transit	
		15-89%	2-90%	13-85%		1-25%	10-47%	10-33%	6-20%	
	Tugboat	Assist low	Assist high	Transit		Standby	Assist low	Assist high	Transit	
		30-71%	80-98%	5-36%		2-20%	2-20%	2-20%	2-20%	

Table 3.6: Relative importance of propulsion power and auxiliary power for different vessels

CARGO SHIPS

For cargo ships, the variations in relative importance of the propulsion and auxiliary power are mainly related to the different size of the vessels, since small cargo ships require much less propulsive power, but only a little less auxiliary power than bigger ships, as shown in Appendix B. With respect to the propulsion power, regardless of their size, the sea margin (which depends on the operational environment), has a noticeable effect on the required propulsion power. As mentioned earlier in this chapter, this can easily lead to a 35-50% increase of the propulsion power with respect to calm sea conditions [103]. Furthermore, the authors of [58] discuss the use of the deck cranes of bulk carriers versus the use of harbour mounted cranes, and the authors of [18] discuss the additional auxiliary power for the transportation of reefer containers instead of normal containers. Another variation is seen for the operational modes *loading* and *unloading*, which lead to a substantial change in the required propulsion power. For example, a mission for a tanker states that it has to sail from harbour A to harbour B, where it will load oil, which it has to transport to harbour C. The trip from A to B can not be made with an empty tanker, since it would be to 'light' to operate. Therefore, the tanker is loaded with seawater in the ballast tanks, to ensure the draught is sufficient. When the tanker arrives at harbour B, it unloads the ballast and loads the oil, and prepares for the trip to harbour C. However, there is a difference in draught between these two situations, resulting in extra resistance for the vessel when it is loaded with oil, which increases the fuel consumption [115]. The implications for the required power are summarized in Table 3.7 and 3.8.

Type of Vessel	Cause	Increase of auxiliary power	Reference
Bulk carrier	Using deck cranes for loading/unloading cargo	26-50%	[58]
Container ship	Reefer containers instead of regular containers	66%	[18]

Table 3.7: Variation in auxiliary power demand for cargo ships

Type of Vessel	Cause	Increase of propulsion power	Reference
All	Increased resistance due to increased sea margin	35-50%	[103]
All	Extra draught due to loaded cargo instead of ballast	27-37%*	[115]

Table 3.8: Variation in propulsion power demand for cargo ships

* : In literature it can be seen that this effect holds for all cargo vessels, but only for a tanker actual data has been found to prove this

An important note is that for transporting reefer containers instead of regular containers, the increase of required power is present until the containers are ready to be unloaded, which is also the case for the increased draught due to the loaded cargo. On the other hand, the additional power for the deck cranes, and additional boiler power is only required when using the loading/unloading mode.

SERVICE SHIPS

While for cargo ships the required propulsion power increases with the size of the vessel, for tugboats this is different. There are small tugboats with less power than large ones, but there are also examples of small tugboats with very powerful power plants, outperforming larger tugboats [116]. Furthermore, due to their missions, power profiles of tugboats show large variations in the required propulsion power, as can be seen from Table 3.6. However, in literature there is no information found which indicates varying auxiliary power demand between different operational modes, for the same vessel. Furthermore, while a clear relation between installed power and maximum required propulsion power can be seen, no clear relation between either the size, required power or installed power is found to indicate the differences in required auxiliary power. To illustrate the difference in the power of tugboats, six different vessels are shown in Table 3.9.

Maximum Required Power*		Propulsion Power*		Auxiliary Power**		Reference
kW	%	kW	%	kW	%	-
1000	100	900	90	100	10	[7]
1780	100	1430	80	350	20	[32]
3230	100	3180	98	50	2	[4]
3460	100	3165	91	295	9	[6]
4100	100	3700	90	400	10	[8]
5000	100	4800	96	200	4	[33]

Table 3.9: Auxiliary and propulsion power for different tugboats

*: Maximum value during a mission, during the operational mode *Assist* or *Assist-high*
**: Assumed constant during a mission

Although the maximum power required for a mission occur during the mode *assist-high*, the required power for this mode can not directly be linked to the size of the cargo ship that has to be assisted. Large cargo ships that normally require four tugboats, often still require four tugboats when more powerful tugboats are available, even if they are twice as powerful. This is due to safety concerns, because in the case of four tugboats, there are still three tugboats left to assist of one breaks down, which is in most cases sufficient for safe handling. However, in the case of two tugboats for such a large cargo ship, only one tugboat is remaining to assist the ship if one breaks down, which would be problematic [116]. Therefore it is more useful to look at the duration of the *assist-low* and *assist-high* mode, to indicate a possible need for modification of the power plant. As shown in Appendix B, these two operational modes together account for 17 – 44% of the mission. One could imagine, if a tugboat requires maximum power for a larger amount of time, it also requires more energy storage in e.g. batteries, since tugboats often use electric or hybrid propulsion, where for the latter the electric motor(s) boosts the mechanical engine(s) for high power operation.

Next to tugboats, required to tow cargo ships, there are also OSVs in this category, which are equipped to fulfil a much more various range of operations, such as assisting a drilling platforms by towing it to another location, by placing or retrieving anchors, or by firefighting, but they are also suited to maintain a steady position at sea using dynamic positioning. Since they have such differing missions, both the propulsion and the auxiliary power for different missions are subject to variations. Furthermore, even within a mission there is much variation of the auxiliary and propulsion power demand, as is shown by the authors of [42], where the auxiliary power demand varies from 1% to 47%, and the propulsion power demand from 4% to 80%, all for the same mission. It has to be noted that this variance is purely caused by the different operational modes, but unfortunately there is not sufficient information found in literature to make a clear comparison between multiple similar missions, other than the different duration of the operational modes as shown in Appendix B.

PASSENGER SHIPS

The last to be discussed are passenger ships, which in this section only includes cruise ships. They are quite different from other vessels, as they require a quite large share of auxiliary power throughout the whole mission. Variations in the auxiliary power demand during the mission are mainly caused by fluctuations in the temperature during the day and between different environments, causing increasing or decreasing auxiliary power demand. More details about the influence of the temperature and the time of day can be seen in Table 3.10. Small variations of the propulsion power between missions depends on the operational environment which affects the resistance of the vessel, but during the mission itself it is mostly affected by the required operational mode. Since the weight of the vessel is much larger than the weight of the passengers, the amount of passenger does not affect the propulsion power, but it does however affect the auxiliary power to a considerable extend, and it is found that every passenger requires about 2-5 kW of the auxiliary systems [113]. Since passenger ships, especially cruise ships, rely on electric propulsion with a mechanical or hybrid power supply, it is important that the electric power production is well designed.

Cause	Effect	Impact
Ambient temperature (warm to cold)	Change of the average hotel load	-7%
	Change of the minimum and maximum hotel load	-7%
	Change of the average service load	23%
	Change of the minimum and maximum service load	34%
Time of the day	Change of auxiliary power demand during mission	25-29%

Table 3.10: Effect of ambient temperature and time of the day on auxiliary power of cruise ships [76]

To conclude, not only during, but also between missions both the propulsion and the auxiliary power demand varies, which could result in possible modifications of the power plant, e.g. to improve efficiency or to produce more power for a longer amount of time. However, before such modifications can be proposed, first the layout of the power plant, (what type of propulsion, power supply, how many of each component, etc.) will be discussed in the next section.

3.2.2. Equipment Modifications for the Power Plant

As discussed in the previous section, different missions lead to different power demands, hence to different power profiles. Using the variations in the power demand and power profile of the previous section, in this section it is discussed how this could result in equipment modifications for the power plant, and how this affects the control system.

Container Ships

Container ships often have constant power profiles, where the propulsion power accounts for approximately 95% of the total power demand. Therefore, most of their power plants use a single mechanical engine (functioning as propulsion plant), providing the required propulsion power, and a separate power supply to provide for the auxiliary power. Therefore, variations in the auxiliary power demand results in modifications of the power supply, and this can for example be seen in the work of [18], where the authors discuss two missions for a 5000 TEU (Twenty-foot Equivalent Unit) container ship. Both missions describe the transportation of containers between two harbours, where for mission 1 only normal containers are involved, but for mission 2 the vessel also carries reefer containers. These containers are temperature controlled, hence they require more electric power from the power plant (approximately 7 kW per reefer), and this results in two power profiles for the container ship, shown in Figure 3.8. The shape of the

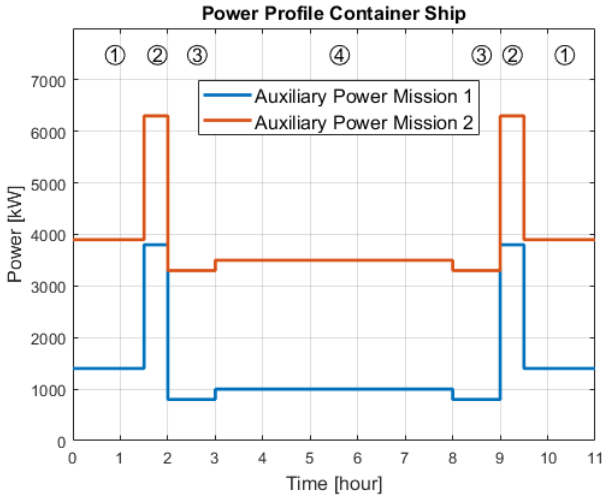

Figure 3.8: Power profiles for two missions of a 5000 TEU container ship [18]

power profile is determined by the operational modes, which in this case are *Transit*(1), *Maneuvering*(2), *Standby*(3), and *Unloading*(4), and can also be seen in the power profile. For both missions the sequence of these modes and the time spend in each is similar, hence the same shape of power profiles, but the auxiliary power demand for mission 2 is increased with 66% due to the reefer containers. For both missions, the authors discuss the use of a mechanical and a hybrid power supply, and they describe the power split, indicating the required components for both power supplies. Using these results, Figure 3.9a, 3.9b, 3.9c, and 3.9d show the required power supplies for both missions, and the capacity of each component is shown in Table 3.11.

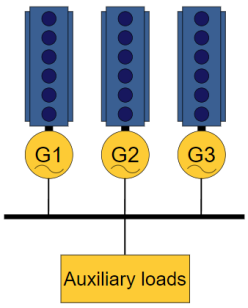

(a) Conventional mechanical power supply for mission 1

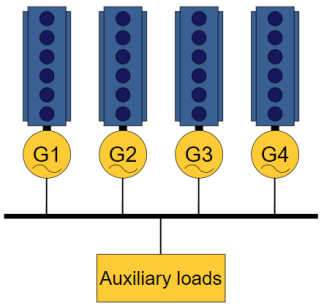

(b) Conventional mechanical power supply for mission 2

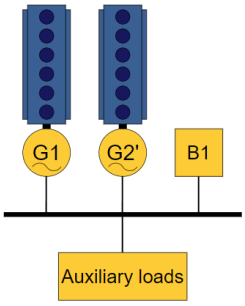

(c) Proposed hybrid power supply for mission 1

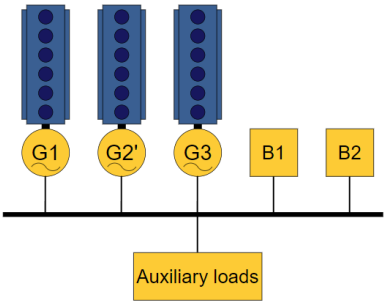

(d) Proposed hybrid power supply for mission 2

Figure 3.9: Power supplies of a container ship [18]

Component	Generator sets					Batteries	
	G1 + engine	G2 + engine	G2' + engine	G3 + engine	G4 + engine	B1	B2
Capacity	1.8 MW	1.8 MW	1.0 MW	1.8 MW	1.8 MW	1.0 MWh	1.0 MWh

Table 3.11: Capacity of each component in the power supply

As can be seen, multiple options are available to increase the power output. If the starting point is the mechanical power plant of Figure 3.9a, and the power profile increases as shown in Figure 3.8 with 66%, there are two options: either a generator set is added, or a generator set is replaced with a generator set of a lower capacity and two batteries are added (in both cases, the authors chose to keep the load factor for the generator sets between 70% and 90% for most time of the power profile, since this is the optimal loading point for most engines and generators). However, if the vessel starts with the power supply of Figure 3.9d and then has to execute mission 1, the process is reversed, so either a generator set and a battery can be removed, or a generator set is replaced with a set with higher capacity and two batteries are removed. Of course, for a lower power demand the equipment could also just be kept in the power plant, but as the weight of a generator set could reach up to the weight of a 20 TEU container [117], it might be desired to remove equipment if not required for the mission.

TUGBOATS

For service ships such as tugboats, the required bollard pull during the operational mode *assist* or *assist-high* is an important criteria for design of a power plant, but how this affects the different components in the power plant depends on the type of propulsion and power supply [6, 33] (e.g. with mechanical propulsion the main engine directly correlates to the bollard pull, but for electric and hybrid propulsion this is different). However, it is not in the scope of this thesis to find how the power plant needs to be designed exactly, but what the effect of a varying power profile can be. Therefore, five tugboats with a similar power plant are investigated. Their power plants consists of an electric propulsion plant with two electric motors, and a hybrid power supply including one or two generator set(s) and one battery, of which an example is shown in Figure 3.10. The

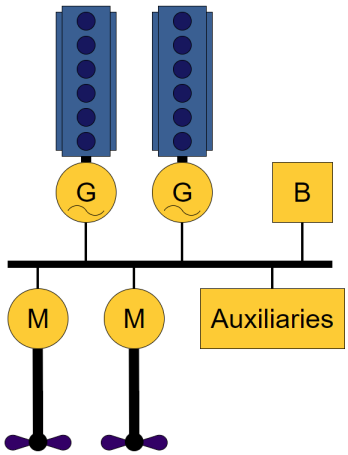

Figure 3.10: Electric-hybrid power plant of a tugboat

power profiles of the vessels are also known, and are used to compare to each other and correlate variations in their power profiles to variations in their power plants. For this analysis the propulsion plant (the electric motors) are not important, so only the power supply will be discussed. The details of the power profiles and power supplies of the different tugboats can be found in Table 3.12.

	Power Profile [kW]					Power Supply				
							Batteries		Installed	
Tugboat	Standby	Transit	Assist Low	Assist Medium	Assist High	Generator Sets [kW]	Capacity [kWh]	Power [kW]	Power [kW]	Reference
1	100	150	500	-	1000	1100	100	600	1700	[7]
2	350	710	1250	-	1780	2000	150	500	2500	[32]
3	50	1050	1710	-	3230	2400	500	1500	3900	[4]
4	200	1250	2500	3750	5000	4080	1250	1250	5330	[33]
5	400	400	950	2400	4100	3890	866	500	4390	[8]

Table 3.12: Details of the tugboats used for comparison

An important note is that the author of [8] states that the same power is required for *Standby* as for *Transit*, which can be explained if it is assumed that the vessel uses dynamic positioning to maintain it's position during this mode, and if this requires the same power as 'normal' sailing.

Using MATLAB the power profiles are plotted and compared, and two of those comparisons can be seen in Figure 3.11. As can be seen, both the actual power profiles as the

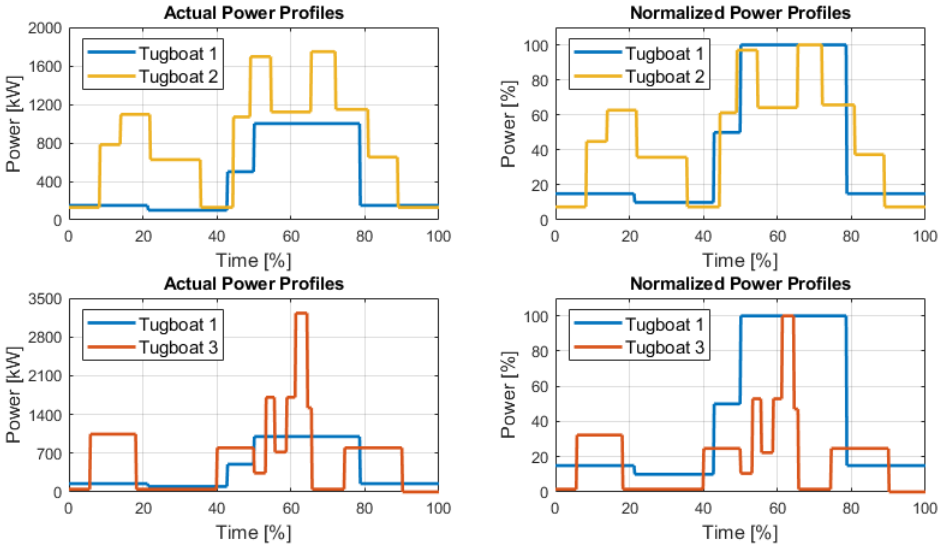

Figure 3.11: Comparison of power profiles

normalized power profiles are used. By comparing the actual power profiles, the effect of an increase or decrease of the power demand can be seen, while by comparing the normalized power profiles the effect of the duration of each mode is more clear. Using these comparisons, which are done for each pair that can be made (10 pairs in total), it is found that instead of adding components to the power supply, as can be seen in Figure 3.9 of the previous section, for these vessels the capacity of the components of the power supply varies, but the number of components remains the same, which is equivalent to replacing the components. Next to this observation, other effects of varying power profiles on the power supply are also seen, and these are listed below. An important note is that the maximum required power always occurs during the mode *assist*, which is only used for 4%-14% of the mission.

- An increase of the maximum power demand results in both an increase of the generator capacity as an increase of the battery capacity
- If the installed power increases, the battery capacity relatively increases more than the generator capacity

- For a certain increase of maximum power demand, the generator power increases with less than this amount, but the battery capacity increases more than this amount
- An increase of the maximum power demand results in less 'reserve' power of the power supply, meaning that the maximum power demand is closer to the total installed power
- If the capacity of the battery increases, the maximum power it can deliver does not necessarily increase too
- The duration of the operational mode *assist* seems to have no clear, direct relation to the capacity of the battery and generator set

Next to these observations, the authors of [33] indicate that at least 75% of the maximum power demand should be provided by generator sets, and except for tugboat 3 this is seen in this analysis. Still, these observations only indicate a possible approach to replace components of the power plant, based on the power profiles and power supplies of five tugboats. In reality, the process of selecting the required components for a power plant is complicated and depends on many factors, as is discussed by the authors of, for example, [8] and [118].

EQUIPMENT MODIFICATIONS

As shown in this section with the examples of the container ship and the tugboats, identifying equipment modifications for the power plant, based on the power profile, is not a simple task. The authors of [6] mention that for the design of the power plant there is a large dependency between the profile profile, the lay-out of the power plant, the control strategy and the size of the components in the power plant, and the author of [8] proposes an approach to select the most optimal power plant, taking into account the desired control objectives, type of propulsion, type of power supply, performance and costs, based on the power profile. However, independently of the process of selecting the optimal power plant, the equipment modification described in this paragraph can be summarized as follows:

- Add components
- Replace components
- Remove components

How these equipment modifications correlate to the automation modifications of the power plant control system is discussed in the next section.

3.2.3. AUTOMATION MODIFICATIONS FOR THE CONTROL SYSTEM

Before the required automation modifications, due to modifications of the equipment in the power plant, can be proposed, the power plant control system needs to be discussed. An example of the power plant control system for a hybrid power plant is shown in Figure 3.12, and it can be seen that the control system consists of two levels; the primary and the secondary level. The controllers in the primary level depend on the type of propulsion and the type of power supply, and for a hybrid power plant (both hybrid propulsion and power supply) containing main engines, generator sets, electric machines and batteries, there are also four type of primary controllers seen. An important note is that for each component there is a controller in the primary level (e.g. for a power plant with two main engines, there are two main engine controllers). The dotted connection be-

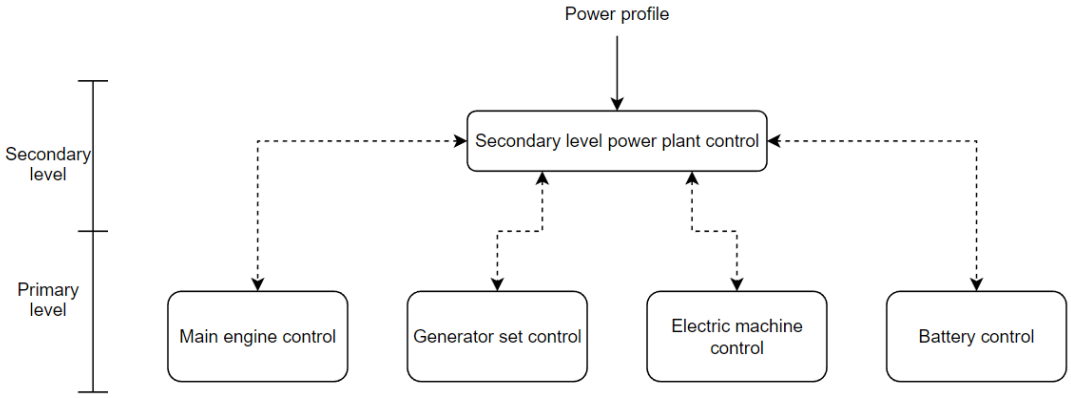

Figure 3.12: General overview of a distributed power plant control system for a hybrid plant

tween the secondary and primary control indicates the flow of communication. Each controller in the primary level receives inputs in the form of reference points for the controlled component, and returns a measurement or estimation of a required parameter back to the high-level power plant control. The latter gives the required settings for the main engines, generator sets, electric machines, and batteries, based on the required power from each component. To compute the required power of each component in the power plant, also refered to as the power split, often three control strategies are used: Equivalent Consumption Minimization Strategy (ECMS), power control, or power management, as can be seen in Chapter 2, Table 2.1. Although all three strategies provide a power split, power control only focuses on a particular type of equipment (e.g. only the power split between generator sets), while ECMS and power management provide the power split for the whole power plant. Furthermore, where ECMS is only a strategy to construct a cost function to compute the power split [4, 6, 12, 17], power management also provides the required reference points for the controllers in the primary level [15, 119]. Now, using one of thee strategies and the power profile as input, as shown in Figure 3.12, the power split throughout the mission can be computed. As discussed in the previous sections, the power profile depends on the mission, which can result in desired equipment modifications for the power plant. Thus, if the power profile for a new mission is known, the power split during the mission can be computed, and it can be checked whether or not the power plant has to be modified by removing, adding or

replacing equipment (e.g. to increase efficiency, or even to prevent overloading of components). To this end, the remainder of this section will discuss how equipment modifications affect the primary and secondary level, and based on these findings the required automation modifications are proposed.

SECONDARY LEVEL

Since the secondary level determines the power split, hence how much power each component in the power plant has to generate or to take in, layout of the power plant is of great importance. If for example the power plant solely consists of a single main engine to provide the propulsion power and a single generator set to provide the auxiliary power, the power split is clear, but as the power plant contains more and more components, which can either be used to provide power for the propulsion loads or for the auxiliary loads, it is more complicated. Therefore, in Figure 3.13 two layouts of a hybrid power plant are shown, which will be used to highlight the relation between the power split and the power plant layout. To determine the power split for such power plants, of-

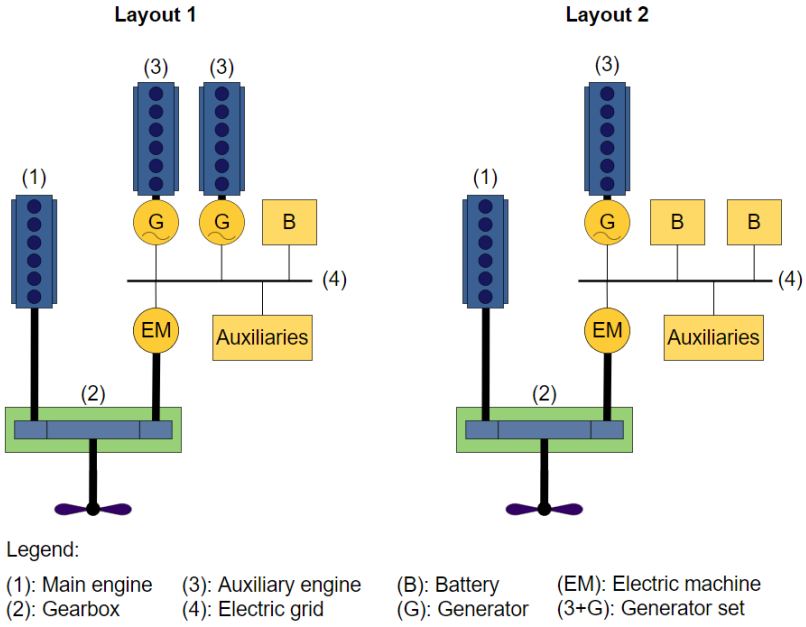

Figure 3.13: Example of two hybrid power plant layouts

ten a cost function and several constraints are used [22]. The cost function translates the power assigned to the components in the power plant to the fuel costs, while the constraints ensure the required propulsion and auxiliary power demands are met, and that the assigned power for the power plant components does not exceed their maximum and minimum power ratings. How this can be applied for the two power plants shown in 3.13 is derived using the work of [7, 100, 120] and can be seen below.

Layout 1 : PTI

Cost Function:

$$C_{tot} = C_{ME} + C_{GS1} + C_{GS2} + C_B$$

Constraints:

$$P_D = (P_{ME} + P_{EM}) \cdot \eta_T$$

$$P_{aux} = P_{GS1} + P_{GS2} + P_B - \frac{P_{EM}}{\eta_{EM}}$$

$$P_{ME,min} \leq P_{ME} \leq P_{ME,max}$$
$$P_{GS1,min} \leq P_{GS1} \leq P_{GS1,max}$$
$$P_{GS2,min} \leq P_{GS2} \leq P_{GS2,max}$$
$$P_{EM,min} \leq P_{EM} \leq P_{EM,max}$$
$$P_{B,min} \leq P_B \leq P_{B,max}$$
$$SOC_{min} \leq SOC \leq SOC_{max}$$

Layout 2 : PTI

Cost Function:

$$C_{tot} = C_{ME} + C_{GS} + C_{B1} + C_{B2}$$

Constraints:

$$P_D = (P_{ME} + P_{EM}) \cdot \eta_T$$

$$P_{aux} = P_{GS} + P_{B1} + P_{B2} - \frac{P_{EM}}{\eta_{EM}}$$

$$P_{ME,min} \leq P_{ME} \leq P_{ME,max}$$
$$P_{GS,min} \leq P_{GS} \leq P_{GS,max}$$
$$P_{EM,min} \leq P_{EM} \leq P_{EM,max}$$
$$P_{B1,min} \leq P_{B1} \leq P_{B1,max}$$
$$P_{B2,min} \leq P_{B2} \leq P_{B2,max}$$
$$SOC_{1,min} \leq SOC_1 \leq SOC_{1,max}$$
$$SOC_{2,min} \leq SOC_2 \leq SOC_{2,max}$$

Layout 1: PTO

Cost Function:

$$C_{tot} = C_{ME} + C_{GS1} + C_{GS2} + C_B$$

Constraints:

$$P_D = P_{ME} \cdot \eta_T - P_{EM}$$

$$P_{aux} = P_{GS1} + P_{GS2} + P_B + P_{EM} \cdot \eta_{EM}$$

$$P_{ME,min} \leq P_{ME} \leq P_{ME,max}$$
$$P_{GS1,min} \leq P_{GS1} \leq P_{GS1,max}$$
$$P_{GS2,min} \leq P_{GS2} \leq P_{GS2,max}$$
$$P_{EM,min} \leq P_{EM} \leq P_{EM,max}$$
$$P_{B,min} \leq P_B \leq P_{B,max}$$
$$SOC_{min} \leq SOC \leq SOC_{max}$$

Layout 2 : PTO

Cost Function:

$$C_{tot} = C_{ME} + C_{GS} + C_{B1} + C_{B2}$$

Constraints:

$$P_D = P_{ME} \cdot \eta_T - P_{EM}$$

$$P_{aux} = P_{GS} + P_{B1} + P_{B2} + P_{EM} \cdot \eta_{EM}$$

$$P_{ME,min} \leq P_{ME} \leq P_{ME,max}$$
$$P_{GS,min} \leq P_{GS} \leq P_{GS,max}$$
$$P_{EM,min} \leq P_{EM} \leq P_{EM,max}$$
$$P_{B1,min} \leq P_{B1} \leq P_{B1,max}$$
$$P_{B2,min} \leq P_{B2} \leq P_{B2,max}$$
$$SOC_{1,min} \leq SOC_1 \leq SOC_{1,max}$$
$$SOC_{2,min} \leq SOC_2 \leq SOC_{2,max}$$

where C_{tot} is the total costs for a certain power split, with C_{ME}, C_{GS}, and C_B the costs of a main engine, generator set, and battery, respectively, η_T is the transmission efficiency (0.95 - 0.98) and η_{EM} is the efficiency of the electric machine (0.93-0.96) [99, 107, 119]. Also, P_{ME} is the mechanical output of the main engine (ME), P_{EM} is the mechanical output (PTI) or input (PTO) the electric machine (EM), P_{GS} is the electric output of a generator set (GS), and P_B is the electric output (discharging) or input (charging, for which P_B is negative) of a battery (B). Since there are two generators sets in layout 1, and

two batteries in layout 2, this is also shown in the cost function and constraints. The electric machine is not considered in the cost function, since it only converts electrical power into mechanical power (PTI), or vice versa (PTO). It can be noted that depending on the used mode for the electric machine, the constraint of the required propulsion and auxiliary power changes. At last, $P_{i,min}$ and $P_{i,max}$ indicate the minimum and maximum power for component i, respectively, and the state-of-charge (SOC) of a battery is constrained by SOC_{min} and SOC_{max}.

Since the cost of each component relates to its generated or consumed power, the power split is found by minimizing the cost functions of the above examples, while meeting the constraints. How exactly the power of the components relates to the costs depends on the used strategy, such as ECMS or power management, but regardless of these specifics, from these examples it can be seen that each components of the power plant is included in the cost function (except for the electric machine) and in the constraints. To ensure the power split can be determined correctly after equipment modifications occur, the secondary control system needs to be updated accordingly. Even more, in order to provide proper control of the components in the power plant once the power split is obtained, the primary level also has to adapt to the equipment modifications.

PRIMARY LEVEL

When modifications of the equipment occur, the layout of the power plant changes. To this end, the example of Figure 3.13 is used, where two different layouts can be seen. For each of these power plants, the primary level control includes controllers for each component, and in Figure 3.14 and 3.15 the power plant control for both layout 1 and 2 can be found, respectively. It can be seen that indeed for each component there is a separate controller, hence to adjust the primary level such that it can be used for layout 2 after the equipment modifications, a generator set controller has to be removed, and a battery controller has to be added. Of course, for a different mission or power plant, the modifications could be different, but process will be similar to this example. Using this information, the automation modifications can be described next.

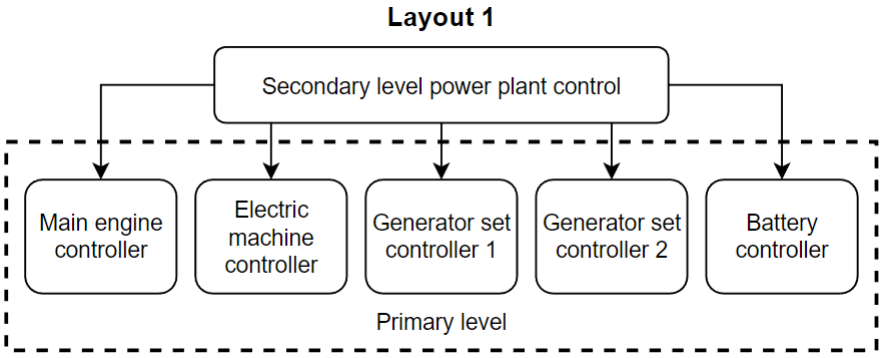

Figure 3.14: Power plant controller for layout 1

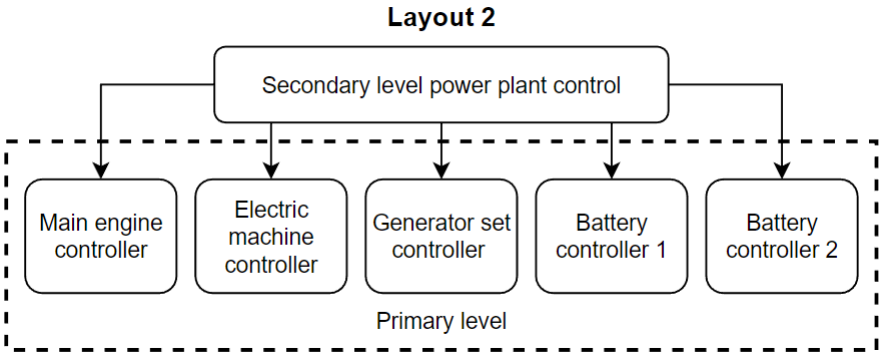

Figure 3.15: Power plant controller for layout 2

AUTOMATION MODIFICATIONS

As shown with the examples in this section, the power profile affects the required power plant of a vessel. To this end, once a mission and the corresponding power profile are known, the vessels control system needs to be able to determine whether or not equipment modifications are required to execute the mission, and if so, which equipment modifications. Furthermore, if the required equipment modifications are determined, in order to control this 'new' power plant of the vessel, the secondary and primary level need to be updated. since the former computes the power split between the power plant components, and the latter includes the local controllers of all the components in the power plant. To this end, the automation modifications as shown in Figure 3.16 are proposed.

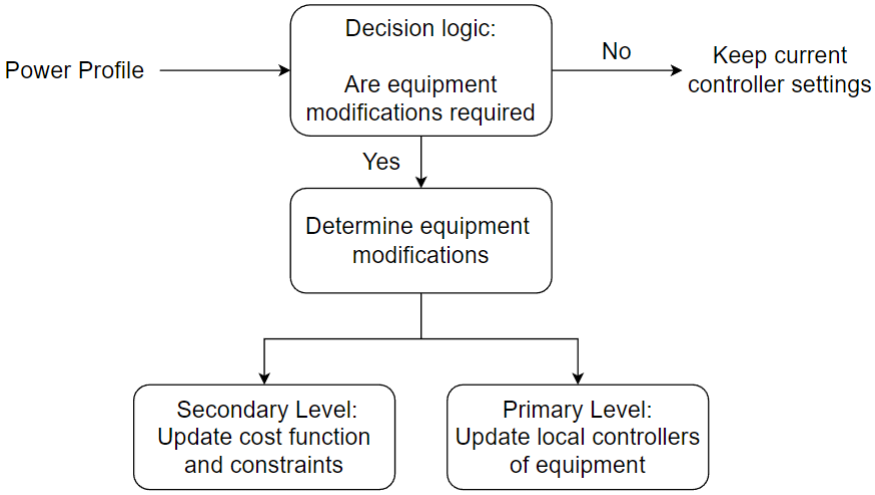

Figure 3.16: Required automation modifications for the power plant control system

3.2.4. MODEL OF CORRELATION POWER PROFILE AND CONTROL SYSTEM

Concluding, the second part of this chapter discussed the required steps to model the correlation between the power profile, the equipment modifications, and the automation modifications, providing an answer to the third research question: "How to model the correlation between the power profile for a mission and the needed modifications in automation of the control systems and the power plant?". We have seen that due to variations missions of a vessel, the power profile changes, and this could lead desired equipment modifications such as addition, removal, or replacement of components. Due to these equipment modifications, automation modifications for the power plant control system are proposed; the layout of the power plant needs to be recognised, where after the cost function and the constraints in the secondary level can be updated, along with the required local controllers in the primary level. A schematic overview of this can be seen in Figure 3.17, along with the previous found relation between the mission and the power profile. A more detailed example of the correlation between the power profile and

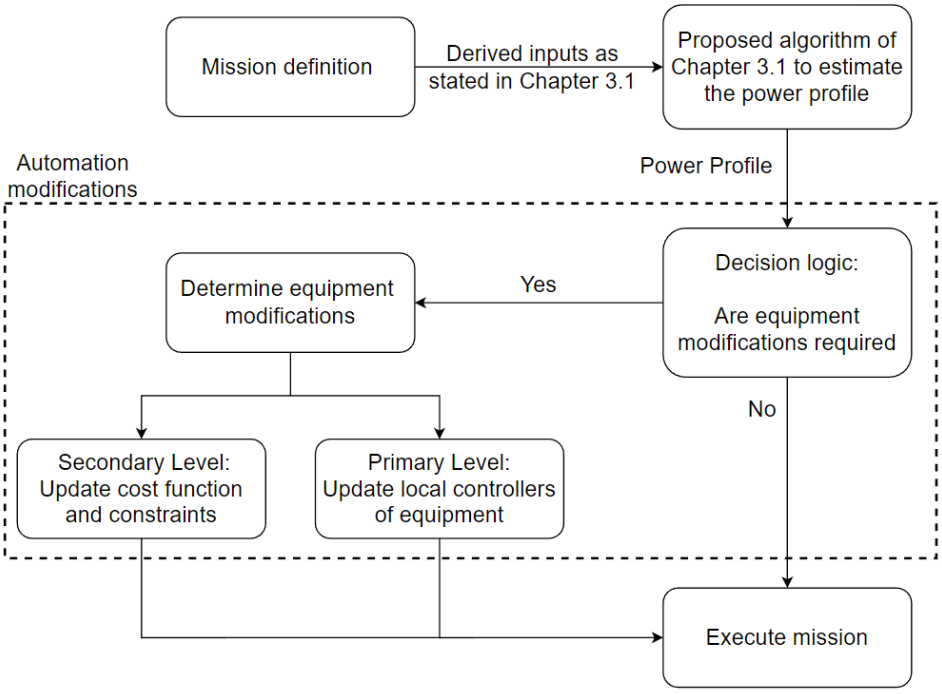

Figure 3.17: Correlation between the power profile and the automation modifications of power plant control system

the control system can be found in Algorithm 2, where a proposal for the decision logic is also shown.

Algorithm 2: Model of Correlation Power Profile and Automation Modifications

Input: From Top-Level
$PF \leftarrow$ Power Profile
$P_{plant,max} \leftarrow$ Maximum power of current power plant
$\lambda \leftarrow$ Fraction of (2) required as reserve power

---

begin
  Decision Logic:
  if $max(PF) \geq (1-\lambda)P_{plant,max}$ **then**
    Proceed with step 13
  else
    Proceed with step 36
  end
end
begin
  Equipment Modifications:
  -Replace/remove/add equipment
end
begin
  System Identification:
  for $i \in \{ME, EM, G, B\}$ **do**
    $x_i \leftarrow$ Occurrence of component i in power plant (e.g. 1,2, or 3)
  end
end
begin
  Update Control System:
  for $i \in \{ME, EM, G, B\}$ **do**
    for $j = 1 : x_i$ **do**
      for *Primary Level:* **do**
        Include a local controller for component i_j
      end
      for *Secondary Level:* **do**
        Include component i_j in the cost function
        Include constraints for component i_j
      end
    end
  end
end
Execute mission

3.3. CONCLUDING REMARKS

In this chapter, the second and third subquestions: "How to model the correlation between the mission and the power profile of the vessel?" and "How to model the correlation between the power profile for a mission and the needed modifications in automation of the control systems and the power plant?" are answered.

First, power profiles and missions of different vessels were analyzed, and using this a general definition of a mission was given, from which the the type of cargo, the locations the vessel has to visit, and the available mission time can be seen. By combining the information given in the mission definition, the type of vessel and its characteristics, the operational modes, the operational environment, and the speed of the vessel throughout the mission could be derived, resulting in the power profile for the mission. Furthermore, a relation-graph showing this correlation and a pseudo-algorithm to construct the power profile were presented.

Second, different missions, power profiles and power plant layouts of a container ship and tugboats were used to specify equipment modifications required between the missions, indicating the correlation between the power profile and the equipment modifications. Using this, and the multi-level control system of a marine vessel described in the previous chapter, automation modifications of the control system were proposed, and this can be summarized as follows. Based on the power profile, it can be decided whether or not equipment modifications, such as additions, removals, or replacements of equipment, are required, and if so, which equipment modifications. If this is determined, the cost function and the constraints included in the secondary level control, required to determine the power split and reference signals for the primary level, have to be updated, together with the controllers in the primary level, such that each component in the power plant is included in the secondary and primary level.

In the next chapter a modular control architecture is designed, in order to meet the proposed automation modifications proposed in this chapter, for which the state-of-the-art described in Chapter 2 is used to select a suitable control strategy. Furthermore, using the correlation between the mission and the power profile, and the described variations of the power profile, multiple missions with corresponding power profiles are constructed, such that the performance of modular control architecture can be shown in Chapter 5.

4

Design of a Modular Power Plant Control Architecture

In this chapter a modular control architecture will be designed to meet the proposed automation modifications of the previous chapter, and therefore providing the answer to the fourth research question: "How can a modular control architecture be designed to meet the proposed automation and power plant modifications?". To this end, first the conventional power plant control system will be analysed, and the primary level controllers and secondary level controllers are designed. Regarding these two levels, the primary level includes all controllers for the components in the power plant, and the secondary level provides the power split and the reference signals for the primary level. Although there are multiple strategies to determine the power split, for this thesis ECMS is selected. After this, a bank of controllers is proposed, based on Supervisory Switching Control (SSC), to allow for modular use of the components in the power plant. Furthermore, following the example of Wärtsilä's ZESPacks [23], the modular control architecture is based on battery modifications, but can easily be adjusted to include more component modifications.

4.1. Power Plant

As discussed in Chapter 1, the power plant consists of the propulsion plant and the power supply, which both can be mechanical, electric, or hybrid. Historically almost all vessels used mechanical propulsion and power supplies [121], but nowadays, all kinds of combinations are seen. Many cargo ships still use a full mechanical power plant with the addition of PTO, but to increase efficiency, some investigate the use of hybrid propulsion, hybrid power supply, or both [15, 17, 18, 58, 63, 64]. For the same reason, also electric propulsion is now used for LNG tankers [19]. Service ships, such as tugboats and OSVs, use electric or hybrid propulsion with mechanical or hybrid power supply [4, 6–9, 12, 32–34, 36, 41–43]. For cruise ships, there are some which still use a mechanical power plant [79], but most use electric propulsion with a mechanical power supply, and also a hybrid power supply has been proposed [20, 77, 79–85]. Therefore, it can be concluded

that hybridization is the trend when designing the power plant, so for this thesis a power plant with hybrid propulsion and hybrid power supply will be used.

Now the type of propulsion and power supply is clear, the remaining degrees of freedom are the amount and type of main engines and electric machines coupled to the shaft, the amount and type of generator sets and batteries in the power supply (and if the latter will be recharged during the mission), a single shaft or a multiple shaft configuration, if the electric machine can only be used in PTO mode, PTI mode, or both, and also the type of electric grid; alternating current (AC) or direct current (DC).

MAIN ENGINES, ELECTRIC MACHINES, AND SHAFT CONFIGURATION

Based on the literature review in the work of [22], the main engines are often diesel engines, and the electric machines are often induction machines. Also, in theory there can be as many diesel engines and induction machines coupled to the shaft as long as the gearbox is properly designed, but usually no more then two diesel engines and a single induction machine are coupled to the same shaft [107]. However, in most hybrid power plants, not more than one diesel engine is coupled to the gearbox, so this will also be used in this thesis. For the induction machine it is assumed that only the PTI mode (motor mode) is used, to reduce complexity. Concerning the shaft configuration, cargo vessels often have a power plant with a single shaft configuration, while service and passenger ships use two shaftlines, as can be found in for example the work of [12, 55, 122, 123]. However, for normal operation they are often assumed to be equally loaded [107], which means that the propulsion loads for each shaft in a two shaft configuration is exactly half of the propulsion load of the shaft in a single shaft configuration. Thus, for a given power profile, the propulsion power demand has to be divided by two to find the load for each of the two shaft lines. Even more, these shaft lines are often identical, hence for the scope of this thesis only one shaft line will be modelled.

GENERATOR SETS AND BATTERIES

For redundancy, at least two generator sets (often diesel generator sets) should be installed [107], but more can be added, based on the required mission of the vessel, and the generator sets can either be of the same or different capacity. For batteries there is no such lower limit found in literature, which can be explained since batteries are often added to assist generator sets. Therefore, for the scope of this thesis it is assumed that the amount of generator sets is fixed at two (minimum amount), and the equipment modifications consist of adding, removing, or replacing batteries. To this end, the number of batteries will just be indicated with K. Furthermore, batteries can be charged or discharged during the mission, and it is assumed that all batteries are fully charged at the start of the mission.

ELECTRIC GRID

Conventionally, most marine vessels use an AC architecture for the electric grid, generally using 3.3, 6.6, or 11 kV at 50 or 60 Hz [14, 124]. Therefore, for this thesis also an AC architecture will be used, which implies that the engines of the generator sets run at synchronous speed, dictated by the required frequency f_{grid} of the AC grid. Furthermore

the DC power of the batteries has to be converted to AC power with frequency converters and since for this architecture the frequency of the grid is regulated by the generator sets, the power for the induction motor has to be converted from AC to AC, as this component often requires different frequencies than the generator sets provide. However, since the stability of the electric grid is not in the scope of this thesis, it is assumed that the required frequency converters (FC) for the batteries and the induction motor have a certain efficiency η_{FC}, and that they work properly.

To conclude, the most important assumptions of this section are listed below, and the described power plant can be seen in Figure 4.1, and will be used for further design in this chapter.

- Only one diesel engine and one induction machine are coupled to the same shaft
- Shaft lines are identical
- The induction machine is only used as motor
- The power plant contains two generator sets
- The power plant contains K rechargeable batteries
- At the start of the mission, each battery is fully charged

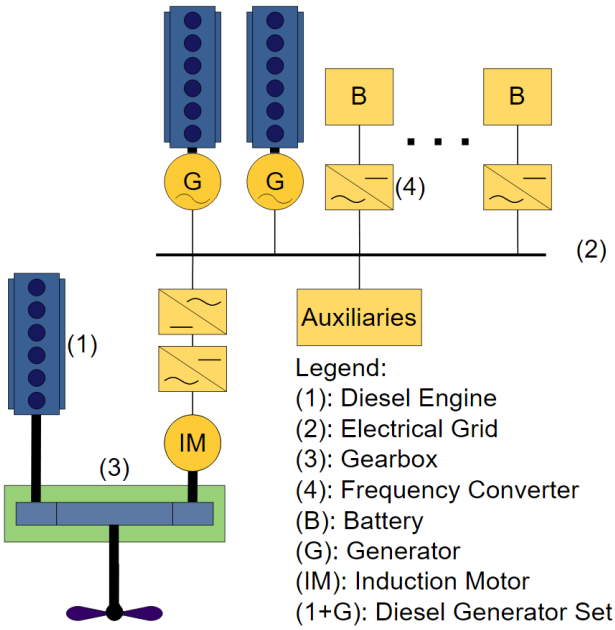

Figure 4.1: Power plant for modular control architecture

4.2. PRIMARY LEVEL CONTROL

The design of the primary level highly depends on the power plant layout of Figure 4.1, as it contains the controllers of the components in the power plant. Therefore, this section both discusses the components of the power plant as their controllers. Furthermore, as discussed in Chapter 1, a power plant consists of two parts; the propulsion and the power supply. To this end, first the propulsion will be discussed, followed by the power supply, and at last a total overview of the primary level control will be given.

4.2.1. PROPULSION PLANT

The power plant of Figure 4.1 uses hybrid propulsion, where a diesel engine (DE) and an induction motor (IM) are both connected to the same shaft. If only one of these two components is operating, shaft/rotor speed control is used, but according to the authors of [122], to be able to run the diesel engine and the induction motor in parallel, either the diesel engine runs in torque control and the induction motor in rotor speed control, or the diesel engine in shaft speed control and the induction motor in torque control. Furthermore, the authors have investigated both scenarios, and conclude that it is more efficient to run the diesel engine in torque control and the induction motor in rotor speed control for parallel operation, hence this will also be used in this thesis. Using this, a schematic of the hybrid propulsion together with the primary level controllers is shown in Figure 4.2.

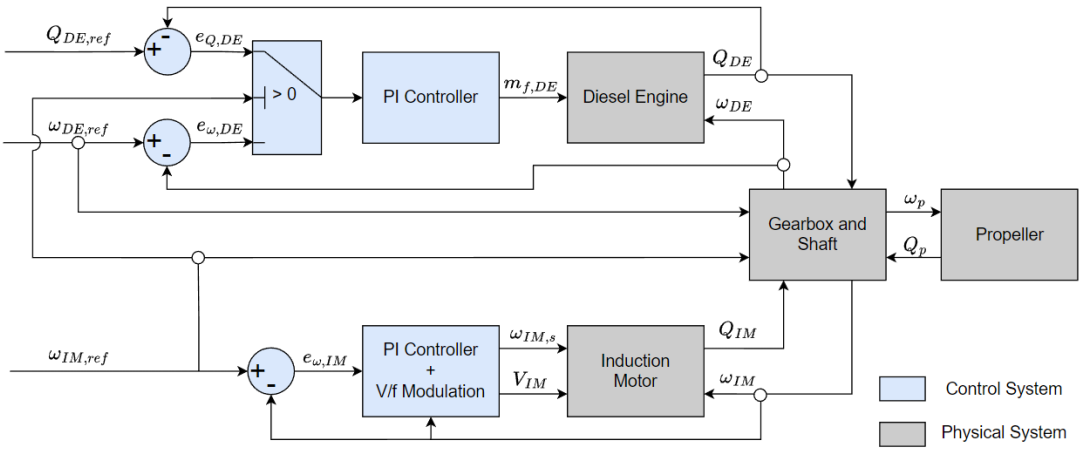

Figure 4.2: Schematic of the hybrid propulsion plant and primary level control

The signals $Q_{DE,ref}, \omega_{DE,ref}, Q_{IM,ref}$ are the reference-signals for the diesel engine torque Q_{DE} and shaft speed ω_{DE}, and the induction motor rotor speed ω_{IM}, respectively, provided by the secondary level of the control system. Also, a switch in front of the PI controller of the diesel engine can be seen, in order to switch from shaft speed control to torque control if the induction motor is switched on.

DIESEL ENGINE AND PI CONTROLLER

Diesel engines can be approximated with nonlinear or linear equations, depending on the level of accuracy needed [125]. Since the scope of this thesis is towards the modular design and control of the power plant, a relatively simple first order differential equation as found in the work of [125] will suffice, which can be seen in Equation 4.1:

$$\dot{Q}_{DE}(t) = -\frac{Q_{DE}(t)}{\tau_{DE}(t)} + k_{DE} \cdot m_{f,DE}(t) \tag{4.1}$$

where k_{DE} is the torque constant, $m_{f,DE}$ is the fuel index, and τ_{DE} is the torque buildup constant which determines the response speed of the diesel engine, as a function of the diesel engine shaft speed ω_{DE}:

$$\tau_{DE}(t) = \frac{0.9}{\omega_{DE}(t)} \tag{4.2}$$

Following the work of [122, 126, 127], the fuel index $m_{f,DE}$ is regulated with a PI controller. This controller, sometimes also refered to as the governor [128], either runs in shaft speed control or in torque control, based on the induction motor reference-signal, and this can be described using Equation 4.3 and 4.4:

Shaft Speed Control :

$$m_{f,DE}(t) = K_{P,DE} \cdot e_{\omega,DE}(t) + K_{I,DE} \int_{t=0}^{t} e_{\omega,DE}(t)\, dt \tag{4.3}$$

Torque Control :

$$m_{f,DE}(t) = K_{P,DE} \cdot e_{Q,DE}(t) + K_{I,DE} \int_{t=0}^{t} e_{Q,DE}(t)\, dt \tag{4.4}$$

where the proportional gain $K_{P,DE}$ and integral gain $K_{I,DE}$ are chosen such that the average acceleration time of the diesel engine is around a minute, as the authors of [127] mention that this is typical for most diesel engines. The shaft speed error e_ω and the torque error e_Q can be found using Equations 4.5 and 4.6:

$$e_{\omega,DE}(t) = \omega_{DE,ref}(t) - \omega_{DE}(t) \tag{4.5}$$

$$e_{Q,DE}(t) = Q_{DE,ref}(t) - Q_{DE}(t) \tag{4.6}$$

where ω_{DE} is the measured shaft speed, Q_{DE} the measured engine torque, and $\omega_{DE,ref}$ and $Q_{DE,ref}$ the references for the shaft speed and engine torque, respectively. At last, a schematic view of the PI controller and the diesel engine dynamics can be seen in Figure 4.3, where, following the notation of [12], the notion of $e_{Q,DE} \,||\, e_{\omega,DE}$ illustrates that either the torque control or the shaft speed control mode can be used.

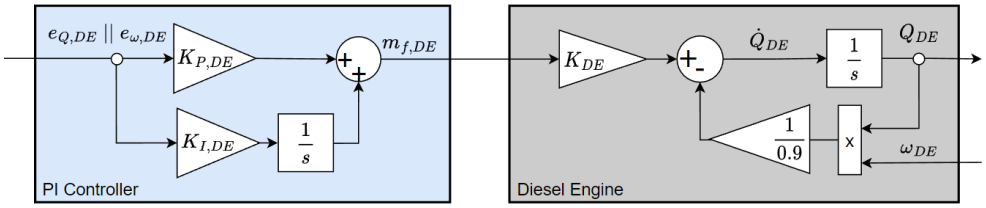

Figure 4.3: Schematic of PI controller for fuel injection and diesel engine dynamics

INDUCTION MOTOR, PI CONTROLLER AND V/F MODULATION

Induction motors are often called the workhorses of the industry [129], as they are simple, easy to maintain, and essentially run at constant speed from zero to full load [130]. The dynamics of an induction motor can be described using Equation 4.7.

$$Q_{IM}(t) = \frac{P_{IM,mec}}{2\omega_{IM}(t)} \frac{V_{IM}^2(t)}{\left(\frac{R_{s,IM}}{s(t)}\right)^2 + \left(\frac{\omega_{IM}(t)}{2\pi}(L_{r,IM} + L_{s,IM})\right)^2} \frac{R_{r,IM}}{s(t)} \tag{4.7}$$

where $P_{IM,mec}$ is the mechanical power, Q_{IM} is the generated torque, p_{IM} is the number of poles, ω_{IM} is the rotor speed, V_{IM} is the input voltage (in literature often refered to as phase voltage), s is the slip, $R_{r,IM}$ is the rotor resistance, $R_{s,IM}$ is the stator resistance, and $L_{r,IM}$ and $L_{s,IM}$ are the rotor inductance and stator inductance, respectively [130, 131]. The slip s is used to express the rotor speed with respect to the rotational speed of the magnetic field in the stator windings as follows:

$$s(t) = \frac{\omega_{IM,s}(t) - \omega_{IM}(t)}{\omega_{IM,s}(t)} \tag{4.8}$$

where $\omega_{IM,s}$ is the rotational speed of the magnetic field in the stator windings, also refered to as the stator speed. The motor dynamics of Equation 4.7 can be used to construct a so called torque-slip curve, shown in Figure 4.4, which shows the produced torque as a function of the stator speed and the slip. For the torque slip curve which includes condition N, when no load is attached to the rotor, $s = 0$ and $n_{IM} = n_s$, but if the motor is loaded, the slip increases linearly with the delivered torque until the full load Q_N is reached. If the induction motor is then loaded with an even higher load, slip increases even more. When the breakdown torque is reached, the rotor stops rotating and is locked, but still delivers torque (locked-rotor torque). However, since in practise the motor is only used between the zero load and full load conditions (between 0 and Q_N), for this thesis only the linear part of the torque-slip curve will be used, and this can be approximated up to 95% accuracy [130] with Equation 4.9:

$$Q_{IM}(t) = s(t) \frac{V_{IM}^2(t)}{R_{r,IM} k_{IM}} \tag{4.9}$$

where k_{IM} is a constant that depends on the motor characteristics. Now to control the induction motor, elaborate control strategies such as field-oriented control [132] or

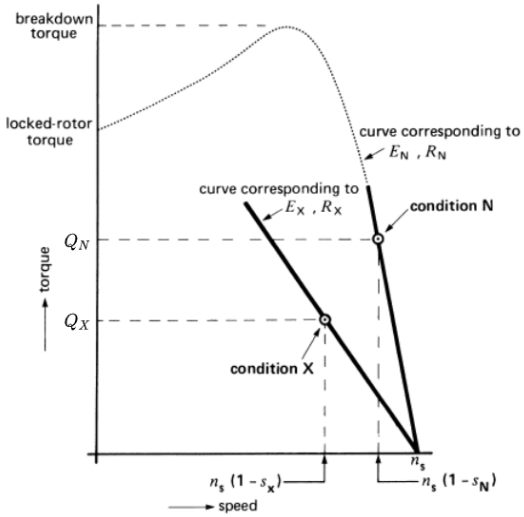

Figure 4.4: Torque-slip curve of an induction motor [130]

direct-torque control [133, 134] are seen in literature, but for the scope of this thesis, constant V/f control as described by the authors of [135, 136] suffices and will be used. This type of control uses constant voltage-frequency ratio, together with a PI controller that determines the required slip speed $\omega_{IM,slip}$ using the rotor speed reference $\omega_{IM,ref}$ and the measured rotor speed ω_{IM}, which can be seen in Equation 4.10:

$$\omega_{IM,slip}(t) = K_{P,IM} \cdot e_{\omega,IM}(t) + K_{I,IM} \int_{t=0}^{t} e_{\omega,IM}(t)\, dt \tag{4.10}$$

where the proportional gain $K_{P,IM}$ and integral gain $K_{I,IM}$ are chosen such that the average acceleration time of the induction motor is around a minute, similar to the diesel engine. The rotor speed error $e_{\omega,IM}$ can be found using equation 4.11:

$$e_{\omega,IM}(t) = \omega_{IM,ref}(t) - \omega_{IM}(t) \tag{4.11}$$

Furthermore, the characterising aspect of this type of control is that the ratio between the voltage V_{IM} and the stator speed $\omega_{IM,s}$ is kept constant, in order to ensure the maximum flux density in the IM and more safe operation [136], and the linear relation between the stator speed and the voltage can be seen in Equation 4.12:

$$\begin{aligned} V_{IM}(t) &= C_{V/f} \cdot \omega_{IM,s}(t) \\ &= C_{V/f} \cdot \big(\omega_{IM,slip}(t) + \omega_{IM}(t)\big) \end{aligned} \tag{4.12}$$

where $\omega_{IM,s}$ is stator speed in rad/s, and $C_{V/f}$ is the constant ratio between the stator speed and the voltage. Finally, a schematic of the described PI controller with V/f modulation and the induction motor dynamics can be seen in Figure 4.5.

*Note: the combination of the V/f control and the simplified IM model is not found in literature, but as will be shown later in this thesis, simulations show good performance

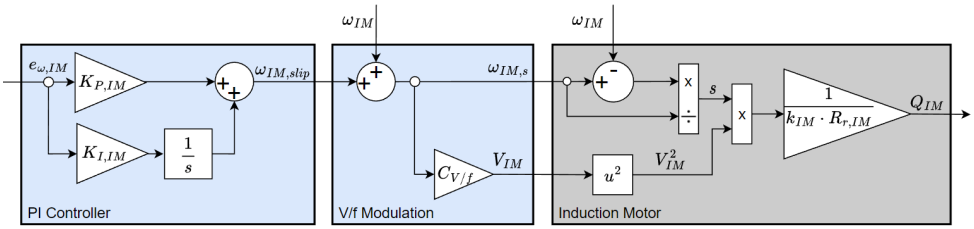

Figure 4.5: Schematic of PI controller with V/f modulation and induction motor dynamics

GEARBOX, SHAFT, AND PROPELLER DYNAMICS

As discussed earlier in this chapter, and also following from Figure 4.2, the diesel engine and the induction motor are both connected to the propeller through the gearbox. If losses are neglected, the gearbox and shaft dynamics can be described using a first order differential equation [12], which can be seen in Equation 4.13:

$$\dot{\omega}_p(t) = \frac{i_{DE} \cdot Q_{DE}(t) + i_{IM} \cdot Q_{IM}(t) - Q_p(t)}{J_{tot}} \tag{4.13}$$

where ω_p is the propeller speed, Q_p is the propeller torque, J_{tot} is the total inertia of the gearbox, induction motor and the diesel engine, and shaft together, and i_{DE} and i_{IM} the gear ratios of the diesel engine and the induction motor, respectively. However, since the gearbox has a certain efficiency η_T [100], the gearbox and shaft dynamics have to be altered such that this is not neglected. Therefore, η_T is included in the new gearbox and shaft dynamics, and this can be seen in Equation 4.14 to 4.16:

$$\dot{\omega}_p(t) = \frac{Q_{p,DE}(t) + Q_{p,IM}(t) - Q_p(t)}{J_{tot}} \tag{4.14}$$

$$Q_{p,DE} = \eta_T \cdot i_{DE} \cdot Q_{DE}(t) \tag{4.15}$$

$$Q_{p,IM} = \eta_T \cdot i_{IM} \cdot Q_{IM}(t) \tag{4.16}$$

Now in order to find the propeller torque Q_p the propeller dynamics are required, which are already discussed in Chapter 3.1.2. As a similar approach is found in the work of [125], the propeller dynamics are approximated as shown in Equation 4.17 and 4.18:

$$Q_p(t) = C_p \cdot |\omega_p(t)| \cdot \omega_p(t) \tag{4.17}$$

$$C_p = \frac{K_Q \cdot \rho \cdot D^5}{4\pi^2} \tag{4.18}$$

where ρ is the density of the seawater, D is the diameter of the propeller, and K_T and K_Q are the thrust and torque coefficients. Since the diesel engine, the induction motor, and the propeller are connected through the gearbox, the propeller speed ω_p can be used to compute the required feedback signals of ω_{DE} and ω_{IM} using their respective gear ratio's i_{IM} and i_{DE} as follows:

$$\omega_{IM} = i_{IM} \cdot \omega_p \tag{4.19}$$

$$\omega_{DE} = i_{DE} \cdot \omega_p \tag{4.20}$$

However, when either the diesel engine or the induction motor is switched off, their reference signals will be equal to zero. Therefore, since the found ω_{DE} and ω_{IM} are used as input to the PI controllers, the gearbox must include two clutches, in order to decouple the diesel engine and/or the induction motor from the propeller. Since this also affects the engine and motor torque used in the gearbox and shaft dynamics, the updated gearbox and shaft dynamics and the dynamics to find the shaft speed and rotor speed ω_{DE} and ω_{IM} are described in Equation 4.21 to 4.24:

$$Q_{p,DE} \begin{cases} \eta_T \cdot i_{DE} \cdot Q_{DE} & \omega_{DE,ref} > 0 \\ 0 & \omega_{DE,ref} = 0 \end{cases} \tag{4.21}$$

$$Q_{p,IM} \begin{cases} \eta_T \cdot i_{IM} \cdot Q_{IM} & \omega_{IM,ref} > 0 \\ 0 & \omega_{IM,ref} = 0 \end{cases} \tag{4.22}$$

$$\omega_{DE} \begin{cases} i_{DE} \cdot \omega_p & \omega_{DE,ref} > 0 \\ \dfrac{Q_{DE} - J_{DE} \cdot \dot{\omega}_{DE}}{D_{DE}} & \omega_{DE,ref} = 0 \end{cases} \tag{4.23}$$

$$\omega_{IM} \begin{cases} i_{IM} \cdot \omega_p & \omega_{IM,ref} > 0 \\ \dfrac{Q_{IM} - J_{IM} \cdot \dot{\omega}_{IM}}{D_{IM}} & \omega_{IM,ref} = 0 \end{cases} \tag{4.24}$$

where $J_{DE}, D_{DE}, J_{IM}, D_{IM}$ are used to describe the inertia and damping of the diesel engine and the induction motor when decoupled from the gearbox, respectively.

4.2.2. POWER SUPPLY

The components in the power plant generate electric power, i.e. for the auxiliary loads and for the induction motor. The power plant of interest includes two diesel generator sets and K batteries in the power supply. As will be discussed in this section, the power output of the diesel generator sets consist of both real and reactive power, while the power profile as discussed throughout this report only defines real power. Therefore, since the electric stability of the electric grid is not in the scope of this thesis, the focus of this section will be on the real power, and relatively simple models can be used to describe the behavior of these components.

DIESEL GENERATOR SETS AND PI CONTROLLERS

For almost a 100 years, a typical diesel generator set (DG) consists of a constant speed diesel engine (CSDE) driving a wounded-rotor synchronous generator [137]. To control such a generator set, traditionally two controllers which do not communicate with each other are used; a controller regulating the fuel intake of the diesel engine to maintain a

stable shaft speed, and a voltage controller to maintain a stable output voltage [138]. To this end, first the diesel engine and its controller are discussed, followed the generator dynamics and its voltage controller, and finally an overview of the total model will be provided.

Although the dynamics of the diesel engine and its controller required for propulsion are already discussed, this section redefines them as they are now used for a different diesel engine, as can be found in Equation 4.25:

$$\dot{Q}_{DG,DE}(t) = -\frac{Q_{DG,DE}(t)}{\tau_{DG}(t)} + k_{DG} \cdot m_{f,DG}(t) \tag{4.25}$$

where $Q_{DG,DE}$ is the generated torque of the diesel engine connected to the generator, k_{DG} is the torque constant, $m_{f,DG}$ is the fuel index, and τ_{DG} is the torque buildup constant which determines the response speed of the diesel engine, as a function of the diesel engine shaft speed ω_{DG}:

$$\tau_{DG}(t) = \frac{0.9}{\omega_{DG}(t)} \tag{4.26}$$

While the fuel index is also regulated with a PI controller, just as the diesel engine used for propulsion, instead of switching between shaft speed and torque control, only shaft speed control is used, and this is shown in Equation 4.27:

$$m_{f,DE}(t) = K_{P,DG_\omega} \cdot e_{\omega,DG}(t) + K_{I,DG_\omega} \int_{t=0}^{t} e_{\omega,DG}(t)\, dt \tag{4.27}$$

where the proportional gain K_{P,DG_ω} and integral gain K_{I,DG_ω} are chosen such that the average acceleration time of the diesel engine is around a minute. At last, the shaft speed error e_ω can be found using Equation 4.28:

$$e_{\omega,DG}(t) = \omega_{DG,ref}(t) - \omega_{DG}(t) \tag{4.28}$$

A typical wounded-rotor synchronous generator consists of a stator with sinusoidally distributed windings and a rotor with electromagnets. Therefore, where a diesel engine can be described with a relatively simple first order differential equations, the generator dynamics are described with a set of algebraic equations [139], based on the equivalent circuit of a diesel generator set as shown in Figure 4.6, where I_X is the excitation current of the rotor coils, V_0 is the induced voltage in the stator windings, X is the synchronous reactance, I_{DG} is the terminal/output current, V_{DG} is the terminal/output voltage, and R_{DG} is the representation of the load connected to the generator. As the focus of this thesis in on the real power, R_{DG} is assumed to be purely resistive, and is assumed to be represented by Equation 4.29:

$$R_{DG}(t) = \frac{V_{DG,ref}^2(t)}{P_{DG}(t)} \tag{4.29}$$

where P_{DG} is the required generator power, provided by the secondary level control, and $V_{DG,ref}$ is the reference signal for the measured voltage V_{DG} across the generators resistive load R_{DG}. Where the latter is independent of generator characteristics and dynamics, the complex internal reactance X is not, as can be seen Equation 4.30:

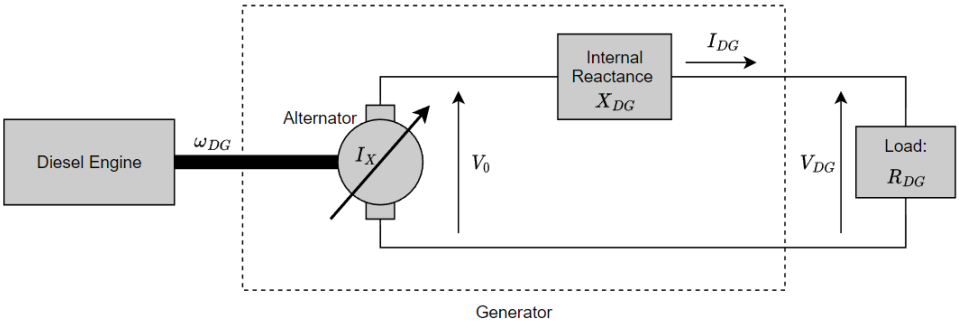

Figure 4.6: Equivalent circuit of a diesel generator set [139]

$$X_{DG}(t) = R_{DG,int} + j \cdot L_{DG} \cdot \omega_{DG}(t) \tag{4.30}$$

where $R_{DG,int}$ is the internal resistance, L_{DG} is the inductance, and j is the imaginary number. Using this, and applying Kirchoff's law to the circuit of Figure 4.6, the complex current I_{DG} and voltage V_{DG} are given by:

$$I_{DG}(t) = \frac{V_0(t)}{X + R_{DG}(t)} \tag{4.31}$$

$$V_{DG}(t) = I_{DG}(t) \cdot R_{DG}(t) = V_0(t) \cdot \frac{R_{DG}(t)}{X_{DG}(t) + R_{DG}(t)} \tag{4.32}$$

From these expressions it can be seen that V_{DG} decreases for increasing values of X, hence the efficiency of the generator (typically around 0.95% [64]) mainly depends on $R_{DG,int}$ and L. The induced voltage V_0 to provide the required output voltage can be described using the shaft speed ω_{DG} and the exciting current I_X as shown in Equation 4.33:

$$V_0(t) = f(I_X(t)) \cdot \frac{\omega_{DG}(t)}{2\pi} \tag{4.33}$$

where $f(I_X(t))$ is experimentally determined by the authors of [139], which they found to be adequately described by Equation 4.34:

$$f(I_X(t)) = a_{G,1} \cdot I_X(t) + a_{G,0} \tag{4.34}$$

with $a_{G,1}$ and $a_{G,0}$ being constant. To maintain a stable output voltage of the generator, typically an Automatic Voltage Regulator (AVR) is used [138, 140], also refered to as excitation control [141]. Furthermore, the authors of [142] mention that for power plants where two or more generator sets are connected to the same grid, 'fighting' can occur, meaning that both generator sets try to pull the grid frequency and voltage to their individual settings. However, since the electrical stability of the grid is not in the scope of

this thesis, the output voltage V_{DG} of the generator is controlled using a PI controller that regulates the excitation current I_X as shown in Equation 4.35:

$$I_X(t) = K_{P,DG_V} \cdot e_{V,DG}(t) + K_{I,DG_V} \int_{t=0}^{t} e_{V,DG}(t)dt \tag{4.35}$$

where K_{P,DG_V} and K_{I,DG_V} are the proportional and integral gains of the PI voltage controller, and e_V is the voltage error as defined in 4.36:

$$e_{V,DG}(t) = V_{DG,ref}(t) - |V_{DG}(t)| \tag{4.36}$$

where $|V_{DG}|$ denotes the absolute value of the output voltage, as this can take complex values. Furthermore, to produce electrical power, torque is required, and this can be expressed using the exciting current and output current, as shown in Equation 4.37.

$$Q_{DG,G}(t) = \frac{f(I_X(t)) \cdot Re(I_{DG}(t))}{2\pi} \tag{4.37}$$

where $Q_{DG,G}$ is the generator torque exerted on the shaft that connects the generator to the diesel engine. Using both the torque of the engine and the generator, the shaft dynamics can be described by Equation 4.38:

$$\dot{\omega}_{DG}(t) = \frac{Q_{DG,DE}(t) - Q_{DG,G}(t)}{J_{DG}} \tag{4.38}$$

where J_{DG} represents the inertia of the shaft. Finally, an overview of the diesel generator set and its controllers can be seen in Figure 4.7.

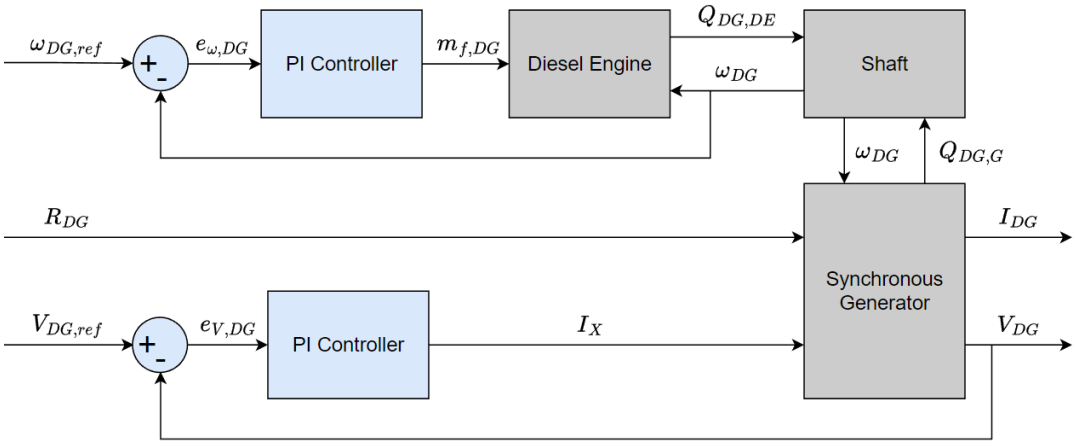

Figure 4.7: Shaft speed and voltage control of a diesel generator set

BATTERIES AND BATTERY CONSTRAINT MODULES

As the power supply contains K batteries, which can either be charged or discharged, a proper battery model has to be included, such that the control system is able to monitor the conditions of each battery, e.g. the state of charge [143]. For the scope of this thesis, a battery is described using the model shown in Figure 4.8, where R_B is the internal

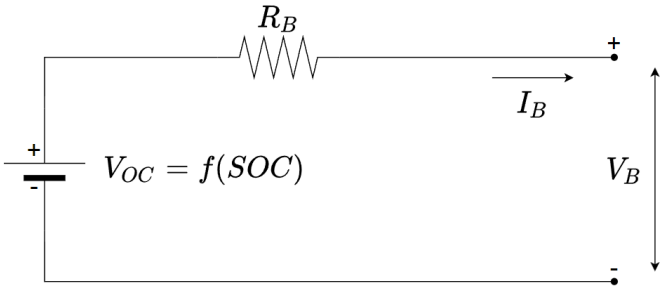

Figure 4.8: Equivalent circuit of a battery [12, 144]

resistance, I_B the battery output current (positive for discharging), V_B is the battery terminal/output voltage, and V_{OC} is the battery open circuit voltage, which is a function of the SOC. Using this, V_B is described as:

$$V_B(t) = V_{OC}(t) - R_B \cdot I_B(t) \tag{4.39}$$

How exactly the V_{OC} relates to the SOC depends on the battery characteristics, but in literature this relation is often described as a nonlinear relation [145–152]. However, as also can be seen in literature, between certain limits of the SOC, the relation between the V_{OC} and the SOC can be approximated linear, although the described values of these limits for which this holds vary. Still, following the notation of the authors of [153], the relation between the V_{OC} and the SOC, will be described using Equation 4.40:

$$V_{OC}(t) = a_{B,1} \cdot SOC(t) + a_{B,0} \tag{4.40}$$

with $a_{B,1}$ and $a_{B,0}$ being constants. Now, to obtain knowledge about the SOC during charging or discharging of the battery, Coulomb counting can be used [152–154]. Using this method, the SOC can be determined as shown in Equation 4.41:

$$SOC(t) = SOC(t_0) - \frac{1}{C_0}\int_{t=0}^{t} I_B(t)dt \tag{4.41}$$

where C_0 is the capacity of the battery, $SOC(t_0)$ is the initial SOC of the battery, and $I_B(t)$ is the (dis)charging current of Figure 4.8. Using this, the model of Figure 4.9 can be used to approximate the battery dynamics and estimate the SOC,

As mentioned, the SOC has to remain between certain limits, affecting the power that can be drawn or supplied to the battery. Furthermore, battery manufacturers prescribe a minimum and a maximum value for the open circuit voltage V_{OC}. Using this, and following the work of [12], a total of four constraints can be constructed, and these are shown in Equation 4.42 to 4.45.

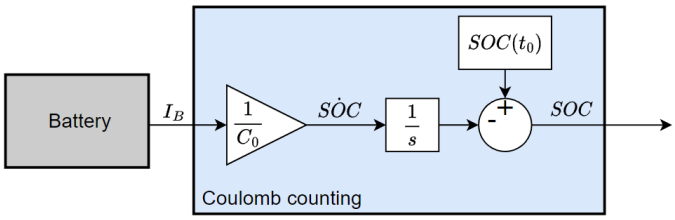

Figure 4.9: Battery and coulomb counting

$$P_{B,V}^{max} = \frac{V_{OC} \cdot V_{B,min} - V_{B,min}^2}{R_B} \tag{4.42}$$

$$P_{B,V}^{min} = \frac{V_{B,max}^2 - V_{OC} \cdot V_{B,max}}{R_B} \tag{4.43}$$

$$P_{B,SOC}^{max} = \frac{SOC - SOC_{min}}{\Delta t} \cdot C_0 \cdot V_{OC} \tag{4.44}$$

$$P_{B,SOC}^{min} = \frac{SOC - SOC_{max}}{\Delta t} \cdot C_0 \cdot V_{OC} \tag{4.45}$$

Here, $V_{B,min}$, $V_{B,max}$, SOC_{min}, and SOC_{max} are the minimum and maximum terminal voltage V_B and minimum and maximum SOC of the battery, respectively, provided by the battery manufacturer. Furthermore, Δt is a discrete timestep, which can be tuned to alter the power constraints related to the SOC of the battery. Now, at each moment during the mission, the secondary level controller has to ensure that the power required from the battery is within these limits, hence the minimum and maximum of the above constraints has to be determined using Equation 4.46 and 4.47:

$$P_B^{min} = max\left(P_{B,SOC}^{min}, P_{B,V}^{min}\right) \tag{4.46}$$

$$P_B^{max} = min\left(P_{B,SOC}^{max}, P_{B,V}^{max}\right) \tag{4.47}$$

Inspired by the work of [155], where hardware is equipped with a memory that contains the required information about that hardware, required by the control system, as in literature the battery constraints are often included in the secondary level of the power plant control system, in this thesis the constraints listed in Equation 4.42 to 4.47, together with the SOC estimation of Equation 4.41, are stored in a battery constraint module, which can be included in the primary level control. Resulting, for battery replacements, additions or removals, these modules also have to be adjusted accordingly, and for the scope of this thesis it is assumed that for replacements or additions of batteries only the capacity of the battery changes. Using this, the constraint module uses the specified discrete timestep Δt, data of the manufacturer, the initial state-of-charge $SOC(t_0)$, measured battery current I_B, the required power of the battery P_B, and the capacity C_0

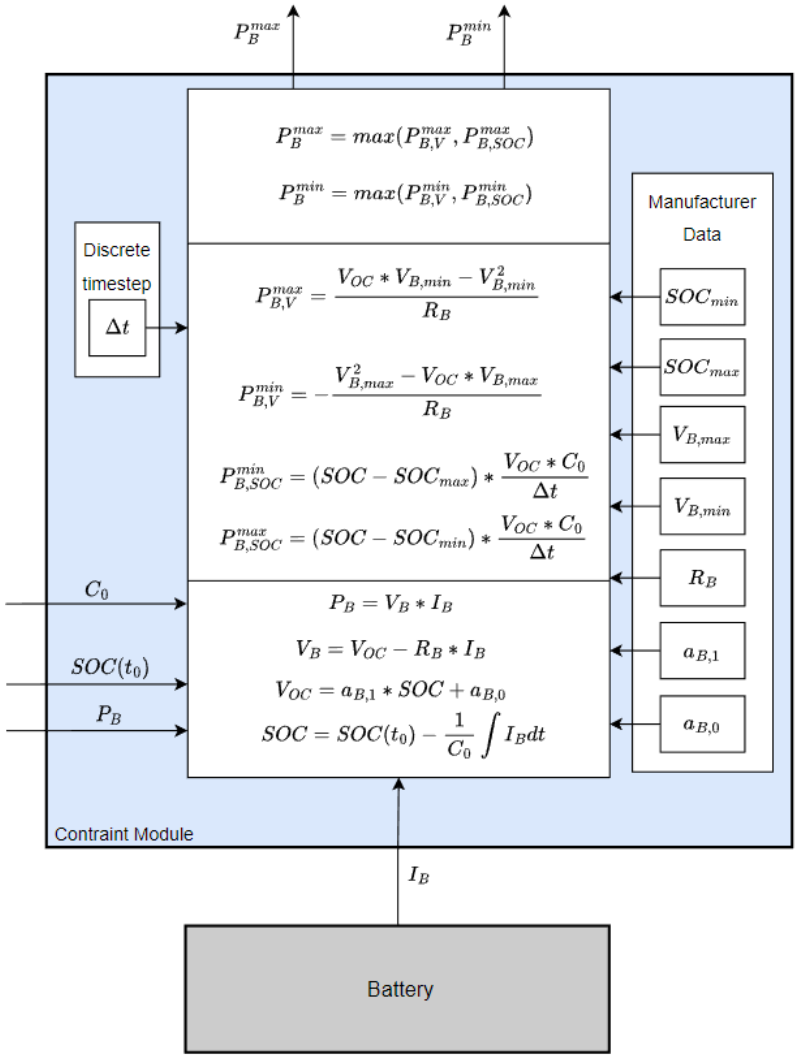

Figure 4.10: Battery and constraint module

to determine the range $[P_B^{min} \quad P_B^{max}]$ for the power of the battery, and this is communicated to the secondary level controller. This removes the need for any reference signals, as the power assigned to the battery can be directly given to the battery constraint module. A schematic representation of the battery and the constraint module can be seen in Figure 4.10. Finally, an overview of all the components in the power plant with their primary level controllers can be give, and this is shown in Figure 4.11. In the next section, the secondary level will be discussed, in order to determine the power split and the required reference-signals for the primary level and the power plant.

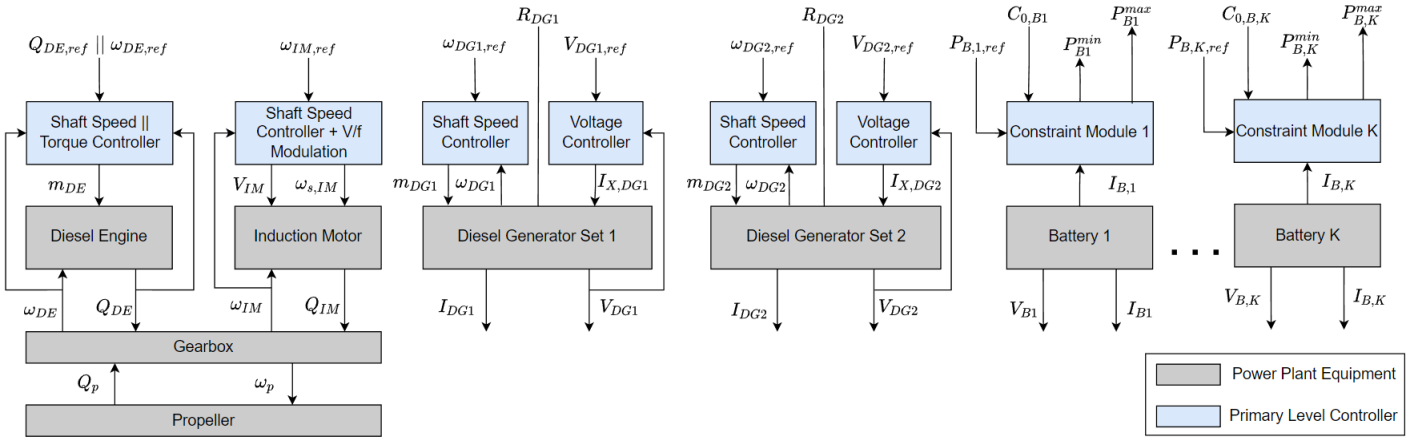

Figure 4.11: Primary level control and power plant

4.3. SECONDARY LEVEL CONTROL

As discussed in the previous sections, the secondary level power plant control determines the power split for the power plant components, and in order to realize this power split, corresponding reference-signals have to be provided for the primary level. It is also shown that often ECMS is used to fulfill the former of these tasks, and in this thesis this will also be the case. Then, after the required power for each component is determined by implementing this strategy, the primary level of the power plant (as described in the previous section) is used to derive the required reference-signals for each controller of that level. Before the ECMS strategy will be discussed, an Energy Flow Diagram (EFD), as described in the work of [100], is provided in Figure 4.12, constructed using the power plant of Figure 4.1. The arrows show the direction of the energy, and are also labeled to be able to clearly describe the power required for each component.

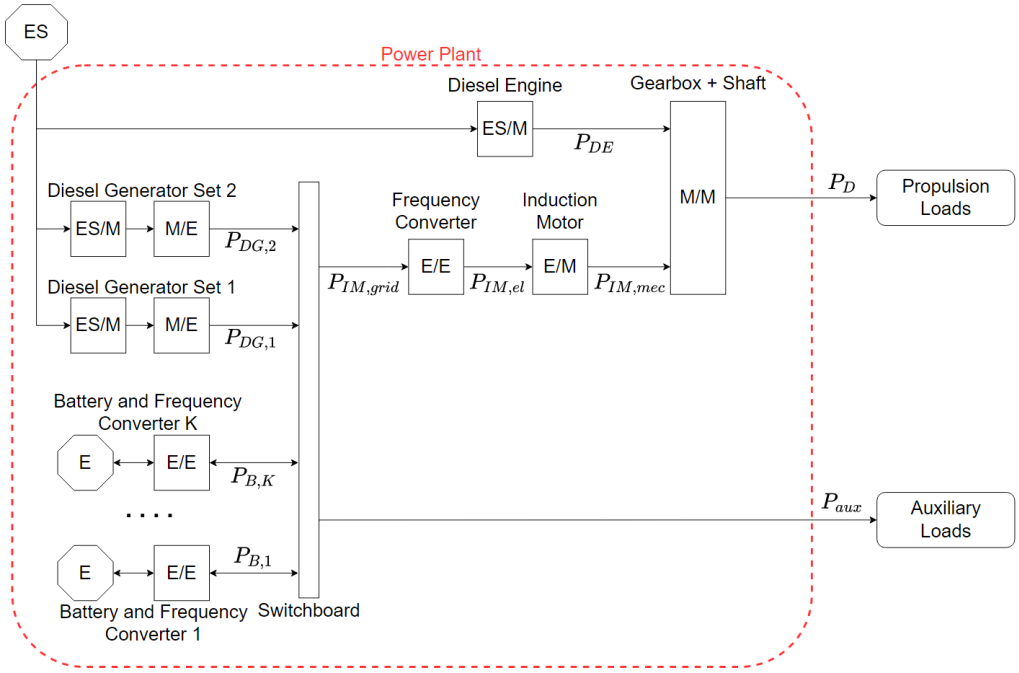

Figure 4.12: Energy flow diagram of the hybrid power plant

Here, the external energy (fuel) for the diesel engine and the diesel generator sets is indicated with ES, the electrical energy sources such as the batteries with an E, mechanical energy as M, the conversion from mechanical energy to electrical energy with M/E (and vice versa with E/M), and for the frequency converters connected to the batteries and the induction motor, the conversion is from electric energy to electric energy, hence indicated with E/E. At last, as the gearbox and shaft take mechanical energy from both the diesel engine as the electric machine and transmits this to the propeller, there is a conversion from mechanical energy to mechanical energy, hence this is indicated with M/M.

4.3.1. EQUIVALENT CONSUMPTION MANAGEMENT STRATEGY

To determine the power split, the Equivalent Consumption Minimization Strategy (ECMS) is used, which is a strategy that expresses the power of each component in terms of fuel consumption, and defines an instantaneous cost function at each time step during the mission [8]. In order to find the the optimum power split, the instantaneous cost function has to be minimized appropriately at each time step. The approach shown in this section is mostly based on the work of [4, 7]. The authors describe that in order to determine the power split using the ECMS, next to the objective to minimize the fuel consumption, the required propulsion and auxiliary power demand has to be met, but also it has to be ensured that the required power from or towards the power plant components does not exceed their capabilities. Therefore, the constraints for the propulsion and auxiliary power demand are derived using Figure 4.12, and are shown in 4.48 and 4.49, respectively.

$$P_D = \eta_T \cdot i \cdot \left(P_{DE} + P_{IM,mec}\right) \tag{4.48}$$

$$P_{aux} = \sum_{j=1}^{2} P_{DG,j} + \sum_{k=1}^{K} P_{B,k} - \frac{i \cdot P_{IM,mec}}{\eta_{IM} \cdot \eta_{FC}} \tag{4.49}$$

where $i \in [1,2]$ denotes the number of shaft lines, η_T is the transmission efficiency, η_{FC} is the frequency converter efficiency, and η_{IM} is the efficiency of the induction motor, and in general the following bounds for these efficiencies are found [64, 99, 119]:

$$0.92 \leq \eta_T \leq 0.95 \tag{4.50}$$

$$0.95 \leq \eta_{IM} \leq 0.97 \tag{4.51}$$

$$0.65 \leq \eta_{FC} \leq 0.99 \tag{4.52}$$

Since the objective is to minimize the fuel consumption, the cost function has to include the fuel consumption for each component, and has to depend on the required power of the components in order to determine a power split. As the induction motor simply converts power provided by the electrical grid to mechanical power for the gearbox, this component can be excluded from the cost function. To this end, the fuel consumption of the diesel engine, diesel generator sets, and the batteries will be discussed next.

DIESEL ENGINE FUEL CONSUMPTION

The diesel engine can work alone to provide propulsion power to the shaft when the induction motor is shut down, work together with the induction motor, or can be shut down, and the induction motor provides the total required propulsion power. Evidently, the power of the engine P_{DE} depends on the required propulsion power P_D and the delivered power of the induction motor $P_{IM,mec}$ as follows:

$$P_{DE} = \frac{P_D}{i \cdot \eta_T} - P_{IM,mec} \tag{4.53}$$

Using the required engine power P_{DE} and the measured engine speed ω_{DE}, the Specific Fuel Oil Consumption (SFOC) can be determined [12], using the relation shown in Equation 4.54:

$$SFOC_{DE} = a_1^{DE} \cdot {P_{DE}}^2 + a_2^{DE} \cdot P_{DE} + a_3^{DE} \cdot \omega_{DE}^2 + a_4^{DE} \cdot \omega_{DE} + a_5^{DE} \cdot P_{DE} \cdot \omega_{DE} + a_6^{DE} \tag{4.54}$$

where $a_1^{DE} - a_6^{DE}$ are constants depending on the engine characteristics. Then, using the work of [156], the fuel consumption (g) after a certian time interval Δt can be expressed as follows:

$$m_{DE} = i \cdot SFOC_{DE} \cdot P_{DE} \cdot \Delta t \tag{4.55}$$

Filling in the found relation for the SFOC of Equation 4.54, the fuel consumption can be written as:

$$m_{DE} = \tag{4.56}$$
$$i \cdot \left(a_1^{DE} \cdot {P_{DE}}^2 + a_2^{DE} \cdot P_{DE} + a_3^{DE} \cdot \omega_{DE}^2 + a_4^{DE} \cdot \omega_{DE} + a_5^{DE} \cdot P_{DE} \cdot \omega_{DE} + a_6^{DE}\right) \cdot P_{DE} \cdot \Delta t$$

DIESEL GENERATOR SETS FUEL CONSUMPTION

The power from the generator sets can be used to supply the auxiliary systems, the induction motor, and also to charge the battery. Therefore, the power required from the generator sets can be described as a function of these three elements, and using Equation 4.49 the required power from the generators is described by Equation 4.57:

$$\sum_{j=1}^{2} P_{DG,j} = P_{aux} - \sum_{k=1}^{K} P_{B,k} + \frac{i \cdot P_{IM,mec}}{\eta_{IM} \cdot \eta_{FC}} \tag{4.57}$$

As a diesel generator set consists of a diesel engine and a generator, and the latter converts mechanical power of a diesel engine into electrical power, the fuel consumption can also be expressed using the SFOC of the diesel engine. Taking into account the efficiency of the generator η_{DG}, typically around 0.95 [64], the SFOC of a diesel generator set can be given by Equation 4.58:

$$SFOC_{DG,j} = a_1^{DG,j} \cdot \left(\frac{P_{DG,j}}{\eta_{DG,j}}\right)^2 + a_2^{DG,j} \cdot \frac{P_{DG,j}}{\eta_{DG,j}} + a_3^{DG,j} \tag{4.58}$$

where $j \in [1,2]$ denotes the j-th diesel generator set, and $a_1^{DG,j} - a_3^{DG,j}$ are constants depending on the engine characteristics. As can be noted, for the diesel generator set the shaft speed is not of importance. This is due to the constant speed of the engine, in order to maintain a stable grid frequency, hence the terms depending on the shaft speed ω_{DG} are captured in the constant $a_3^{DG,j}$. Now the fuel consumption of the diesel generator sets can be found by multiplying the SFOC with the required power and a certain time interval, as described with Equation 4.59:

$$m_{DG,j} = SFOC_{DG,j} \cdot \frac{P_{DG,j}}{\eta_{DG,j}} \cdot \Delta t \tag{4.59}$$

Filling in the details, this can be written as:

$$m_{DG,j} = \left(a_1^{DG,j} \cdot \left(\frac{P_{DG,j}}{\eta_{DG,j}} \right)^3 + a_2^{DG,j} \cdot \left(\frac{P_{DG,j}}{\eta_{DG,j}} \right)^2 + a_3^{DG,j} \cdot \frac{P_{DG,j}}{\eta_{DG,j}} \right) \cdot \Delta t \tag{4.60}$$

At last, since there are two generator sets, to find the total fuel consumption the sum of their individual fuel consumption has to be taken, such that:

$$m_{DG} = \sum_{j=1}^{2} m_{DG,j} \tag{4.61}$$

BATTERIES EQUIVALENT CONSUMPTION

The batteries can be used to supply power to the auxiliaries, to the induction motor, or they can be charged with power from the generator sets. A positive sign for the battery power indicates discharging, and a negative sign indicates charging. As for diesel engines the SFOC curve describes the fuel consumption for a given power output, for batteries this is not the case. Therefore the approach from the ECMS strategy described in [12] is used to express the equivalent fuel consumption (g/kWh) of each battery $k \in [1, ..., K]$ as given by Equation 4.62:

$$c_{sfoc,eqv} = \frac{s_{eqv} \cdot \eta_{B,k}{}^{sign(P_{B,k})}}{Q_{lhv}} \tag{4.62}$$

where $\eta_{B,k}$ is the efficiency of the k-th battery, typically 0.98 [4] , Q_{lhv} is the lower heating value of the fuel, and s_{eqv} is the equivalence factor. In the first formulation of ECMS by [157], s_{eqv} depends on whether the battery is charging or discharging, but according to the authors of [12], using a constant value practically yields the same results. They also state that the value of the equivalence factor s_{eqv} can be chosen such that it reflects the nominal fuel consumption of the diesel engines, corrected for the efficiency of the components between the batteries and the shaft. Since the battery power is defined as the power of the electrical grid from/towards the battery's frequency converter, as can be seen in Figure 4.12, there is a single frequency converter and an induction motor left between the battery and the shaft, resulting the equivalence factor given in Equation 4.63:

$$s_{eqv} = SFOC_{DE,nom} \cdot \eta_{FC} \cdot \eta_{IM} \cdot Q_{lhv} \tag{4.63}$$

where $SFOC_{DE,nom}$ is the nominal fuel consumption of the diesel engine. Using this result and Equation 4.62, the equivalent consumption of a battery can be written as:

$$c_{sfoc,eqv} = SFOC_{DE,nom} \cdot \eta_{FC} \cdot \eta_{IM} \cdot \eta_{B,k}{}^{sign(P_{B,k})} \tag{4.64}$$

where the chosen value for $SFOC_{DE,nom}$ could be adjusted to affect the use of the battery power during a mission, as this value acts as a weighting function [4]. Using the found equivalent consumption of a battery, the fuel consumption can be expressed as shown in Equation 4.65 and Equation 4.66:

$$m_{B,k} = c_{sfoc,eqv} \cdot P_{B,k} \cdot \Delta t \tag{4.65}$$

$$m_{B,k} = SFOC_{DE,nom} \cdot \eta_{FC} \cdot \eta_{IM} \cdot \eta_{B,k}{}^{sign(P_{B,k})} \cdot P_{B,k} \cdot \Delta t \tag{4.66}$$

Now the total fuel consumption of all the batteries is just the sum of the fuel consumption of each battery, as shown in Equation 4.67:

$$m_B = \sum_{k=1}^{K} m_{B,k} \tag{4.67}$$

TOTAL FUEL CONSUMPTION

The total fuel consumption consist of the contributions of all the relevant components in the power plant. Since the objective is to minimize the fuel consumption for a mission, and the power split is not known a priori, it is also not known how long each component delivers a certain amount of power. Therefore, instead of the fuel consumption, the fuel consumption rate will be minimized at each time instant, in order to provide the optimum power split throughout the whole mission. Therefore, the derivation of the total fuel consumption rate can be found in Equation 4.68 to 4.70, which can be used to construct the final ECMS structure.

$$m_{T,K} = m_{DE} + \sum_{j=1}^{2} m_{DG,j} + \sum_{k=1}^{K} m_{B,k} \tag{4.68}$$

$$\dot{m}_{T,K} = \frac{1}{\Delta t} \cdot m_T = \frac{1}{\Delta t} \cdot \left(m_{DE} + \sum_{j=1}^{2} m_{DG,j} + \sum_{k=1}^{K} m_{B,k} \right) \tag{4.69}$$

$$\begin{aligned} \dot{m}_{T,K} = i \cdot \Big(& a_1^{DE} \cdot {P_{DE}}^3 + a_2^{DE} \cdot {P_{DE}}^2 + a_3^{DE} \cdot \omega_{DE}^2 \cdot P_{DE} \\ & + a_4^{DE} \cdot \omega_{DE} \cdot P_{DE} + a_5^{DE} \cdot {P_{DE}}^2 \cdot \omega_{DE} + a_6^{DE} \cdot P_{DE} \Big) \\ & + \sum_{j=1}^{2} \left(a_1^{DG,j} \cdot \left(\frac{P_{DG,j}}{\eta_{DG,j}} \right)^3 + a_2^{DG,j} \cdot \left(\frac{P_{DG,j}}{\eta_{DG,j}} \right)^2 + a_3^{DG,j} \cdot \frac{P_{DG,j}}{\eta_{DG,j}} \right) \\ & + \sum_{k=1}^{K} \left(SFOC_{DE,nom} \cdot \eta_{FC} \cdot \eta_{IM} \cdot {\eta_{B,k}}^{sign(P_{B,k})} \cdot P_{B,k} \right) \end{aligned} \tag{4.70}$$

where $m_{T,K}$ is the total fuel consumption of the discussed power plant with K batteries.

ADDITIONAL CONSTRAINTS

As discussed in [8], the ECMS strategy defines a minimization problem which has to be solved at each time step to find the optimum power split. Also, the authors of [4, 7] indicate that the power split has to meet several constraints, such as meeting the propulsion and auxiliary power demand, and that the power required of each component is within its limits. However, to the best knowledge of the authors of this paper, little to no literature exists on an ECMS problem with multiple batteries operating next to each other. In fact, in for example the work of [12] the discussed power plant includes two identical batteries, but the authors model and simulate them as a single battery. Where in that case this leads to no significant issues, for scenarios where the power plant includes two or more batteries which are not identical, this can cause significant errors, as will be

shown Chapter 5. When for example two batteries with different capacities C_0 are both discharged at the same rate, the battery with a smaller C_0 will be drained sooner than the other. However, if these batteries are modeled as one, the control system fails to recognise that the smaller battery is already drained, so the power split will still include this battery (as the system thinks it still has some energy left). As there is actually no energy left in the smaller battery, the power split is not being met.

When only the constraints and cost function found in existing work on the ECMS are used to compute the power split for multiple batteries, it is found that batteries will charge each other, meaning that for example a larger battery will be discharged, in order to charge the smaller battery. One way to deal with this problem is by adding constraints for the batteries, and it is experimentally found that the constraints shown in Equation 4.71 and 4.72 are required to provide a stable power split, as these constraints ensure that at each point in the mission, all K batteries in the power plant either charge or discharge.

$$P_{B,K} \cdot P_{B,1} \geq 0 \tag{4.71}$$

$$P_{B,n} \geq P_{B,n-1} \qquad \text{for } k \in [2,...,K] \tag{4.72}$$

FINAL ECMS FORMULATION

Using these additional constraints, the ECMS, which is basically a minimization problem, required to find the power split for a power plant with K batteries can be found below. Note that in the notation the number K is used, which indicates that for the discussed power plant with any number of batteries K, the same formulation can be used, and only K has to be filled in to find the required ECMS formulation.

$$\min\{\dot{m}_{T,K}\} \tag{4.73}$$

subject to the following constraints:

$$0 \leq P_{DE} \leq P_{DE}^{max} \tag{4.74}$$

$$P_{DE} \geq \frac{P_D}{i \cdot \eta_T} - P_{IM,mec} \tag{4.75}$$

$$0 \leq P_{DG,j} \leq P_{DG,j}^{max} \qquad \text{for } j \in [1,2] \tag{4.76}$$

$$\sum_{j=1}^{2} P_{DG,j} \geq P_{aux} - \sum_{k=1}^{K} P_{B,k} + \frac{i \cdot P_{IM,mec}}{\eta_{IM} \cdot \eta_{FC}} \tag{4.77}$$

$$0 \leq P_{IM,mec} \leq P_{IM,mec}^{max} \tag{4.78}$$

$$P_{B,k}^{min} \leq P_{B,k} \leq P_{B,k}^{max} \qquad \text{for } k \in [1,...,K] \tag{4.79}$$

$$P_{B,K} \cdot P_{B,1} \geq 0 \qquad \text{for } K \geq 2 \tag{4.80}$$

$$P_{B,k} \geq P_{B,k-1} \qquad \text{for } k \in [2,...,K] \tag{4.81}$$

where the output of the ECMS is the power split: $[P_{DE}; P_{IM,mec}; P_{DG,1}; P_{DG,2}; P_{B,1}; ...; P_{B,K}]$.

REFERENCE-SIGNALS

Once the power split is found with the aforementioned ECMS, the reference-signals can be generated, which are determined using the power plant of Figure 4.1 and the discussed primary controllers. First the components in the propulsion are discussed, hence the required propeller speed is required. The latter can be found using the required propulsion power P_D from the power profile and Equation 3.21, such that the propeller speed reference $\omega_{p,ref}$ can be written as:

$$\omega_{p,ref} = \sqrt[3]{\frac{P_D}{C_p}} \tag{4.82}$$

Since the propeller is coupled to the gearbox together with the diesel engine and the induction motor, the required propeller speed $\omega_{p,ref}$ dictates the shaft speed reference-signal for the diesel engines and induction motors shaft speed controllers, $\omega_{DE,ref}$ and $\omega_{IM,ref}$ as shown in Equation 4.83 and 4.84.

$$\omega_{DE,ref} \begin{cases} i_{DE} \cdot \omega_{p,ref} & P_{DE} > 0 \\ 0 & P_{DE} = 0 \end{cases} \tag{4.83}$$

$$\omega_{IM,ref} \begin{cases} i_{IM} \cdot \omega_{p,ref} & P_{IM,mec} > 0 \\ 0 & P_{IM,mec} = 0 \end{cases} \tag{4.84}$$

where i_{DE} and i_{IM} are the gearbox ratios of the diesel engine and the induction motor to the propeller, respectively. Now, using the assigned power to the diesel engine P_{DE} (from the power split), the torque reference-signal for the diesel engines torque controller $Q_{DE,ref}$ can be found using Equation 4.85:

$$Q_{DE,ref} \begin{cases} \dfrac{P_{DE}}{\omega_{DE,ref}} & P_{DE} > 0 \\ 0 & P_{DE} = 0 \end{cases} \tag{4.85}$$

Second, the components in the power supply of the power plant are discussed. This system includes two generator sets and K batteries, all connected to the grid. To ensure a stable grid frequency f_{grid} and grid voltage V_{grid}, proper reference-signals for the generator sets and batteries are required, and the shaft speed reference for each generator set is given by Equation 4.86:

$$\omega_{DG,j,ref} = f_{grid} \cdot \frac{4\pi}{p_{G,j}} \qquad \text{for } j \in [1,2] \tag{4.86}$$

where $p_{G,j}$ is the amount of poles of the generator j. The grid voltage V_{grid} is given as reference-signal to the voltage controller of the generator as shown in Equation 4.87

$$V_{DG,j,ref} = V_{grid} \tag{4.87}$$

At last, to simulate the behavior or the generator set, the load resistance R_{DG} is required (as described in Section 4.2), and is determined using Equation 4.88

$$R_{DG,j} = \frac{V_{DG,j,ref}^2}{P_{DG,j}} \qquad \text{for } j \in [1,2] \tag{4.88}$$

where $P_{DG,j}$ is the power assigned to generator set j as defined by the power split. As the required battery power $P_{B,k}$ can be directly given to the battery constraint module, for further use in this report, the reference-signals can be given as:

$$u_{ref,K} = [Q_{DE,ref},\ \omega_{DE,ref},\ \omega_{IM,ref},\ \omega_{DG,1,ref},\ R_{DG,1},\ V_{DG,1,ref},\ \omega_{DG,2,ref},\ R_{DG,2},\ V_{DG,2,ref}, P_{B,1}, ..., P_{B,K}] \tag{4.89}$$

4.3.2. BANK OF CONTROLLERS

As shown with the above ECMS formulation, the required objective function ($\dot{m}_{T,K}$) and the constraints depend on the power plant equipment. Therefore, in order to realize the secondary level control for a retrofittable power plant with a variable number of batteries, the vessel control system needs to include a controller for each possible power plant layout. In the work of for example [90, 91], the authors discuss supervisory switching control, using a bank of controllers. Using this, for a variable layout power plant, a bank of controllers should be included in the secondary level. In this bank of controller, for each $k \in [0, ..., K_{max}]$ there needs to be an ECMS structure, hence this bank will include a total of $K_{max} + 1$ controllers. A schematic view of this can be found in Figure 4.13, where each controller in the bank of controllers contains the ECMS formulation for the amount of batteries shown.

The exact value of K_{max} greatly depends on two factors; the type of vessel and the available batteries. The type of vessel gives information about the variability of the power profile, as shown in Section 3.2.1, hence if the available batteries for the vessel's power plant are known, an upper bound for the maximum required batteries the power plant required during a mission of the vessel, K_{max} can be estimated. However, for the scope of this thesis, the exact value of K_{max} is not determined, since next to the type of vessel, specific information about the other components of the power plant and the expected missions of the vessel is required. Therefore, simply the notation of K_{max} will be used, and it is left for future research to investigate how to properly determine the exact value of this.

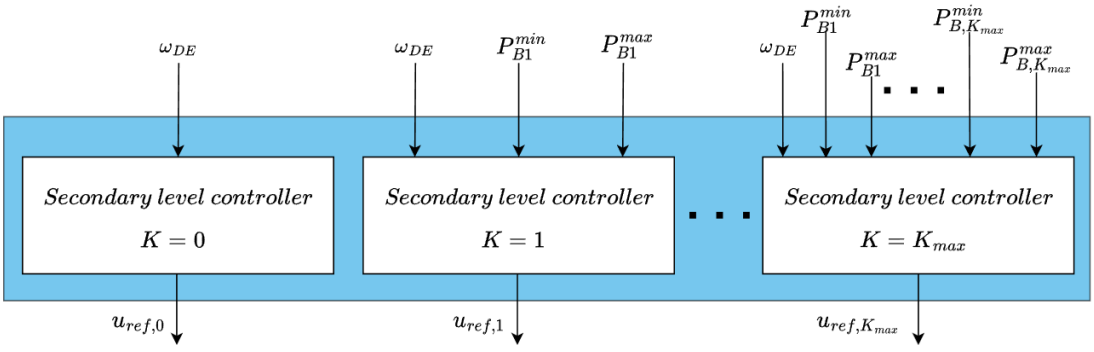

Figure 4.13: Bank of controllers for secondary level control

4.4. SUPERVISORY LEVEL

As discussed in Chapter 3.2, the equipment modifications for this thesis consist of battery additions, removals or replacements. Although the primary and secondary level are designed to cope with a varying number of batteries in the power plant, without further design, the control system would not know which controller to select from the bank and which batteries are in the plant. Therefore, just as the supervisor to select the required controller in the example of [90, 91], a supervisory level is added to the control architecture, which includes a supervisor that is able to decide which batteries are required, which secondary level controller from the bank of controllers is needed, and which can initialize the battery constraint modules in the primary level, such that they can correctly be used for the batteries in the power plant. Using this description, the following requirements for the supervisor can be formulated:

- Before the mission:
  - Estimate the required batteries to execute the mission
  - Initialize the constraint modules in the primary level
- During the mission:
  - Detect if all batteries in the power plant are working correctly
  - If a fault is detected:
    - Select fitting secondary level controller for the remaining batteries
    - Ensure the battery at fault is not used for the remainder of the mission

In order to design a supervisor that is able to perform well on the aforementioned tasks, while remaining in the scope of this thesis, a few assumptions have to be made:

- The power profile is known, or can be approximated using Chapter 3.1
- Of the two diesel generator sets, only one is used during the mission (the other is for redundancy)
- Batteries are only used when the diesel generator set can not provide the required power *
- The diesel engine is only used when induction motor can not provide the required propulsion power **
- At each harbour there are two available types of batteries: type 1 and type 2
- The capacity of type 2 is twice the capacity of type 1
- A proper fault diagnosis is installed in the supervisor, which can detect and identify the battery/batteries at fault

* : The ECMS is solved with fmincon in MATLAB, and since this is a nonlinear problem the solution depends on the initial guess for the power split. Tuning this results in fmincon preferring generator power over battery power, vice versa, or approach them as equally important.
** : Same as the above, only now regarding the diesel engine and the induction motor. However, it is seen that for scenarios where no preference was given, fmincon chose induction motor power over diesel engine power, but this depends on the SFOC of the diesel engine.

Using the requirements for the supervisor and the assumptions listed above, an initial design can be made, and this will be discussed in this section in twofold. First it is shown how the power profile can be used to estimate which batteries are required to execute the mission, and second the decision logic will be discussed, in order to select the required secondary level controller from the bank of controllers, which is especially important for the scenario of detecting a battery fault during the mission.

4.4.1. REQUIRED BATTERIES FOR THE MISSION

In order to determine the required batteries for the mission, the power profile (or the mission statement), characteristics of the equipment in the power plant, and the assumptions listed above are required. Then, using this information, first the required battery capacity of the power plant needs to be determined, where after a suitable battery configuration that matches the required battery capacity can be selected using the designed algorithm.

REQUIRED BATTERY CAPACITY

To illustrate the steps to determine the required battery capacity, a tugboat is used as an example. To this end, first a typical power profile of a tugboat is shown in Figure 4.14, based on the work of [4, 7].

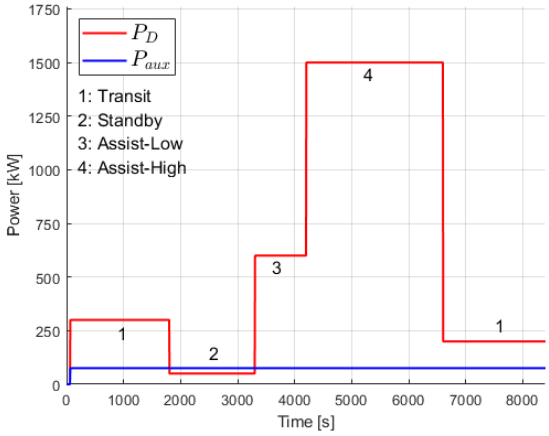

Figure 4.14: Typical power profile of a tugboat

In the power profile, the operational modes are indicated with 1,2,3, and 4. It has to be noted that the authors use electric propulsion for the tugboat in their work, while

this thesis considers hybrid propulsion. However, this is not much of a problem since for this analysis the specifics of the diesel engine(s) do not have to be known, only the specifics of the induction motor(s) and the diesel generator sets. Also, as the aim of this section is to illustrate how to estimate the required batteries based on the power profile, a single shaft configuration will be used. Furthermore, the maximum power $P^{max}_{IM,mec}$ of the induction motor is assumed to be 800 kW [158], and the generator sets are assumed to have a maximum power of 700 kW, based on the work of [12].

The first step is to determine the maximum electric power the induction motor can request from the electric grid, and according to Figure 4.12, this can be found using Equation 4.90:

$$P^{max}_{IM,grid} = \frac{P^{max}_{IM,mec}}{\eta_{IM} \cdot \eta_{FC}} \tag{4.90}$$

The second step is to find the optimum working point of the diesel generator set, and this can be done using the SFOC. Based on SFOC data shown in the work of [4, 7, 12] it is found that the optimum working point of the diesel generator sets is between 70% and 80% of the maximum load, hence 75% will be used as approximation. This leads to the results shown in Figure 4.15, where next to the power profile, the optimum working point of the diesel generator set $P^{opt}_{DG,1}$ (only one DG is active) and the maximum electric power for the induction motor are shown. Now, the power required for the auxiliary loads and

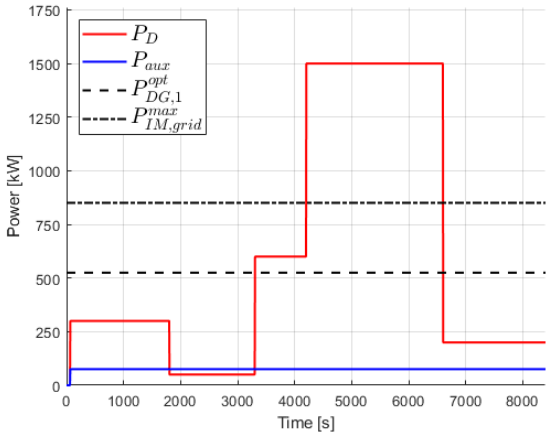

Figure 4.15: Power profile of a tugboat and equipment characteristics

the power for the induction motor, up to $P^{max}_{IM,grid}$, will be provided by the generator sets and the batteries. Therefore, the propulsion load has to be expressed as an electric load:

$$P_{D,elec} = \frac{P_D}{\eta_T \cdot \eta_{IM} \cdot \eta_{FC}} \tag{4.91}$$

Furthermore, since the ECMS as described above tries to balance the power assigned to the generator set around the optimum working point, for power demands higher than

the optimum load of the diesel generator set, the batteries will be used. Combining this with the notion that the induction motor can only take a maximum amount of electric power from the grid, the maximum power $P_{B,max}$ from the batteries will be equal to:

$$P_{B,max} = \max\left\{0,\ P_{aux} + \min\left\{P_{D,elec}, P^{max}_{IM,grid}\right\} - P^{opt}_{DG,1}\right\} \tag{4.92}$$

At last, to find the total energy the batteries have to deliver during the mission, the found battery power has to be integrated over time, and this can be seen in Figure 4.16 and 4.17.

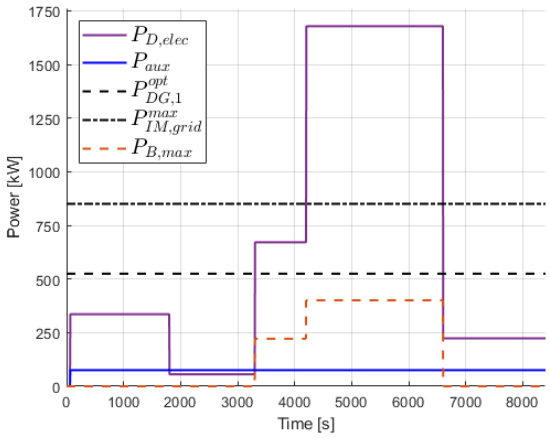

Figure 4.16: Power profile of a tugboat and required battery power

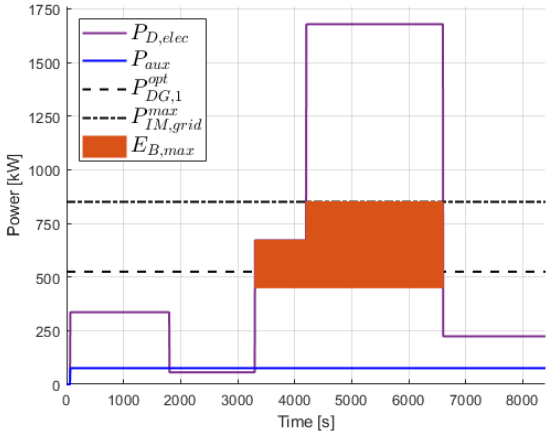

Figure 4.17: Power profile of a tugboat and required battery energy

Summarizing, if the steps taken in this section are used, the maximum energy the

batteries have to deliver during the mission can be found as shown in Equation 4.93:

$$E_{B,max} = \int_{t=0}^{t_m} \left(\left\{ 0,\ P_{aux}(t) + \min\left\{ \frac{P_D(t)}{\eta_T \cdot \eta_{IM} \cdot \eta_{FC}},\ \frac{P_{IM,mec}^{max}}{\eta_{IM} \cdot \eta_{FC}} \right\} - P_{DG,1}^{opt} \right\} \right) dt \tag{4.93}$$

where t_m is the total mission time, and P_D and P_{aux} are known from the power profile. Although it is assumed that each battery is charged fully at the start of the mission, they could be restricted to be discharged completely, and therefore it is important to take this into account when estimating the required batteries. Furthermore, as seen in literature during the analysis of the tugboats power profiles shown in Table 3.12, most tugboats have a buffer of 10%-30% of the total installed power, which is, under normal circumstances, not required during the mission. Therefore, for the battery energy a buffer of 20% is chosen, such that the required energy capacity of the batteries for the power plant is equal to:

$$E_{B,plant} = 1.2 \cdot \frac{E_{B,max}}{SOC_{max} - SOC_{min}} \tag{4.94}$$

where SOC_{max} and SOC_{min} are the prescribed battery limits, and $E_{B,plant}$ denotes the required battery energy capacity. With the required battery capacity of the batteries in the power plant known, a suited the battery configuration can be selected.

BATTERY CONFIGURATIONS

The power plant can contain up to K_{max} batteries, and each battery can either be of type 1 or type 2, where the energy capacity of type 1 is equal to $E_{0,1}$ and the energy capacity of type 2 is equal to $E_{0,2} = r_{2/1} \cdot E_{0,1}$, with $r_{2/1}$ an integer. Consequently, there are numerous configurations possible to obtain a power plant with the required capacity. To illustrate this, each unique configuration for a power plant that can contain up to 6 batteries is shown in Table 4.1, where '1' denotes a battery of type 1, and '2' a battery of type 2.

Number of Batteries	Configuration						
	1	2	3	4	5	6	7
1	1	2	-	-	-	-	-
2	1,1	1,2	2,2	-	-	-	-
3	1,1,1	1,1,2	1,2,2	2,2,2	-	-	-
4	1,1,1,1	1,1,1,2	1,1,2,2	1,2,2,2	2,2,2,2	-	-
5	1,1,1,1,1	1,1,1,1,2	1,1,1,2,2	1,1,2,2,2	1,2,2,2,2	2,2,2,2,2	-
6	1,1,1,1,1,1	1,1,1,1,1,2	1,1,1,1,2,2	1,1,1,2,2,2	1,1,2,2,2,2	1,2,2,2,2,2	2,2,2,2,2,2

Table 4.1: Battery configurations

From this example it can be noted that for K batteries in the power plant, $K+1$ unique configurations can be made, and in total there are 27 different configurations seen in Table 4.1. Upon closer inspection, the following relation can be derived for the maximum amount of batteries in the power plant and the number of possible configurations:

$$K_{config} = \begin{cases} K_{max} \cdot \left(\frac{K_{max}}{2} + 2 \right) - \frac{K_{max}}{2} & \text{for } K_{max} = \text{ even} \\ K_{max} \cdot \left(\frac{K_{max}+1}{2} + 1 \right) & \text{for } K_{max} = \text{ odd} \end{cases} \tag{4.95}$$

where K_{max} denotes the maximum number of batteries in the power plant, and K_{config} is the number of unique battery configurations. Now to find a suitable configuration, the total battery capacity of each configuration is required, which is done by assigning weighting factors, proportional to the ratio of the battery capacities, to each battery type. In this case, a battery of type 1 receives weighting factor 1, but a battery of type 2 receives weighting factor $r_{2/1}$, since that is the ratio between the capacity of a type 2 and a type 1 battery. In this case, this would yield the same results as Table 4.1, only with each 2 replaced by $r_{2/1}$. Now if for each configuration the sum of the weights is taken, the results is a factor, expressing the total energy capacity of that configuration in terms of the capacity of a type 1 battery. For the example shown in Table 4.1 this is also done, and this can be seen in Table 4.2.

Number of Batteries	Configuration						
	1	2	3	4	5	6	7
1	1	1+($r_{2/1}$-1)	-	-	-	-	-
2	2	2+($r_{2/1}-1$)	2+2($r_{2/1}-1$)	-	-	-	-
3	3	3+($r_{2/1}-1$)	3+2($r_{2/1}-1$)	3+3($r_{2/1}-1$)	-	-	-
4	4	4+($r_{2/1}-1$)	4+2($r_{2/1}-1$)	4+3($r_{2/1}-1$)	4+4($r_{2/1}-1$)	-	-
5	5	5+($r_{2/1}-1$)	5+2($r_{2/1}-1$)	5+3($r_{2/1}-1$)	5+4($r_{2/1}-1$)	5+5($r_{2/1}-1$)	-
6	6	6+($r_{2/1}-1$)	6+2($r_{2/1}-1$)	6+3($r_{2/1}-1$)	6+4($r_{2/1}-1$)	6+5($r_{2/1}-1$)	6+6($r_{2/1}-1$)

Table 4.2: Total capacity of battery configurations

In order to decide which configuration is selected for a certain $E_{B,plant}$, it is assumed that the configuration with the least amount of batteries is prefered, since this reduces the amount of equipment, reducing the total weight of the vessel, and therefore reduces the resistance of the vessel during the mission. As the remaining steps to determine the required batteries for the power plant are purely mathematical, this is shown in in Algorithm 3, together with the steps taken to estimate the required battery capacity, and this algorithm can be used to determine the required battery configuration for any two types of batteries, as long as the ratio of their capacities is an integer. Finally, with the found batteries, the capacity in ampere-seconds, required as input for the primary level battery constraint modules, can be computed. This is based on the work of [145] and Equation 4.40, and can be seen in Equation 4.96 to 4.98:

$$\boldsymbol{C}_0 = \frac{\boldsymbol{E}_0}{V_{avg}} \tag{4.96}$$

$$V_{avg} = a_{B,1} \cdot SOC_{avg} + a_{B,0} \tag{4.97}$$

$$SOC_{avg} = \frac{SOC_{max} + SOC_{min}}{2} \tag{4.98}$$

where $\boldsymbol{C}_0$ contains the capacity in ampere-seconds for each battery in the desired battery configuration, and V_{avg} and SOC_{avg} are the average voltage and SOC, respectively.

Algorithm 3: Selection algorithm for the optimal battery configuration

Input: Battery and Power Plant Specifics

$K_{max} \leftarrow$ Maximum number of batteries in the power plant
$E_{0,1} \leftarrow$ Capacity of battery type 1
$E_{0,2} \leftarrow$ Capacity of battery type 2
$E_{B,plant} \leftarrow$ Required battery capacity

$r_E = \dfrac{E_{0,2} - E_{0,1}}{E_{0,1}}$ Express difference in capacity in terms of $E_{0,1}$

$\mathbf{E}_K = \text{zeros}(K_{max}, K_{max}+1)$
for $i = 1 : K_{max}$ **do**
  for $j = 1 : i+1$ **do**
    $E_K(i,j) = (j \cdot r_E + (i - r_E)) \cdot E_{0,1}$ Capacity of configurations
  end
end
$[\boldsymbol{I}, \boldsymbol{J}] = \text{find}(\mathbf{E}_K >= E_{B,plant})$ Find suitable configurations
$K_{plant} = \min(\boldsymbol{I})$ Select minimum of batteries
$J_{min} = \min(\boldsymbol{J}(\boldsymbol{I}(:) == K_{plant}))$ Select closest to required capacity
$\boldsymbol{E}_0 = \text{ones}(1, K_{plant}) \cdot E_{0,1}$ Fill configuration with battery type 1
if $J_{min} \geq 2$ **then**
  for $j = 1 : J_{min} - 1$ **do**
    $E_0(K_{plant} - j + 1) = E_{0,2}$ Replace type 1 with type 2 if necessary
  end
end

Output: Battery Configuration

$K_{plant} \leftarrow$ Number of batteries in the power plant required for the mission
$\boldsymbol{E}_0 \leftarrow$ Battery configuration closest to $E_{B,plant}$ with minimum number of K_{plant} batteries

4.4.2. DECISION LOGIC

Opposed to the section before, where the power profile is used to give an estimate of the required batteries for the mission before the mission starts, during the mission the decision logic is more important. This logic receives as inputs how many batteries are installed in the power plant, the required battery power assigned by the ECMS, and the battery constraints provided by the constraint modules. During normal operation, the decision logic will not intervene, but when a battery fault is detected by the fault diagnosis module, the latter gives a signal to the decision logic, such that it switch between the secondary level controllers in the bank of controllers. Furthermore, the decision logic will rearrange the battery power and constraints, such that the malfunctioning battery is not used during remainder of the mission, or until the battery is fixed. To illustrate this, in Figure 4.18 and 4.19 a power plant with three batteries can be seen, where in Figure 4.18 the batteries are working correctly, and in Figure 4.19 battery 2 is malfunctioning. In the figures it can be seen how the signals from and towards the batteries must be rearranged in order to give the proper inputs to the secondary level controllers and to the batteries, indicating the role of the supervisor.

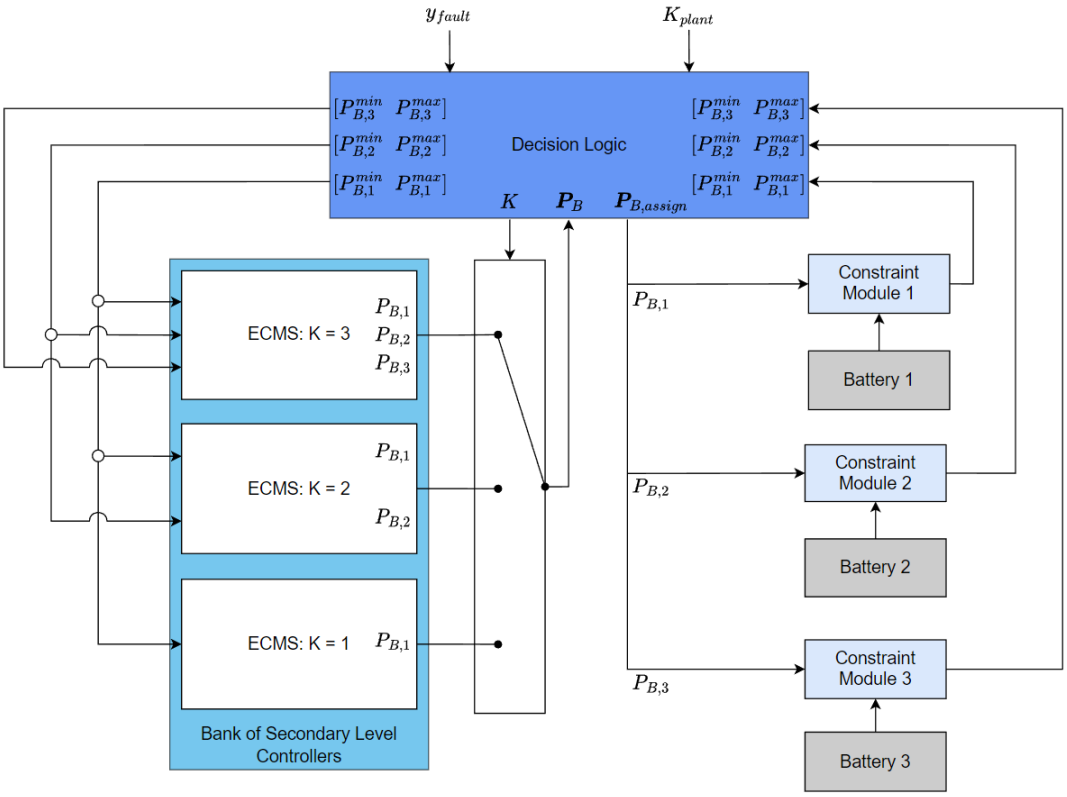

Figure 4.18: Simplified scenario for a power plant with three batteries

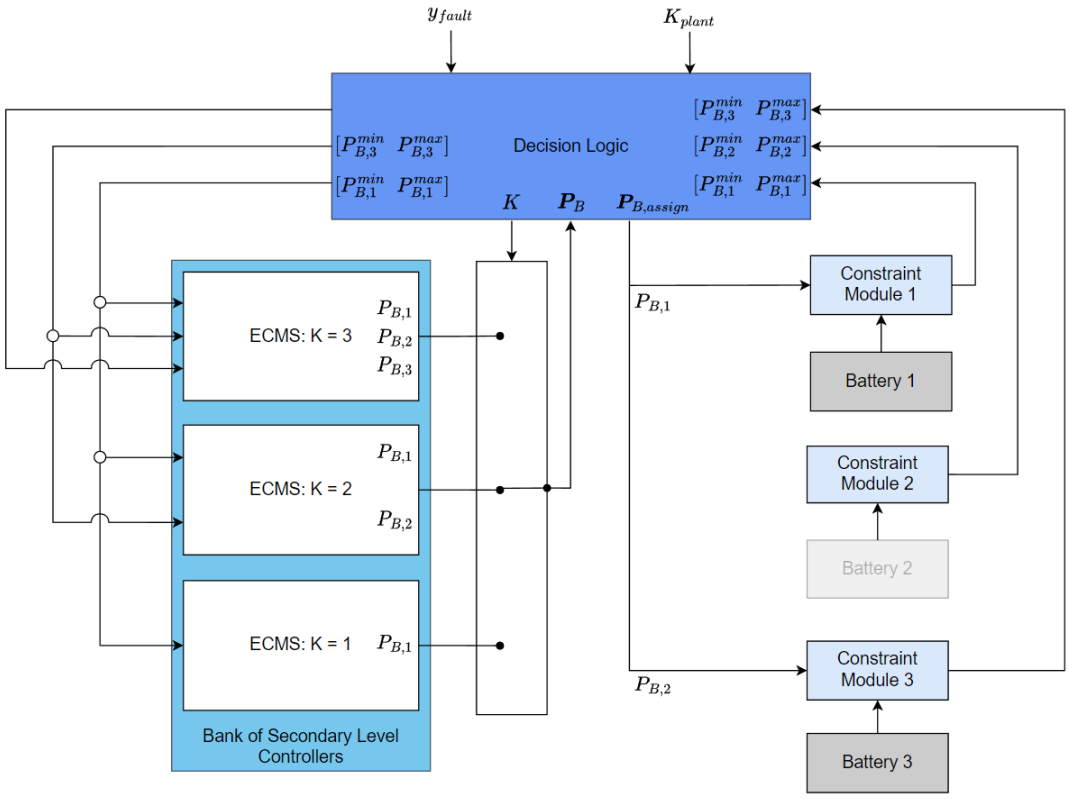

Figure 4.19: Simplified scenario with a battery fault

From this example it can be seen that the supervisor receives the battery constraints from the constraint modules, reassigns them (if necessary), and distributes them to the secondary level. In order to give a more compact view of this, the battery constraints as provided by the battery modules are listed in $\mathbf{P}_{B,con}$, and the battery constraints assigned to the secondary level are listed in $\mathbf{P}_{B,con,assign}$, and regarding the above example this lead to the following notation:

No faults:

$$\mathbf{P}_{B,con} = \begin{bmatrix} P^{min}_{B,1} & P^{max}_{B,1} \\ P^{min}_{B,2} & P^{max}_{B,2} \\ P^{min}_{B,3} & P^{max}_{B,3} \end{bmatrix} \qquad \mathbf{P}_{B,con,assign} = \begin{bmatrix} P^{min}_{B,1} & P^{max}_{B,1} \\ P^{min}_{B,2} & P^{max}_{B,2} \\ P^{min}_{B,3} & P^{max}_{B,3} \end{bmatrix}$$

Fault for Battery 2:

$$\mathbf{P}_{B,con} = \begin{bmatrix} P^{min}_{B,1} & P^{max}_{B,1} \\ P^{min}_{B,2} & P^{max}_{B,2} \\ P^{min}_{B,3} & P^{max}_{B,3} \end{bmatrix} \qquad \mathbf{P}_{B,con,assign} = \begin{bmatrix} P^{min}_{B,1} & P^{max}_{B,1} \\ P^{min}_{B,3} & P^{max}_{B,3} \end{bmatrix}$$

The same can be done for the battery power. If the power fed to the batteries in the power plant is denoted as $\boldsymbol{P}_{B,assign}$ and the power for the batteries received from the power split as $\boldsymbol{P}_B$, they can be described as:

No faults:

$$\boldsymbol{P}_B = \begin{bmatrix} P_{B,1} \\ P_{B,2} \\ P_{B,3} \end{bmatrix} \qquad \boldsymbol{P}_{B,assign} = \begin{bmatrix} P_{B,1} \\ P_{B,2} \\ P_{B,3} \end{bmatrix}$$

Fault for Battery 2:

$$\boldsymbol{P}_B = \begin{bmatrix} P_{B,1} \\ P_{B,2} \end{bmatrix} \qquad \boldsymbol{P}_{B,assign} = \begin{bmatrix} P_{B,1} \\ - \\ P_{B,2} \end{bmatrix}$$

Note that for both $\mathbf{P}_{B,con}$ and $\boldsymbol{P}_{B,assign}$ the number of elements does not change, while the size of $\mathbf{P}_{B,con,assign}$ and $\boldsymbol{P}_B$ depends on the amount of working batteries in the power plant. This is because $\mathbf{P}_{B,con}$ and $\boldsymbol{P}_{B,assign}$ are directly connected to the batteries in the power plant, hence this number does not change if one of the batteries fails. However, as $\mathbf{P}_{B,con,assign}$ and $\boldsymbol{P}_B$ are connected to the secondary level control, the selected secondary level controller (which on its turn depends on the amount of working batteries in the power plant plant), determines the size of these signals.

At last, it is assumed that the supervisor contains a well-designed and well-functioning fault diagnosis scheme, that can adequately communicate to the supervisor which battery is malfunctioning, if a fault is detected, such that K can be determined and the described rearrangements of above can be performed. An example of the output y_{fault} of such a fault diagnosis scheme for the example shown above can be seen in Equation 4.99 and 4.100:

No faults:

$$y_{fault} = [0;\ 0;\ 0] \tag{4.99}$$

Fault for Battery 2:

$$y_{fault} = [0;\ 1;\ 0] \tag{4.100}$$

Thus, y_{fault} is a vector filled with zeros when all batteries are properly functioning. When a battery fault is detected, a '1' is written at the position of which the index in y_{fault} corresponds to the battery at fault. Using this, the decision logic can be designed as shown in Algorithm 4.

Algorithm 4: Decision Logic of the Supervisor

Input: Signals from the required batteries, fault diagnosis and secondary level

$K_{plant} \leftarrow$ Required number of batteries in the power plant
$y_{fault} \leftarrow$ Signal of the fault diagnosis
$\boldsymbol{P}_B \leftarrow$ Battery power provided by the secondary level
$\mathbf{P}_{B,con} \leftarrow$ Battery constraints from the constraint modules

---

$K = K_{plant} - \text{sum}(y_{fault})$ Determine working batteries in power plant
$\boldsymbol{P}_{B,assign} = \text{zeros}(K_{plant}, 1)$ Empty vector to be filled
$\mathbf{P}_{B,con,assign} = \text{zeros}(K, 2)$ Empty matrix to be filled
$I = \text{find}(y_{fault} == 0)$ Find indices of working batteries
for $j = 1 : K_{plant}$ **do**
  for $i = 1 : K$ **do**
    if $j == I(i)$ **then**
      $P_{B,assign}(j) = P_B(i)$
      $P_{B,con,assign}(i,:) = P_{B,con}(j,:)$
    end
  end
end

Output: Power for the batteries and power constraints for the secondary level

$\boldsymbol{P}_{B,assign} \leftarrow$ Battery power for the working batteries in the power plant
$\mathbf{P}_{B,con,assign} \leftarrow$ Power constraints of the working batteries for the secondary level

4.5. Final Design of Modular Power Plant Control Architecture

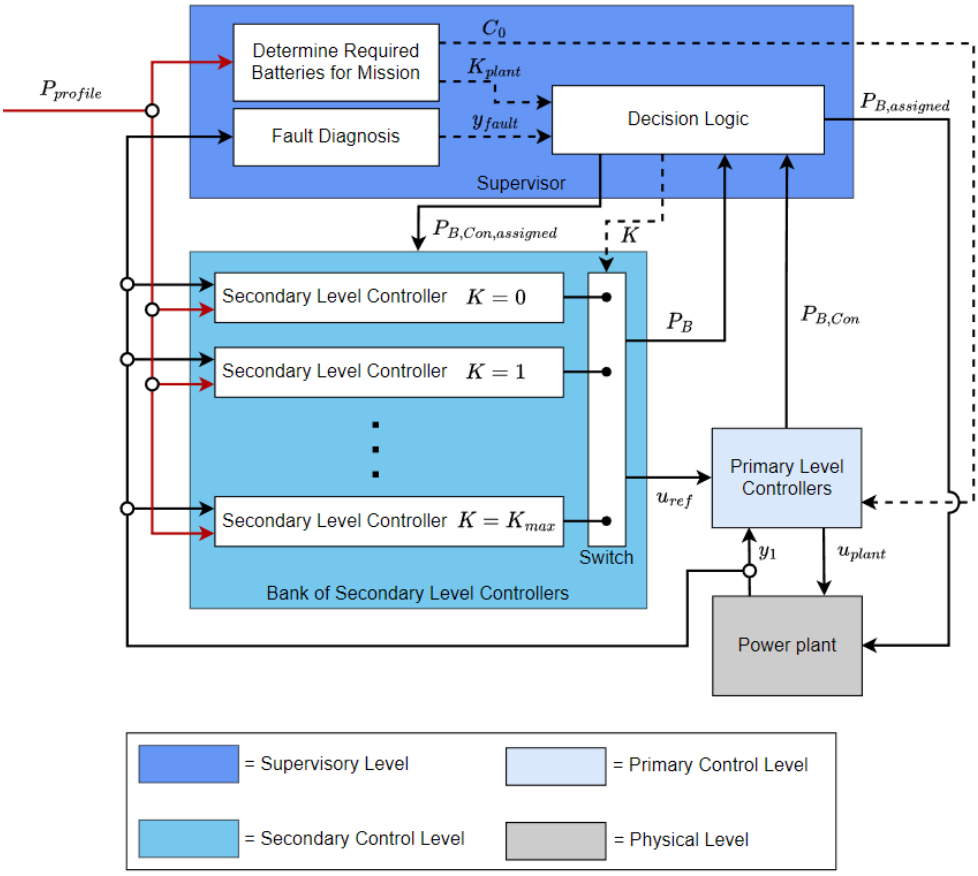

Figure 4.20: Schematic view of the designed modular power plant control architecture

In Figure 4.20 the final design of the modular control architecture can be seen. At the top the supervisor is shown, which uses the power profile to determine the required batteries for the power plant K_{plant}, and provides the required battery capacity C_0 of each battery to the primary level, in order to initialize the constraints modules of the batteries. Furthermore, the proposed fault diagnosis module can be seen, which tells the decision logic whether there is a battery at fault or not with a certain signal y_{fault}. This decision logic first uses K_{plant} to select the required secondary level controller from the bank of controllers. Furthermore, if a fault signal y_{fault} is received, the decision logic is responsible for the following three tasks:

- Update K, such that the secondary level controller corresponding to the still working batteries in the power plant is selected

- Assign the required battery power $\boldsymbol{P}_B$ as provided by the secondary level controller to the remaining working batteries $P_{B,assign}$
- Rearrange the battery power constraints $\mathbf{P}_{B,con}$ to $\mathbf{P}_{B,con,assign}$ such that it can be used by the secondary level controller

Regardless of the batteries in the power plant, the fixed equipment in the power plant, being the diesel engines, induction motor, and diesel generator sets, are controlled by their primary level controllers. From the power plant, the shaft speed of the diesel engine is fed directly to the (selected) secondary level controller, and also the batteries are monitored by the fault diagnosis module, in order to detect and act on battery faults.

4.6. PROPOSED KEY PERFORMANCE INDICATORS

In the next chapter, the modular power plant control architecture will be verified, by showing the stability and robustness of the designed control architecture. However, in order to assess the performance in a more quantitative manner, Key Performance Indicators (KPI's) are required. The main goal of this thesis is to present a methodology that can be used to design a modular control system, in order to allow modular use of the power plant components. Since the modular use of the power plant components is based on the power profile, dictated by the mission, a good performance indicator would be the error with respect to the power profile. To this end, using the root-mean-square error (RMSE) and the scatter index (SI) with respect to the propulsion power and the auxiliary power, but also of the individual power plant components, the performance is measured. How these can be determined is seen in Equation 4.101 and 4.102:

$$\text{RMSE} = \sqrt{\text{mean}\left(\left(y_{ref} - y\right)^2\right)} \tag{4.101}$$

$$\text{SI} = \frac{\text{RMSE}}{\text{mean}(y)} \tag{4.102}$$

where y is the measured data, and y_{ref} is the corresponding reference-signal.

4.7. CONCLUDING REMARKS

In this chapter, the fourth subquestion: "How can a modular control architecture be designed to meet the proposed automation and power plant modifications?" is answered.

A modular control architecture is designed, allowing modular use of the batteries. The control system consists of three levels: a supervisory, a secondary, and a primary level. In the supervisory level, a supervisor determines the required batteries for the mission, using the power profile. Then, it selects the required controller from the bank of the secondary level controllers, and the mission can be executed. Furthermore, battery constraint modules are proposed, which provide a limit for the power that can be assigned to/requested of the battery during the mission. Regular PI controllers are used for the rest of the (fixed) power plant equipment. Furthermore, if a fault diagnosis is included (not designed or presented in this thesis), the supervisor is able to cope with

battery faults. At last, KPI's are presented to measure the performance of the modular control system:

- RMSE:
  Root-mean-square error between measured data and the corresponding reference-signal
- SI:
  Scatter-index, which is the normalized RMSE, to give a more insightfull measure of the performance

In the next chapter, multiple power profiles are used to simulate the behavior of the modular control architecture in a Simulink/MATLAB environment, and with the aforementioned KPI's and plotted data, the performance (stability and robustness) of the presented modular control architecture is verified.

5

VERIFICATION OF THE MODULAR POWER PLANT CONTROL ARCHITECTURE

In this chapter the research question: "How to verify the performance (stability and robustness) of the developed modular control scheme?" will be addressed. To this end, four scenarios will be examined, based on a typical mission of a tugboat and the variations of the power profile discussed in this report. For each scenario, the mission of the tugboat is translated to a power profile, which is given as input to the supervisor. The latter uses the power profile to determine the amount of batteries, and their capacities, such that it can initialize the battery constraint modules, and select the required secondary controller from the bank of controllers. Using these scenarios, multiple simulations in a Simulink/MATLAB environment are executed, and in order to verify the performance of the modular control scheme and the behavior of the components in the power plant, the proposed KPI's are used. Furthermore, it will be shown that the designed modular control architecture can also be used for missions where a battery fails during operation will be shown, if the fault diagnosis is properly designed.

5.1. SCENARIOS

The baseline for the different scenarios is the typical mission of the tugboat, described by e.g. the authors of [7]. At the start of the mission, the tugboat travels to the specific location in the harbour, where the cargo vessel will arrive. It waits there for the cargo vessel to arrive, where after the tugboat assists the cargo vessel - either with relatively low or high bollard pull - and afterwards it travels back to a specified location in the harbour. To summarize this, this typical mission can be described by the following sequence of operational modes:

Transit-Standby-Assist-low-Assist-high-Transit

How the power profile correlates with the different operational modes is described in Chapter 3.1. Furthermore, Equation 3.41 and 3.42 describe the quantitative relation between the mission and the power profile, but these are not yet validated. Still, the found correlation can be used to indicate changes of the power profile for changes in the mission, and hence four missions are constructed. For each of these missions, the auxiliary power is assumed to be constant and fixed to 100 kW. The first mission is the baseline mission, and for this mission the environmental conditions such as wave, wind, and water currents are average. The second mission requires a higher towing force during the modes *Assist-low* and *Assist-high*, due to a larger cargo vessel, and therefore these modes have a higher propulsion power demand. For the third mission, not only a higher towing force is required, but also the environmental conditions change. The wave, wind, and currents increase for the whole mission, and this leads to an increase in the propulsion power demand. The last mission is similar to mission 3, but now the tugboat has to travel longer to the cargo vessel, and during the last part of the transit it has to sail faster, increasing the propulsion power demand. Also the vessel spends less time in the mode *Assist-low*, and more time in the mode *Assist-high* compared to mission 1, 2, and 3. These changes and variations are summarized in Table 5.1, and the resulting power profiles can be seen in Figure 5.1. Note that instead fixed slopes, exponential slopes are used to construct the power profile, as this generally leads to better performance, which is shown Appendix C.

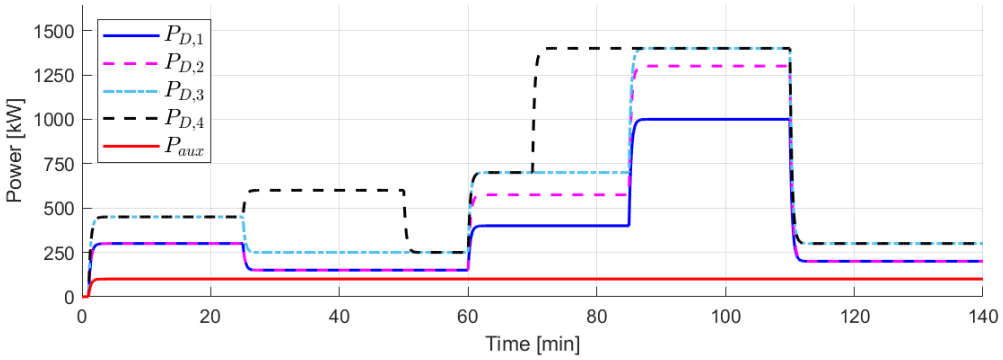

Figure 5.1: Power profile of missions

For each mission, the supervisor uses the power profile to estimate the required batteries for the mission. As discussed, it is assumed that at any time, two batteries are

	Change with respect to mission 1	Change with respect to power profile 1			
		Transit	Standby	Assist-low	Assist-high
Mission 2	Larger cargo ship to assist	-	-	Increase of F_{tow} → P_D increases	Increase of F_{tow} → P_D increases
Mission 3	Larger cargo ship to assist	-	-	Increase of F_{tow} → P_D increases	Increase of F_{tow} → P_D increases
	Increase of wave, wind, and currents	Increase of s_s, w_s, c_s → P_D increases	Increase of s_s, w_s, c_s → P_D increases	Increase of s_s, w_s, c_s → P_D increases	Increase of s_s, w_s, c_s → P_D increases
Mission 4	Larger cargo ship to assist	-	-	Increase of F_{tow} → P_D increases	Increase of F_{tow} → P_D increases
	Increase of wave, wind, and currents	Increase of s_s, w_s, c_s → P_D increases	Increase of s_s, w_s, c_s → P_D increases	Increase of s_s, w_s, c_s → P_D increases	Increase of s_s, w_s, c_s → P_D increases
	Cargo ship arrives further from starting point of tugboat, but total mission time remains the same	Longer duration of mode* Speed increase halfway during mode* → P_D increases*	Shorter duration of mode	Shorter duration of mode	Longer duration of mode

Table 5.1: Changes in mission and power profile

*: Only applies for the first use of this mode. For the second use of this mode, at the end of the mission, this is not applicable.

available, which can be characterized by their capacity. Now, while there are already quite large batteries with a lot of capacity, such as the modular battery packs of Wärtsilä [159], since the missions are based on a tugboat, the battery capacity is also chosen such that it represents the average tugboat battery as seen in literature. As a result, the characteristics of the available batteries for the scenarios in this report are shown Table 5.2. (Note that the capacity C_0 is derived using E_0 and Equation 4.96 to 4.98.)

Battery	Capacity			Voltage
	E_0 [kWh]	E_0 [MJ]	C_0 [kAs]	$V_{avg}[V]$
Type 1	150	540	1200	450
Type 2	300	1080	2400	450

Table 5.2: Characteristics of available batteries for the missions

5.2. SIMULATION RESULTS REGULAR MISSIONS

The power plant of the tugboat is designed conform Figure 4.1, together with the control architecture of Figure 4.20. The required parameters the describe the behavior of (the components in) the power plant, the primary level controllers and the parameters to constructs the bank of controllers are shown in Table 5.3. With respect to the parameters of the power plant equipment, these are mostly based on the literature mentioned in Chapter 4.2. The controller gains are found by trial and error, although data of the work mentioned in Chapter 4.2 was used as an initial guess. The bank of controllers is build using Equation 4.73 up to Equation 4.82, in which an secondary level controller is included for each $K \in [0,1,2,3,4]$. At last, the supervisor is constructed using the formulation of section 4.4, such that the shown modular control architecture of Figure 4.20 is build in a Simulink/Matlab environment, using MATLAB R2021b and a PC with an Intel Core i7 processor and 24 GB memory.

Diesel Engine

Model Parameters

k_{DE}	3000	$\frac{m^2}{s^2}$
J_{DE}	4167	kgm^2
D_{DE}	1000	kgm^2/s

Controller Gains

$K_{P,DE}$	20	[-]
$K_{I,DE}$	2	[-]

SFOC and ECMS Parameters

a_1^{DE}	$5.48 \cdot 10^{-5}$	$\frac{kg}{GW^3h}$
a_2^{DE}	-0.206	$\frac{kg}{MW^2h}$
a_3^{DE}	$5.545 \cdot 10^{-4}$	$\frac{kgs^2}{kWh}$
a_4^{DE}	-0.271	$\frac{kgs}{kWh}$
a_5^{DE}	$-3.55 \cdot 10^{-5}$	$\frac{kgs}{MW^2h}$
a_6^{DE}	600	$\frac{kg}{kWh}$
P_{DE}^{max}	$1200 \cdot 10^3$	W

Induction Motor

Model Parameters

k_{IM}	1000	[-]
R_r	0.01	Ω
J_{DE}	4167	kgm^2
D_{DE}	1000	$\frac{kgm^2}{s}$

Controller Gains

$K_{P,IM}$	10	[-]
$K_{I,IM}$	10	[-]
$C_{V/f}$	2	$\frac{kgm^2}{As^3}$

ECMS Parameters

η_{IM}	0.95	[-]
P_{IM}^{max}	$800 \cdot 10^3$	W

Shaft and Gearbox

J_{tot}	12500	kgm^2
i_{DE}	7.5	[-]
i_{IM}	24	[-]
η_T	0.95	[-]

Propeller

C_p	670	kgm^2

Diesel Generator Sets

Model Parameters

k_{DG}	4000	$\frac{m^2}{s^2}$
J_{DG}	4167	kgm^2
R_{int}	0.150	Ω
L	0.0021	H
$a_{G,1}$	3.34	$\frac{kgm^2}{As^2}$
$a_{G,0}$	0.57	$\frac{kgm^2}{A^2s^2}$

Controller Gains

$K_{P,DG,DE}$	200	[-]
$K_{I,DG,DE}$	30	[-]
$K_{P,DG,G}$	30	[-]
$K_{I,DG,G}$	12	[-]

SFOC and ECMS Parameters

a_1^{DG}	$5.55 \cdot 10^{-4}$	$\frac{kg}{GW^3h}$
a_2^{DG}	-0.580	$\frac{kg}{MW^2h}$
a_3^{DG}	$2.15 \cdot 10^2$	$\frac{kg}{kWh}$
η_{DG}	0.95	[-]
P_{DG}^{max}	$665 \cdot 10^3$	W
P_{DG}^{opt}	$524 \cdot 10^3$	W

Batteries

Model Parameters

$SOC(t_0)$	1	[-]
$a_{B,1}$	111	V
$a_{B,0}$	389	V
R_B	0.0225	Ω

Constraint Module Parameters

Δt	1000	s
SOC_{min}	0.1	[-]
SOC_{max}	1	[-]
$V_{B,min}$	300	V
$V_{B,max}$	600	V

SFOC and ECMS Parameters

η_B	0.97	[-]
$SFOC_{DE,nom}$	72.1	$\frac{kg}{kWh}$

Electric Grid

V_{grid}	3300	V
f_{grid}	50	$\frac{1}{s}$
η_{FC}	0.99	[-]

Table 5.3: Parameters of the power plant components, primary and secondary level controllers

5.2.1. RESULTS OF THE SUPERVISOR

The required batteries for the mission are determined at the start of the mission, hence this will be discussed first. Following the same steps as shown in section 4.4.1, the required batteries for each mission are determined by using the power profile. In Figure 5.2 this is visualized, and for each mission, the output of the supervisor, the required batteries and their capacity, is shown in Table 5.4. As can be seen from the supervisor

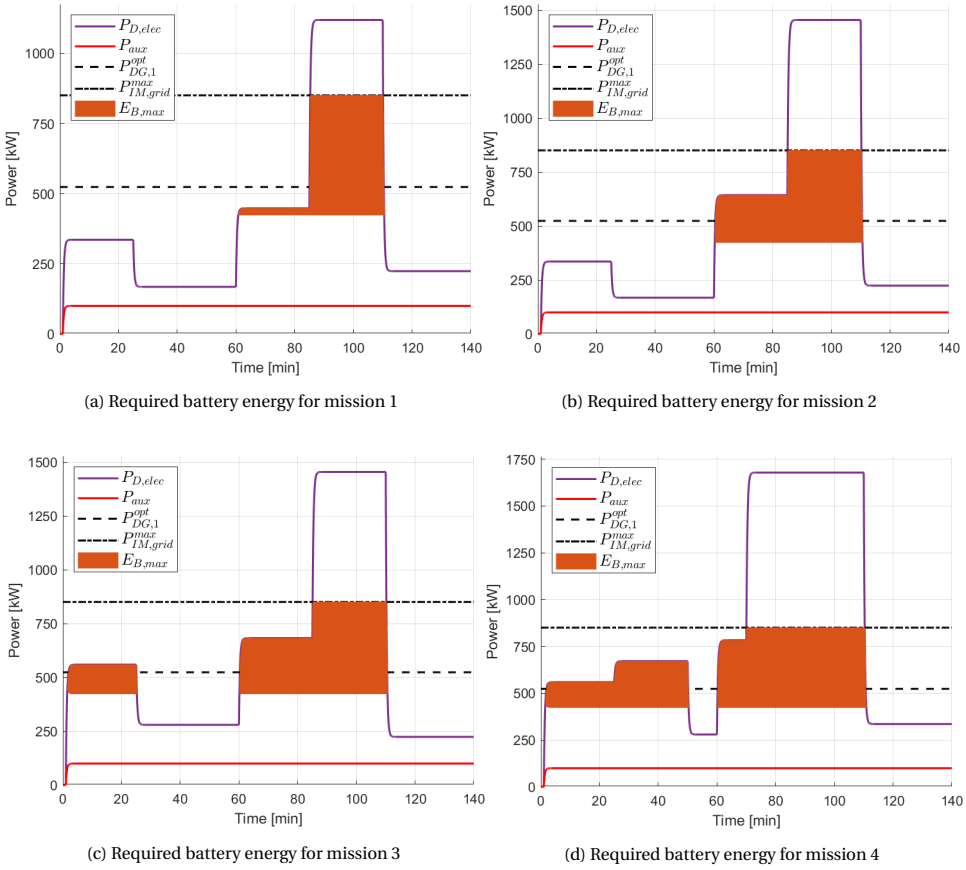

(a) Required battery energy for mission 1

(b) Required battery energy for mission 2

(c) Required battery energy for mission 3

(d) Required battery energy for mission 4

Figure 5.2: Required battery energy for the missions

results, mission 1 requires a single battery, mission 2 requires two batteries of different capacity, mission 3 also requires requires two batteries, but now of the same capacity, and mission 4 requires three batteries; one of type 1 and two of type 2. Next, the simulations results are shown for each mission, and it can be seen that for each mission the modular control architecture yields stable behavior. Since the power demand varies during the mission, but also between the missions, it can be concluded that the modular control architecture is also robust. Additionally, it will be shown that indeed, modelling batteries with different capacities as one (as is the approach of the authors of [12]) may result in wrong results regarding the tracking of the SOC.

	Required Battery Capacity ($E_{B,max}$)	Required Batteries					
		K	Type	Capacity			
				E_0		C_0	
Mission 1	904 MJ	1	2	1080	MJ	2.4	MAs
Mission 2	1294 MJ	2	[1,2]	[540 1080]	MJ	[1.2 2.4]	MAs
Mission 3	1625 MJ	2	[2,2]	[1080 1080]	MJ	[2.4 2.4]	MAs
Mission 4	2404 MJ	3	[1,2,2]	[540 1080 1080]	MJ	[1.2 2.4 2.4]	MAs

Table 5.4: Supervisor results for different missions

5.2.2. RESULTS MISSION 1

As the supervisor stated that only one battery is used for this mission, the corresponding secondary level controller is, automatically, selected from the bank of controllers. The power profile, also shown in Figure 5.3a, is used by the secondary level to determine the power split throughout the mission, and this can be seen in Figure 5.3b and 5.3c, for the fixed equipment and the battery, respectively. The found power split is then converted to reference signals, and fed to the primary level. In order to check if the power demand of the power profile is being met, the propulsion power tracking error ($P_{D,error}$) and the auxiliary power tracking error ($P_{aux,error}$) are required. First, as the propulsion power demand has to be delivered by the propeller, and the propeller speed ω_p is simulated, this can be used to find the propulsion power tracking error as follows:

$$P_{D,error} = \frac{P_D - P_p}{P_D} \cdot 100\% \tag{5.1}$$

$$P_p = C_p \cdot \omega_p \tag{5.2}$$

where C_p is a vessel dependent constant, and the used value can be found in Table 5.3. The auxiliary power error can be determined by taking the simulated power of each component in the power plant as follows:

$$P_{aux,error} = \frac{P_{aux} - P_{aux,plant}}{P_{aux}} \cdot 100\% \tag{5.3}$$

$$P_{aux,plant} = \sum_{j=1}^{2} V_{DG,j} \cdot I^*_{DG,j} + \sum_{k=1}^{K} V_{B,k} \cdot I_{B,k} - \frac{Q_{IM} \cdot \omega_{IM}}{\eta_{IM} \cdot \eta_{FC}} \tag{5.4}$$

where $P_{aux,plant}$ is the auxiliary power provided by the power plant, and * is noted for the complex conjugate. (For this mission, $K = 1$.) The resulting tracking errors of the propulsion and the auxiliary power can be seen in Figure 5.4a and 5.4b, respectively. Evidently, the tracking of the power profile is affected by the performance of the primary level, which can be seen in Figure 5.4c up to 5.4f. The tracking errors for the power plant components are obtained at the PI controllers, and expressed in terms of the reference signals. For each of the tracking errors the same behavior can be seen. When the power demand changes, an error is introduced, which recedes withing a few minutes. With respect to the magnitude of the tracking errors, for the physical components the errors are

negligible, for the propulsion power the errors are significant, but quickly receding, while for the auxiliary power the observed errors can be quite large (although also quickly receding). This behavior is mainly caused by the modelling and simulation approach of this thesis. As the electrical stability of the grid is outside the scope of this thesis no attention is paid to the inductive and reactive loading of components. However, these type of loads tend to dampen out electrical power peaks and surges, hence by not including this in the design, the errors as shown for the electrical loads can be expected.

Furthermore, as the power constraint modules attached to the batteries are, to the best knowledge of the authors, not used in literature, the battery results are discussed in more detail. The SOC of the battery can be found in Figure 5.3d, the output current is shown in Figure 5.3e, and finally the batteries terminal voltage can be seen in Figure 5.3f. The used battery model, as described in section 4.9, dictates that the terminal voltage of the battery V_B follows the SOC, and as a consequence, for a constant power demand, the batteries output current I_B should increase over time, since the SOC decreases when the battery is discharged. The results confirm this behavior, and it is best visible for the high power demand during the mode *Assist-high*. To conclude, the results of the baseline mission show good performance, both for the fixed equipment in the power plant and the battery, and it also shows good tracking of the power profile.

5.2.3. RESULTS MISSION 2

For the second mission, the supervisor states that two batteries of different capacity are used, while the fixed components, as the name already indicates, do not change. The results are shown in a similar fashion as the results for the baseline mission, only now with two batteries. The performance of the fixed components can be seen in Figures 5.6c to 5.6f, and also for this mission the tracking errors are negligible. Similar to the baseline mission, the propulsion tracking error is significant, but quickly receding to zero each time the power profile changes, and the same holds for the auxiliary power tracking error. Both can be seen in Figure 5.6a and Figure 5.6b.

As stated in this report, no literature has considered modeling of multiple batteries in a vessels power plant, hence the results for the batteries can be quite insightful. Just as for the baseline mission, for a constant power demand, the terminal voltage decreases, along with the SOC, and the output current increases. However, from the results it can also be concluded that batteries with different capacities can not be approximated as one, single battery with a single capacity. Using Figure 5.5c to Figure 5.5e, it can be seen that during the mission, both batteries are discharged to approximately the same SOC, but the power demand, and hence the output current, of battery 2 is nearly twice as high (regardless of the power demand, since their SOC behaves similar for the discharging part, their terminal voltage should behave similar too, and this is confirmed in Figure 5.5f). Even more, for charging the batteries with approximately the same power, battery 1 charges much faster. This shows that, for batteries of different capacity, wrongful results would be obtained if they were treated as one.

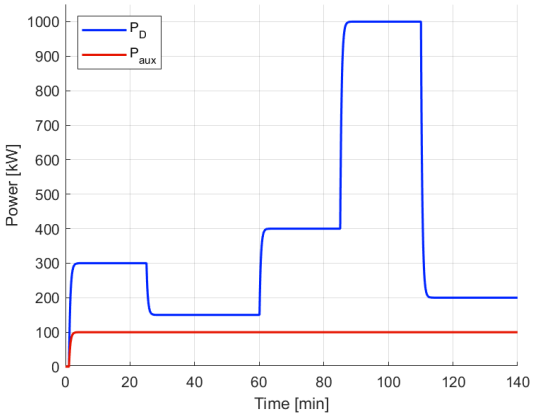

(a) Power profile

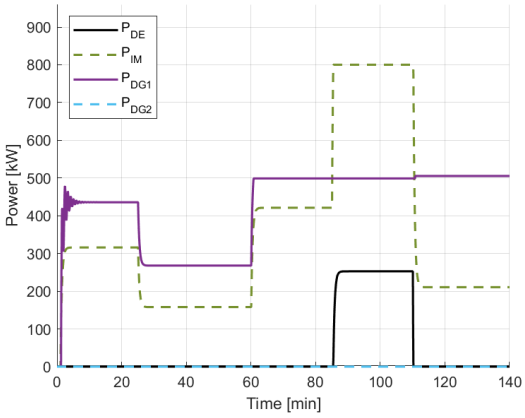

(b) Power split for the fixed equipment

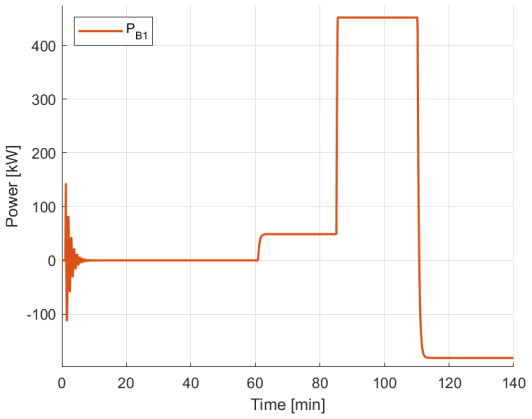

(c) Power split for the batteries

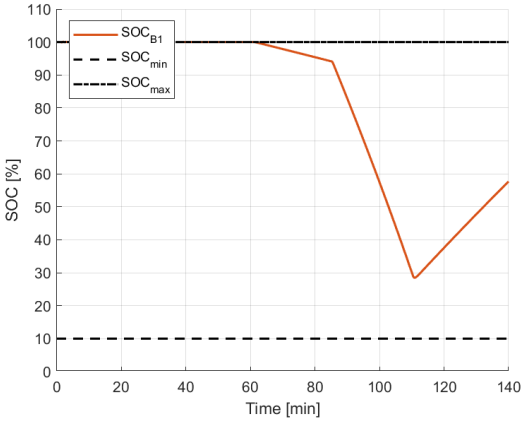

(d) SOC of the batteries

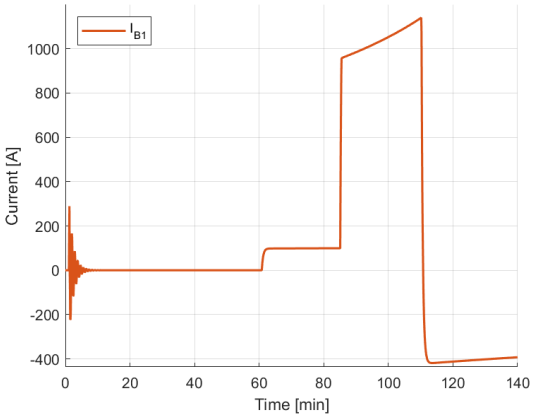

(e) Output current of the batteries

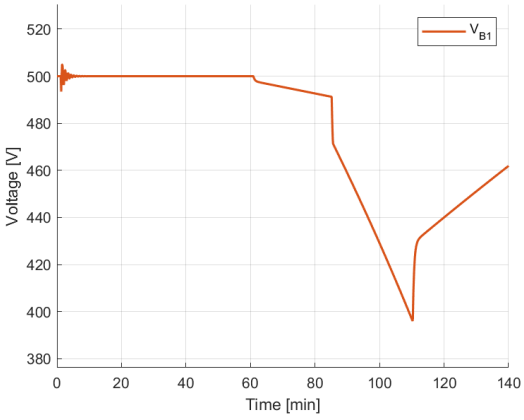

(f) Terminal voltage of the batteries

Figure 5.3: Power profile, power split, and battery performance for mission 1

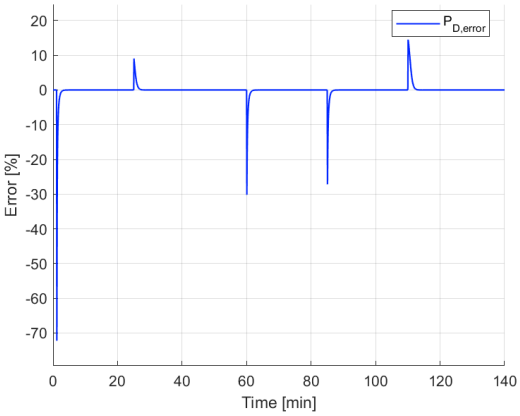

(a) Propulsion power demand error

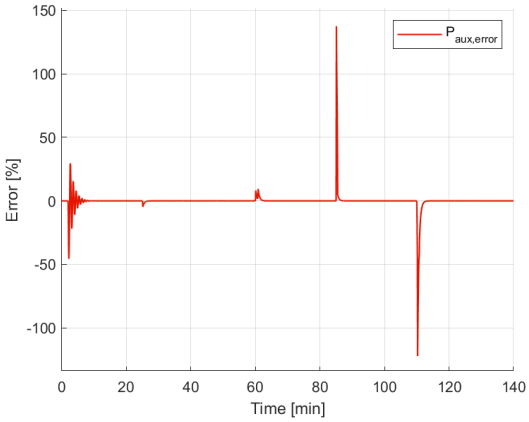

(b) Auxiliary power demand error

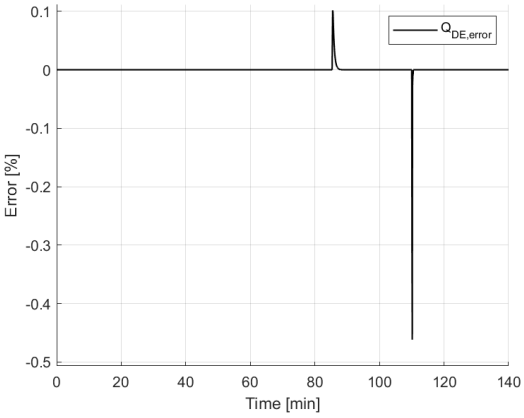

(c) Diesel engine torque error

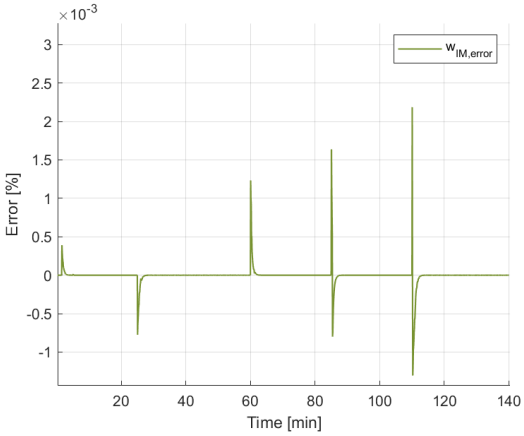

(d) Induction motor shaft speed error

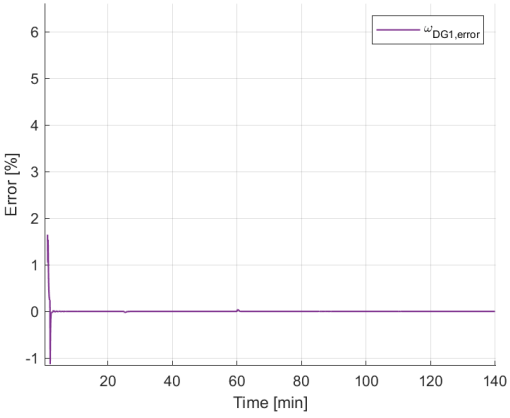

(e) Diesel generator set 1 shaft speed error

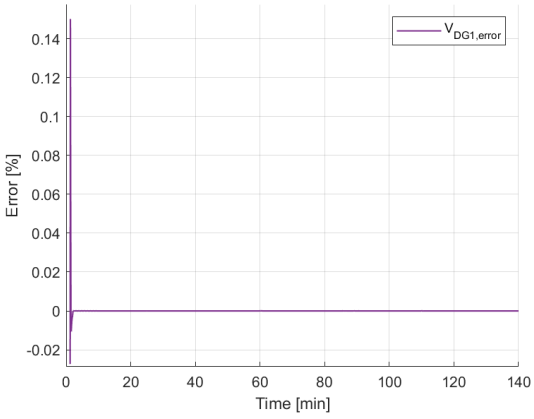

(f) Diesel generator set 1 voltage error

Figure 5.4: Tracking errors for mission 1

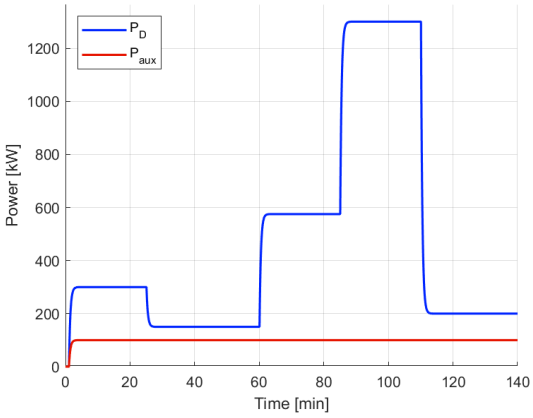

(a) Power profile

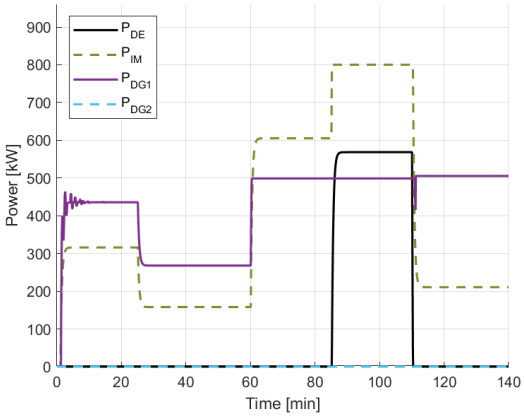

(b) Power split for the fixed equipment

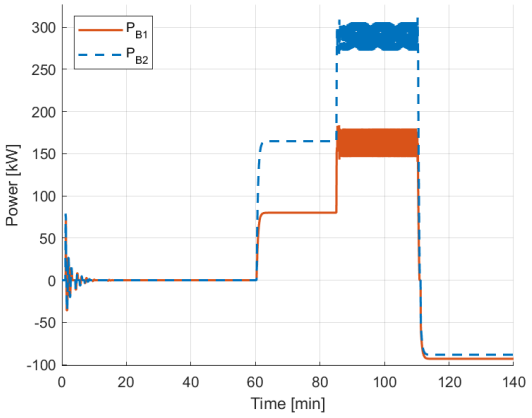

(c) Power split for the batteries

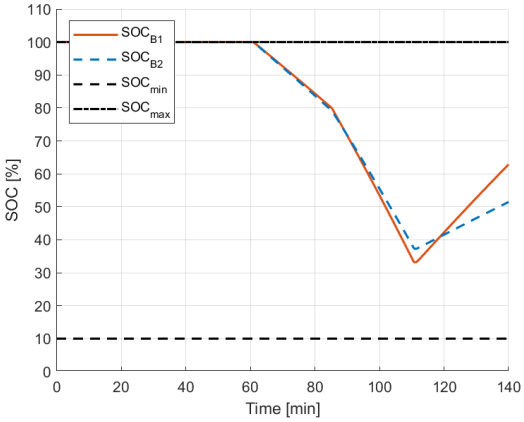

(d) SOC of the batteries

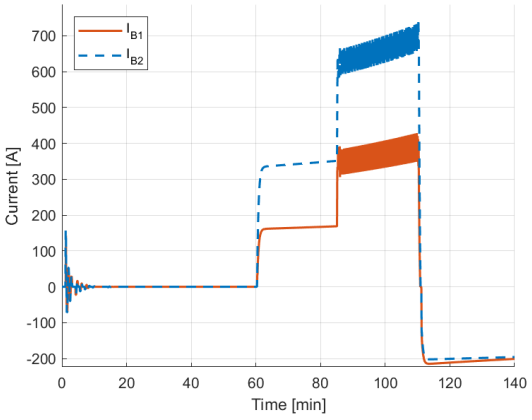

(e) Output current of the batteries

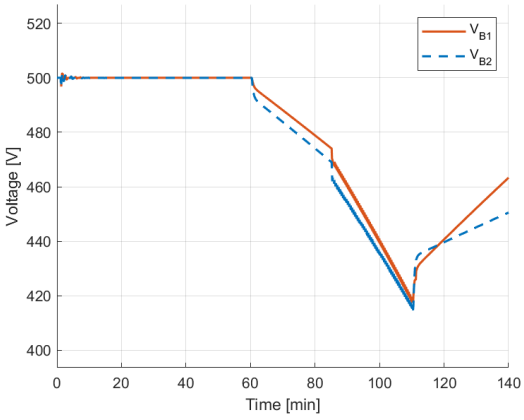

(f) Terminal voltage of the batteries

Figure 5.5: Power profile, power split, and battery performance for mission 2

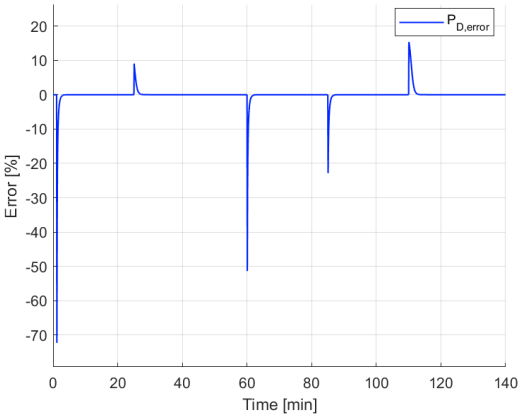

(a) Propulsion power demand error

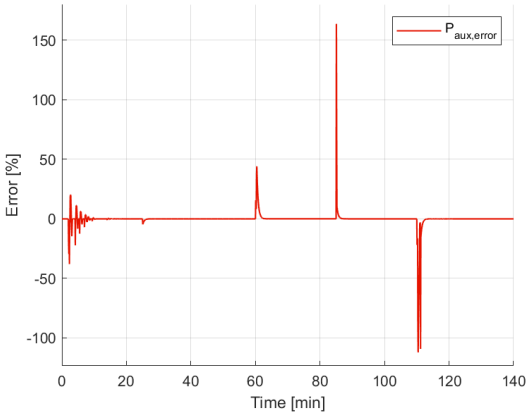

(b) Auxiliary power demand error

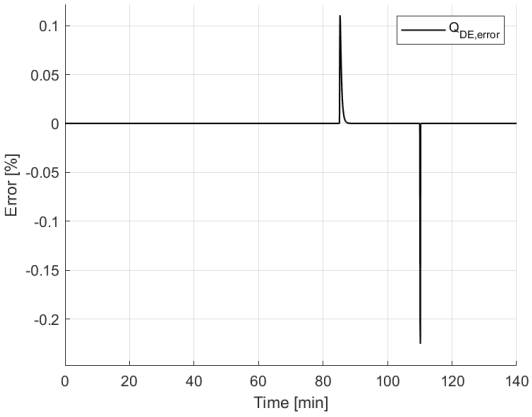

(c) Diesel engine torque error

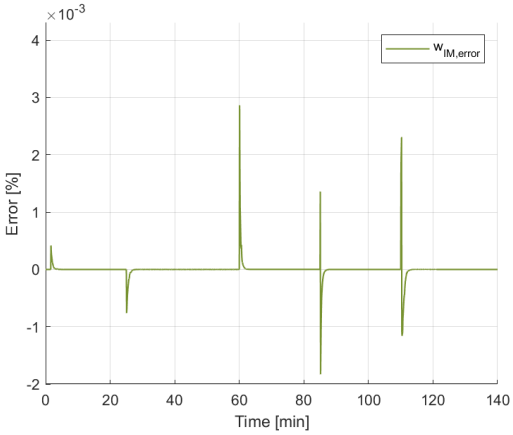

(d) Induction motor shaft speed error

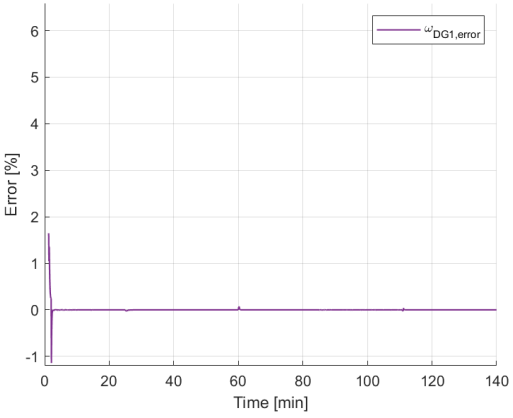

(e) Diesel generator set 1 shaft speed error

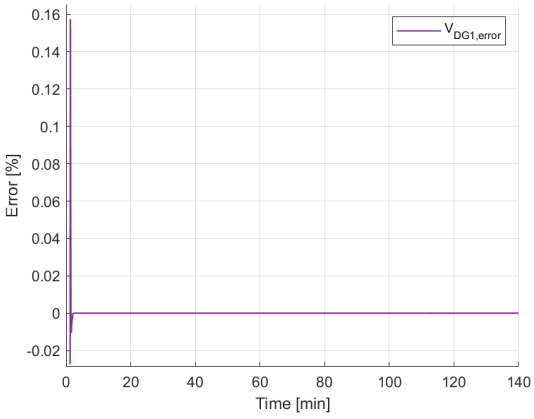

(f) Diesel generator set 1 voltage error

Figure 5.6: Tracking errors for mission 2

5.2.4. RESULTS MISSION 3

This mission also requires two batteries, but now of the same capacity. The results are shown in Figure 5.7 and 5.8, and since the performance of the fixed power plant is similar to that of the previous missions, the emphasis will be on the behavior of the batteries. With respect to the latter, as the batteries have the same capacity, the power is also split equally between them, and this is also seen in the SOC of the batteries. As a result, the aforementioned approach to treat two batteries as one, could yield similar performance. However, as also stated in this report, batteries could fail during the mission. Therefore it is still better to model the batteries separately, as the bank of controllers can then be used to work around battery faults. It can also be noted that there is more activity in the error tracking signal of the auxiliary power, around 25 minutes. This is due to the batteries, which, after a short period of discharging, are charged to their maximum SOC. Around 25 minutes, they are both fully charged, and the secondary level has to recalculate the power split, resulting in a short period of indecisiveness of the secondary level regarding power from/to the batteries and power from the diesel generator set. However, this is quickly resolved, and the remaining peaks and surges of the auxiliary power can be explained by the 'regular' changing of the power profile.

5.2.5. RESULTS MISSION 4

For the last mission, three batteries are required; two of type 2 and one of type 1. With respect to the batteries, it can be argued that this mission combines features of mission 2: two batteries with different capacity, with features of mission 3: two batteries with the same capacity, and the results can be found in Figure 5.9 and 5.10. It can, again, be seen that the fixed power plant shows the same, stable and robust, behavior as for the previous mission, indicating the variety of conditions in which the power plant can operate. Also, the batteries show similar results as for the previous missions. In fact, a combination of behavior can be found when a closer look is taken at Figure 5.9c and 5.9d. From the start of the mission to approximately 50 minutes, battery 2 and 3 are equally loaded, and since their capacity is the same, the SOC of both batteries is also similar. Now between 70 and 110 minutes, battery 1 and 2 are equally loaded, and resulting, battery 1 is drained twice as fast as battery 2. This shows that the system is well able to use multiple batteries in the power plant, either of the same or of different capacity.

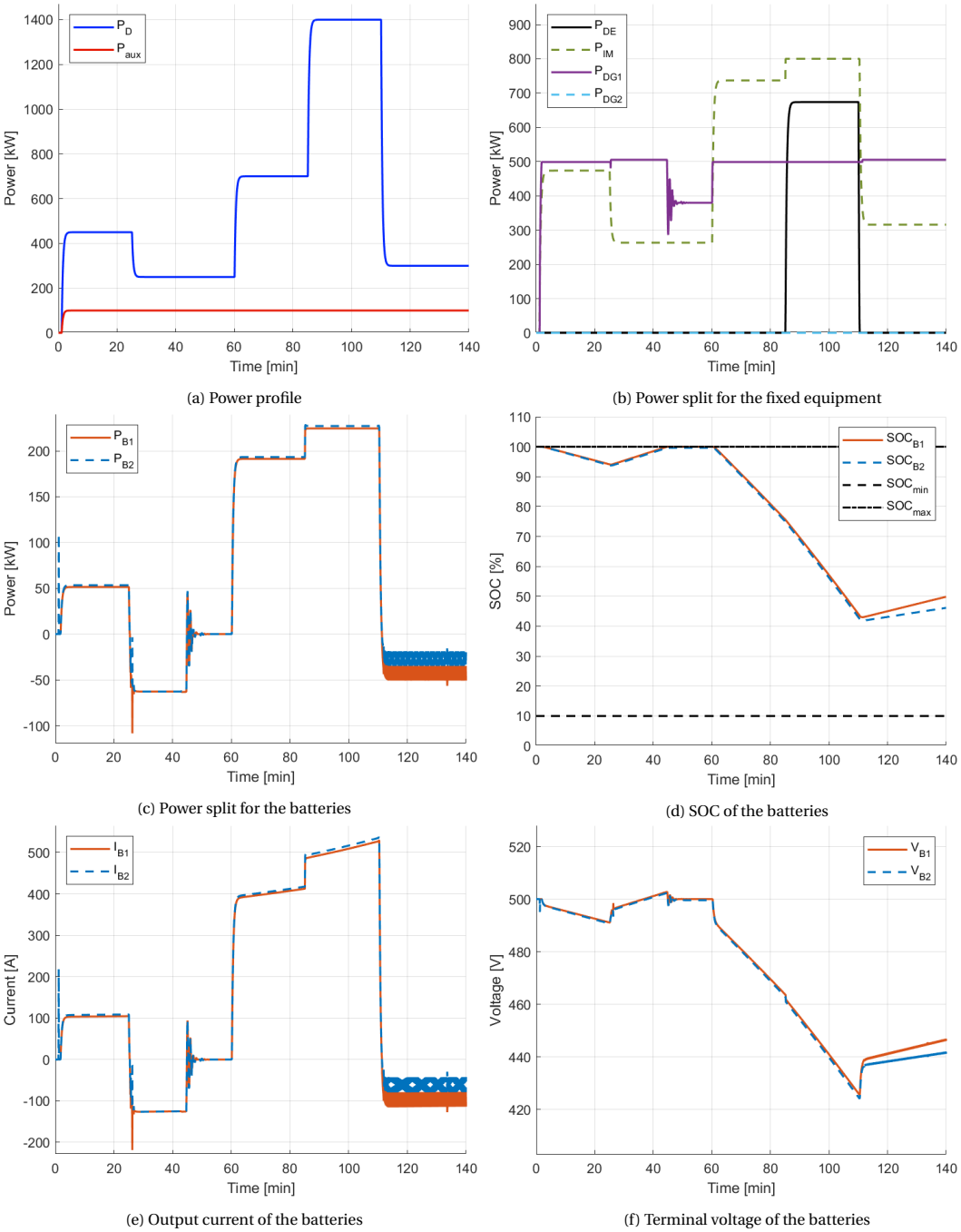

(a) Power profile

(b) Power split for the fixed equipment

(c) Power split for the batteries

(d) SOC of the batteries

(e) Output current of the batteries

(f) Terminal voltage of the batteries

Figure 5.7: Power profile, power split, and battery performance for mission 3

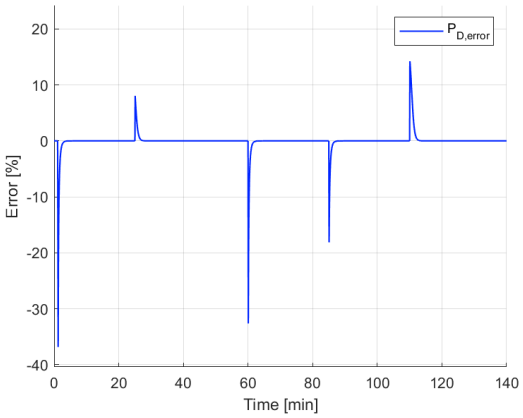

(a) Propulsion power demand error

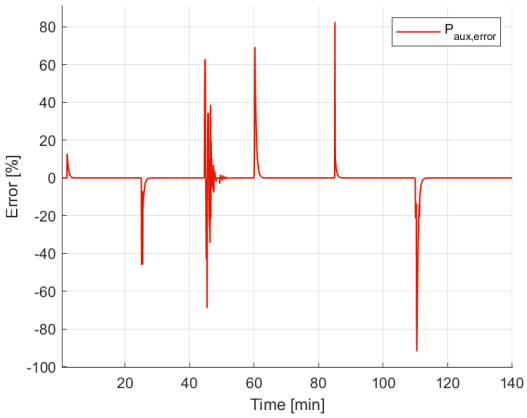

(b) Auxiliary power demand error

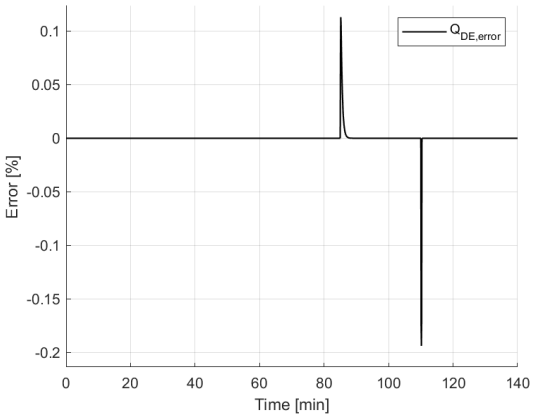

(c) Diesel engine torque error

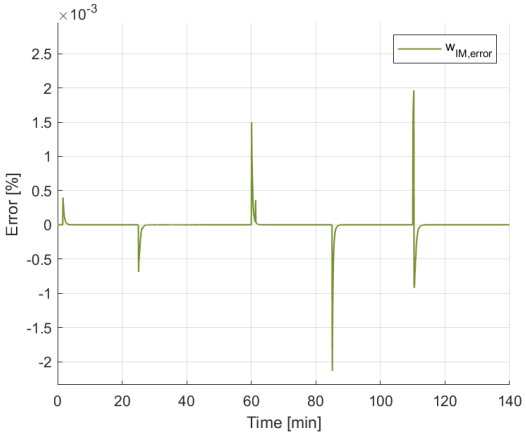

(d) Induction motor shaft speed error

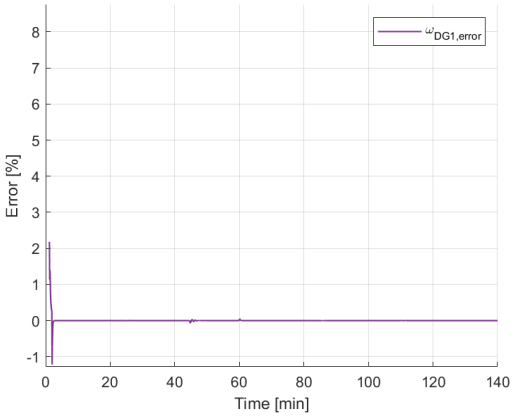

(e) Diesel generator set 1 shaft speed error

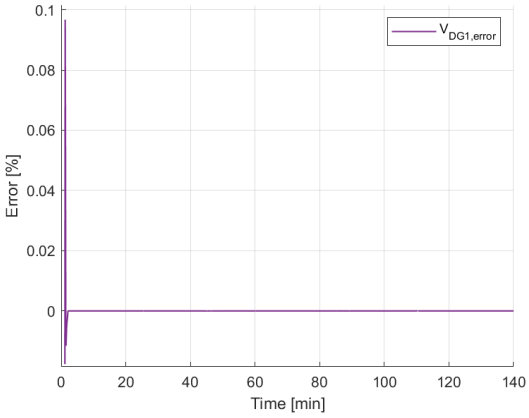

(f) Diesel generator set 1 voltage error

Figure 5.8: Tracking errors for mission 3

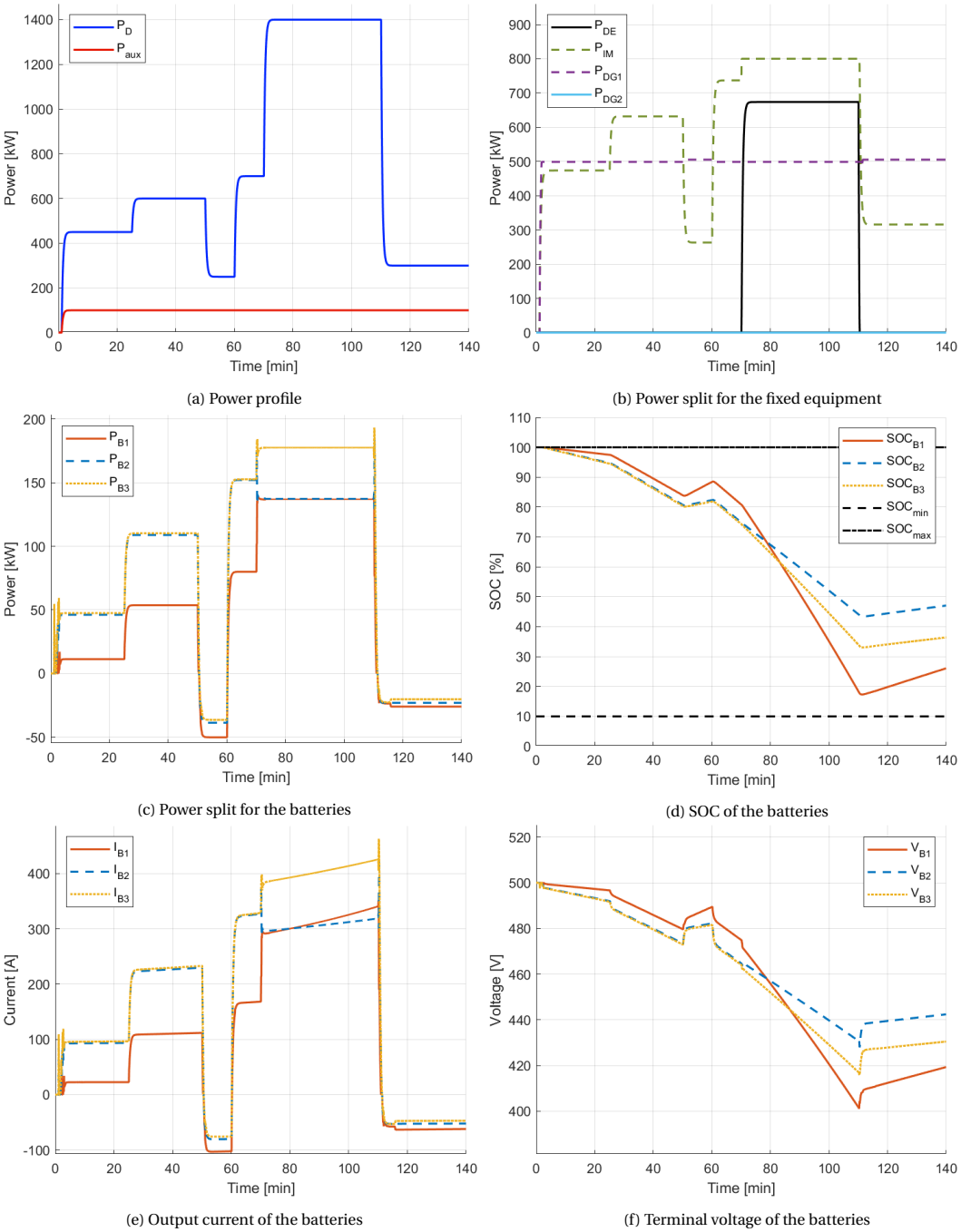

(a) Power profile

(b) Power split for the fixed equipment

(c) Power split for the batteries

(d) SOC of the batteries

(e) Output current of the batteries

(f) Terminal voltage of the batteries

Figure 5.9: Power profile, power split, and battery performance for mission 4

5

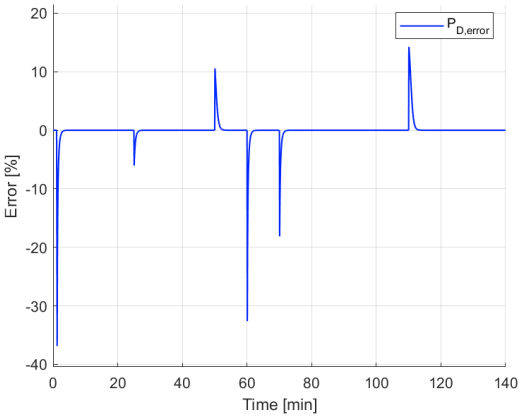

(a) Propulsion power demand error

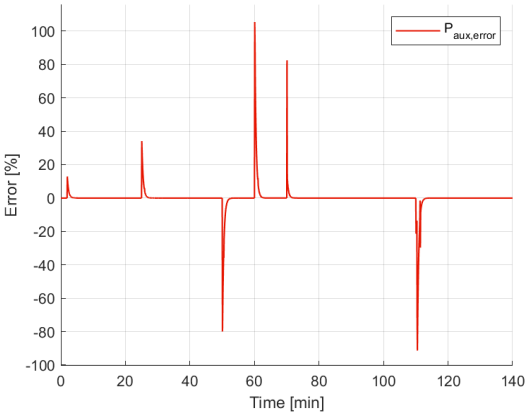

(b) Auxiliary power demand error

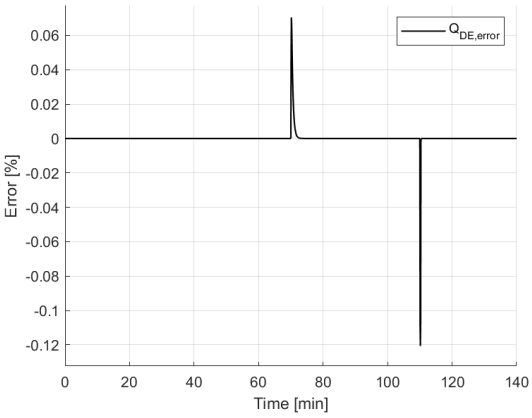

(c) Diesel engine torque error

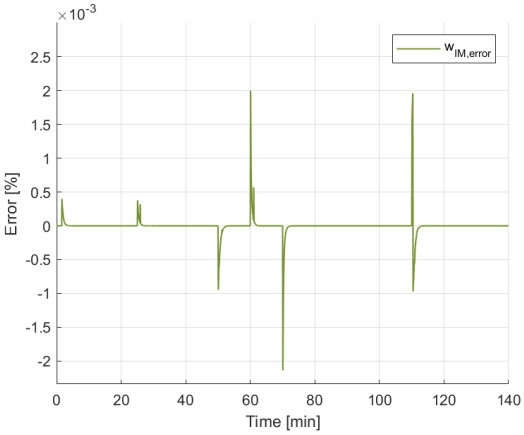

(d) Induction motor shaft speed error

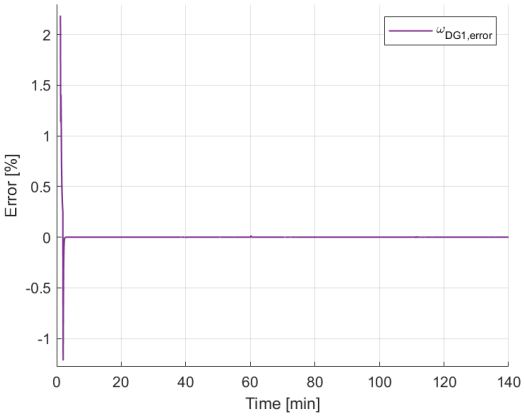

(e) Diesel generator set 1 shaft speed error

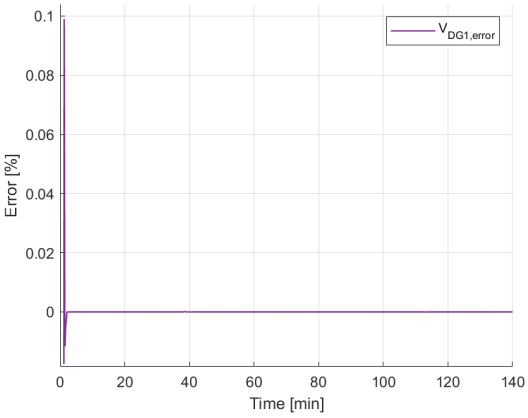

(f) Diesel generator set 1 voltage error

Figure 5.10: Tracking errors for mission 4

5.3. SIMULATION RESULTS BATTERY FAULTS

As illustrated in Chapter 4.4, the supervisor is designed to cope with battery faults. Therefore, mission 1 and mission 4 are used to illustrate the behavior of the power plant and the modular control system for a battery fault, resulting in mission 5 and mission 6, respectively, and these missions are discussed in this section. It has to be highlighted that the required fault diagnosis is not included in the design of the supervisor, only the proposed fault signal y_{fault} is manually set at a certain time t_{fault}. Both for mission 5 and 6, a battery fails at t_{fault} = 5500 seconds, approximately 92 minutes.

5.3.1. RESULTS MISSION 5

This mission is similar to mission 1, but now battery 1 fails at t_{fault}. In Figures 5.11, 5.12 and 5.13 the results for this mission can be seen, where the fault is highlighted with vertical lines. From Figure 5.11b and 5.11c, is can be noted that diesel generator set 2 is switched on when the battery fails, and also that no more power is requested from the battery. Since the battery has 'failed', the SOC, voltage, and current are no longer monitored, as the battery could be short-fused, malfunctioning, or something else, but that is not known in this report. Furthermore, using Figure 5.12a and 5.12b, the tracking errors of the propulsion and auxiliary power during the mission are seen, and it can be noted that next to the errors introduced by the changes in the power profile, an extra error at t_{fault} is observed. This error can be explained by the switching from battery power to diesel generator set power, as this is not an immediate switch but takes some time. Although the error is significant, the results still show stable behavior, as this error is only present for a few seconds. At last, since this mission uses diesel generator set 2, the tracking errors with respect to the shaft speed $\omega_{DG,2}$ and output voltage $V_{DG,2}$ can be found in Figure 5.13c and 5.13d, respectively.

5.3.2. RESULTS MISSION 6

Mission 6 is the same as mission 4, but now battery 2 fails at t_{fault}. The results show an almost perfectly stable power split for the fixed equipment, as seen in Figure 5.14b, and using Figure 5.14c, it is observed that instead of switching on another diesel generator set when a battery fails, as is the case for mission 5, the two remaining batteries are used to cover for the faulty battery. Since batteries do not have the starting time the diesel generator set has, the error introduced with respect to the auxiliary power is considerably smaller than for mission 5, as can be concluded using Figure 5.12b and 5.15b. Also, it can be noted from Figure 5.14c and 5.14d that battery 1 reaches its minimum SOC level before the high power demand of the mode *Assist-high* ends, hence battery 3 is discharged with a very high rate, for the remaining duration of this mode.

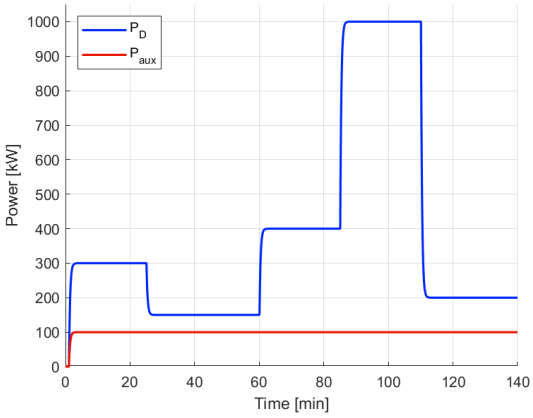

(a) Power profile

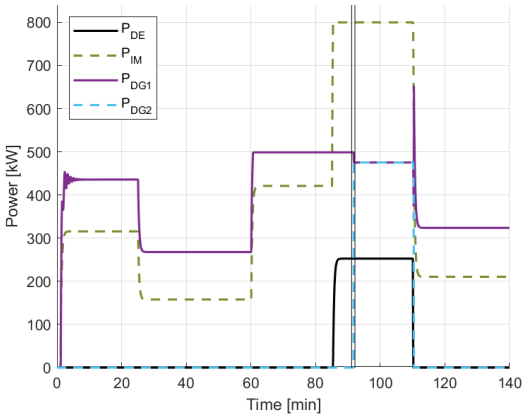

(b) Power split for the fixed equipment

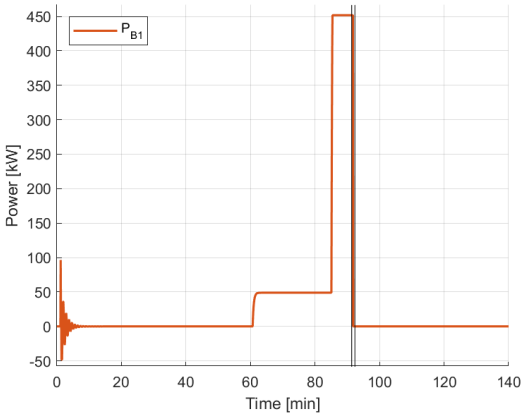

(c) Power split for the batteries

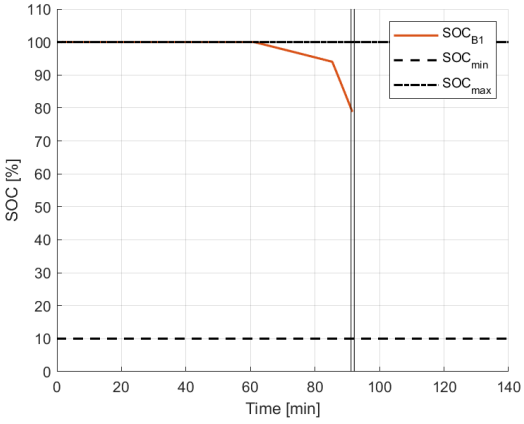

(d) SOC of the batteries

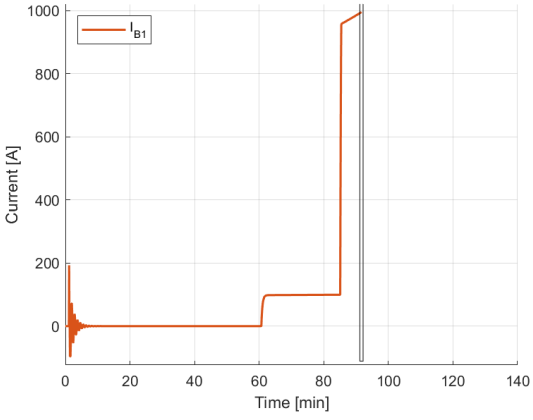

(e) Output current of the batteries

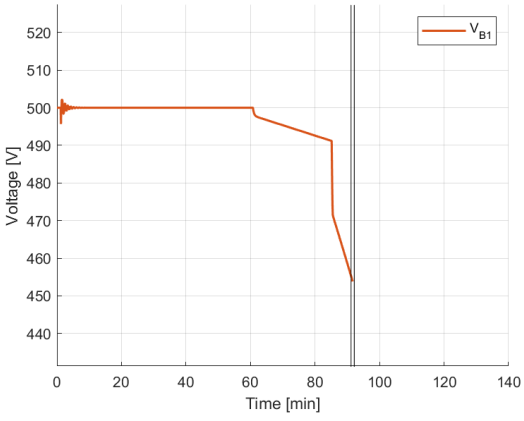

(f) Terminal voltage of the batteries

Figure 5.11: Power profile, power split, and battery performance for mission 5

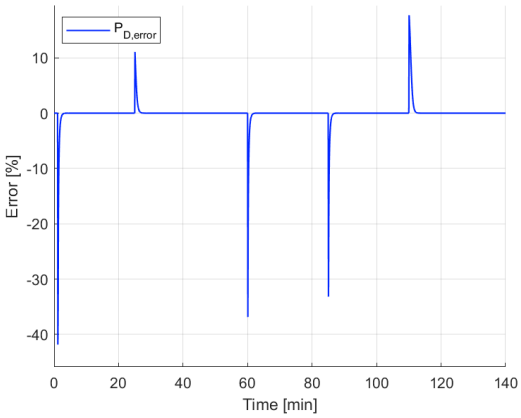

(a) Propulsion power demand error

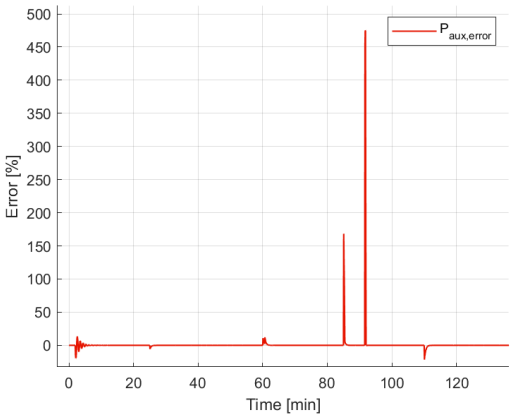

(b) Auxiliary power demand error

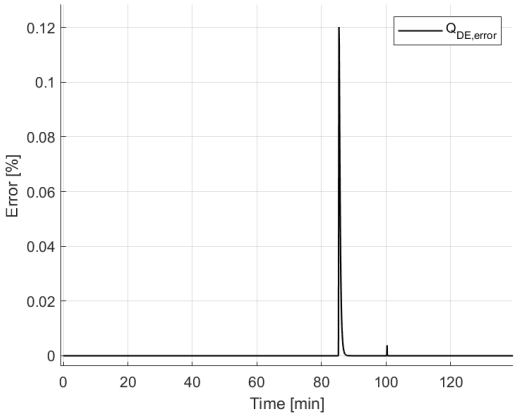

(c) Diesel engine torque error

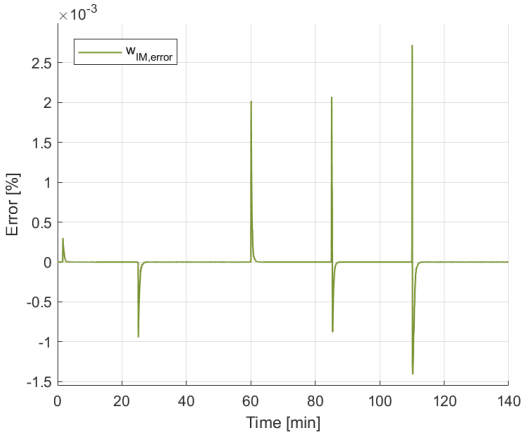

(d) Induction motor shaft speed error

Figure 5.12: Tracking errors propulsion, auxiliary, diesel engine and induction motor for mission 5

5

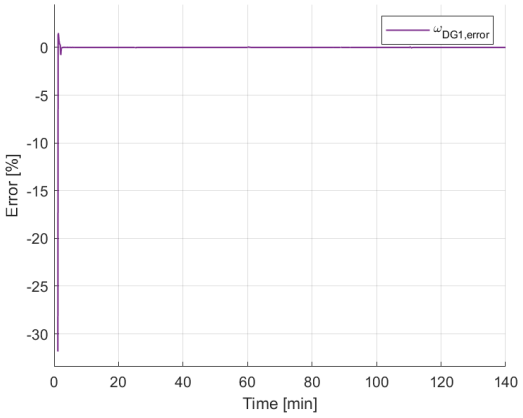

(a) Diesel generator set 1 shaft speed error

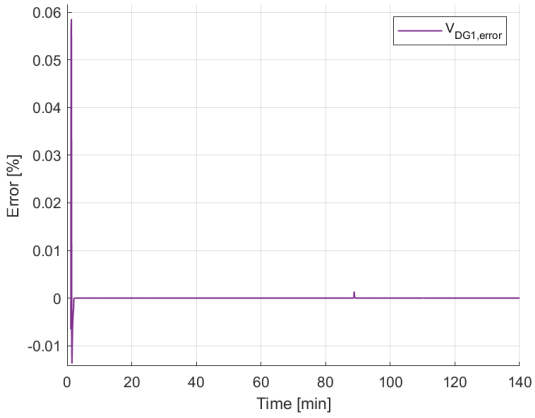

(b) Diesel generator set 1 voltage error

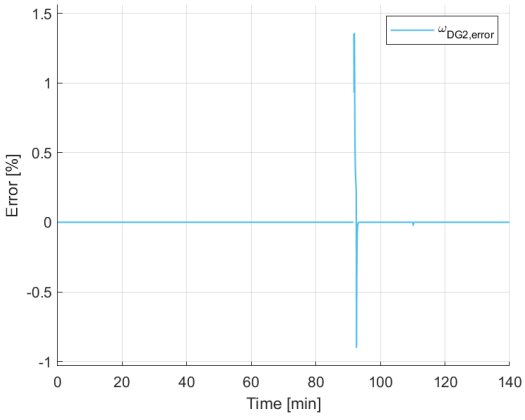

(c) Diesel generator set 2 shaft speed error

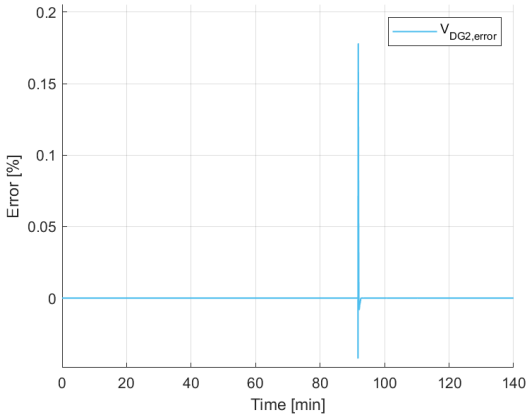

(d) Diesel generator set 2 voltage error

Figure 5.13: Tracking errors of diesel generator sets for mission 5

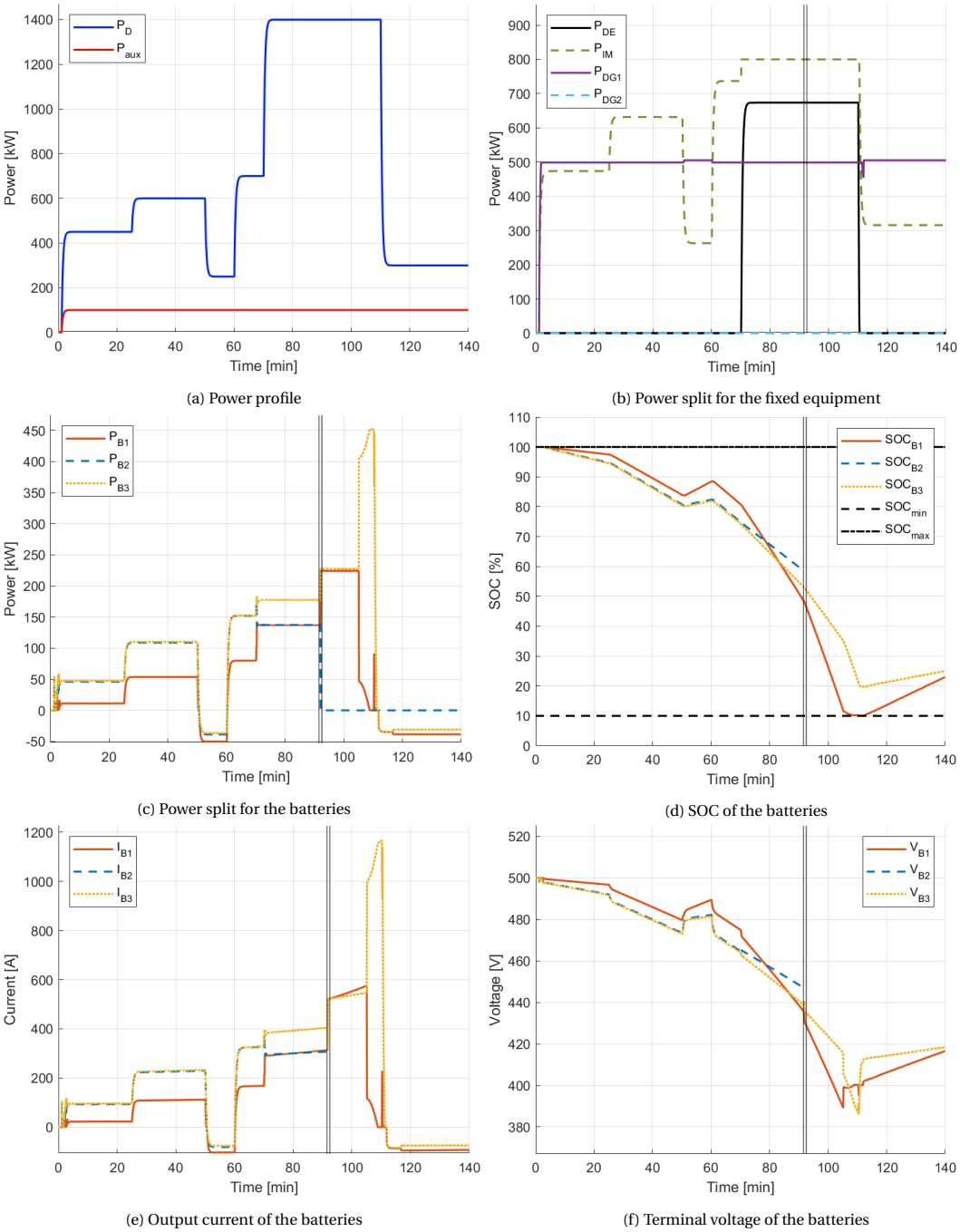

(a) Power profile

(b) Power split for the fixed equipment

(c) Power split for the batteries

(d) SOC of the batteries

(e) Output current of the batteries

(f) Terminal voltage of the batteries

Figure 5.14: Power profile, power split, and battery performance for mission 6

5

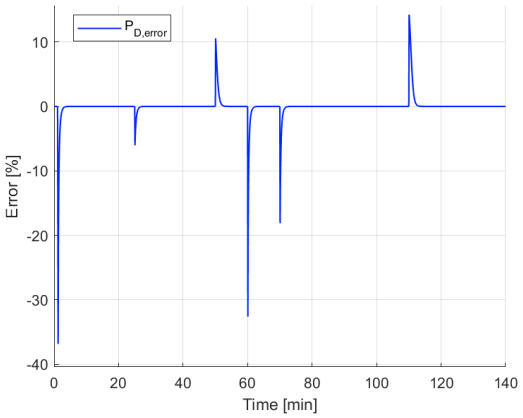

(a) Propulsion power demand error

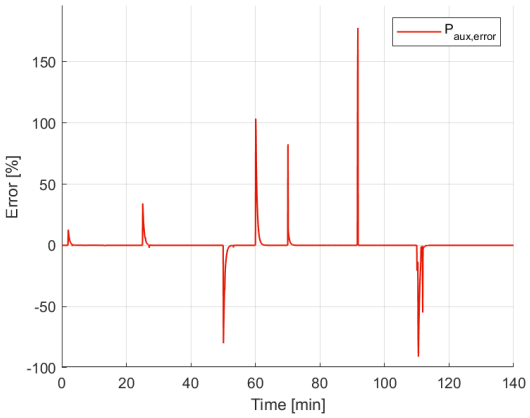

(b) Auxiliary power demand error

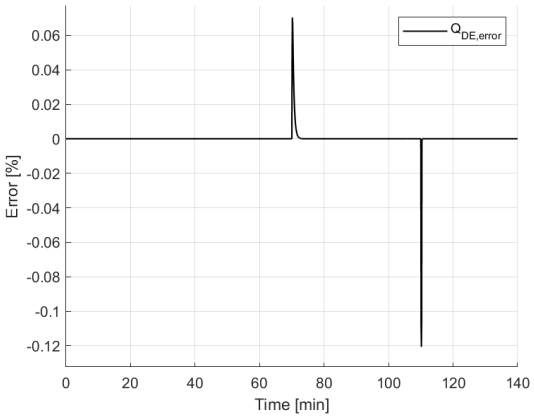

(c) Diesel engine torque error

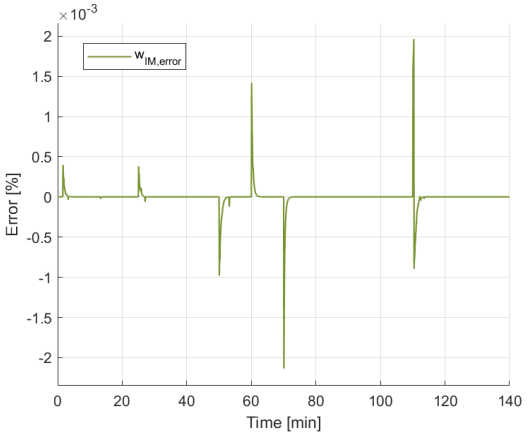

(d) Induction motor shaft speed error

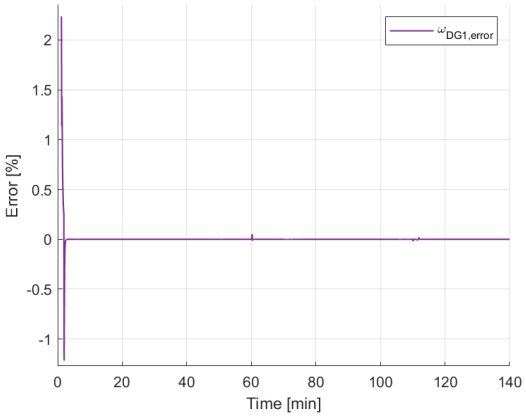

(e) Diesel generator set 1 shaft speed error

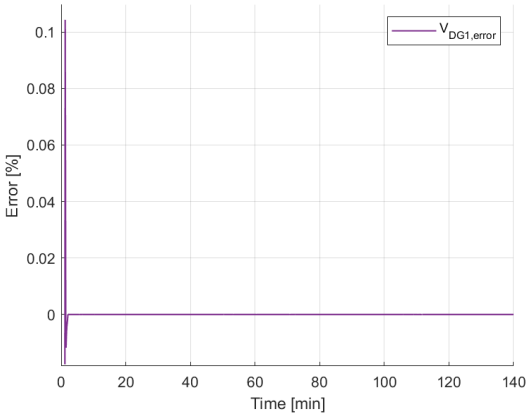

(f) Diesel generator set 1 voltage error

Figure 5.15: Tracking errors for mission 6

5.4. EVALUATION OF KPI'S

Next to visual inspection as shown with the simulation results, the KPI's can be used to measure the performance, and for each mission the tracking error of the propulsion and auxiliary power is determined, and can be found in Table 5.5. Note that these results include the performance of the whole control architecture, including the models used for the components of the power plant, as the measured error is constructed using the input for the supervisor, and output data of the power plant. To this end, it can be concluded that the propulsion power is tracked with a very good accuracy, and that the auxiliary power is also tracked to a good extent. This difference is mainly explained due to the absence of inductive and reactive loads, which tend to dampen the electric power surges that can now be seen in the simulation results, potentially decreasing the errors. Therefore, in order to improve the results with respect to the auxiliary power, a proper electric grid analysis should be included, and loads should not be assumed to be purely resistive. At last, in order to improve the performance with respect to the propulsion power, communication between the controllers for the diesel engine and induction machine might reduce the errors introduced when switching off one of the components, as now a large error is introduced (although for a short moment) when this occurs.

	Propulsion Power Error		Auxiliary Power Error	
	RMSE [kW]	SI [%]	RMSE [kW]	SI [%]
Mission 1	8.23	2.16	10.26	10.39
Mission 2	10.88	2.34	10.02	10.15
Mission 3	10.99	1.90	10.54	10.68
Mission 4	11.27	1.58	10.50	10.64
Mission 5	9.12	2.39	21.96	22.52
Mission 6	11.27	1.58	11.19	12.04

Table 5.5: Performance of modular power plant controller

Furthermore, the KPI's can be used to measure the performance of the primary level controllers and the models for the power plant components, and this is shown in Table 5.6. Since the batteries are not modelled with respect to dynamic behavior, they are not included in this analysis. It can be noted that for the induction motor, very small errors are measured, and this is mainly due to the algebraic model for this component, allowing instant changes of the induction motor torque and hence the rotor speed, where the

	Diesel Engine		Induction Motor		Diesel Generator Set 1				Diesel Generator Set 2			
	Torque		Rotor Speed		Shaft Speed		Voltage		Shaft Speed		Voltage	
	RMSE [Nm]	SI [%]	RMSE [rad/s]	SI [%]	RMSE [rad/s]	SI [%]	RMSE [V]	SI [%]	RMSE [rad/s]	SI [%]	RMSE [V]	SI [%]
Mission 1	0.0761	0.0149	6.16e-4	3.29e-4	0.0573	0.0369	96.95	2.97	-	-	-	-
Mission 2	0.123	0.0115	6.71e-4	3.41e-4	0.0578	0.0372	95.01	2.91	-	-	-	-
Mission 3	0.132	0.0106	6.67e-4	2.98e-4	0.0635	0.0409	101.95	3.12	-	-	-	-
Mission 4	0.128	0.0064	6.59e-4	2.82e-4	0.0632	0.0407	100.82	3.08	-	-	-	-
Mission 5	0.0714	0.0139	6.31e-4	3.37e-4	0.6386	0.0344	107.80	3.30	0.639	0.419	111.29	3.43
Mission 6	0.1363	0.0068	6.38e-4	2.73e-4	0.0632	0.0407	99.47	3.04	-	-	-	-

Table 5.6: Performance of the primary level and power plant components

diesel engine connected to the shaft, and the diesel engines of the diesel generator sets are modeled using a first-order differential equation, resulting in a slower response and a larger error. However, algebraic equations are also used to model the generator of the diesel generator sets, but here a quite large error is measured. This could be explained by the interconnection between the generator and the diesel engine in the diesel generator set, as the voltage equations also include the shaft speed, where the latter affected by the first-order differential equation of the diesel engine model. Furthermore, due to this interconnection, the PI shaft speed controller and the PI voltage controller affect each other, while they have no communication. This could introduce some difficulties, and it could be that the approach of this thesis results in a preference of shaft speed stability over voltage stability. Also, simple models and PI controllers are used, where the fuel intake of the diesel engines is modelled as instantaneous, resulting in very fast torque response of the engines. Then, if for example the gains of PI controller of the generators voltage controller are too low, this could also explain the difference in errors the measured error signals. However, as a proper stability analysis is missing in this thesis, this has to be investigated in future research.

At last, the impact of the battery faults can also be seen from this analysis. Using Table 5.5, it can be seen that indeed for mission 5, where diesel generator set 2 is used to generate the power when the battery fails, a quite large error regarding the auxiliary power is present, while the propulsion power is not much affected. As for mission 6 the second diesel generator set is not used, but the remaining batteries provide the power for the failed battery, this error is much smaller, and for the propulsion power this error is almost similar to the error of a mission with no failing batteries. Now, using Table 5.6, it can be noted that failing batteries do not, or very little, affect the remaining equipment with respect to tracking their reference-signals.

5.5. CONCLUDING REMARKS

In this chapter, the fifth and last subquestion "How to verify the performance (stability and robustness) of the developed modular control scheme?" is answered.

Using the simulations results of four missions, data from the supervisor, secondary level, and the primary level is plotted and the KPI's are used to measure the performance. Stable behavior of the control system is shown, with a relative tracking error of only 3% for the propulsion power, and 11% for the auxiliary power. Furthermore, for two of the four missions battery faults are introduced, and also in these scenarios stable behavior is seen, with the same relative tracking error for the propulsion power (3%). Regarding the auxiliary power, if a second diesel generator set has to be switched on, the relative error of the auxiliary power increases up to 22%, while for a scenario where the remaining batteries are able to supply the power when a battery fails, the error of the auxiliary power is less than 12%, which is only a slight increase with respect to a regular mission. At last, since the designed modular control architecture shows stable behavior for multiple power power profiles and multiple power plant layouts, it can be concluded to be robust.

6

Conclusions and Recommendations

This chapter presents the research conclusion by answering the main research question: "How can mission-oriented modular control of marine vessels be designed?", using the concluding remarks of each chapter, where the five subquestions are discussed. This is following by the recommendations, which will for example provide insight in how the design of a mission-oriented modular control system can be improved, but also how this can be used for future vessel design.

6.1. Conclusion

This thesis presented a methodology to design a mission-oriented, modular power plant for a retrofittable power plant. First, in Chapter 1 the background and motivation was stated, and it was shown that current marine vessels use a fixed power plant and fixed control system, while their missions introduced variability in the loading of their power plants. This introduced the need for a mission-oriented power plant design, where equipment modifications are allowed, and consequently, a control system that allows for equipment modification had to be designed. Then, the methodology was presented, by showing the main research question, the subquestions, and also the outline of this thesis and how the research questions would be addressed. To this end, the state-of-the-art was discussed in the second chapter.

In Chapter 2 the first subquestion: "What is the state-of-the art in marine power plant control?", is answered, by means of a literature review. It is seen that there are many control strategies used for marine vessels, each with their own characteristics. Most ships have a control system consisting of multiple levels, resulting in a multi-level control architecture, as was already shown in Figure 1.5. The highest level is the guidance and navigation system, which measures the position and motion of the ship, and determines the course and the heading. This is fed to a general secondary level controller, which uses

this input to optimize the voyage and follow the desired path. This creates set-points for the rudder angle, which is then applied by the primary level rudder controller, but also set-points for the total power needed for propulsion of the ship. The latter is used by the secondary level plant control, which converts this input to settings for the primary level controllers for the engines, generator sets, electric machines, and batteries, using a cost function and constraints, based on the specific equipment in the power plant. The primary level control and the secondary level plant control are responsible for the power plant of the ship, and are therefore refered to as the power plant control system. There are various control strategies for this system, and the specific strategy depends on the type of vessel. Service ships often have hybrid propulsion and a hybrid power supply, hence they often use ECMS, power management, or coordinated control, but a simple rule-based controller of dynamic programming is also seen. Cargo ships have more simple power plants, consisting mainly of mechanical propulsion and a mechanical power supply, and therefore the control system focuses on maintaining the required shaft speed. However, ECMS or power management is also seen on bulk carriers and tankers with a hybrid power supply. Passenger ships, such as ferries and cruise ships, often have mechanical or hybrid propulsion, combined with a hybrid power supply, and hence the control system often uses strategies to provide the optimal power split between the equipment. Furthermore, it is seen that although there are multiple batteries installed in the power plant, they are described by a single model, hence from the perspective of the vessels control system, only one battery is present. At last, this chapter showed a taxonomy, presented in Table 2.1, which includes information such as the type of vessel, type of propulsion, type of power supply, and the control strategy. Next, the different vessels discussed in this chapter were used to discuss the correlation between the mission, power profile, and the automation modifications.

Chapter 3 answered the second and third subquestions: "How to model the correlation between the mission and the power profile of the vessel?" and "How to model the correlation between the power profile for a mission and the needed modifications in automation of the control systems and the power plant?". First, in Chapter 3.1, power profiles and missions of different vessels were analyzed, and using this a general definition of a mission was given, providing the type of cargo, the locations the vessel has to visit, and the available mission time. By combining the information given in the mission definition, the type of vessel and its characteristics, the operational modes, the operational environment, and the speed of the vessel throughout the mission could be derived, resulting in the power profile for the mission. Furthermore, a relation-graph showing this correlation and a pseudo-algorithm to construct the power profile were presented in Figure 3.7 and Algorithm 1, respectively. Next, in Chapter 3.2 different power profiles of a container ship and tugboats were used to specify equipment modifications required between the mission, indicating the correlation between the power profile (dictated by the mission) and the equipment modifications. Using this, and the multi-level control system of a marine vessel described in the previous chapter, automation modifications of the control system were proposed, as presented in Figure 3.17, and summarizing this resulted in the following. Based on the power profile, it can be decided whether or not equipment modifications, such as additions, removals, or replacements of equipment,

are required, and if so, which equipment modifications. If this is determined, the cost function and the constraints included in the secondary level control, required to determine the power split and reference signals for the primary level, have to be updated, together with the controllers in the primary level, such that each component in the power plant is included in the secondary and primary level. Next, using the found equipment and automation modifications, a modular control system was designed.

In Chapter 4 the fourth subquestion: "How can a modular control architecture be designed to meet the proposed automation and power plant modifications?" was answered. The first step was to identify the power plant for which the control system would be designed. In this thesis, a hybrid power plant, shown in Figure 4.1, was selected. With respect to the propulsion, a single shaft line, where a propeller is connected to a diesel engine and an induction motor through a gearbox is used. The power supply consists of two diesel generator sets and a variable amount of batteries, where batteries can be replaced, added, or removed, inspired by the ZESPacks of Wärtsilä, and hence the primary level control and the models used to describe the power plant equipment was discussed next. For each component and its primary level controller, a relatively simple model and PI control is used, as found in literature. Only for the batteries, a different approach was used, and this thesis proposed the use of a so called battery constraint module, which measures the output current of the battery, and using the (known) battery characteristics the module provides a window for the power that can be supplied to or requested of the battery. Using this, the secondary level control was designed, where an ECMS structure is used to provide the power split for each possible layout of the power plant, resulting in a bank of controllers (inspired by the concept of supervisory switching control). In order to select the required controller from this bank a supervisor was designed, which determines the required batteries for the mission, based on the power profile, and selects the corresponding secondary level controller. Furthermore, the supervisor was designed to handle battery faults, assuming proper fault diagnosis (not designed nor presented) was available. The designed modular control architecture was shown in Figure 4.20. Next, different missions were simulated, in order to verify the performance of the designed control architecture with respect to the stability and robustness.

Finally, in Chapter 5 the fifth and last subquestion "How to verify the performance (stability and robustness) of the developed modular control scheme?" was answered. First a baseline mission for a tugboat was established, as found in literature. Second, variations in the mission were used to manually alter the power profile, using the found correlation between the mission and the power profile of Chapter 3.1, to create a total of four different missions with corresponding power profiles, as presented in Table 5.1 and Figure 5.1. Using these profiles, a MATLAB/Simulink environment was used to simulate the missions. First, the supervisor determined the required batteries for the missions, where after it automatically selected the required secondary level controller from the bank, and initialized the battery constraint modules. Then, each mission was simulated, and the output of the power plant equipment was used to derive the delivered propulsion power and auxiliary power, such that a tracking error could be determined. It is found that the designed modular control system is able to follow the required propul-

sion power with an RMSE less than 3% of the nominal propulsion power, and the auxiliary power was tracked with an RMSE less than 11% of the nominal auxiliary power, and therefore stability was verified. Furthermore, as both during each mission as between the missions the power demand varied, and each mission is executed with different batteries in the power plant, it can be concluded that the designed modular control architecture is also robust. After these four missions were simulated, two more missions where considered: mission 5 and mission 6, which where similar to mission 1 and 4, respectively, but now including battery faults. For these missions a battery was assumed to fail at a certain time, and it was also assumed that there was a fault diagnosis that could detect and identify which battery was at fault. It has to be noted that no design was included for the fault diagnosis, and only the proposed output of this fault diagnosis as discussed in section 4.4 was used in the simulations. Using this, the simulation results showed that for multiple batteries in the power plant, the remaining batteries took over when a battery failed, and for a power plant with a single battery, the redundant diesel generator set was turned on when the battery failed. As a diesel generator set has a certain starting time in order to reach the desired power output, a larger tracking error for the auxiliary power was observed here (23% versus 14% when multiple batteries can take over), but the propulsion tracking error remained less than 3% for both fault scenarios. This showed that next to stable and robust behavior for a variable power plant layout (different batteries in the power plant), battery faults can be handled, under the assumption of properly designed fault diagnosis.

In conclusion, this thesis presented a methodology to design a mission-oriented modular control architecture for retrofittable power plants. First, the correlation between the mission and the power profile, and also how variations in the power profile lead to needed automation modifications of the control system and the power plant were discussed. Based on the concept of supervisory switching control, a modular control architecture for a hybrid power plant which allows modular use of batteries is designed. The modular control architecture consists of a supervisory level, a secondary level, and a primary level, and for a given mission, the control system is able to select the required batteries and corresponding secondary level controller. By means of simulating multiple missions, the designed modular control architecture is found stable and robust, while switching between secondary level controllers when batteries are added, removed, or replaced. Even more, it was found that the designed modular architecture can accommodate battery faults, provided that a (not designed nor presented in this thesis) fault diagnosis is included.

6.2. RECOMMENDATIONS

In this thesis, the correlation between the mission and the power profile is modeled, and an algorithm is proposed to determine the power profile from the inputs defined by the mission. However, future research could improve this model, by including more specifics related to the auxiliary power, and by validating the proposed algorithm. Regarding the correlation between the power profile and the automation modifications, the decision logic to determine the required equipment modification is limited to batteries in this thesis, and future work could include multiple power plant components to allow for a more optimal solution for the power plant layout, given a power profile.

A modular control architecture for a retrofittable power plant was designed, allowing batteries to be added, replaced, or removed, and the performance is verified using simulations based on different missions for a tugboat. While the results regarding the performance showed stable and robust behavior, the architecture still has to be validated. Also, using the proposed architecture, future research could include modular use of different power plant components, such as the diesel generator sets or induction motors, or the addition of for example fuel cells as energy source. Furthermore, the induction motor could be used as shaft generator, which would have to be adequately included in the control system. With respect to the secondary level, two additional constraints were proposed for the ECMS structure, in order to keep batteries for charging each other. Future research could focus on this problem, to determine if there are more solutions to this problem, and which is best. Regarding the battery fault scenario's, a proper fault diagnosis was only assumed, not designed. Hence, future research could include this in the supervisor. The primary level control of this thesis includes non-communicating PI controllers, but it could be beneficial to have communication between some of these controllers, for example between the diesel engine and the induction motor, or between the two controllers for the diesel generator set. Future research could therefore investigate the added value of communication between the primary level controllers. Also, this thesis proposed the use of battery constraint modules, shifting the required battery constraints from the secondary level to the primary level. The exact design of such modules can be investigated in future research, and possibly this concept can be expanded to other components of the power plant to enhance modularity, just as the authors of [155] proposed. At last, the stability of the electric grid is not included in the design, and also only resistive loads are assumed. Future research could therefore focus on including reactive and inductive loads, and e.g. connecting the power input of the induction motor to the power output of the diesel generator sets and batteries, to get a more closed-loop power analysis.

A

Relation between Effective Power and Vessel Speed

In Figure A.1 the relation between the effective power and the speed of the chemical tanker can be seen, for both trial condition (very calm sea) and 15% sea margin ('roughness' of the sea increases with 15%) [64]. As shown in Chapter 3, the required effective power of each vessel can be described by the vessel speed and two parameters [99–101]:

$$P = c * V^a \tag{A.1}$$

where P is the required effective power, V is the vessel speed, c is a scaling factor, and a determines the proportionality between the power and the speed. For a tanker, normally $a \approx 3.2$ [103] for low vessel speeds, and $a > 3.2$ for high vessel speeds. Furthermore, c can be assumed constant for low vessel speeds, but not for high vessel speeds. This section will approximate a and c, to verify if this theory can be used for a chemical tanker.

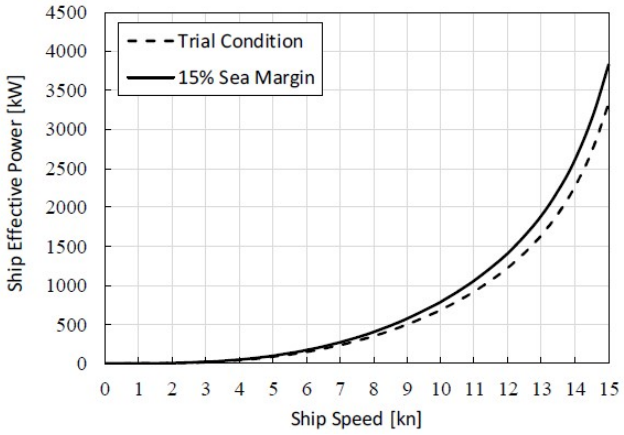

Figure A.1: Effective power versus ship speed [64]

A

Since the shown relation between the speed of the vessel and the effective power (in this section also refered to as power curve) of Figure A.1 is only graphical, to be able to find a proper approximation of a and c, first the effective power for all integer values of the vessel speed for both the trial condition and 15% sea margin are measured from the figure. These measurements are shown in Tables A.1 and A.2 respectively, and used to plot discrete power curves on top of the graphical data, which can be seen in Figure A.2. It can be noted that the discrete power curves aligns almost perfectly with the original power curves.

P_{tc} [kW]	0	0*	0*	15	44	88	147	221	338	500	706	941	1235	1662	2324	3324
V [kn]	0	1	2	3	4	5	6	7	8	9	10	11	12	13	14	15

Table A.1: Effective power (P_{tc}) versus vessel speed (V) for the trial condition

P_{sm} [kW]	0	0*	0*	15	44	88	162	265	412	588	809	1088	1441	1926	2706	3853
V[kn]	0	1	2	3	4	5	6	7	8	9	10	11	12	13	14	15

Table A.2: Effective power (P_{sm}) versus vessel speed (V) for 15% sea margin

*: For these vessel speeds a proper reading of the effective power could not be made, and since the real values would be relatively very small, they are assumed to be zero.

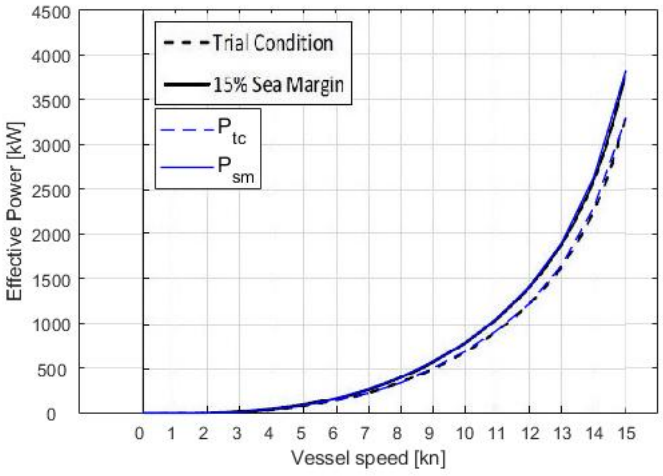

Figure A.2: Discrete power curves (blue) based on the original power curves (black)

The next step is to use the discrete power curves to approximate a and c. Since the curves are discrete, each interval of $P_{k+1} - P_k$ has a unique a_k. Furthermore, since c can be assumed constant for low vessel speeds, it can also be assumed that $c_{k+1} \approx c_k$. Using

this, the following relations for a_k and c_k are found:

$$P_k = c_k * V_k^{a_k}$$

$$P_{k+1} = c_{k+1} * V_{k+1}^{a_k} = c_k * V_{k+1}^{a_k}$$

$$\frac{P_{k+1}}{P_k} = \frac{V_{k+1}^{a_k}}{V_k^{a_k}} = \left(\frac{V_{k+1}}{V_k}\right)^{a_k}$$

$$a_k = \frac{log\left(\frac{P_{k+1}}{P_k}\right)}{log\left(\frac{V_{k+1}}{V_k}\right)} \quad , \quad c_k = \frac{P_k}{V_k^{a_k}} \tag{A.2}$$

With these relations and the data from Table A.1 and A.2, MATLAB is used to derive first approximations for a_k and c_k, and the results can be seen in Table A.3. They show that

Interval (Vessel speed)		0-1	1-2	2-3	3-4	4-5	5-6	6-7	7-8
Trial Condition	a_k	-	-	-	3.74	3.10	2.81	2.65	3.18
	c_k	-	-	-	0.24	0.59	0.94	1.29	0.45
15% Sea State	a_k	-	-	-	3.74	3.10	3.35	3.19	3.03
	c_k	-	-	-	0.24	0.59	0.40	0.53	0.73
Interval (Vessel speed)		8-9	9-10	10-11	11-12	12-13	13-14	14-15	
Trial Condition	a_k	3.32	3.07	3.07	3.18	3.74	4.47	5.24	
	c_k	0.34	0.59	0.59	0.45	0.11	0.02	0.02	
15% Sea State	a_k	3.13	2.90	3.22	3.31	3.69	4.42	5.41	
	c_k	0.59	0.98	0.47	0.38	0.15	0.02	0.02	

Table A.3: Approximations for a_k and c_k

a_k fluctuates around the expected value of 3.2 for vessel speeds up till 12 knots for the trial conditions, and up till 11 knots for the 15% sea state, indicating the upper bound for 'low vessel speed'. However, the assumption that c_k is constant for these low vessel speeds seems to be invalidated by the results, as it ranges from 0.24 to 1.29. Therefore, a new approach is chosen. Based on the results shown in Table A.3, a_k will range from 2 to 4, and c_k from 0 to 2, and these are used to calculate a new set of effective (discrete) power curves. For each power curve, the method of the least square error will be used to find the best fit to the data of Table A.1 and A.2. In Table A.4 the required variables are shown, and in Equation A.3 the used approach can be seen.

*An important note is that since the power for vessel speeds 0-2 knots are manually set to zero, and the upper bound for low vessel speed is between 11-12 knots, only vessel speeds from 3 to 12 knots will be used compute the square errors and find the best fit.

A

Variable	Description	Size
a	Row vector of candidates for a	1x1000
a_{tc}	Approximation of a, trial condition	1x1
a_{sm}	Approximation of a, 15% sea margin	1x1
c	Row vector of candidates for c	1x1000
c_{tc}	Approximation of c, trial condition	1x1
c_{sm}	Approximation of c, 15% sea margin	1x1
a	Row vector of candidates for a	1x1000
V	Row vector of vessel speed	1x16
V_{fit}	Row vector of vessel speed for plot of best fit	1x100
P_{tc}	Row vector of effective power, trial condition	1x16
P_{sm}	Row vector of effective power, 15% sea margin	1x16
P	Matrix of effective power for all a,c and V	1000x16x1000
$P_{fit,tc}$	Row vector of best fit effective power, trial condition	1x100
$P_{fit,sm}$	Row vector of best fit effective power, 15% sea margin	1x100
e_{tc}	Matrix of squared errors, trial condition	1000x9x1000
e_{sm}	Matrix of squared errors, 15% sea margin	1000x9x1000
$e_{sum,tc}$	Matrix of squared errors summed over vessel speed, trial condition	1000x1000
$e_{sum,sm}$	Matrix of squared errors summed over vessel speed, 15% sea margin	1000x1000
$e_{c,tc}$	Row vector of minimum errors for each a, trial condition	1x1000
$e_{c,sm}$	Row vector of minimum errors for each a, 15% sea margin	1x1000
$e_{a,tc}$	Smallest squared error, trial condition	1x1
$e_{a,sm}$	Smallest squared error,15% sea margin	1x1
$P_{fit,sm}$	Best fit to power curve,15% sea margin	1x100

Table A.4: Required variables for approximation of power curves

Variable	Approximation
a_{tc}	3.10
a_{sm}	3.09
c_{tc}	0.55
c_{sm}	0.64

Table A.5: Approximations of a and c

```
for i = 1 : 1000
    for j = 1 : 16
        for z = 1 : 1000
            P(i, j, z) = c(i) * V(j)^a(z)
        end
    end
end
for i = 1 : 1000
    for j = 1 : 9
        for z = 1 : 1000
            e_tc(i, j, z) = (P(i, j + 3, z) − P_tc(i, j + 3, z))^2
            e_sm(i, j, z) = (P(i, j + 3, z) − P_sm(i, j + 3, z))^2
        end
    end
end
for i = 1 : 1000
    for z = 1 : 1000
        e_sum,tc(i, j, z) = sum(e_tc(i, :, z))
        e_sum,sm(i, j, z) = sum(e_sm(i, :, z))
    end
end

e_c,tc = min(e_s,tc)
e_a,tc = min(e_c,tc)
[I_c,tc I_a,tc] = find(e_s,tc == e_a,tc)

e_c,sm = min(e_s,sm)
e_a,sm = min(e_c,sm)
[I_c,sm I_a,sm] = find(e_s,sm == e_a,sm)

c_tc = c(I_c,tc)
a_tc = c(I_a,tc)
c_cm = c(I_c,sm)
a_sm = c(I_a,sm)

P_fit,tc = c_tc * V_fit^a_tc
P_fit,sm = c_sm * V_fit^a_sm
```

(A.3)

In Table A.5 the final approximations of a and c can be seen, for both the trial condition as for the 15% sea margin. It can be seen that the approximated value for $a = 3.09 - 3.10$ is close to the theoretical value of 3.2 for a tanker, with an error of 3%. Furthermore, it can be seen from Figure A.3 that the found (constant) approximations of c lead to a very good approximation of the power curves. Chapter 3 also states that to find the required power for the 15% sea margin, the required power for calm sea conditions (in this case trial conditions), can just be multiplied by this sea margin. This implies that $\frac{c_{sm}}{c_{tc}}$ has to be equal to the sea margin (since $a_{tc} \approx a_{sm}$). Using the found approximations for these parameters, it is found that $\frac{c_{sm}}{c_{tc}} = 1.16$, which means a sea margin of 16%. Therefore, it is concluded that these results verify the described theory about the relation between the required effective power and the vessel speed, and for the sea margin.

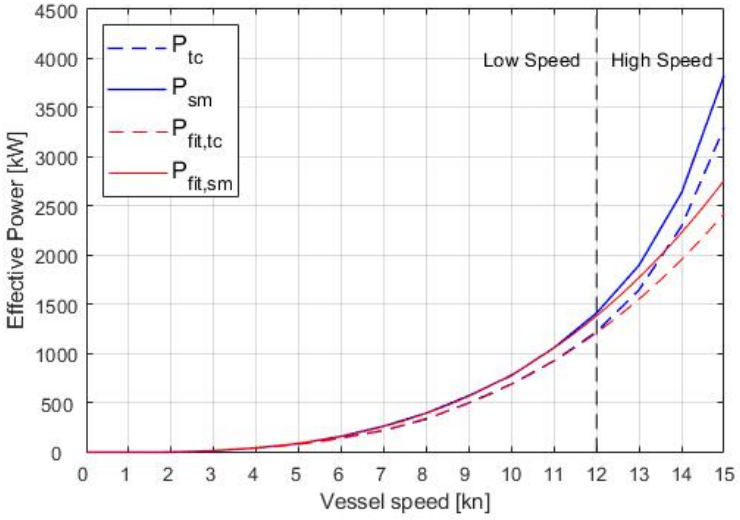

Figure A.3: Result of the best fit approximations using the method of the least square error

B

Operational Modes

This appendix shows the analysis of the different operational modes of multiple vessels. Since each mode has different power requirements, it also affects the relative importance of the propulsion and auxiliary power, and this is shown in Tables B.1, B.2, and B.3 below. The required propulsion and auxiliary power for each mode is indicated with a share (%) of the total power, where this total power is based on maximum required total power. Furthermore, based on the work of [33, 76, 85], for passenger and service ships it is assumed that the required auxiliary power is constant during the mission, unless stated otherwise.

For the analysis on tugboats, data from [4, 6–8, 12, 32, 33, 160] is used, the work of [9, 36, 41, 43, 107, 161] is used for OSVs, and for cruise ships the work of [76, 77, 79, 80, 162] is used. They all provide clear information on the used operational modes, the propulsion power and auxiliary power, and also the total required power. Ferries are also analyzed, but only the authors of [33, 107] provided useful data. Research vessels also have been found, and limited information for the power requirements for each operational mode is provided by [49], but no useful data for a clear division between propulsion power and auxiliary power has been found.

For the analysis on cargo vessels, a slightly different approach was used. On the contrary with the other vessels, large data sets were available for a part of the required information, but this had to be combined with other work to be able to display it as shown below. The authors of [113] is used for the required auxiliary power for each mode and propulsion power from thrusters for the maneuvering mode. They describe four distinct modes: anchorage, at berth, maneuvering, and transit. These modes for cargo vessels seem different than the ones described in this thesis (standby, loading/unloading, maneuvering, transit), but are actually the same. During 'anchorage', the vessel is at rest (standby) at the quay, while auxiliary systems are still running, and 'at berth' also includes the loading and unloading of the vessel. Furthermore, while it is stated in Chapter 3 that maneuvering of cargo vessels is realized with tugboats, the authors state that

some vessels use bow thrusters to maneuver alongside, which means that the resulting propulsion power for this mode is an upper bound, where zero propulsion power is the lower bound. To further analyse the data, it is assumed that the only difference between 'at berth' and 'anchorage' is the required auxiliary power for loading and unloading, the difference between 'maneuvering' and 'at berth' is the required propulsion power for the thrusters, and that the main engines are only active for transit. The propulsion power required for 'transit' is found in the work of [112, 163, 164]. Furthermore, the duration and share of each operational modes with respect to the mission is found using other sources. The authors of [165] discuss how much time each cargo vessel spends in the port, and the authors of [166, 167] discuss the average travel time at sea for a cargo vessel. Since most seagoing cargo vessels travel (transit) at approximately the same speed (container ships a bit faster) [168, 169], this average travel time will be used for the analysis of container ships, bulk carriers, and tankers. It is assumed that cargo vessels require at least half of the time in the port to load/unload the cargo [18, 107], and the rest of the time is spend in other operational modes, such as 'maneuvering' or 'standby'. To this end, Tables B.4, B.5, B.6, B.7, and B.8 contain the data used to compose the data in Table B.3

Passenger ships				
Type	Mode	Share [%] of mission	Typical Characteristics	Description
Cruise ships	Standby	27-46%	V = 0 kn P_D = 0% P_{aux} = 24-32%	At quay or at water, waiting for instructions
	Boarding/ Unboarding*		V = 0 kn P_D = 0% P_{aux} = 24-32%	Boarding or unboarding passengers
	Maneuvering	3-47%	V = 2-5 kn P_D = 2-9% P_{aux} = 29-42%	Sailing in or out of the harbour
	Transit low	7-55%	V = 4-15 kn P_D = 2-20% P_{aux} = 29-42%	Sailing at open sea with low speed
	Transit high		V > 15 kn P_D = 17-66% P_{aux} = 34-42%	Sailing at open sea with high speed
Ferries	Standby	40%	V = 0 kn P_D = 0% P_{aux} = 3-4%	At quay or at water, waiting for instructions
	Loading/ Unloading*		V = 0 kn P_D = 0% P_{aux} = 3-4%	Boarding or unboarding passengers and loading/unloading cargo
	Maneuvering	10-14%	V = 3-6 kn P_D = 30-53% P_{aux} = 4-9%	Sailing in or out of the harbour
	Transit	47-50%	V = 7-8 kn P_D = 87-96% P_{aux} = 4%	Sailing at open water

Table B.1: Overview of the main operational modes of passenger ships

*The Boarding/unboarding and Loading/unloading mode is assumed to be the same as the standby mode (only for passenger ships)

Service ships				
Type	Mode	Share [%] of mission	Typical Characteristics	Description
Tugboats	Standby	21-40%	V = 0 kn P_D = 0% P_{aux} = 2-20%	At quay or at water, waiting for instructions
	Transit	27-70%	V < 15 kn P_D = 5-36% P_{aux} = 2-20%	Sailing towards or back from a cargo ship
	Assist low	14-30%	V < 6 kn P_D = 30-71% P_{aux} = 2-20%	Towing the cargo ship with low to modest power
	Assist high	3-14%	V = 0-2 kn P_D = 80-98% P_{aux} = 2-20%	Towing the cargo ship with modest to high power
OSV	Standby	4-20%	V = 0 kn P_D = 0% P_{aux} = 1-25%	At quay or at water, waiting for instructions
	Transit	23-47%	V = 10-18 kn P_D = 13-85% P_{aux} = 6-20%	Sailing towards a platform, or another destination
	Assist*	10-16%	$V \rightarrow$ no clear data P_D = 15-89% P_{aux} = 10-47%	Towing a vessel
	Dynamic positioning	15-55%	V = 0 kn P_D = 2-90% P_{aux} = 10-33%	Maintaining a fixed position at sea, e.g. to transfer provisions or personnel from OSV to platform
Research vessels	Standby	-	V = 0 kn P_{total} < 3%	At quay or at water, waiting for instructions
	Transit	-	V = 8-12 kn P_{total} = 18-100%	Sailing towards or back from destination, often high speed
	Maneuvering	-	V = 3-6 kn P_{total} = 3-14%	Sailing at destination, often low speed
	Other**	-	$V \rightarrow$ no clear data $P_{total} \rightarrow$ no clear data	

Table B.2: Overview of the main operational modes of service ships

*The assist mode of OSVs also contains a fire fighting mode, for which a lot of auxiliary power is required. Without this mode, the required auxiliary power would remain less than 33%

**Each research vessel has a mission dependent mode, such as a fishing mode for a fishing research vessel, and hence this is not included here

Cargo ships				
Type	Mode	Share [%] of mission	Typical Characteristics	Description
Container ships	Standby	1%	V = 0 kn P_D = 0% P_{aux} = 1-11%	At quay or at water, waiting for instructions
	Loading/ Unloading	2%	V = 0 kn P_D = 0% P_{aux} = 1-11%	Loading or unloading of the cargo, realized with quay cranes
	Maneuvering	1%	V < 6 kn P_D = 1-7% P_{aux} = 1-11%	Sailing in or out of the harbour, assisted by tugboats
	Transit	96%	V = 12-19 kn P_D = 93-99% P_{aux} = 1-7%	Sailing at open sea
Bulk carriers	Standby	2%	V = 0 kn P_D = 0% P_{aux} = 3-12%	At quay or at water, waiting for instructions
	Loading/ Unloading	5%	V = 0 kn P_D = 0% P_{aux} = 4-17%	Loading or unloading of the cargo, realized with quay cranes or deck cranes
	Maneuvering	2%	V < 6 kn P_D = 1-6% P_{aux} = 3-12%	Sailing in or out of the harbour, assisted by tugboats
	Transit	91%	V = 13-15 kn P_D = 90-98% P_{aux} = 2-10%	Sailing at open sea
Tankers	Standby	1%	V = 0 kn P_D = 0% P_{aux} = 8-21%	At quay or at water, waiting for instructions
	Loading/ Unloading	2%	V = 0 kn P_D = 0% P_{aux} = 8-25%	Loading or unloading of the cargo, realized with piping systems
	Maneuvering	1%	V = < 6 kn P_D = 3-7% P_{aux} = 8-21%	Sailing in or out of the harbour, assisted by tugboats
	Transit	96%	V = 13-17 kn P_D = 82-94% P_{aux} = 6-18%	Sailing at open sea

Table B.3: Overview of the main operational modes of (seagoing) cargo ships

	Capacity	Capacity Units	Anchorage	Maneuvering	Loading/unloading	Transit	Anchorage	Maneuvering	Loading/unloading	Transit	Propulsion Power [kW]	
Bulk carrier	0–9999	dwt	190	310	280	190	50	50	50	0	0	3500
	10,000–34,999	dwt	190	310	280	190	50	50	50	0	3500	6000
	35,000–59,999	dwt	260	420	370	260	100	100	100	0	6000	8500
	60,000–99,999	dwt	420	680	600	420	200	200	200	0	8500	11000
	100,000–199,999	dwt	420	680	600	420	200	200	200	0	11000	16000
	200,000+	dwt	420	680	600	420	200	200	200	0	16000	25000
Container	0–999	teu	340	550	340	300	120	120	120	0	0	7650
	1000–1999	teu	600	1320	600	820	290	290	290	0	7650	13500
	2000–2999	teu	700	1800	700	1230	350	350	350	0	13500	18000
	3000–4999	teu	940	2470	940	1390	450	450	450	0	18000	23500
	5000–7999	teu	970	2600	970	1420	450	450	450	0	23500	36500
	8000–11,999	teu	1000	2780	1000	1630	520	520	520	0	36500	452500
	12,000–14,500	teu	1200	3330	1200	1960	630	630	630	0	452500	520000
	14,500+	teu	1320	3670	1320	2160	700	700	700	0	520000	650000
Crude oil tanker	0–4999	dwt	250	375	250	250	100	100	500	0	0	6000
	5000–9999	dwt	375	563	375	375	150	150	750	0	6000	6500
	10,000–19,999	dwt	625	938	625	625	250	250	1250	0	6500	7250
	20,000–59,999	dwt	750	1125	750	750	300	300	1500	150	7250	10000
	60,000–79,999	dwt	750	1125	750	750	300	300	1500	150	10000	11250
	80,000–119,999	dwt	1000	1500	1000	1000	400	400	2000	200	11250	14000
	120,000–199,999	dwt	1250	1875	1250	1250	500	500	2500	250	14000	19250
	200,000+	dwt	1500	2250	1500	1500	600	600	3000	300	19250	25000
Products/ gas/ chemical tanker	0–4999	dwt	250	375	250	250	371	371	371	0	0	6000
	5000–9999	dwt	375	563	375	375	371	371	371	0	6000	6500
	10,000–19,999	dwt	625	938	625	625	371	371	371	0	6500	7250
	20,000–59,999	dwt	750	1125	750	750	371	371	371	0	7250	10000
	60,000–79,999	dwt	750	1125	750	750	371	371	371	0	10000	11250
	80,000–119,999	dwt	1000	1500	1000	1000	371	371	371	0	11250	14000
	120,000–199,999	dwt	1250	1875	1250	1250	371	371	371	0	14000	19250
	200,000+	dwt	1500	2250	1500	1500	371	371	371	0	19250	25000

Table B.4: Raw data for propulsion and auxiliary power of cargo ships [36, 112, 163, 164]

			Aux Power [kW]	Aux Power [kW]	Prop Power [kW]	Aux Power [kW]	Prop Power [kW]	Aux Power [kW]	Max Power [kW]
	Capacity	Capacity Units	Standby	Loading/unloading	Maneuvering		Transit		->transit
Bulk carrier	0–9999	dwt	240	330	120	240	1750	190	1940
	10,000–34,999	dwt	240	330	120	240	4750	190	4940
	35,000–59,999	dwt	360	470	160	360	7250	260	7510
	60,000–99,999	dwt	620	800	260	620	9750	420	10170
	100,000–199,999	dwt	620	800	260	620	13500	420	13920
	200,000+	dwt	620	800	260	620	20500	420	20920
Container ship	0–999	teu	460	460	210	460	3825	300	4125
	1000–1999	teu	890	890	720	890	10575	820	11395
	2000–2999	teu	1050	1050	1100	1050	15750	1230	16980
	3000–4999	teu	1390	1390	1530	1390	20750	1390	22140
	5000–7999	teu	1420	1420	1630	1420	30000	1420	31420
	8000–11,999	teu	1520	1520	1780	1520	244500	1630	246130
	12,000–14,500	teu	1830	1830	2130	1830	486250	1960	488210
	14,500+	teu	2020	2020	2350	2020	585000	2160	587160
Crude oil tanker	0–4999	dwt	350	750	125	350	3000	250	3250
	5000–9999	dwt	525	1125	188	525	6250	375	6625
	10,000–19,999	dwt	875	1875	313	875	6875	625	7500
	20,000–59,999	dwt	1050	2250	375	1050	8625	900	9525
	60,000–79,999	dwt	1050	2250	375	1050	10625	900	11525
	80,000–119,999	dwt	1400	3000	500	1400	12625	1200	13825
	120,000–199,999	dwt	1750	3750	625	1750	16625	1500	18125
	200,000+	dwt	2100	4500	750	2100	22125	1800	23925
Products/ gas/ chemical tanker	0–4999	dwt	621	621	125	621	3000	250	3250
	5000–9999	dwt	746	746	188	746	6250	375	6625
	10,000–19,999	dwt	996	996	313	996	6875	625	7500
	20,000–59,999	dwt	1121	1121	375	1121	8625	750	9375
	60,000–79,999	dwt	1121	1121	375	1121	10625	750	11375
	80,000–119,999	dwt	1371	1371	500	1371	12625	1000	13625
	120,000–199,999	dwt	1621	1621	625	1621	16625	1250	17875
	200,000+	dwt	1871	1871	750	1871	22125	1500	23625

Table B.5: Combined data for propulsion and auxiliary power of cargo ships

			Aux Power [kW]	Aux Power [kW]	Prop Power [kW]	Aux Power [kW]	Prop Power [kW]	Aux Power [kW]	Max Power [kW]
	Capacity	Capacity Units	Standby	Loading/unloading	Maneuvering		Transit		->transit
Bulk carrier	0–9999	dwt	12%	17%	6%	12%	90%	10%	100%
	10,000–34,999	dwt	5%	7%	2%	5%	96%	4%	100%
	35,000–59,999	dwt	5%	6%	2%	5%	97%	3%	100%
	60,000–99,999	dwt	6%	8%	3%	6%	96%	4%	100%
	100,000–199,999	dwt	4%	6%	2%	4%	97%	3%	100%
	200,000+	dwt	3%	4%	1%	3%	98%	2%	100%
Container ship	0–999	teu	11%	11%	5%	11%	93%	7%	100%
	1000–1999	teu	8%	8%	6%	8%	93%	7%	100%
	2000–2999	teu	6%	6%	6%	6%	93%	7%	100%
	3000–4999	teu	6%	6%	7%	6%	94%	6%	100%
	5000–7999	teu	5%	5%	5%	5%	95%	5%	100%
	8000–11,999	teu	1%	1%	1%	1%	99%	1%	100%
	12,000–14,500	teu	0%	0%	0%	0%	100%	0%	100%
	14,500+	teu	0%	0%	0%	0%	100%	0%	100%
Crude oil tanker	0–4999	dwt	11%	23%	4%	11%	92%	8%	100%
	5000–9999	dwt	8%	17%	3%	8%	94%	6%	100%
	10,000–19,999	dwt	12%	25%	4%	12%	92%	8%	100%
	20,000–59,999	dwt	11%	24%	4%	11%	91%	9%	100%
	60,000–79,999	dwt	9%	20%	3%	9%	92%	8%	100%
	80,000–119,999	dwt	10%	22%	4%	10%	91%	9%	100%
	120,000–199,999	dwt	10%	21%	3%	10%	92%	8%	100%
	200,000+	dwt	9%	19%	3%	9%	92%	8%	100%
Products/ gas/ chemical tanker	0–4999	dwt	19%	19%	4%	19%	92%	8%	100%
	5000–9999	dwt	11%	11%	3%	11%	94%	6%	100%
	10,000–19,999	dwt	13%	13%	4%	13%	92%	8%	100%
	20,000–59,999	dwt	12%	12%	4%	12%	92%	8%	100%
	60,000–79,999	dwt	10%	10%	3%	10%	93%	7%	100%
	80,000–119,999	dwt	10%	10%	4%	10%	93%	7%	100%
	120,000–199,999	dwt	9%	9%	3%	9%	93%	7%	100%
	200,000+	dwt	8%	8%	3%	8%	94%	6%	100%

Table B.6: Propulsion and auxiliary power with respect to the maximum power of cargo ships

		Aux Power [kW]	Aux Power [kW]	Prop Power [kW]	Aux Power [kW]	Prop Power [kW]	Aux Power [kW]
		Standby	Loading/unloading	Maneuvering		Transit	
Bulk carrier	MIN	3%	4%	1%	3%	90%	2%
	MAX	12%	17%	6%	12%	98%	10%
Container ship	MIN	0%	0%	0%	0%	93%	0%
	MAX	11%	11%	7%	11%	100%	7%
Crude oil tanker	MIN	8%	17%	3%	8%	91%	6%
	MAX	12%	25%	4%	12%	94%	9%
Products/gas/ chemical tanker	MIN	8%	8%	3%	8%	92%	6%
	MAX	19%	19%	4%	19%	94%	8%

Table B.7: Minimum and maximum propulsion and auxiliary power with respect to the maximum power of cargo ships

		Aux Power [kW]	Aux Power [kW]	Prop Power [kW]	Aux Power [kW]	Prop Power [kW]	Aux Power [kW]
		Standby	Loading/unloading	Maneuvering		Transit	
Bulk carrier	MIN	3%	4%	1%	3%	90%	2%
	MAX	12%	17%	6%	12%	98%	10%
Container	MIN	0%	0%	0%	0%	93%	0%
	MAX	11%	11%	7%	11%	100%	7%
Tanker	MIN	8%	8%	3%	8%	91%	6%
	MAX	19%	25%	4%	19%	94%	9%

Table B.8: Final minimum and maximum propulsion and auxiliary power with respect to the maximum power of cargo ships

C

Simulation Results for Different Power Profiles

As mentioned in Chapter 5.1, instead of building the power profile with exponential slopes, the power profile can also be constructed with fixed slopes. Therefore, in this appendix multiple exponential and fixed slopes will be discussed, and the performance of the modular control architecture will be shown. It is expected that for a very steep increase in the power profile, the introduced errors also increase, and the smoother the power profile evolves, the lower the errors.

For both exponential and fixed slopes, two different rates are considered, resulting in four different power profiles. Each power profile is similar to the power profile required for Mission 1 in Chapter 5. For the exponential slopes, two different rates are considered, indicated with 'tau'. The higher the value of 'tau', the less steep the change. For the fixed slope also two rates are considered, indicated with the time it takes to reach a new power demand. An example of the four different slopes can be found in Figure C.1. The total power profiles can be found in Figures C.2, C.3, and C.4, together with the simulation results for the propulsion tracking error and the auxiliary tracking error. The measured KPI's for the propulsion and auxiliary power are shown in Table C.1.

		Propulsion		Auxiliary	
		RMSE [kW]	SI [%]	RMSE [kW]	SI [%]
Exponential Rates	tau = 45	6.19	1.63	8.66	8.79
	tau = 20	8.23	2.16	10.26	10.39
Fixed Rates	60 s	7.61	2.00	9.54	9.67
	6s	21.92	5.75	20.00	20.19

Table C.1: Comparison of performance of different power profiles for mission 1

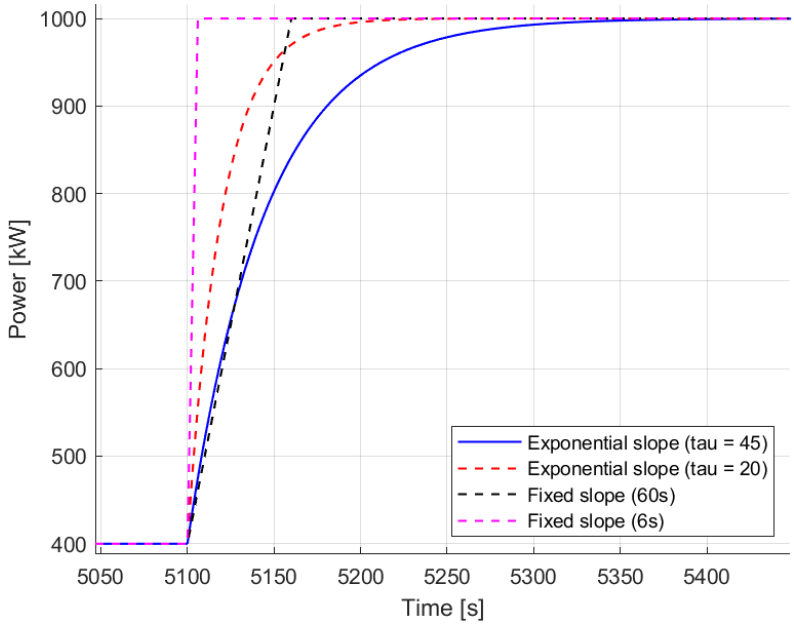

Figure C.1: Comparison of exponential and fixed rates

From the results it can be concluded that the steeper the changes in the power profile, the larger the errors. When comparing the results of the steepest exponential rate (tau=20) and the least steep fixed rate (60s), it can be noted that the latter outperforms the former. This is due to the fact that even for the exponential slopes, only the last part of a slope change is gradual, but the first part is similar to a fixed slope increase. Even more, for 'tau=20' a steeper increase of the power profile can be seen than for '60s', at the first instance of a change in the power profile, see Figure C.1, hence larger errors are present. Also, by comparing 'tau=20' to '6s' and 'tau=45' to '60s', where for each pair the first part of a power increase is similar, but for the last part the exponential profile is more smooth, smaller errors are observed for the exponential profiles. To this end, it can be concluded that performance of the modular control architecture can be improved by using exponential slopes for the power profile, rather than fixed slopes.

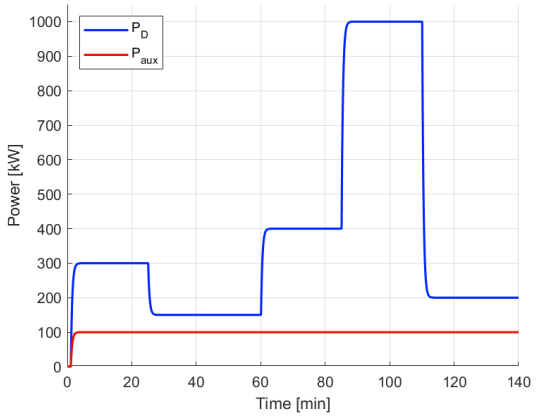

(a) Power profile exponential (tau=20)

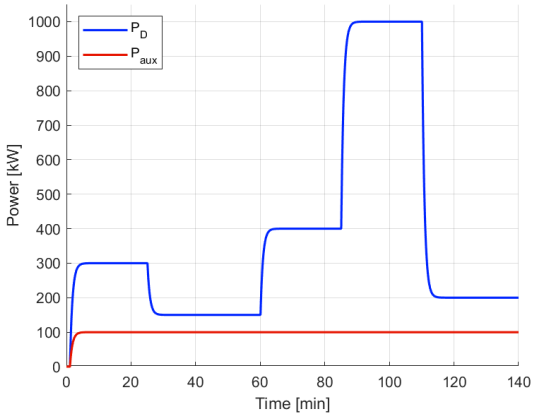

(b) Power profile exponential (tau=45)

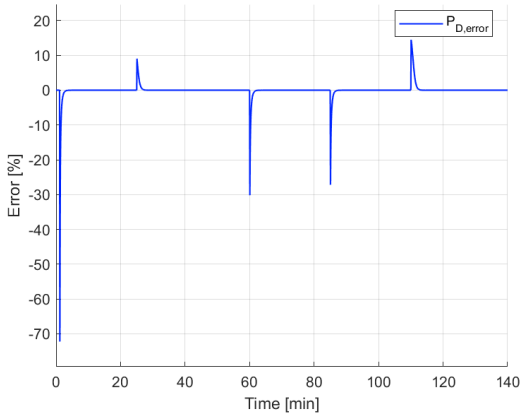

(c) Propulsion power tracking error exponential (tau=20)

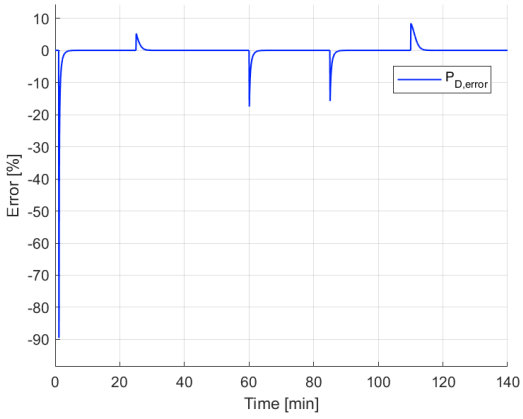

(d) Propulsion power tracking error exponential (tau=45)

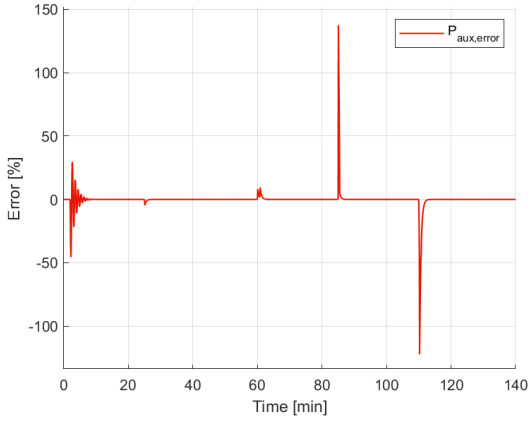

(e) Auxiliary power tracking error exponential (tau=20)

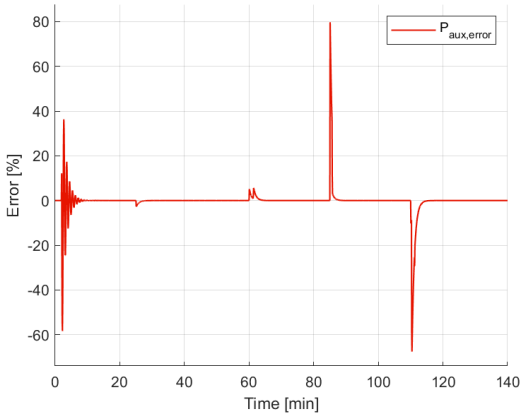

(f) Auxiliary power tracking error exponential (tau=45)

Figure C.2: Comparison of performance between exponential increases of the power profile

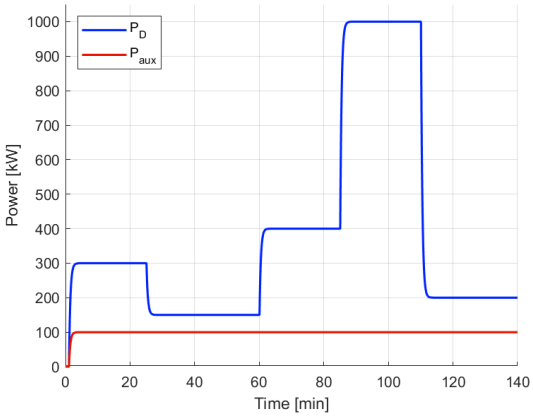

(a) Power profile exponential (tau=20)

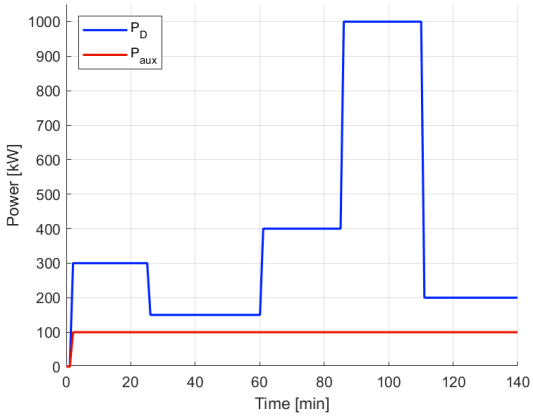

(b) Power profile fixed slope (60s)

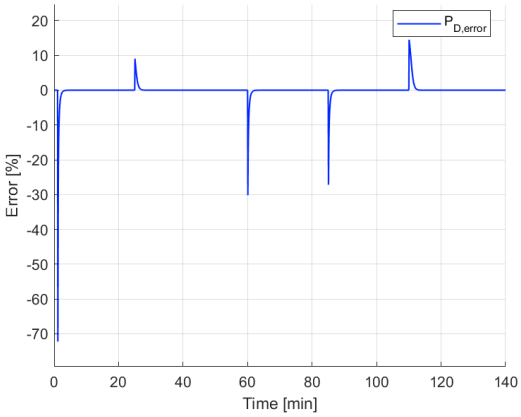

(c) Propulsion power tracking error exponential (tau=20)

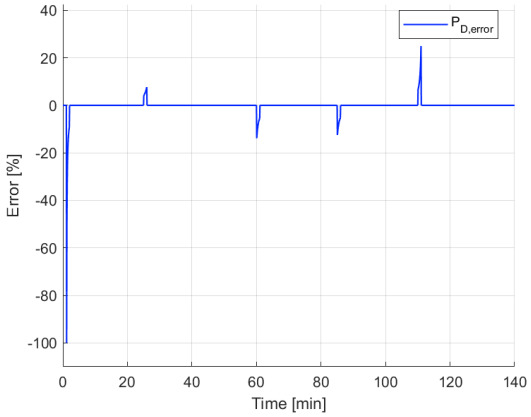

(d) Propulsion power tracking error fixed slope (60s)

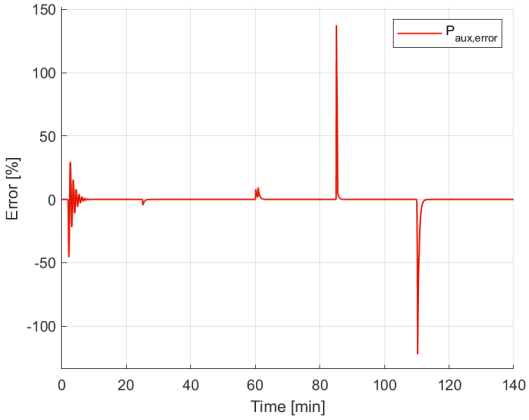

(e) Auxiliary power tracking error exponential (tau=20)

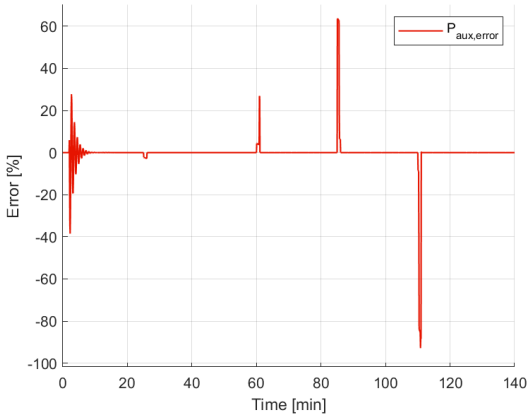

(f) Auxiliary power tracking error fixed slope (60s)

Figure C.3: Comparison of performance between exponential increases and fixed slope increases of the power profile

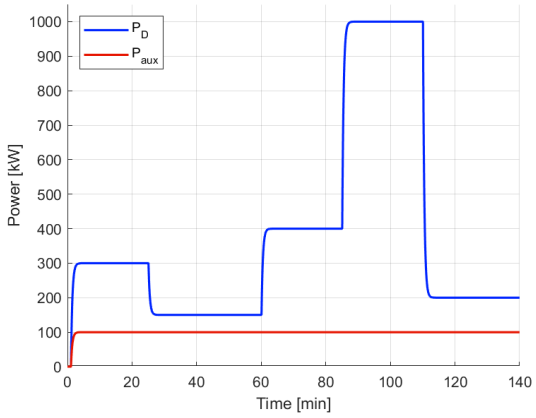

(a) Power profile exponential (tau=20)

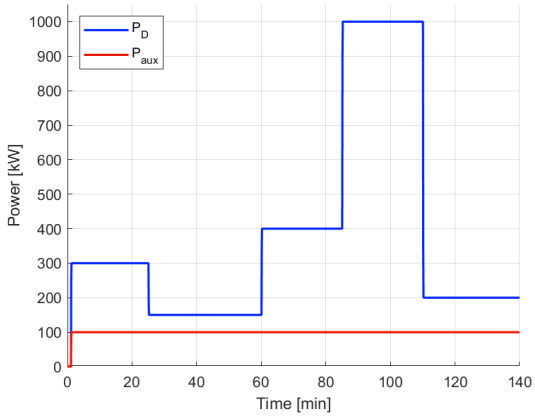

(b) Power profile fixed slope (6s)

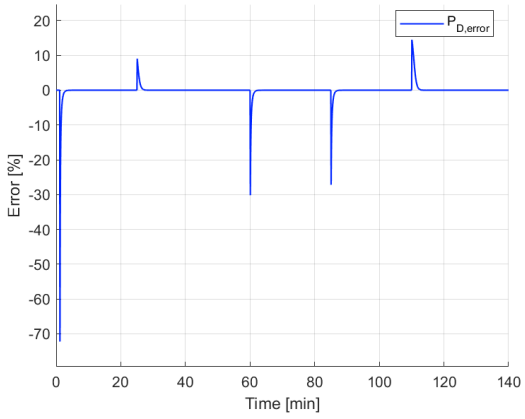

(c) Propulsion power tracking error exponential (tau=20)

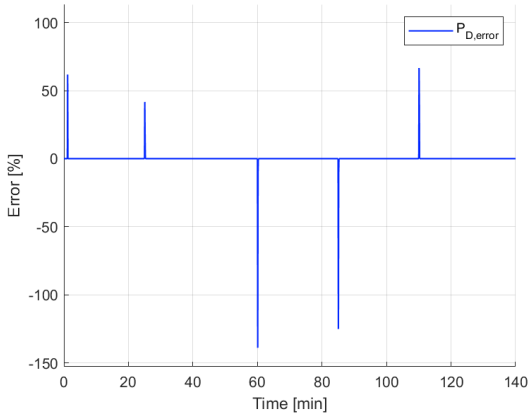

(d) Propulsion power tracking error fixed slope (6s)

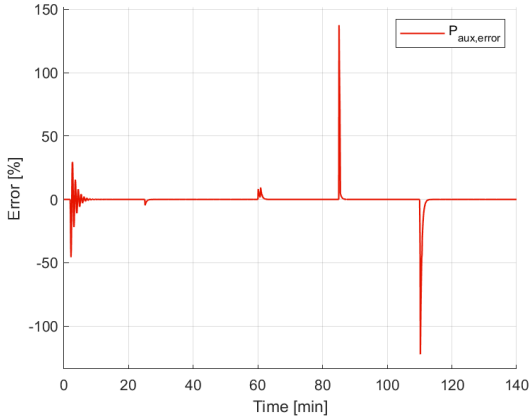

(e) Auxiliary power tracking error exponential (tau=20)

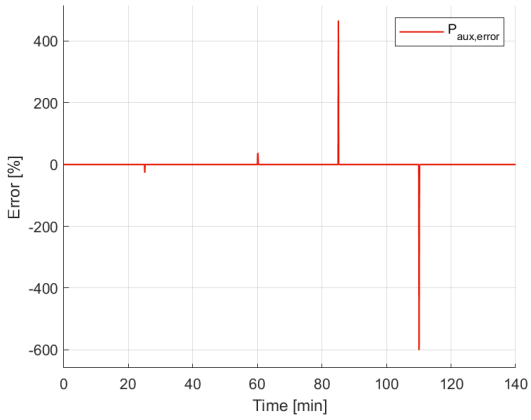

(f) Auxiliary power tracking error fixed slope (6s)

Figure C.4: Comparison of performance between exponential increases and fixed slope (6s) increases of the power profile

Mission-oriented Modular Control of Retrofittable Marine Power Plants

M.C. van Benten*, Dr. V. Reppa[a], N. Kougiatsos[a]

[a]*Maritime and Transport Technology, Faculty of Mechanical, Maritime and Materials Engineering, Delft University of Technology, 2628CD, the Netherlands*

*Corresponding author. Email: marcel_vanbenten@hotmail.com

Synopsis

Marine vessels execute many missions during their life cycle, each associated with a different required power profile. The required power is to be provided by the power plant, which has a fixed set of equipment such as diesel engines, generator sets, electric machines, and batteries. Typically, the control of vessel's power plants consist of two levels; a primary level with local controllers for the power plant components, and a secondary level that determines the distribution of the required power to the various components in the power plant. The state-of-the-art only considers a multi-level power plant control architecture assuming a fixed power plant layout, but in practice, the fixed power plant layout may not suffice for generating the power demand dictated by a new mission. This may lead to inefficient use of components, risk of overloading components, or the inability to deliver the required power. To handle this issue, equipment modifications such as additions, removals or replacements would probably be necessary, along with modifications in the multi-level control scheme. To enable the seamless operation of the multi-level plant control system after the modifications is essential for guaranteeing safety and reducing the downtime, which could be achieved by a control architecture that allows for modular use of the power plant components.

This paper presents the design methodology of a mission-oriented modular control system for marine power plants. To this end, first power profiles, power plant layouts and control systems of multiple vessels such as tugboats, offshore support vessels, cargo ships and cruise ships are analyzed. By decomposing the power profile in two components, the propulsion and auxiliary power demand, the correlation between the power profile of a vessel and its mission is derived, and an algorithm that computes the power profile using mission and vessel data is proposed. Furthermore, the correlation between the power profile and the layout of the power plant is also investigated, with emphasis on how changes in the power profile result in power plant automation modifications. A modular secondary control level is then designed to cope with the required power plant automation modifications, by combining the Equivalent Consumption Minimization Strategy (ECMS) with Supervisory Switching Control (SSC). In this paper we consider battery modifications, following the example of Wärtsilä's ZESPacks. Simulation results are used to show the performance of the proposed switching control methodology, in relation to the stability of the components in the power plant after automation modifications occur.

The main contribution of this paper is the novel approach for the secondary level power plant control system, introducing modularity to the otherwise assumed fixed layout of the power plant. Furthermore, the proposed algorithm can be used to determine the expected power profile for a new mission, to identify required modifications of the power plant equipment.

Keywords: Marine control systems, Modular control architecture, Hybrid power plant, Battery modifications

1 Introduction

1.1 Motivation

Marine vessels are used for many purposes, such as shipping cargo, (supporting) offshore operations, transporting passengers, or even to tow other marine vessels. During their lifetime they execute many missions, and each mission requires power, either for propulsion or for other tasks. The power required for a mission can be used to construct the power profile, and is generated by the power plant. How the power plant is designed is partly based on the mission statement which includes the expected missions the vessel will execute (Hanbidge, 2001), resulting in a fixed power plant, and therefore a fixed control system. However, each mission results in a different power profile, since for each mission there are different environmental conditions (such as wind, waves and currents)

Authors' Biographies

Marcel van Benten is currently a master student at Delft Universtiy of Technology, track Multi-Machine Engineering, and is graduating on the topic of this paper.

Dr. Vasso Reppa is a tenure-track Assistant Professor with the Transport Engineering and Logistics Section of the Maritime and Transport Technology Department, Delft University of Technology. Dr. Reppa's research interests include fault tolerant control, fault diagnosis, interconnected uncertain systems, multi-agent control, autonomous shipping operations and waterborne transport.

Nikos Kougiatsos MSc is currently a PhD researcher at Delft University of Technology. His research involves scalable, modular control and fault-tolerant control strategies for marine vessels. During his Master's in Naval Architecture and Marine Engineering, he has been awarded scholarships from the American Bureau of Shipping (ABS).

and operational conditions (e.g. the frequency of the required actions of the vessel, such as loading or unloading cargo, sail across open sea or towing another vessel). Therefore, each mission implies a certain required amount of equipment in the power plant. By using only a fixed set of equipment, this could result in situations where the power plant is not able to suffice for generating the power demand dictated by a new mission, which may lead to to inefficient use of the power plant components, risk of overloading the components, or even the inability to execute the mission properly. To handle this issue, equipment modification such as additions, removals, or replacements would probably be necessary, along with modifications of the control architecture.

1.2 Literature review

Many different power layouts seen in literature, and both for the propulsion plant and the power supply there are three main configurations; mechanical, electric, and hybrid. In this paper, a hybrid propulsion plant with a hybrid power supply is considered, and an example is shown in Figure 1. The control system of the power plant is part of

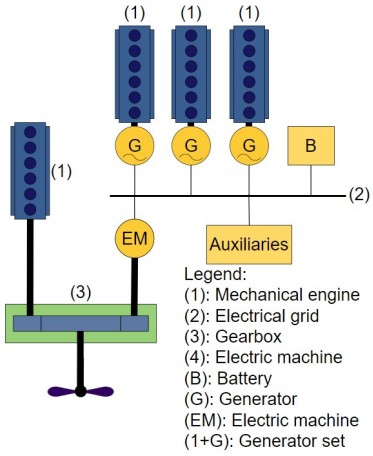

Figure 1: Hybrid propulsion and hybrid power supply

the marine control system, and the latter is more and more developed in a hierarchical, distributed architecture, and combining the work of (Geertsma et al., 2017; Smogeli et al., 2005; Smogeli, 2006; Smogeli et al., 2008; Smogeli and Sørensen, 2009), most of these systems can be divided into three levels:

- Local optimizer/tertiary level
- Secondary level
- Primary level

The local optimizer is also known as the guidance and navigation system, and is actually not a controller, and the main task of this system is to determine the desired path for the ship, and to provide the reference signals for the general secondary level control (Wang et al., 2018). This level includes a path-following controller, which uses the reference signal and the generated path from the guidance and navigation system to determine the reference signals for the secondary level plant control and other controllers, for example the rudder control. The secondary level plant control determines the distribution of power to the components in the power plant, from now on this will be refered to as the power split, and based on the found power split the set-points for the primary level control are generated, where the latter consists of the controllers of all the components in the power plant (Geertsma et al., 2017). Combining this with the general control architectures presented in (Negenborn and Hellendoorn, 2010), a schematic of the ship control architecture is made and can be seen in Figure 2. For this example, hybrid propulsion with hybrid power supply, as shown in Figure 1, is used. As each vessel is designed with a certain power plant layout, the multi-level control system shown above is designed to control a specific set of power plant equipment, and often Equivalent Consumption Minimization Strategy (ECMS) is used in the secondary level plant control. This strategy requires a cost function, that expresses the power of each component in terms of fuel use, and determines the power split by minimizing the cost function at each instance, while meeting several constraints that limit the power of each component and ensure the power demand is being met. However, it is seen in literature

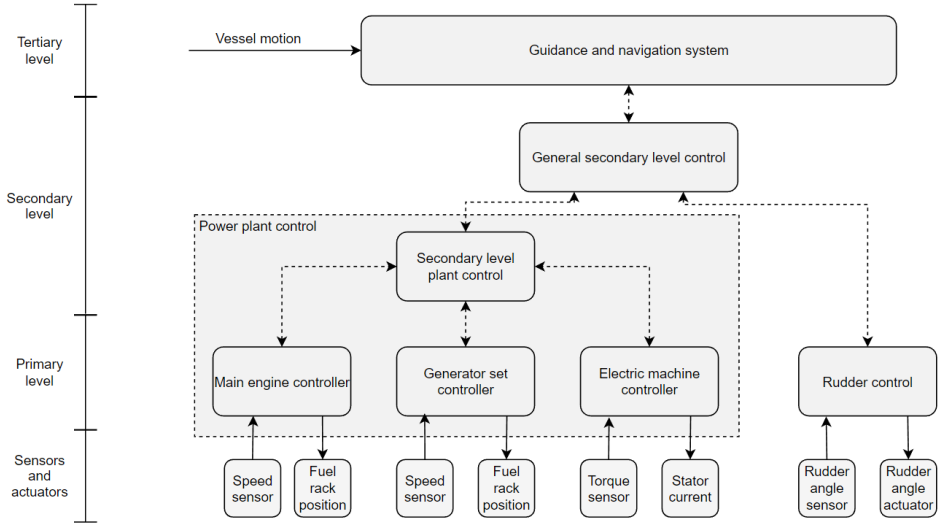

Figure 2: General marine vessel control system

that vessels often have a fixed power plant, and a fixed control system while their missions lead to different power requirements. This could introduce inefficient use, or overloading of the power plant equipment, or even the inability to carry out future missions, and therefore it could be beneficial to be able to change the power plant of the vessel between or during mission. Unfortunately, with the state-of-the-art marine vessels, the control system would have to be manually tuned to be able to control the new power plant. To this end, this paper presents a design for a modular control system for a retrofittable power plant, allowing modular use of the power plant equipment, without the need to manually tune the control system.

1.3 Approach

In order to design a control system for a retrofittable power plant, first the correlation between the mission and the power profile of the vessel should be investigated, in order to find the impact of varying missions on the power demand during and between missions. Then, to connect changes in the power profile to changes in the power plant and the control system, the correlation between the power profile and the needed modifications in automation of the control system and the power plant is discussed. Using this, a modular power plant architecture can be proposed to meet these automation modifications. At last, the designed architecture is verified, with respect to stability and robustness.

1.4 Structure

This paper is structured as follows. In Section 2 the problem formulation is presented, which discusses the used models for the design of the power plant and control system. In Section 3 a model for the correlation between the mission and the power profile is shown, but also the correlation between the power profile and the needed automation modifications in the control system and power plant is discussed. Then, in Section 4 a design for a modular control architecture is proposed, to meet the required automation modifications. In Section 5 the performance of the proposed design is verified, showing the stability and robustness of the modular control architecture. At last, in Section 6 a conclusion is formulated, and recommendations for further research are given.

2 Problem formulation

The main goal of this paper is to present the design of a modular control architecture, where the main contributions are in the supervisory and the secondary level. To this end, the used models for the power plant components are directly taken from literature, and for each component, except for the batteries, a PI controller is used as primary level controller. For the batteries, a constraint module is used instead of a regular controller.

2.1 Diesel engine

For the diesel engine, a first-order differential equation as found in the work of Haseltalab and Negenborn (2019) is used:

$$\dot{Q}_{DE}(t) = -\frac{Q_{DE}(t)}{\tau_{DE}(t)} + k_{DE} \cdot m_{f,DE}(t) \tag{1}$$

where k_{DE} is the torque constant, $m_{f,DE}$ is the fuel index (regulated by a PI controller), and τ_{DE} is the torque buildup constant which determines the response speed of the diesel engine, as a function of the shaft speed ω_{DE}:

$$\tau_{DE}(t) = \frac{0.9}{\omega_{DE}(t)} \tag{2}$$

2.2 Induction motor

For the induction motor, instead of a first-order differential equation, an algebraic equation is used, derived from the work of (Eijkhout and Jovanova, 2021; Wildi et al., 2002):

$$Q_{IM}(t) = \frac{\omega_{IM,s}(t) - \omega_{IM}(t)}{\omega_{IM,s}(t)} \cdot \frac{V_{IM}^2(t)}{R_{r,IM} \cdot k_{IM}} \tag{3}$$

where Q_{IM} is the generated torque, ω_{IM} is the rotor speed, $\omega_{IM,s}$ is the rotational speed of the magnetic field in the stator windings, also refered to as the stator speed, V_{IM} is the input voltage (in literature often refered to as phase voltage), $R_{r,IM}$ is the rotor resistance, and k_{IM} is a constant that depends on the motor characteristics. As $\omega_{IM,s}$ is regulated by a PI controller, the input voltage V_{IM} is proportional to $\omega_{IM,s}$ (Vahedpour et al., 2015):

$$V_{IM}(t) = C_{V/f} \cdot \omega_{IM,s}(t) \tag{4}$$

where $C_{V/f}$ is a motor dependent constant.

2.3 Gearbox, shaft, and propeller

To model the shaft dynamics of the gearbox, shaft and propeller, the work of (Kalikatzarakis et al., 2018; Woud and Stapersma, 2019; Haseltalab and Negenborn, 2019) is used, resulting in the following relation:

$$\dot{\omega}_p(t) = \frac{\eta_T(i_{DE} \cdot Q_{DE}(t) + i_{IM} \cdot Q_{IM}(t)) - Q_p(t)}{J_{tot}} \tag{5}$$

where ω_p is the propeller speed, Q_p is the propeller torque, J_{tot} is the total inertia of the gearbox, induction machine and the diesel engine together, i_{DE} and i_{IM} the gear ratios of the diesel engine and the induction motor, respectively, and η_T is the transmission efficiency. The propeller torque Q_p is found using the work of (Izadi-Zamanabadi and Blanke, 1999; Smogeli, 2006):

$$Q_p(t) = C_p \cdot |\omega_p(t)| \cdot \omega_p(t) \tag{6}$$

$$C_p = \frac{K_Q \cdot \rho \cdot D^5}{4\pi^2} \tag{7}$$

where ρ is the density of the seawater, D is the diameter of the propeller, and K_T and K_Q are the thrust and torque coefficients. Since the diesel engine, the induction machine, and the propeller are rigidly coupled, ω_{DE} and ω_{IM} can be expressed in terms of ω_p:

$$\omega_{IM}(t) = i_{IM} \cdot \omega_p(t) \tag{8}$$

$$\omega_{DE}(t) = i_{DE} \cdot \omega_p(t) \tag{9}$$

2.4 Diesel generator sets

The engine of the diesel generator set is modeled using the work of (Haseltalab and Negenborn, 2019):

$$\dot{Q}_{DG,DE}(t) = -\frac{Q_{DG,DE}(t)}{\tau_{DG}(t)} + k_{DG} \cdot m_{f,DG}(t) \tag{10}$$

where $Q_{DG,DE}$ is the torque of the diesel engine connected to the generator, k_{DG} the torque constant, $m_{f,DG}$ the fuel index (regulated by a PI controller), and τ_{DG} is the torque buildup constant which determines the response speed of the diesel engine, as a function of the shaft speed ω_{DG}:

$$\tau_{DG}(t) = \frac{0.9}{\omega_{DG}(t)} \tag{11}$$

The dynamics of the generator are described with a set of algebraic equations, as found in (Cheong et al., 2010):

$$Q_{DG,G}(t) = \frac{(a_{G,1} \cdot I_X(t) + a_{G,0}) \cdot Re(I_{DG}(t))}{2\pi} \tag{12}$$

$$I_{DG}(t) = \frac{(a_{G,1} \cdot I_X(t) + a_{G,0}) \cdot \omega_{DG}(t)}{2\pi(R_{DG,int} + j \cdot L_{DG} \cdot \omega_{DG}(t) + R_{DG}(t)} \tag{13}$$

$$\dot{\omega}_{DG}(t) = \frac{Q_{DG,DE}(t) - Q_{DG,G}(t)}{J_{DG}} \tag{14}$$

where $Q_{DG,G}$ is the generator torque, I_X the excitation current (regulated by a PI controller), $a_{G,1}$ and $a_{G,0}$ are constants, I_{DG} the generator output current, $R_{DG,int}$ the internal resistance, L the inductance, j the imaginary number, J_{DG} the generator inertia, and R_{DG} the load resistance, in this paper assumed to be purely resistive, and determined with the assigned power P_{DG} and the reference-voltage $V_{DG,ref}$ as follows:

$$R_{DG}(t) = \frac{V_{DG,ref}^2(t)}{P_{DG}(t)} \tag{15}$$

2.5 Batteries and constraint modules

Batteries are described with a set of algebraic equation, as found in (Sun and Shu, 2011; Kularatna and Gunawardane, 2021; Chang, 2013; Haseltalab et al., 2020):

$$P_B(t) = V_B(t) \cdot I_B(t) \tag{16}$$

$$V_B(t) = V_{OC}(t) - R_B \cdot I_B(t) \tag{17}$$

$$V_{OC}(t) = a_{B,1} \cdot SOC(t) + a_{B,0} \tag{18}$$

$$SOC(t) = SOC(t_0) - \frac{1}{C_0} \int_{t=0}^{t} I_B(t) dt \tag{19}$$

where P_B and I_B are the battery power and the battery current, respectively (both positive for discharging), V_B the battery output voltage, V_{OC} the open-circuit voltage, $a_{B,0}$ and $a_{B,1}$ are constants, C_0 the capacity, and $SOC(t_0)$ the initial SOC. The main goal of the constraint module is to provide a window $[P_B^{min} \;\; P_B^{max}]$ for P_B to the secondary level, such that the SOC and V_B are kept within their predescribed limits, and based on the work of (Kalikatzarakis et al., 2018) this leads to the following constraints:

$$P_{B,V}^{max} = \frac{V_{OC} \cdot V_{B,min} - V_{B,min}^2}{R_B} \tag{20}$$

$$P_{B,V}^{min} = \frac{V_{B,max}^2 - V_{OC} \cdot V_{B,max}}{R_B} \tag{21}$$

$$P_{B,SOC}^{max} = \frac{SOC - SOC_{min}}{\Delta t} \cdot C_0 \cdot V_{OC} \tag{22}$$

$$P_{B,SOC}^{min} = \frac{SOC - SOC_{max}}{\Delta t} \cdot C_0 \cdot V_{OC} \tag{23}$$

$$P_B^{min} = max\left(P_{B,SOC}^{min}, P_{B,V}^{min}\right) \tag{24}$$

$$P_B^{max} = min\left(P_{B,SOC}^{max}, P_{B,V}^{max}\right) \tag{25}$$

Here, $V_{B,min}$, $V_{B,max}$, SOC_{min}, and SOC_{max} are the minimum and maximum terminal voltage V_B and minimum and maximum SOC of the battery, respectively, provided by the battery manufacturer, and Δt is a discrete timestep, which can be tuned to alter the power constraints related to the SOC of the battery.

3 Correlation between the mission, power profile, and the required automation modifications

The correlation between the mission, the power profile and the required automation modifications is discussed in twofold. First, to answer the second research question, a model for the correlation between the mission and the power profile is discussed. Second, the answer to the third research question is formulated by describing the correlation between the power profile and the required automation modifications, using the power plant equipment modifications implied by variations of the power profile.

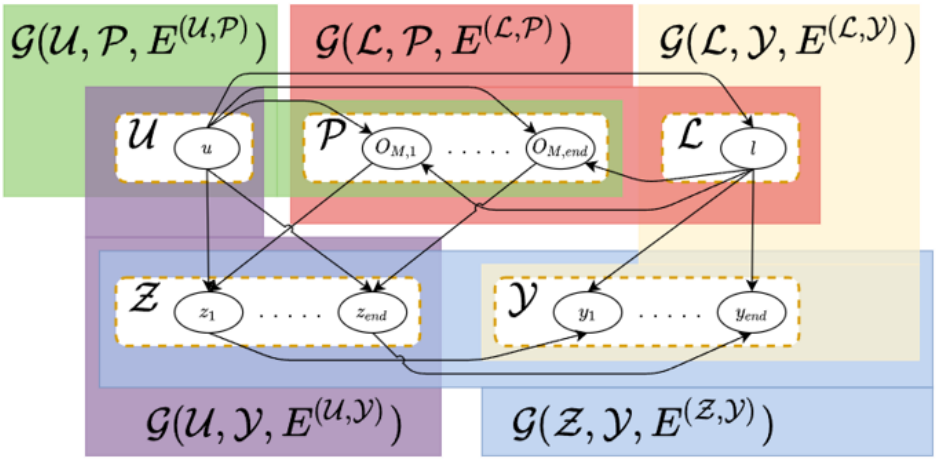

Figure 3: Correlation between the mission and the power profile

3.1 Mission and power profile

In literature, there is no consensus of a general definition for a mission, hence this paper proposes the following mission definition:

"Transport X from A to B (optionally via C, D, etc.), leaving at t_0 (time and date), arriving at destination at t_{end} (time and date)."

where X denotes the cargo (amount/size and type), and $A \in R^2$ and $B \in R^2$ the locations visited. Using this definition, three important aspects can be derived: the type of vessel and its characteristics ($\mathcal{L}$), the operational modes required throughout the mission ($\mathcal{P}$), and other mission parameters ($\mathcal{Z}$) such as travelled route, the environment (waves, currents, wind, temperature, water depth, and waterway width) along this route, the speed of the vessel, and also details such as the displacement, and the towing force during the mode *assist*, if applicable. Together, these aspects determine the power required during the mission, hence they determine the power profile ($\mathcal{Y}$). A graph-model of the correlation between the mission, power profile, and the different aspects can be seen in Figure 3.

Now, using a mission with two locations (A and B) to be visited, cargo X, starting time t_0 and total mission time $t_m = t_{end} - t_0$, an algorithm that determines the required power profile for a given mission can be proposed, as shown in Algorithm 1.

Algorithm 1: Correlation between mission and power profile

Input: $\mathcal{U} = \{A,\ B,\ t_0,\ t_m,\ X\}$ ← Derived from mission definition or historic data

$\mathcal{L} = f(\mathcal{U}) = \{X_v,\ a,\ D\ ,f_h,\ K_Q,\ K_T,\ \eta_D\}$ ← Type of vessel X_v and vessel parameters

$\mathcal{P} = f(\mathcal{U},\mathcal{L}) = \{O_{M,1},\ ...,\ O_{M,end}\}$ ← List of operational modes used during the mission

$\mathcal{Z} = f(\mathcal{U},\mathcal{P}) = \{z_1,\ ...,\ z_{end}\}$ ← Mission dependent parameters , where:

$z_t = \{\ S_m,\ F_{tow}(t),\ O_e(t),\ \nabla(t),\ V_{O_m}(t),\ c_0(t)\}$ ← Route S_m, towing force F_{tow}, displacement ∇, operational environment O_e, vessel speed V_{O_m}, and a speed dependent parameter c_0

$O_e(t) = \{s_s(t),\ c_s(t),\ w_s(t),\ h(t),\ T_a(t),\ w_w(t)\}$ ← seas state s_s, current c_s, wind w_s, water depth h, ambient temperature T_a, and waterway width w_w

Output: $\mathcal{Y} = f(\mathcal{L},\mathcal{Z}) = \{y_1,\ ...,\ y_{end}\}$ ← Power demands to construct the power profile, where:

$y_t = \{P_{tot}(t),\ P_D(t),\ P_{aux}(t)\}$ ← Total power P_{tot}, propulsion power P_D, and auxiliary power P_{aux}

$P_{aux} = P_{aux,c}(X_v) + \Delta P_{aux}(O_m, T_a, X_v)$ ← A constant auxiliary power demand based on the type of vessel, with fluctuations due to the operational modes and temperature

$$P_D = \frac{f(s_s, w_s, c_s, h, w_w, f_h, \nabla) * c_0 * V_s^a}{\eta_D} + |F_{tow}|^{\frac{3}{2}} \frac{2\pi K_Q}{\sqrt{\rho} D K_T^{\frac{3}{2}}}$$

3.2 Power profile and automation modifications

If multiple diesel-electric tugboats, found in the works of (Vu et al., 2015), (Kumar et al., 2020), and (Yuan et al., 2016) are compared, it can be found that although their operations are alike, the power profile differs, and also the installed equipment is different. To this end, the three power profiles are shown in Figure 4.

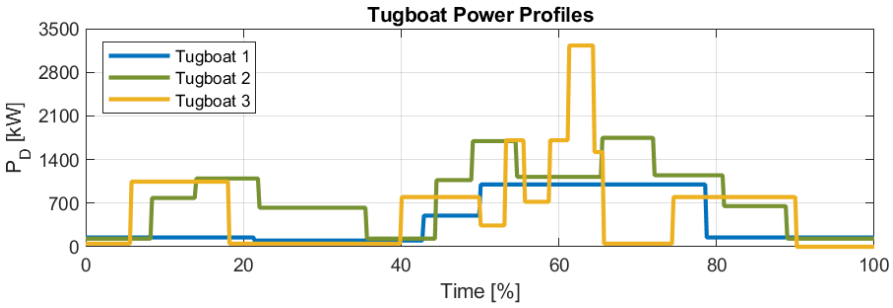

Figure 4: Comparison of different tugboats

By comparing the shown power profiles and the power plants of the corresponding tugboats, it is noted that for missions with more power demand, the capacity of the generator sets and the batteries increase. Now, if for example tugboat 1 has to carry out the mission associated with tugboat 2, both a generator set and a battery has to be added or replaced. Vice versa, tugboat 2 could execute the mission associated with tugboat 1 with less equipment, reducing the weight of the ship. This leads to the following equipment modifications:

- Add components
- Replace components
- Remove components

As described in the introduction, state-of-the-art power plant control systems consist of two levels: a secondary level to compute the power split and reference signals, and a primary level that controls the equipment in the power plant, using the derived reference signals. Since a primary level controller for each component in the power plant has to be included, and the secondary level determines the required power of each component, these two levels depend on the current layout of the power plant. Therefore, if equipment is added or removed, the layout definitely changes, but also for replacements, the characteristics of the equipment may change, hence for all three equipment modifications the control system needs to be updated. To be able to automate this process, a control system that can determine the required equipment modifications based on the power profile is proposed, where after it can use these modifications to update the secondary and primary level, and a schematic can be seen in Figure 5.

4 Design of a modular control architecture

In this section, a modular control architecture is proposed, and a schematic view of the design can be found in Figure 7. The architecture is designed for the retrofittable power plant shown in Figure 6, and the control system consist of a supervisory level, a secondary level, and a primary level, and allows for modular use of the batteries in the power plant.The modular controller presented in this paper is mainly based on SSC, first introduced by Hespanha (Hespanha, 1998), which he later improved (Hespanha and Morse, 1999; Hespanha et al., 1999; Hespanha, 2001; Hespanha and Morse, 2002), and is for example used by (Nguyen et al., 2007) to handle changing environmental conditions. SSC has two characteristics; a supervisor and a bank of controllers. At any moment, the supervisor can decide to switch between the controllers in the bank, and in this paper, the supervisor switches based on the power profile for the mission, where the bank of controllers contains controllers which use ECMS to determine the power split for the power plant equipment.

4.1 Supervisor

In this paper, only batteries can be added, replaced, or removed, and therefore the main task of the supervisor is to determine the amount of batteries required for a given power profile, dictated by the mission. As this process can be quite complicated, due to the charging and discharging of the batteries during the mission, in this paper an upper bound for the required batteries ($P_{B,ub}$) will be determined. Therefore, it is assumed that diesel generator set 2 is only used for emergencies, and that the batteries are only discharged when the total electric power demand

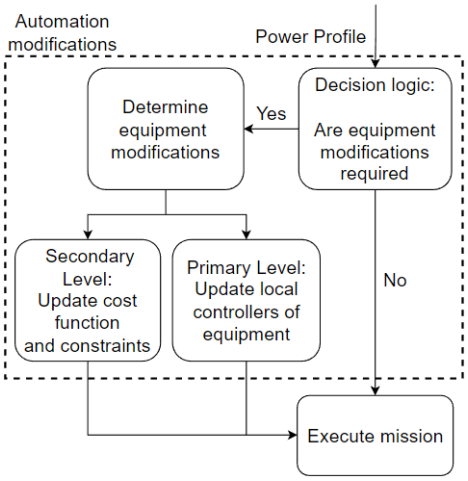

Figure 5: Correlation between the mission, power profile and the automation modifications

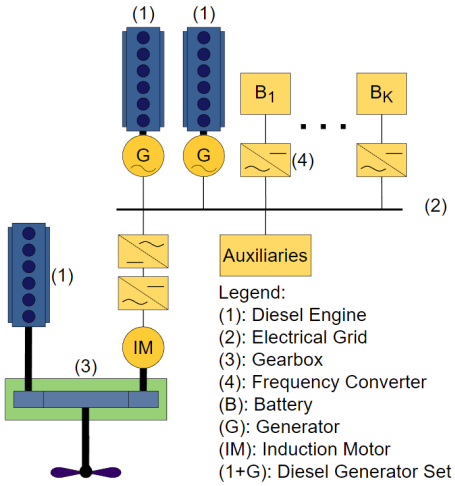

Figure 6: Modular power plant layout

is higher than the optimal working point of diesel generator set 1 ($P^{opt}_{DG,1}$). Furthermore, it is assumed that the induction motor is used for propulsion, and only assisted by the diesel engine for high loads, and that there are two available batteries for the power plant: type 1 and type 2, where the capacity of type 2 is is twice the capacity of type 1. At last, it is assumed that each battery is charged to SOC_{max} at the beginning of the mission, such that:

$$P_{B,ub}(t) = max\Big\{0,\ P_{aux}(t) + min\Big\{P_{D,elec}(t), P^{max}_{IM,grid}\Big\} - P^{opt}_{DG,1}\Big\} \tag{26}$$

$$P_{D,elec}(t) = \frac{P_D(t)}{\eta_T \cdot \eta_{IM} \cdot \eta_{FC}} \tag{27}$$

$$P^{max}_{IM,grid} = \frac{P^{max}_{IM,mec}}{\eta_{IM} \cdot \eta_{FC}} \tag{28}$$

where $P^{max}_{IM,mec}$ and $P^{max}_{IM,grid}$ denote the maximum mechanical power output of the induction motor, and the corresponding electric input power required from the grid, respectively, $P_{D,elec}$ is the propulsion power in terms of electric power of the induction motor, and η_{FC} and η_{IM} are the efficiency of the frequency converter and the induction motor, respectively. The required battery capacity ($E_{B,plant}$) can be found by integrating the found $P_{B,ub}$, and using the batteries SOC limits and a safety factor SF as follows:

$$E_{B,plant} = \frac{\int_{t=0}^{t_m} P_{B,ub}(t)dt}{SOC_{max} - SOC_{min}} \cdot SF \tag{29}$$

with SF (1.1 - 1.2), as often in literature extra battery capacity is installed. It is assumed that the configuration with the least amount of batteries that satisfies $E_{B,plant}$ is selected, and also the capacity of each battery $C_{0,1}$ and $C_{0,2}$ in ampere-seconds (As) is known, such that the configuration can be found with Algorithm 2.

4.2 Bank of secondary level controllers

The supervisor determines the required batteries for the power plant, while the rest of the equipment is fixed, and since there is a certain physical limit of batteries (K_{max}) in the power plant, due to limited space, this results in K_{max} different layouts for the power plant. Also, if for example no batteries are required at all, the vessel also needs to be able to operate, hence the amount of different power plant layouts is equal to $K_{max} + 1$. This can be represented as shown in Figure 7, where each controller in the bank uses ECMS to determine the power split for the installed equipment in the power plant. To this end, the next section will discuss the required ECMS structure to find the power split for each layout, where after the found power split can be converted to reference-signals for the primary level.

Algorithm 2: Selection algorithm for the optimal battery configuration

Input: Battery and Power Plant Specifics

$K_{max} \leftarrow$ Maximum number of batteries in the power plant
$E_{0,1} \leftarrow$ Capacity of battery type 1 (J)
$C_{0,1} \leftarrow$ Capacity of battery type 1 (As)
$E_{0,2} \leftarrow$ Capacity of battery type 2 (J)
$C_{0,2} \leftarrow$ Capacity of battery type 2 (As)
$E_{B,plant} \leftarrow$ Required battery capacity (J)

$r_E = \dfrac{E_{0,2} - E_{0,1}}{E_{0,1}}$ ← Express difference in capacity in terms of $E_{0,1}$
$\mathbf{E}_K = \text{zeros}(K_{max}, K_{max}+1)$
for $i = 1 : K_{max}$ **do**
  for $j = 1 : i+1$ **do**
    $E_K(i,j) = (j \cdot r_E + (i - r_E)) \cdot E_{0,1}$ ← Compute capacity (J) of battery configurations
  end
end
$[\boldsymbol{I}, \boldsymbol{J}] = \text{find}(\mathbf{E}_K >= E_{B,req})$ ← Find indices of suitable configurations
$K_{plant} = min(\boldsymbol{I})$ ← Select configuration with minimum of batteries
$J_{min} = min(\boldsymbol{J}(\boldsymbol{I}(:) == K_{plant}))$ ← Select configuration closest to required capacity
$\boldsymbol{C}_0 = \text{ones}(1, K_{plant}) \cdot C_{0,1}$ ← Fill configuration with battery type 1
if $J_{min} \geq 2$ **then**
  for $j = 1 : J_{min} - 1$ **do**
    $C_0(K_{plant} - j + 1) = C_{0,2}$ ← Replace type 1 with type 2 if necessary
  end
end

Output: Battery Configuration

$K_{plant} \leftarrow$ Amount of batteries in the power plant
$\boldsymbol{C}_0 \leftarrow$ Capacity of each battery

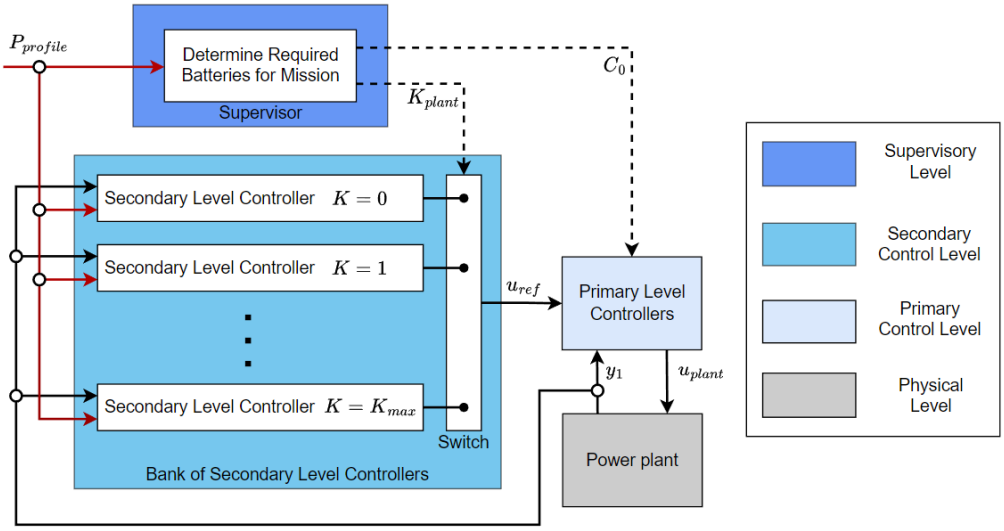

Figure 7: Modular power plant control architecture

4.3 ECMS and reference-signals

The secondary level control used for the modular control system is mainly based on the work of (Kalikatzarakis et al., 2018; Yuan et al., 2016; Vu et al., 2015), and consists of an ECMS with cost function and constraints, and a conversion of the power split to the reference signals. The cost function expresses the power of each components in terms of fuel use, while the constraints limit the power of each component to their capabilities, and ensure the required power, as specified by the power profile, is met. Opposed to the work of Kalikatzarakis et al. (2018); Yuan et al. (2016); Vu et al. (2015), the constraint that keeps the *SOC* of a battery between its limits is replaced by a constraint for the power of the battery (Eq. 37), and furthermore, during simulations it was found that in order to use ECMS for multiple batteries, additional constraints are required. To the best knowledge of the authors, no literature exists on this problem, and therefore two additional constraints (presented in Eq. 38 and Eq. 39) are proposed. The constraints are experimentally found sufficient for this problem, and the final ECMS formulation for any number of batteries K can be found below.

$$minimize\{\dot{m}_{T,K}\} \tag{30}$$

where:

$$\begin{aligned}\dot{m}_{T,K} = {} & a_1^{DE} \cdot {P_{DE}}^3 + a_2^{DE} \cdot {P_{DE}}^2 + a_3^{DE} \cdot \omega_{DE}^2 \cdot P_{DE} + a_4^{DE} \cdot \omega_{DE} \cdot P_{DE} + a_5^{DE} \cdot {P_{DE}}^2 \cdot \omega_{DE} + a_6^{DE} \cdot P_{DE} \\ & + \sum_{j=1}^{2} \left(a_1^{DG,j} \cdot \left(\frac{P_{DG,j}}{\eta_{DG,j}} \right)^3 + a_2^{DG,j} \cdot \left(\frac{P_{DG,j}}{\eta_{DG,j}} \right)^2 + a_3^{DG,j} \cdot \frac{P_{DG,j}}{\eta_{DG,j}} \right) \\ & + \sum_{k=1}^{K} \left(SFOC_{DE,nom} \cdot \eta_{FC} \cdot \eta_{IM} \cdot {\eta_{B,k}}^{sign(P_{B,k})} \cdot P_{B,k} \right)\end{aligned} \tag{31}$$

subject to:

$$P_{DE} \geq \frac{P_D}{\eta_T} - P_{IM,mec} \tag{32}$$

$$\sum_{j=1}^{2} P_{DG,j} \geq P_{aux} - \sum_{k=1}^{K} P_{B,k} + \frac{P_{IM,mec}}{\eta_{IM} \cdot \eta_{FC}} \tag{33}$$

$$0 \leq P_{DE} \leq P_{DE}^{max} \tag{34}$$

$$0 \leq P_{IM,mec} \leq P_{IM,mec}^{max} \tag{35}$$

$$0 \leq P_{DG,j} \leq P_{DG,j}^{max} \qquad \text{for } j \in [1,2] \tag{36}$$

$$P_{B,k}^{min} \leq P_{B,k} \leq P_{B,k}^{max} \qquad \text{for } k \in [1,...,K] \tag{37}$$

$$P_{B,k} \geq P_{B,k-1} \qquad \text{for } k \in [2,...,K] \tag{38}$$

$$P_{B,K} \cdot P_{B,1} \geq 0 \qquad \text{for } K \geq 2 \tag{39}$$

Here, $\dot{m}_{T,K}$ is the fuel consumption rate for a power plant with K batteries, $P_{DE}, P_{IM,mec}, P_{DG,j}$, and $P_{B,k}$ denote the power split regarding the diesel engine, induction motor, diesel generator set $j \in 1,2$, and battery $k \in [1,...K]$, respectively, with limits P_{DE}^{max}, $P_{IM,mec}^{max}$, $P_{DG,j}^{max}$, $P_{B,k}^{min}$, and $P_{B,k}^{max}$. Furthermore, a_i^{DE} for $i = [1,2,3,4,5,6]$, $a_i^{DG,j}$ for $i = [1,2,3]$ are constants to characterize the fuel consumption, $SFOC_{DE,nom}$ is the nominal diesel engine fuel consumption, $\eta_{B,k}$ is the efficiency of battery k, and $\eta_{DG,j}$ the j-th diesel generator sets efficiency.

5 Simulation results

This paper aims to investigate the behaviour of the modular power plant control architecture when used for a tugboat such as the Smith Elbe (Kalikatzarakis et al., 2018). A typical mission consists of: *Transit* to the arrival location of the cargo vessel, remain *standby* at position until cargo vessel arrives, *assist-low*, following by *assist-high*, in order to guide the cargo vessel into the harbour, and *transit* back to a specific location in the harbour when finished. Each operational mode dictates a certain power demand, but also the operational environment and the time spend in each mode has an impact. To this end, four missions are composed, where for the baseline, mission 1, the power profile found in (Yuan et al., 2016) is assumed. As mission 2, 3, and 4 are all variations on mission 1, the described correlation between the mission and the power profile can be used to indicate changes in the power profile, based on the changes in the mission, and this is shown in Table 1. Note that only the propulsion power is affected, and for the auxiliary power a constant load of 100 kW is assumed for each mission.

The described variation in the mission and the power profile, as shown in Table 1, are used to construct the four different power profiles shown in Figure 8. For each mission, at $t = 0$ the supervisor determines the required batteries for the mission, selects the corresponding secondary level controller from the bank, automatically initializes

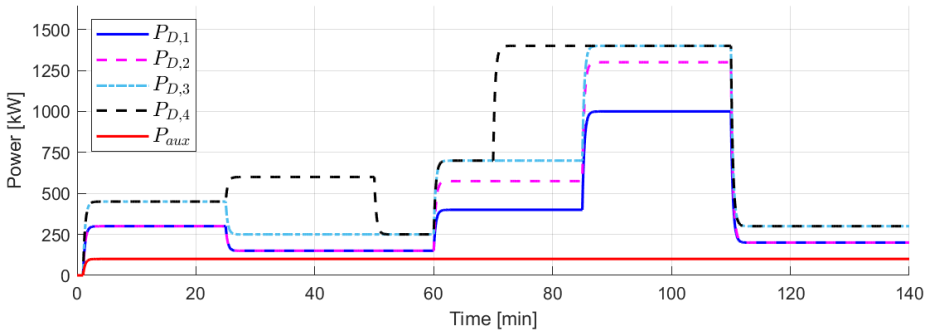

Figure 8: Power profiles of different scenarios

	Change with respect to mission 1	Change with respect to power profile 1			
		Transit	Standby	Assit-low	Assist-high
Mission 2	Larger cargo ship to assist	-	-	Increase of F_{tow} $\rightarrow$ P_D increases	Increase of F_{tow} $\rightarrow$ P_D increases
Mission 3	Larger cargo ship to assist	-	-	Increase of F_{tow} $\rightarrow$ P_D increases	Increase of F_{tow} $\rightarrow$ P_D increases
	Increase of wave, wind, and currents	Increase of s_s, w_s, c_s $\rightarrow$ P_D increases	Increase of s_s, w_s, c_s $\rightarrow$ P_D increases	Increase of s_s, w_s, c_s $\rightarrow$ P_D increases	Increase of s_s, w_s, c_s $\rightarrow$ P_D increases
Mission 4	Larger cargo ship to assist	-	-	Increase of F_{tow} $\rightarrow$ P_D increases	Increase of F_{tow} $\rightarrow$ P_D increases
	Increase of wave, wind, and currents	Increase of s_s, w_s, c_s $\rightarrow$ P_D increases	Increase of s_s, w_s, c_s $\rightarrow$ P_D increases	Increase of s_s, w_s, c_s $\rightarrow$ P_D increases	Increase of s_s, w_s, c_s $\rightarrow$ P_D increases
	Cargo ship arrives further from starting point of tugboat, but total mission time remains the same	Longer duration of mode*	Shorter duration of mode	Shorter duration of mode	Longer duration of mode
		Speed increase halfway during mode* $\rightarrow$ P_D increases*			

Table 1: Changes in mission and power profile

*: Only applies for the first use of this mode. For the second use of this mode, at the end of the mission, this is not applicable.

the primary level battery constraint modules, and also selects the required battery models in the power plant model, and in Table 2 the required batteries and their capacity for each mission can be found. During the simulations, the behavior of the secondary level, the primary level, and also of the power plant components is monitored. The parameters used for the simulations are shown in Table 4, and the simulation results are presented in Figure 9. In Figure 9a, 9d, 9g, and 9j the power split for the fixed equipment can be seen, in Figure 9b, 9e, 9h, and 9k the power split for the batteries is shown, and in Figure 9c, 9f, 9i, and 9l the batteries *SOC* levels are presented. Note that the power split is provided by the secondary level, while the *SOC* levels are given by the battery constraint modules in the primary level. From the results it can be seen that the modular control architecture performs well for each mission, as the power split for all the components appears stable, and the *SOC* of the batteries is kept within its limits. The robustness of the modular control architecture follows from the stable behavior for both different power profiles, as different power plant layouts.

Furthermore, using the shown power split and the *SOC* of the batteries, it can be noted that either the battery

	$E_{B,max}$	Selected Batteries					
		K	Type	Capacity			
				E_0		C_0	
Mission 1	904 MJ	1	2	1080	MJ	2.4	MAs
Mission 2	1294 MJ	2	[1,2]	[540 1080]	MJ	[1.2 2.4]	MAs
Mission 3	1625 MJ	2	[2,2]	[1080 1080]	MJ	[2.4 2.4]	MAs
Mission 4	2404 MJ	3	[1,2,2]	[540 1080 1080]	MJ	[1.2 2.4 2.4]	MAs

Table 2: Supervisor results for different missions

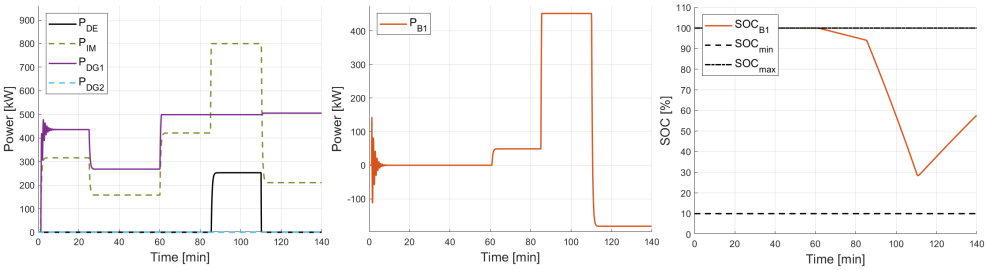

(a) Mission 1: Fixed equipment power

(b) Mission 1: Battery power

(c) Mission 1: Battery SOC

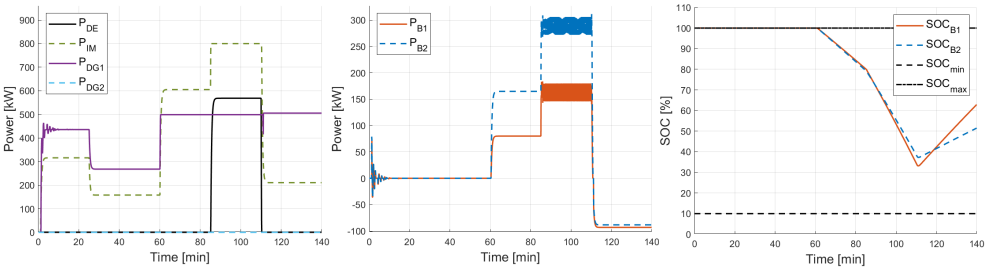

(d) Mission 2: Fixed equipment power

(e) Mission 2: Battery power

(f) Mission 2: Battery SOC

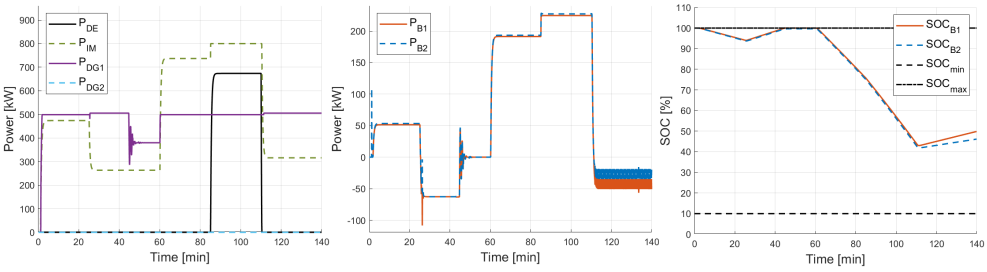

(g) Mission 3: Fixed equipment power

(h) Mission 3: Battery power

(i) Mission 3: Battery SOC

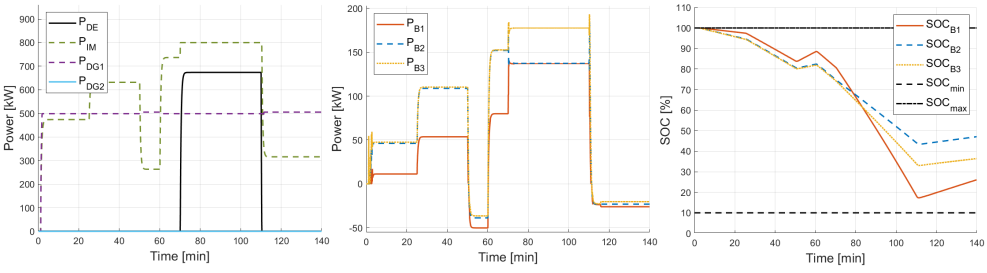

(j) Mission 4:Fixed equipment power

(k) Mission 4: Battery power

(l) Mission 4: Battery SOC

Figure 9: Simulation results

power or the *SOC* behaves proportional to the ratio of the batteries capacities. An example of this is seen using Figure 9e and 9f, where a battery of type 2 shows similar *SOC* decrease for a discharging power twice as much as for a battery of type 1. Even more, for the same charging rate, a battery of type 1 charges much faster than a battery of type 2, as it has a smaller capacity. At last, it can be noted that although batteries in the power plant have the same capacity, the secondary level could decide to discharge or charge them with different rates, as can be seen in Figure 9h and 9k.

	Propulsion Power Error		Auxiliary Power Error	
	RMSE [kW]	SI [%]	RMSE [kW]	SI [%]
Mission 1	9.12	2.39	10.43	10.55
Mission 2	10.88	2.34	10.02	10.15
Mission 3	10.99	1.90	10.54	10.68
Mission 4	11.27	1.58	10.50	10.64

Table 3: Performance of modular power plant controller

In order to give quantitative results, for each mission the output of the power plant components is measured and used to determine the delivered propulsion $P_{D,plant}$ and auxiliary power $P_{aux,plant}$, as shown in Equation 40 and 41.

$$P_{D,plant} = Q_p \cdot \omega_p \tag{40}$$

$$P_{aux,plant} = \sum_{j=1}^{2} V_{DG,j} \cdot I^*_{DG,j} + \sum_{k=1}^{K} V_{B,k} \cdot I_{B,k} - \frac{Q_{IM} \cdot \omega_{IM}}{\eta_{IM} \cdot \eta_{FC}} \tag{41}$$

where * denotes the complex conjugate. Using this, the RMSE and the scatter index (SI) with respect to the requested propulsion P_D and auxiliary power P_{aux}, as stated by the power profile, can be determined, and the results are presented in Table 3.

$$\text{Propulsion} \begin{cases} \text{RMSE} &= \sqrt{\text{mean}\left(\left(P_D - P_{D,plant}\right)^2\right)} \\ \text{SI} &= \dfrac{\text{RMSE}}{\text{mean}(P_{D,plant})} \end{cases} \tag{42}$$

$$\text{Auxiliary} : \begin{cases} \text{RMSE} &= \sqrt{\text{mean}\left(\left(P_{aux} - P_{aux,plant}\right)^2\right)} \\ \text{SI} &= \dfrac{\text{RMSE}}{\text{mean}(P_{aux,plant})} \end{cases} \tag{43}$$

$$\tag{44}$$

Induction Motor

Model Parameters

k_{IM}	1000	-
R_2	0.01	Ω
J_{DE}	4167	kgm^2
D_{DE}	1000	$\frac{\mathrm{kgm}^2}{\mathrm{s}}$

Controller Gains

$K_{P,IM}$	10	[-]
$K_{I,IM}$	10	[-]
$C_{V/f}$	2	$\frac{\mathrm{kgm}^2}{\mathrm{As}^3}$

ECMS Parameters

η_{IM}	0.95	[-]
P_{IM}^{max}	$800 \cdot 10^3$	W

Shaft and Gearbox

J_{tot}	12500	kgm^2
i_{DE}	7.5	[-]
i_{IM}	24	[-]
η_T	0.95	[-]

Batteries

Model Parameters

$SOC(t_0)$	1	[-]
$a_{B,1}$	111	V
$a_{B,0}$	389	V
R_B	0.0225	Ω

Constraint Module Parameters

Δt	1000	s
SOC_{min}	0.1	[-]
SOC_{max}	1	[-]
$V_{B,min}$	300	V
$V_{B,max}$	600	V

ECMS Parameters

η_B	0.97	[-]
$SFOC_{DE,nom}$	72.1	$\frac{\mathrm{kg}}{\mathrm{kWh}}$

Electric Grid

V_{grid}	3300	V
f_{grid}	50	$\frac{1}{\mathrm{s}}$
η_{FC}	0.99	[-]

Diesel Engine

Model Parameters

k_{DE}	3000	$\frac{\mathrm{m}^2}{\mathrm{s}^2}$
J_{DE}	4167	kgm^2
D_{DE}	1000	$\frac{\mathrm{kgm}^2}{\mathrm{s}}$

Controller Gains

$K_{P,DE}$	20	[-]
$K_{I,DE}$	2	[-]

ECMS Parameters

a_1^{DE}	$5.48 \cdot 10^{-5}$	$\frac{\mathrm{kg}}{\mathrm{GW}^3\mathrm{h}}$
a_2^{DE}	-0.206	$\frac{\mathrm{kg}}{\mathrm{MW}^2\mathrm{h}}$
a_3^{DE}	$5.545 \cdot 10^{-4}$	$\frac{\mathrm{kgs}^2}{\mathrm{kWh}}$
a_4^{DE}	-0.271	$\frac{\mathrm{kgs}}{\mathrm{kWh}}$
a_5^{DE}	$-3.55 \cdot 10^{-5}$	$\frac{\mathrm{kgs}}{\mathrm{MW}^2\mathrm{h}}$
a_6^{DE}	600	$\frac{\mathrm{kg}}{\mathrm{kWh}}$
P_{DE}^{max}	$1200 \cdot 10^3$	W

Propeller

C_p	670	kgm^2

Diesel Generator Sets

Model Parameters

k_{DG}	4000	$\frac{\mathrm{m}^2}{\mathrm{s}^2}$
J_{DG}	4167	kgm^2
$R_{DG,int}$	0.150	Ω
L_{DG}	0.0021	H
$a_{G,1}$	3.34	$\frac{\mathrm{kgm}^2}{\mathrm{A}^2\mathrm{s}^2}$
$a_{G,0}$	0.57	$\frac{\mathrm{kgm}^2}{\mathrm{As}^2}$

Controller Gains

$K_{P,DG,DE}$	200	[-]
$K_{I,DG,DE}$	30	[-]
$K_{P,DG,G}$	30	[-]
$K_{I,DG,G}$	12	[-]

ECMS Parameters

a_1^{DG}	$5.55 \cdot 10^{-4}$	$\frac{\mathrm{kg}}{\mathrm{GW}^3\mathrm{h}}$
a_1^{DG}	-0.580	$\frac{\mathrm{kg}}{\mathrm{MW}^2\mathrm{h}}$
a_3^{DG}	$2.15 \cdot 10^2$	$\frac{\mathrm{kg}}{\mathrm{kWh}}$
η_{DG}	0.95	[-]
P_{DG}^{max}	$665 \cdot 10^3$	W
P_{DG}^{opt}	$524 \cdot 10^3$	W

Table 4: Parameters of the power plant components

6 Conclusions

In this paper, a graph-model for the correlation between the mission and the power profile is presented, and the correlation between the power profile and the automation modifications of the control system is discussed. Using this, a modular control architecture for a retrofittable power plant is proposed, which allows modular use of the batteries. Simulations showed the performance of the modular control architecture, regarding the stability and robustness. The results indicate a tracking error less than 3% and 11% of the propulsion and auxiliary power requested by the power profile, respectively.

References

Chang, W., 2013. The state of charge estimating methods for battery: A review. International Scholarly Research Notices 2013.

Cheong, K., Li, P., Xia, J., 2010. Control oriented modeling and system identification of a diesel generator set (genset), in: Proceedings of the 2010 American Control Conference, IEEE. pp. 950–955.

Eijkhout, T., Jovanova, J., 2021. Active heave compensation of a floating crane using electric drive, in: 2021 IEEE/ASME International Conference on Advanced Intelligent Mechatronics (AIM), pp. 1089–1094. doi:10.1109/AIM46487.2021.9517502.

Geertsma, R., Negenborn, R., Visser, K., Hopman, J., 2017. Design and control of hybrid power and propulsion systems for smart ships: A review of developments. Applied Energy 194, 30–54.

Hanbidge, P., 2001. A mission-based approach to vessel design the royal institution of naval architects (rina) small craft safety. URL: https://www.academia.edu/14563968/A_MISSION_BASED_APPROACH_TO_VESSEL_DESIGN_The_Royal_Institution_of_Naval_Architects_RINA_SMALL_CRAFT_SAFETY.

Haseltalab, A., van Biert, L., Mestemaker, B., Negenborn, R., 2020. Energy Management for Hybrid Power Generation Using Solid Oxide Fuel Cell, Zenodo. URL: https://doi.org/10.24868/issn.2631-8741.2020.006, doi:10.24868/issn.2631-8741.2020.006.

Haseltalab, A., Negenborn, R., 2019. Model predictive maneuvering control and energy management for all-electric autonomous ships. Applied Energy 251, 113308.

Hespanha, J., 1998. Logic-based switching algorithms in control.

Hespanha, J., 2001. Tutorial on supervisory control, in: Lecture Notes for the workshop Control using Logic and Switching for the 40th Conf. on Decision and Contr., Orlando, Florida, Citeseer.

Hespanha, J., Liberzon, D., Morse, A., 1999. Logic-based switching control of a nonholonomic system with parametric modeling uncertainty. Systems & Control Letters 38, 167–177.

Hespanha, J., Morse, A., 1999. Certainty equivalence implies detectability. Systems & Control Letters 36, 1–13.

Hespanha, J., Morse, A., 2002. Switching between stabilizing controllers. Automatica 38, 1905–1917.

Izadi-Zamanabadi, R., Blanke, M., 1999. A ship propulsion system as a benchmark for fault-tolerant control. Control Engineering Practice 7, 227–239.

Kalikatzarakis, M., , R., Boonen, E., Visser, K., Negenborn, R., 2018. Ship energy management for hybrid propulsion and power supply with shore charging. Control Engineering Practice 76, 133–154.

Kularatna, N., Gunawardane, K., 2021. Rechargeable battery technologies: An electronic circuit designer's viewpoint. pp. 65–98. doi:10.1016/B978-0-12-820778-9.00001-2.

Kumar, B., Selvaraj, R.and Desingu, K., Chelliah, T., Upadhyayula, R., 2020. A coordinated control strategy for a diesel-electric tugboat system for improved fuel economy. IEEE Transactions on Industry Applications 56, 5439–5451.

Negenborn, R., Hellendoorn, H., 2010. Intelligence in transportation infrastructures via model-based predictive control, in: Intelligent Infrastructures. Springer, pp. 3–24.

Nguyen, T.D., Sørensen, A.J., Quek, S.T., 2007. Design of hybrid controller for dynamic positioning from calm to extreme sea conditions. Automatica 43, 768–785.

Smogeli, Ø., 2006. Control of marine propellers: from normal to extreme conditions .

Smogeli, Ø., Ruth, E., Sorensen, A., 2005. Experimental validation of power and torque thruster control, in: Proceedings of the 2005 IEEE International Symposium on, Mediterrean Conference on Control and Automation Intelligent Control, 2005., IEEE. pp. 1506–1511.

Smogeli, Ø., Sørensen, A., 2009. Antispin thruster control for ships. IEEE transactions on control systems technology 17, 1362–1375.

Smogeli, Ø., Sørensen, A., Minsaas, K., 2008. The concept of anti-spin thruster control. Control Engineering Practice 16, 465–481.

Sun, K., Shu, Q., 2011. Overview of the types of battery models, in: Proceedings of the 30th Chinese Control Conference, IEEE. pp. 3644–3648.

Vahedpour, M., Noei, A., Kholerdi, H., 2015. Comparison between performance of conventional, fuzzy and frac-

tional order pid controllers in practical speed control of induction motor, in: 2015 2nd International Conference on Knowledge-Based Engineering and Innovation (KBEI), IEEE. pp. 912–916.

Vu, T., Ayu, A., Dhupia, J., Kennedy, L., Adnanes, A., 2015. Power management for electric tugboats through operating load estimation. IEEE Transactions on Control Systems Technology 23, 2375–2382.

Wang, S., Wang, L., Qiao, Z., Li, F., 2018. Optimal robust control of path following and rudder roll reduction for a container ship in heavy waves. Applied Sciences 8, 1631.

Wildi, T., et al., 2002. Electrical machines, drives, and power systems. New Jersey: Upper Saddle River .

Woud, H.K., Stapersma, D., 2019. Design of propulsion and electric power generation systems. IMarEST, Institute of Marine Engineering, Science and Technology.

Yuan, L., Tjahjowidodo, T., Lee, G., Chan, R., dnanes, A.K., 2016. Equivalent consumption minimization strategy for hybrid all-electric tugboats to optimize fuel savings, in: 2016 American Control Conference (ACC), IEEE. pp. 6803–6808.

REFERENCES

[1] G. Storhaug. *Digital Twins and Sensor Monitoring - DNV*. Jan. 2019. URL: https://www.dnv.com/expert-story/maritime-impact/Digital-twins-and-sensor-monitoring.html.

[2] D.T. Nguyen and A.J. Sørensen. "Switching control for thruster-assisted position mooring". In: *Control Engineering Practice* 17.9 (2009), pp. 985–994.

[3] P. Hanbidge. *A MISSION-BASED APPROACH TO VESSEL DESIGN The Royal Institution of Naval Architects (RINA) SMALL CRAFT SAFETY*. May 2001. URL: https://www.academia.edu/14563968/A_MISSION_BASED_APPROACH_TO_VESSEL_DESIGN_The_Royal_Institution_of_Naval_Architects_RINA_SMALL_CRAFT_SAFETY.

[4] L.C.W Yuan et al. "Equivalent consumption minimization strategy for hybrid all-electric tugboats to optimize fuel savings". In: *2016 American Control Conference (ACC)*. IEEE. 2016, pp. 6803–6808.

[5] F. Zhao et al. "Power management of vessel propulsion system for thrust efficiency and emissions mitigation". In: *Applied Energy* 161 (2016), pp. 124–132.

[6] H. Grimmelius et al. "Control of hybrid ship drive systems". In: *10th International conference on computer and IT applications in the maritime industries*. 2011, pp. 1–15.

[7] T.L. Vu et al. "Power management for electric tugboats through operating load estimation". In: *IEEE Transactions on Control Systems Technology* 23.6 (2015), pp. 2375–2382.

[8] L. Chen. "Integrated design and control optimization of hybrid electric marine propulsion systems based on battery performance degradation model". PhD thesis. 2019.

[9] P.J. Chauhan et al. "Fuel efficiency improvement by optimal scheduling of diesel generators using PSO in offshore support vessel with DC power system architecture". In: *2015 IEEE PES Asia-Pacific Power and Energy Engineering Conference (APPEEC)*. IEEE. 2015, pp. 1–6.

[10] A.J. Sørensen. "Marine control systems". In: *Propulsion and Motion Control of Ships and Ocean Structures* 3 (2013).

[11] T.I. Bø et al. "Marine vessel and power plant system simulator". In: *IEEE Access* 3 (2015), pp. 2065–2079.

[12] M. Kalikatzarakis et al. "Ship energy management for hybrid propulsion and power supply with shore charging". In: *Control Engineering Practice* 76 (2018), pp. 133–154.

[13] R.D. Geertsma et al. “Design and control of hybrid power and propulsion systems for smart ships: A review of developments”. In: *Applied Energy* 194 (2017), pp. 30–54.

[14] M.D.A Al-Falahi et al. “AC ship microgrids: control and power management optimization”. In: *Energies* 11.6 (2018), p. 1458.

[15] K.K. Yum et al. “Simulation of a hybrid marine propulsion system in waves”. In: *Proceedings of 28th CIMAC World Congress*. 202. 2016.

[16] A.F. Molland, S.R. Turnock, and D.A. Hudson. *Ship resistance and propulsion*. Cambridge university press, 2017.

[17] E.K. Dedes, D.A. Hudson, and S.R. Turnock. “Investigation of Diesel Hybrid systems for fuel oil reduction in slow speed ocean going ships”. In: *Energy* 114 (2016), pp. 444–456.

[18] K. Kim et al. “Analysis of battery/generator hybrid container ship for co 2 reduction”. In: *IEEE Access* 6 (2018), pp. 14537–14543.

[19] J.F. Hansen and F. Wendt. “History and state of the art in commercial electric ship propulsion, integrated power systems, and future trends”. In: *Proceedings of the IEEE* 103.12 (2015), pp. 2229–2242.

[20] V. Bolbot et al. “Cruise ship optimal power plants design identification and quantitative safety assessment”. In: *environmental pollution* 9 (2019), p. 11.

[21] X. Zhaoxia et al. “Coordinated control of a hybrid-electric-ferry shipboard microgrid”. In: *IEEE Transactions on Transportation Electrification* 5.3 (2019), pp. 828–839.

[22] M.C. van Benten. *Multi-Level Propulsion Control in Complex Ships*. 2021. URL: https://www.dropbox.com/s/lybtqzln6obc0rm/Multi-Level%5C%20Propulsion%5C%20Control%5C%20in%5C%20Complex%5C%20Ships.pdf?dl=0.

[23] M. Holmlund-Sund. *Wärtsilä and partners develop emissions-free barge concept*. June 2020. URL: https://www.wartsila.com/media/news/02-06-2020-wartsila-and-partners-develop-emissions-free-barge-concept-2720925.

[24] A.J. Sørensen. “Structural issues in the design and operation of marine control systems”. In: *Annual Reviews in Control* 29.1 (2005), pp. 125–149.

[25] Ø.N. Smogeli, E. Ruth, and A.J. Sorensen. “Experimental validation of power and torque thruster control”. In: *Proceedings of the 2005 IEEE International Symposium on, Mediterrean Conference on Control and Automation Intelligent Control, 2005*. IEEE. 2005, pp. 1506–1511.

[26] Ø.N. Smogeli. “Control of marine propellers: from normal to extreme conditions”. In: (2006).

[27] Ø.N. Smogeli, A.J. Sørensen, and K.J. Minsaas. “The concept of anti-spin thruster control”. In: *Control Engineering Practice* 16.4 (2008), pp. 465–481.

[28] Ø.N. Smogeli and A.J. Sørensen. “Antispin thruster control for ships”. In: *IEEE transactions on control systems technology* 17.6 (2009), pp. 1362–1375.

[29] S. Wang et al. “Optimal robust control of path following and rudder roll reduction for a container ship in heavy waves”. In: *Applied Sciences* 8.9 (2018), p. 1631.

[30] R.R. Negenborn and H. Hellendoorn. “Intelligence in transportation infrastructures via model-based predictive control”. In: *Intelligent Infrastructures*. Springer, 2010, pp. 3–24.

[31] Equasis. *Equasis Statistics: The world merchant fleet in 2018*. 2018. URL: https://www.equasis.org/Fichiers/Statistique/MOA/Documents%20availables%20on%20statistics%20of%20Equasis/Equasis%20Statistics%20-%20The%20world%20fleet%202018.pdf.

[32] B.A. Kumar et al. “A Coordinated Control Strategy for a Diesel-Electric Tugboat System for Improved Fuel Economy”. In: *IEEE Transactions on Industry Applications* 56.5 (2020), pp. 5439–5451.

[33] T. Völker. “Hybrid propulsion concepts on ships”. In: (2015).

[34] B.A. Kumar et al. “Control strategy for fuel saving in asynchronous generator driven electric tugboats”. In: *2016 IEEE Uttar Pradesh Section International Conference on Electrical, Computer and Electronics Engineering (UPCON)*. IEEE. 2016, pp. 467–472.

[35] *Container vessel Ever Glory welcomed and assisted in Rotterdam*. June 2019. URL: https://www.boluda.eu/news/Container-vessel-Ever-Glory-welcomed-and-assisted-in-Rotterdam.

[36] A.T. Hoang et al. “Aalyzing and selecting the typical propulsion systems for ocean supply vessels”. In: *2020 6th International Conference on Advanced Computing and Communication Systems (ICACCS)*. IEEE. 2020, pp. 1349–1357.

[37] R.S.K. Rose. “Future Characteristics of Offshore Support Vessels”. PhD thesis. Massachusetts Institute of Technology, 2011.

[38] M. Sano et al. “Design issues and trends for the new generation of offshore support vessels”. In: *Offshore Technology Conference*. Offshore Technology Conference. 2012.

[39] S.O. Erikstad and K. Levander. “System based design of offshore support vessels”. In: *Proceedings 11th International Marine Design Conference—IMDC201*. 2012.

[40] B. Głowacki and C. Behrendt. “Energy Efficiency of Offshore Support Vessel”. In: (2017).

[41] H.E. Lindstad, G.S. Eskeland, and A. Rialland. “Batteries in offshore support vessels–Pollution, climate impact and economics”. In: *Transportation Research Part D: Transport and Environment* 50 (2017), pp. 409–417.

[42] J. Herdzik. “Problems of propulsion systems and main engines choice for offshore support vessels”. In: *Zeszyty Naukowe/Akademia Morska w Szczecinie* (2013).

[43] K.S. Rao et al. “Optimal scheduling of diesel generators in offshore support vessels to minimize fuel consumption”. In: *IECON 2015-41st Annual Conference of the IEEE Industrial Electronics Society*. IEEE. 2015, pp. 004726–004731.

[44] DNV-GL. *Offshore service vessels (OSV)*. URL: https://www.dnvgl.com/maritime/Offshore/vessels/osv.html.

[45] MMA-Offshore. *MMA Centurion*. URL: https://www.mmaoffshore.com/vessel-fleet/mma-centurion.

[46] O. Vennemann, I. Frazer, R. Tornqvist, et al. “Extending the Use of Conventional Construction Technology for the Installation of Subsea Production Facilities in Deep Water”. In: *Offshore Technology Conference*. Offshore Technology Conference. 2008.

[47] MI-News-Network. *What is a Research Vessel?* Apr. 2019. URL: https://www.marineinsight.com/types-of-ships/what-is-a-research-vessel/.

[48] C. Capasso et al. “Preliminary design of the hybrid propulsion architecture for the research vessel “G. Dallaporta””. In: *2016 International Conference on Electrical Systems for Aircraft, Railway, Ship Propulsion and Road Vehicles & International Transportation Electrification Conference (ESARS-ITEC)*. IEEE. 2016, pp. 1–6.

[49] F. Mauro et al. “An hybrid-electric solution for station-keeping and propulsion of a small coastal research vessel”. In: *2018 International Symposium on Power Electronics, Electrical Drives, Automation and Motion (SPEEDAM)*. IEEE. 2018, pp. 607–612.

[50] M. Placek. *Container shipping*. Sept. 2021. URL: https://www.statista.com/topics/1367/container-shipping/#dossierKeyfigures.

[51] N. Xiros. *Robust control of diesel ship propulsion*. Springer Science & Business Media, 2012.

[52] M. van der Meijden. *Triple E – making the impossible possible*. Aug. 2013. URL: https://www.portofrotterdam.com/en/news-and-press-releases/triple-e-%5C%E2%5C%80%5C%93-making-the-impossible-possible.

[53] C. Guan et al. “Computational investigation of a large containership propulsion engine operation at slow steaming conditions”. In: *Applied Energy* 130 (2014), pp. 370–383.

[54] C. Shi, C. Guo, and C. Sun. “Simulation and optimal control of diesel engine propulsion system”. In: *2009 WRI World Congress on Computer Science and Information Engineering*. Vol. 5. IEEE. 2009, pp. 87–91.

[55] K. Kharroubi and O.S. Söğüt. “Modelling of the propulsion plant of a large container ship by the partition of the cycle of the main diesel engine”. In: *Proceedings of the Institution of Mechanical Engineers, Part M: Journal of Engineering for the Maritime Environment* 234.2 (2019), pp. 475–489.

[56] N.I. Xiros and N.P. Kyrtatos. “A neural predictor of propeller load demand for improved control of diesel ship propulsion”. In: *Proceedings of the 2000 IEEE International Symposium on Intelligent Control. Held jointly with the 8th IEEE Mediterranean Conference on Control and Automation (Cat. No. 00CH37147)*. IEEE. 2000, pp. 321–326.

[57] BergeBulk. *Welcome to the fleet – Berge Snaefell*. Jan. 2018. URL: https://www.bergebulk.com/welcome-to-the-fleet-berge-snaefell/.

[58] K. Kim et al. “Analysis of a supercapacitor/battery hybrid power system for a bulk carrier”. In: *Applied Sciences* 9.8 (2019), p. 1547.

[59] J.E. Buckingham and D.R. Pearson. “Modelling Alternative Propulsion Technologies for Merchant Vessels”. In: *RINA, Power & Propulsion Alternatives for Ships, 23rd January* (2019).

[60] *VLCC and ULCC*. URL: https://maritime-connector.com/wiki/vlcc/.

[61] P. Manuelle, B. Singam, and S. Siala. “Induction motors fed by PWM MV7000 converters enhance electric propulsion performance”. In: *2009 13th European Conference on Power Electronics and Applications*. IEEE. 2009, pp. 1–9.

[62] C. Sui et al. “Energy effectiveness of ocean-going cargo ship under various operating conditions”. In: *Ocean Engineering* 190 (2019), p. 106473.

[63] C. Sui et al. “Fuel consumption and emissions of ocean-going cargo ship with hybrid propulsion and different fuels over voyage”. In: *Journal of Marine Science and Engineering* 8.8 (2020), p. 588.

[64] C. Sui et al. “Impact of Battery-Hybrid Cargo Ship Propulsion on Fuel Consumption and Emissions during Port Approaches”. In: June 2019.

[65] A.J. Sørensen. “A survey of dynamic positioning control systems”. In: *Annual reviews in control* 35.1 (2011), pp. 123–136.

[66] F. D’Agostino et al. “Development of a Multiphysics Real-Time Simulator for Model-Based Design of a DC Shipboard Microgrid”. In: *Energies* 13.14 (2020), p. 3580.

[67] T.R. Torben, A.H. Brodtkorb, and A.J. Sørensen. “Control allocation for double-ended ferries with full-scale experimental results”. In: *IFAC-PapersOnLine* 52.21 (2019), pp. 45–50.

[68] URL: https://www.cruisemapper.com/ships/Galicia-ferry-1714.

[69] R. Izadi-Zamanabadi and M. Blanke. “A ship propulsion system as a benchmark for fault-tolerant control”. In: *Control Engineering Practice* 7.2 (1999), pp. 227–239.

[70] S. Krüger and T. Haack. “Design of propulsion control systems based on the simulation of nautical manoeuvres”. In: *9th Symposium on Practical Design of Ships and Other Floating Structures*. Citeseer. 2004.

[71] R. Banning, M.A. Johnson, and M.J. Grimble. “Advanced control design for marine diesel engine propulsion systems”. In: (1997).

[72] M. Blanke and R. Izadi-Zamanabadi. “Nonlinear observer for signal and parameter fault detection in ship propulsion control”. In: *New Directions in nonlinear observer design*. Springer, 1999, pp. 375–397.

[73] U. Campora and M. Figari. “Numerical simulation of ship propulsion transients and full-scale validation”. In: *Proceedings of the Institution of Mechanical Engineers, Part M: Journal of Engineering for the Maritime Environment* 217.1 (2002), pp. 41–52.

[74] A. Bassam. “Use of voyage simulation to investigate hybrid fuel cell systems for marine propulsion”. PhD thesis. University of Southampton, 2017.

[75] H. Gao et al. “Improved control of propeller ventilation using an evidence reasoning rule based Adaboost. M1 approach”. In: *Ocean Engineering* 209 (2020), p. 107329.

[76] M. Rivarolo, D. Rattazzi, and L. Magistri. “Best operative strategy for energy management of a cruise ship employing different distributed generation technologies”. In: *International journal of hydrogen energy* 43.52 (2018), pp. 23500–23510.

[77] A. Armellini et al. “Evaluation of gas turbines as alternative energy production systems for a large cruise ship to meet new maritime regulations”. In: *Applied energy* 211 (2018), pp. 306–317.

[78] H. Sampson. *Coral Princess cruise ship heads to Florida with sick passengers, as Zaandam awaits its fate with the same port*. Apr. 2020. URL: https://www.washingtonpost.com/travel/2020/04/01/coral-princess-cruise-ship-heads-florida-with-sick-passengers-zaandam-awaits-its-fate-with-same-port/.

[79] F. Baldi et al. “Energy and exergy analysis of a cruise ship”. In: *Energies* 11.10 (2018), p. 2508.

[80] T. Iannaccone et al. “Sustainability of cruise ship fuel systems: Comparison among LNG and diesel technologies”. In: *Journal of Cleaner Production* 260 (2020), p. 121069.

[81] V. Bolbot, G. Theotokatos, and D. Vassalos. “Using system-theoretic process analysis and event tree analysis for creation of a fault tree of blackout in the Diesel-Electric Propulsion system of a cruise ship”. In: *International Marine Design Conference XIII*. 2018, pp. 691–9.

[82] V. Mrzljak and T. Mrakovčić. “Comparison of COGES and diesel-electric ship propulsion systems”. In: *Pomorski zbornik* 1 (2016), pp. 131–148.

[83] J. Kivimäki. “Effects of electronically commutated motors used in passenger cabin air conditioning on low voltage network of a cruise ship”. MA thesis. 2016.

[84] I. Atutxa, G. Abad, and J. Carlton. “Electric Propulsion Drives and Power Electronics”. In: *Encyclopedia of Maritime and Offshore Engineering* (2017), pp. 1–17.

[85] C. Ghenai et al. “Hybrid solar PV/PEM fuel Cell/Diesel Generator power system for cruise ship: A case study in Stockholm, Sweden”. In: *Case Studies in Thermal Engineering* 14 (2019), p. 100497.

[86] T. D. Nguyen, A. J. Sorensen, and S. T. Quek. “Multi-operational controller structure for station keeping and transit operations of marine vessels”. In: *IEEE Transactions on Control Systems Technology* 16.3 (2008), pp. 491–498.

[87] T. V. R. Torben, A.J. Sørensen, and A. Brodtkorb. “Hybrid control of autonomous ferries”. In: *December. Project thesis, Department of Marine Technology. Norwegian University of Science and Technology (NTNU), Trondheim. doi* 10 (2018), p. 13140.

[88] J.P. Hespanha. *Logic-based switching algorithms in control*. 1998.

[89] J.P. Hespanha, D.l Liberzon, and A.S. Morse. “Logic-based switching control of a nonholonomic system with parametric modeling uncertainty”. In: *Systems & Control Letters* 38.3 (1999), pp. 167–177.

[90] J.P. Hespanha. “Tutorial on supervisory control”. In: *Lecture Notes for the workshop Control using Logic and Switching for the 40th Conf. on Decision and Contr., Orlando, Florida*. Citeseer. 2001.

[91] J.P. Hespanha and A.S. Morse. “Switching between stabilizing controllers”. In: *Automatica* 38.11 (2002), pp. 1905–1917.

[92] J.P. Hespanha, D. Liberzon, and A. S. Morse. “Hysteresis-based switching algorithms for supervisory control of uncertain systems”. In: *Automatica* 39.2 (2003), pp. 263–272.

[93] T. D. Nguyen. “Design of hybrid marine control systems for dynamic positioning”. PhD thesis. Citeseer, 2005.

[94] T. D. Nguyen, A. J. Sørensen, and S. T. Quek. “Design of hybrid controller for dynamic positioning from calm to extreme sea conditions”. In: *Automatica* 43.5 (2007), pp. 768–785.

[95] M. Tomera. “Hybrid Switching Controller Design for the Maneuvering and Transit of a Training Ship”. In: *International Journal of Applied Mathematics and Computer Science* 27.1 (2017), pp. 63–77.

[96] I.R. Bertaska and K.D. von Ellenrieder. “Experimental evaluation of supervisory switching control for unmanned surface vehicles”. In: *IEEE Journal of Oceanic Engineering* 44.1 (2018), pp. 7–28.

[97] S. Yin, H. Yang, and O. Kaynak. “Coordination task triggered formation control algorithm for multiple marine vessels”. In: *IEEE Transactions on Industrial Electronics* 64.6 (2016), pp. 4984–4993.

[98] E. Ruth. “Propulsion control and thrust allocation on marine vessels”. In: (2008).

[99] G.J. Nuij. “Introduction of PEM Fuel Cells on Inland Ships”. In: (2021).

[100] H. Klein Woud and D. Stapersma. *Design of propulsion and electric power generation systems*. IMarEST, Institute of Marine Engineering, Science and Technology, 2019.

[101] *Chapter 7 Resistance and Powering of Ships - USNA*. URL: https://dokumen.tips/documents/chapter-7-resistance-and-powering-of-ships-usna-resistance-and-powering-of-ships.html.

[102] L. Birk. “Holtrop and Mennen’s Method”. In: *Fundamentals of Ship Hydrodynamics* (Apr. 2019), pp. 611–627. DOI: 10.1002/9781119191575.ch50.

[103] MAN. *Technical papers: Basic principles of ship propulsion*. URL: https://www.man-es.com/marine/products/planning-tools-and-downloads/technical-papers/2.

[104] G. Guedes Soares and T.A. Santos. *Maritime Technology and Engineering*. Oct. 2014. URL: https://books.google.nl/books?hl=nl&lr=&id=kg7NBQAAQBAJ&oi=fnd&pg=PA119&dq=%5C%22sea%5C%2Bmargin%5C%22%5C%2B%5C%22inland%5C%2Bwaterways%5C%22&ots=hkSBYfODml&sig=SFaOD2iBJlL-PQL-vvlLiONXMIY&redir_esc=y#v=onepage&q=%5C%22sea%5C%20margin%5C%22%5C%20%5C%22inland%5C%20waterways%5C%22&f=false.

[105] P.K. Patel and M. Premchand. “Numerical Investigation of the Influence of Water Depth on Ship Resistance”. In: *International Journal of Computer Applications* 116 (2015), pp. 10–17.

[106] H. Schneekluth and V. Bertram. *Ship design for efficiency and economy*. Vol. 218. Butterworth-Heinemann Oxford, 1998.

[107] B. Kwasieckyj. “Efficiency analysis and design methodology of hybrid propulsion systems”. In: (2013).

[108] A. Menon. *What is bollard pull - everything you wanted to know*. Mar. 2021. URL: https://www.marineinsight.com/naval-architecture/bollard-pull-everything-you-wanted-to-know/.

[109] V. Krasilnikov, N. Berchiche, and K. Koushan. “Thrust Losses and Dynamic Loads on a Ducted Pushing Thruster in Regular Waves”. In: *Proceedings of the 6th International Symposium on Marine Propulsors SMP*. Vol. 19. 2019.

[110] Z. Zeng et al. “A survey on path planning for persistent autonomy of autonomous underwater vehicles”. In: *Ocean Engineering* 110 (2015), pp. 303–313.

[111] K.J. Rawson and E.C. Tupper. “11 - Powering of ships: application”. In: *Basic Ship Theory (Fifth Edition)*. Ed. by K.J. Rawson and E.C. Tupper. Fifth Edition. Oxford: Butterworth-Heinemann, 2001, pp. 411–456. ISBN: 978-0-7506-5398-5. DOI: https://doi.org/10.1016/B978-075065398-5/50014-5. URL: https://www.sciencedirect.com/science/article/pii/B9780750653985500145.

[112] MAN. *Technical papers: Propulsion trends in bulk carriers*. URL: https://www.man-es.com/marine/products/planning-tools-and-downloads/technical-papers/2.

[113] B. Goldsworthy and L. Goldsworthy. “Assigning machinery power values for estimating ship exhaust emissions: Comparison of auxiliary power schemes”. In: *Science of the Total Environment* 657 (2019), pp. 963–977.

[114] G.M. Milis, C.G. Panayiotou, and M.M. Polycarpou. “Semiotics: Semantically enhanced Iot-enabled intelligent control systems”. In: *IEEE Internet of Things Journal* 6.1 (2017), pp. 1257–1266.

[115] H.N. Psaraftis and C.A. Kontovas. “Speed models for energy-efficient maritime transportation: A taxonomy and survey”. In: *Transportation Research Part C: Emerging Technologies* 26 (2013), pp. 331–351.

[116] H. Hensen. “Using experience to assess required tug power”. In: *Port Technol. Int* 26 (2003), pp. 95–97.

[117] *Wärtsilä generating sets*. URL: https://www.wartsila.com/marine/products/engines-and-generating-sets/generating-sets/wartsila-gensets.

[118] Y. Zhang et al. “Collaborative Optimization of the Battery Capacity and Sailing Speed Considering Multiple Operation Factors for a Battery-Powered Ship”. In: *World Electric Vehicle Journal* 13.2 (2022), p. 40.

[119] A. Bordianu and G. Samoilescu. “Electric and Hybrid Propulsion in the Naval Industry”. In: *2019 11th International Symposium on Advanced Topics in Electrical Engineering (ATEE)*. IEEE. 2019, pp. 1–6.

[120] L. Castelo Branco Menano de Figueiredo. “The Yacht of 2030”. In: (2018).

[121] Z. Duan et al. “Analysis of Key Technologies for New Green Marine Propulsion Systems”. In: *E3S Web of Conferences*. Vol. 194. EDP Sciences. 2020, p. 02008.

[122] R.D. et al. “Parallel control for hybrid propulsion of multifunction ships”. In: *IFAC-PapersOnLine* 50.1 (2017), pp. 2296–2303.

[123] N. Bennabi et al. “Hybrid propulsion systems for small ships: Context and challenges”. In: *2016 XXII International Conference on Electrical Machines (ICEM)*. IEEE. 2016, pp. 2948–2954.

[124] J.F. Hansen et al. “Onboard DC Grid for enhanced DP operation in ships”. In: *Dynamic Positioning Conference, Houston*. 2011.

[125] A. Haseltalab and R.R. Negenborn. “Model predictive maneuvering control and energy management for all-electric autonomous ships”. In: *Applied Energy* 251 (2019), p. 113308.

[126] R.D. Geertsma et al. “Pitch control for ships with diesel mechanical and hybrid propulsion: Modelling, validation and performance quantification”. In: *Applied Energy* 206 (2017), pp. 1609–1631.

[127] R.D. Geertsma et al. “Torque control for diesel mechanical and hybrid propulsion for naval vessels”. In: *Proceedings of the 13th international naval engineering conference. Bristol, UK*. 2016, pp. 476–92.

[128] D. Stapersma. “Interaction between propulsor and engine”. In: *Proceedings of the 34th WEGEMT School" Developments in the Design of Propulsors and Propulsion Systems", AULA, TUDelft, June 2000, Edited by: PW de Heer, Paper: P2000-7 Proceedings.* (2000).

[129] L. Warnes. “Induction motors”. In: *Electronic and Electrical Engineering*. London: Macmillan Education UK, 1998, pp. 312–332. ISBN: 978-1-349-15052-6. DOI: 10.1007/978-1-349-15052-6_17. URL: https://doi.org/10.1007/978-1-349-15052-6_17.

[130] T. Wildi et al. “Electrical machines, drives, and power systems”. In: *New Jersey: Upper Saddle River* (2002).

[131] T. Eijkhout and J. Jovanova. “Active heave compensation of a floating crane using electric drive”. In: *2021 IEEE/ASME International Conference on Advanced Intelligent Mechatronics (AIM)*. 2021, pp. 1089–1094. DOI: 10.1109/AIM46487.2021.9517502.

[132] M.A.W. Begh and H.G. Herzog. “Comparison of field oriented control and direct torque control”. In: *Technical University of Munich, Germany* (2018).

[133] S. Karpe, S.A. Deokar, and A.M. Dixit. “Switching losses minimization by using direct torque control of induction motor”. In: *Journal of electrical systems and information technology* 4.1 (2017), pp. 225–242.

[134] E. Flach, R. Hoffmann, and P. Mutschler. “Direct mean torque control of an induction motor”. In: *European Conference on Power Electronics and Applications*. Vol. 3. Proceedings published by various publishers. 1997, pp. 3–672.

[135] R. Bharti, M. Kumar, and B.M. Prasad. “V/f control of three phase induction motor”. In: *2019 International Conference on Vision Towards Emerging Trends in Communication and Networking (ViTECoN)*. IEEE. 2019, pp. 1–4.

[136] M. Vahedpour, A.R. Noei, and H.A. Kholerdi. “Comparison between performance of conventional, fuzzy and fractional order PID controllers in practical speed control of induction motor”. In: *2015 2nd International Conference on Knowledge-Based Engineering and Innovation (KBEI)*. IEEE. 2015, pp. 912–916.

[137] J. Lee, S. Lee, and S. Sul. “Variable-speed engine generator with supercapacitor: Isolated power generation system and fuel efficiency”. In: *IEEE Transactions on Industry Applications* 45.6 (2009), pp. 2130–2135.

[138] D.J. McGowan, D.J. Morrow, and M. McArdle. “A digital PID speed controller for a diesel generating set”. In: *2003 IEEE Power Engineering Society General Meeting (IEEE Cat. No. 03CH37491)*. Vol. 3. IEEE. 2003, pp. 1472–1477.

[139] K.L. Cheong, P.Y. Li, and J. Xia. “Control oriented modeling and system identification of a diesel generator set (genset)”. In: *Proceedings of the 2010 American Control Conference*. IEEE. 2010, pp. 950–955.

[140] S. Ayasun and A. Gelen. “Stability analysis of a generator excitation control system with time delays”. In: *Electrical Engineering* 91.6 (2010), pp. 347–355.

[141] L. Luo, L. Gao, and H. Fu. “The control and modeling of diesel generator set in electric propulsion ship”. In: *International Journal of Information Technology and Computer Science (IJITCS)* 3.2 (2011), p. 31.

[142] A.A. Renjit et al. “Modeling and control of a natural gas generator set in the CERTS microgrid”. In: *2013 IEEE Energy Conversion Congress and Exposition*. IEEE. 2013, pp. 1640–1646.

[143] K. Sun and Q. Shu. “Overview of the types of battery models”. In: *Proceedings of the 30th Chinese Control Conference*. IEEE. 2011, pp. 3644–3648.

[144] M.I. Wahyuddin, P.S. Priambodo, and H. Sudibyo. “State of charge (SOC) analysis and modeling battery discharging parameters”. In: *2018 4th International Conference on Science and Technology (ICST)*. IEEE. 2018, pp. 1–5.

[145] M. Coleman, W.G. Hurley, and C.K. Lee. “An Improved Battery Characterization Method Using a Two-Pulse Load Test”. In: *IEEE Transactions on Energy Conversion* 23.2 (2008), pp. 708–713. DOI: 10.1109/TEC.2007.914329.

[146] H. Pandžić and V. Bobanac. “An accurate charging model of battery energy storage”. In: *IEEE Transactions on Power Systems* 34.2 (2018), pp. 1416–1426.

[147] T. Wu et al. “Voltage-SOC balancing control scheme for series-connected lithium-ion battery packs”. In: *Journal of Energy Storage* 25 (2019), p. 100895.

[148] F. Zheng et al. “Influence of different open circuit voltage tests on state of charge online estimation for lithium-ion batteries”. In: *Applied energy* 183 (2016), pp. 513–525.

[149] S. Lee, J. Kim J.and Lee, and B.H. Cho. “State-of-charge and capacity estimation of lithium-ion battery using a new open-circuit voltage versus state-of-charge”. In: *Journal of power sources* 185.2 (2008), pp. 1367–1373.

[150] A.A. Hussein and I. Batarseh. “An overview of generic battery models”. In: *2011 IEEE Power and Energy Society General Meeting*. IEEE. 2011, pp. 1–6.

[151] J. Kim et al. “Stable configuration of a Li-ion series battery pack based on a screening process for improved voltage/SOC balancing”. In: *IEEE Transactions on Power Electronics* 27.1 (2011), pp. 411–424.

[152] N. Kularatna and K. Gunawardane. “Rechargeable battery technologies: An electronic circuit designer’s viewpoint”. In: Jan. 2021, pp. 65–98. ISBN: 9780128207789. DOI: 10.1016/B978-0-12-820778-9.00001-2.

[153] W. Chang. “The state of charge estimating methods for battery: A review”. In: *International Scholarly Research Notices* 2013 (2013).

[154] A. Haseltalab et al. “Energy Management for Hybrid Power Generation Using Solid Oxide Fuel Cell”. In: Zenodo, Oct. 2020. DOI: 10.24868/issn.2631-8741.2020.006. URL: https://doi.org/10.24868/issn.2631-8741.2020.006.

[155] J. Friedrich et al. “Flexible and Modular Control and Manufacturing System”. In: *Procedia CIRP* 33 (Dec. 2015), pp. 115–120. DOI: 10.1016/j.procir.2015.06.022.

[156] T. Ananth. *3 Important Calculations Every Marine Engineer Must Know On Ships*. Sept. 2021. URL: https://www.marineinsight.com/guidelines/3-important-calculations-every-marine-engineer-must-know/.

[157] G. Paganelli. “Conception et commande d’une chaine de traction pour véhicule hybride parallèle thermique et électrique”. PhD thesis. Valenciennes, 1999.

[158] C. N. Mueller. *Siship Eco Prop - Central Commission for navigation on the Rhine*. URL: https://ccr-zkr.org/temp/wrshp120411/Informations/SISHIP_ECO_PROP_Siemens_CMueller.pdf.

[159] Wärtsilä. *GRIDSOLV Max specification sheet*. URL: https://www.wartsila.com/docs/default-source/power-plants-documents/downloads/specification-sheets/gridsolv-max.pdf.

[160] M.A. El-Reedy. "5 - Fabrication and installation". In: *Offshore Structures (Second Edition)*. Ed. by M.A. El-Reedy. Second Edition. Gulf Professional Publishing, 2020, pp. 269–357. ISBN: 978-0-12-816191-3. DOI: https://doi.org/10.1016/B978-0-12-816191-3.00005-5. URL: https://www.sciencedirect.com/science/article/pii/B9780128161913000055.

[161] B. Zahedi, L.E. Norum, and K.B. Ludvigsen. "Optimized efficiency of all-electric ships by dc hybrid power systems". In: *Journal of power sources* 255 (2014), pp. 341–354.

[162] I. Emmanuel-Douglas. "Performance evaluation of combined cycles for cruise ship applications". In: *ASME International Mechanical Engineering Congress and Exposition*. Vol. 48692. 2008, pp. 183–194.

[163] MAN. *Technical papers: Propulsion trends in container vessels*. URL: https://www.man-es.com/marine/products/planning-tools-and-downloads/technical-papers/2.

[164] MAN. *Technical papers: Propulsion of 46,000-50,000 dwt MR tankers*. URL: https://www.man-es.com/marine/products/planning-tools-and-downloads/technical-papers/2.

[165] S.N. Sirimanne et al. *Review of maritime transport 2019*. Tech. rep. tech. rep, 2019.

[166] *Shipping time calculator*. Sept. 2021. URL: https://www.freightos.com/freight-resources/transit-time-calculator/.

[167] H. Xu and D. Yang. "LNG-fuelled container ship sailing on the Arctic Sea: Economic and emission assessment". In: *Transportation Research Part D: Transport and Environment* 87 (2020), p. 102556.

[168] M. Agarwal. *What is the speed of a ship at sea?* Mar. 2020. URL: https://www.marineinsight.com/guidelines/speed-of-a-ship-at-sea/.

[169] F. Frese. *How slow steaming impacts shippers and carriers*. June 2021. URL: https://container-xchange.com/blog/slow-steaming/.